THE UNIVERSITY
of EDINBURGH

Wave Energy Resource Modelling and Energy Pattern Identification Using a Spectral Wave Model

George Lavidas

Doctor of Philosophy

THE UNIVERSITY OF EDINBURGH

2016

To my mother and father for their support throughout the years,

your son George

Layout Summary

Globally the electricity needs are expected to increase with climate change significantly affected by the energy production sector. Estimations for future climates made by the International Energy Agency (IEA), suggest that increasing renewable energy production will tackle some of the major climate change issues.

This work was undertaken at the University of Edinburgh, by George Lavidas under the supervision of Dr. Vengatesan Venugopal and Dr. Daniel Friedrich, on investigating the wave climate, resource capabilities and uncertainty towards energy production. The work was funded by the Engineering and Physical Sciences Research Council (EPSRC) under grant number J12DTA.

Waves constitute an abundant renewable source of energy that ranks amongst the highest in energy content. Their predictability is higher and variations are reduced compared to other renewable energy forms. This work, starts by identifying the resource of areas through extensive assessment and custom models of high temporal and spatial resolutions. The results obtained allow quantification of energy, extremes, and climate variations of the resource.

Under this context, the applicability of a numerical wave model and its physical alterations was investigated to establish long-term wave data. Apart from the analysis and detailed instruction on operation of the numerical wave model, the quantification of exploitable energy by waves and their financial viability are also estimated. The results can be utilized not only by the wave energy industry but also for examination of the wave climate, fisheries, naval and offshore marine activities.

They can also be utilized in the decision making process by institutions and legislative bodies which examine the incorporation of wave energy into the production cycle. It is expected that the work, offers information to the wave modelling and renewable energy community towards the importance of numerical resource assessments, in providing clear and substantial considerations. A state-of-the-art database generated from this work is publicly available and can be used to aid the dissemination activities of decision making for wave energy application and the long-term wave climate as a whole.

Abstract

The benefits of the Oceans and Seas have been exploited by societies for many centuries; the marine offshore and naval sectors have been the predominant users of the waters. It has been overlooked until recently, that significant amounts of energy can be harnessed by waves, providing an additional abundant resource for renewable energy generation.

The increasing energy needs of current societies have led to the consideration of waves as an exploitable renewable resource. During the past decades, advancements have been made towards commercialising wave energy converters (WECs), though significant knowledge gap exists on the accurate estimation of the potential energy that can be harnessed. In order, to enhance our understanding of opportunities within wave energy highly resolved long-term resource assessment of potential sites are necessary, which will allow for not only a detailed energy estimation methodology but also information on extreme waves that are expected to affect the survivability and reliability of future wave energy converters.

This research work aims to contribute the necessary knowledge to the estimation of wave energy resources from both highly energetic and milder sea environment, exhibiting the opportunities that lay within these environments. A numerical model SWAN (Simulating WAves Nearshore), based on spectral wave formulation has been utilised for wave hindcasting which was driven by high resolution temporal and spatially varying wind data. The capabilities of the model, allow a detailed representation of several coastal areas, which are not usually accurately resolved by larger ocean models.

The outcome of this research provides long-term data and characterisation of the wave environment and its extremes for the Scottish region. Moreover, investigation on the applicability of wave energy in the Mediterranean Sea, an area which was often overlooked, showed that wave energy is more versatile than expected. The outcomes provide robust estimations of extreme wave values for coastal waters, alongside valuable information about the usage of numerical modelling and WECs to establish energy pattern production. Several key tuning factors and inputs such as boundary wind conditions and computational domain parameters are tested. This was done in a systematic way in order to establish a customized solution and detect parameters that may hinder the process and lead to erroneous results.

The uncertainty of power production by WECs is reduced by the introduction of utilization rates based on the long-term data, which include annual and seasonal variability. This will assist to minimize assumptions for energy estimates and financial returns in business plans. Finally, the importance of continuous improvements in resource assessment is stressed in order to enhance our understanding of the wave environment.

Acknowledgements

I owe gratitude to my supervisor Dr. Vengatesan Venugopal for his support and guidance under stressful situations, your comments, guidelines and valuable help made this thesis possible. I would like also like to thank my second supervisor, Dr. Daniel Friedrich for his helpful comments.

My many thanks go to the team of the ECDF computer facility, the TU Delft University team that maintains the SWAN code, as well as to the ocean and wave departments of ECMWF, NOAA, NCEP, HCMR, CEFAS, for providing access to various data.

Gratitude and thanks are also due to my friends, and especially (the current) Dr. Atul Agarwal. Whose discussions and insights always proved to be a valuable different point of view, which added something more to my thoughts. You are one of the few people that I am proud to call my friend.

Many thanks to my colleagues, office mates and friends Brian, Duncan, Paul hopefully i didn't made your life to hard. To the whole family of IES which often provided fun times with coffee. To Dimitris Tsikritsis, Konstantinos Markakis my friends that we spent hours of procrastination and laughter. Special thanks go to my outside university friends Dave, Mike, Colin , Zach and Louie, it has been a privilege to have met you all and spent so many hours discussing and training, through the passing of these years.

My parents, Leonidas and Panagiota, for their unlimited support towards the hard path I choose, I hope you are pleased and proud where ever my future career takes me. Without your help I wouldn't be able to pull till the end. I hope I can always make you feel happy for my achievements.

Finally, I would like to thank Zoe, for your love and support, even through the hardships, the distance and moments that intervened until the completion of this work. You are a significant reason that pushed me to complete my dream. You always stayed with me regardless the hard times and complaints.

Declaration

I declare that this thesis was composed by myself, that the work contained herein is my own except where explicitly stated otherwise in the text, and that this work has not been submitted for any other degree or professional qualification except as specified.

Contents

List of Figures

List of Tables

Abbreviations

AMM	Annual Maxima Method
BERR	Department for Business Enterprise and Regulatory Reform
BODC	British Oceanographic Data Centre
BOF	Bottom Oscillating Flap (resembling Oyster 2)
CfD	Contracts for Difference
CAPEX	Cital Expenditure
CFL	Courant-Friedrich-Levy criterion
CFSR	Climate Forecast System Re-Analysis
CIESM	Mediterranean Science Commission
CPE	Caspian Environment Program
DIA	Discrete Interaction Approximations
DTA	Discrete Triad Approximation
ECDF	Edinburgh Compute and Data Facility
ECMWF	European Centre for Medium Range Weather Forecasts
ECWM	European Centre WAve Model
ETS	Emissions Trading Scheme
EVA	Extreme Value Analysis
EU	European Union
F2HB	Floating two body heave converter (resembling WaveBob)
FC_n	Fixed Cost
FIT	Feed in Tarrif
GEV	Generalized Extreme Value
GB	Gigabytes
GHSS	Global Shelf-consistent,Hierarchical,High-resolution Shoreline
GMD	Generalized Multiple Discrete Interaction Approximation
GPD	Generalized Pareto Distribution
IC_n	Initial Capital Cost (ex-works)
IC_o	Initial Capital Cost (including works)
IEA	International Energy Agency
IES	Institute for Energy Systems
i.i.d	identically independent distributed
IFS	Integrated Forecasting System
IRR	Internal Rate of Return
JODC	Japanese Oceanographic Data Centre

JONSWAP	Joint North Sea Wave Project
LCOE	Levelized Cost of Energy
LTA	Lumped Triad Approximation
MLM	Maximum Likehood Method
MPI	Message Passing Interface
NPV	Net Present Value
NCAR	National Centre for Atmospheric Research
NCEP	National Centre for Environmental Prediction
NDGC	National Data Geophysical Centre
NetCDF	network Common Data Form
OMP	Open Multi-Processing
OPNML	Ocean Processes Numerical Modelling Laboratory
POT	Peak-Over-Threshold
PTO	Power Take Off
PM	Pierson-Moskowitz
RE	Renewable Energy
ROC	Renewable Obligation Certificates
SWAMP	Sea Wave Modelling Project
SWAN	Simulating WAves Nearshore
TB	Terra-bytes
TPAR	Boundary conditions file in SWAN
WAM	WAve Model
WEC	Wave Energy Converter
*WW*3	WaveWatch3
XNL	Exact Non Linear solvers

Chapter 1

Introduction

"Men should strive to think much and know little."

Democritus, 460-370 B.C.

Power generation from renewable energy sources has been proven to result in significant energy security, climate change mitigation, and economic benefits. Wave energy, as one form of renewable energy sources from the ocean, has enormous potential worldwide to provide significant contribution to electricity generation. Wave energy resources are best between 30^o and 60^o latitude in both hemispheres, hence the United Kingdom and Europe are well placed to harness this particular form of renewable energy. Indicatively for the European region the available wave power resource amounts to 300 GW (Gunn and Stock-Williams, 2012).

Ocean wave climate is highly variable across the globe on temporal and spatial scales, and the local geography greatly influences the wave formation and propagation. Currently third generation numerical wave models are utilised for wave hindcasting and forecasting. A properly calibrated, validated wave numerical model is the basis, proving that it can reduce uncertainties both long and short term wave predictions.

Consequently, the focus is solely on the wave potential, though understanding of the resource itself is important and should be the primary driver for the development not only of engineering technologies but energy policies as well. So starting from a resource assessment point of view, the assumptions on energy productions are kept at a minimum, since a good long-term hindcast reveals not only possibilities but also uncertainties in the prediction of waves.

During the past years attempts to develop wave energy converters and test them at real sea location have increased (Cruz, 2008; Falcão, 2010; EMEC, 2009, 2013; Bozzi *et al.*, 2011a). The dependence of wave and climatic investigation, prompted further development of techniques and numerical models that allow insight in past and future events.

With computer advancements, the goal to establish better and more accurate models has improved. Developments in wave theory and infrastructure have allowed significant improvements in understanding of waves. This has put the use of numerical models for climatic research, climate change, and in recent years wave energy estimations (Sterl *et al.*, 1998; Gulev

and Hasse, 1999; Dodet *et al.*, 2010; Reguero *et al.*, 2012; Stopa *et al.*, 2013; Reguero *et al.*, 2015).

With accuracy improved (Komen *et al.*, 1994; Cavaleri *et al.*, 2007; Janssen, 2008), numerical wave models have found their way and utilization within the research community and energy industries. This does not mean though that accuracy is always high. Proper set-up of a numerical wave model, comprises from many inputs, starting with the drivers of models, up to interactions and proper calibration of activated physical processes. Different models, though they obtain similar results if properly used, have different numerical solutions which affect their applicability.

Thus far, large scale or oceanic numerical models are typically used to provide wave parameters. Their use is adopted from international, governmental, research institutes, and when used correctly they pose a significant resource of information, this has spurred various research studies on wave environments. Global energy estimations in the past have quantified the available resource amounts to significant levels, which are accessible to most countries but have not been taken into advantage. Some have tried to quantify the global resource (Cornett, 2008; Reguero *et al.*, 2015), while others focused on more specific areas such as the North of Europe Agarwal (2015). Baltic Sea and United Kingdom (Smith and Maisondieu, 2014; Neill and Hashemi, 2013; Venugopal and Nemalidinne, 2015), the Spanish and Portuguese coastlines (Pilar *et al.*, 2008; Ratsimandresy *et al.*, 2008), the Mediterranean (Medatlas Group, 2004; Cavaleri and Bertotti, 2006; Soukissian *et al.*, 2012; Ayat, 2013; Liberti *et al.*, 2013; Mentaschi *et al.*, 2015), the French North coast Cañellas *et al.* (2007), the Chinese Seas (Liang *et al.*, 2014), the Black Sea (Akpinar and Kömürcü, 2013) and other numerous to list here.

These constitute a large scientific database, which can be expanded upon for general offshore and climate investigations in various regions. Numerical model results are applicable to offshore structural analysis studies, wind evaluation, climate forecasts, extreme statistics, wave energy and many more.

Though the information from such studies enhance our knowledge, a significant gap exist in resource assessments concerning the coastal and nearshore wave environments. The representation of these zones is often limited by the larger models. While computational, storage, and data requirements pose a barrier in the detailed examination. Majority of information are usually extrapolated assumptions based on larger models. Most of the times lack of appropriate data hinders the accurate representation of coastal zones, increasing uncertainties and assumptions for offshore applications.

Increased uncertainties and lack of information means that the exploitation and establishment of wave energy as a viable generation alternative is reduced. Numerical wave models apart from the local wave climate, can provide information concerning the energy potential of an area, assisting in the identification of energetic locations. Assessing energy production, through

long-term data reduces uncertainties in the energy flux. These benefits will help us to reduce the intermittent nature of waves in energy production considerations. At the same time a significant knowledge on the variation of energy content over a large period of time, will allow future extrapolations in a robust way.

1.1 Research Objectives

The main objective of this doctoral thesis is to assess the wave power, predominately around Scottish waters using a third generation numerical wave model. The study focuses in the energetic coastline of Scotland and North Sea, aiming to establish a robust approach to estimate the potential energy production levels available to wave energy devices. In addition, as similar opportunities exist in the Mediterranean and Aegean Seas for wave power production, this research has also been extended to include these zones and wave modelling was carried out.

The thesis uses the popular wave model SWAN and addresses the following questions:

- How to optimally set up a spectral model? What are key considerations to customize and improve it? How different wave theories can be incorporated and what effects will they have on accuracy and demands of the model?
- Can a customizable model provide better data than existing studies? To what extent can they be improved and what limitations exist within the wave model itself?
- Is the selection process of customizable parameters, able to provide high confidence data at other locations?
- How does the previous studies and scientific literature on wave modelling explain barriers in the models e.g. under or over-estimation of wave parameters? What are the alternatives to minimizing these effects?
- How does the intra-annual variability of wave parameters affect the resource for waves and energy potential? Based on this variation, what locations are exposed to less variance and have the potential of a better environment for wave energy applications?
- What are the actual energy capabilities of operation for wave energy converters?

With the production of a resource assessment map, based on high-resolution data of spatial input information and physical customization of the model for the area. It is expected that energy resource estimations for Scotland and the Mediterranean sea can be highly improved. The ability of the model to perform at coastal and deeper water locations will be assessed, to show that results strengthen the notion that wave hindcasts can be used reliably for investigation of the wave climate, with out the deployment of expensive equipment for many years i.e. buoys.

The necessity for coastal wave resource information e.g. wave height, energy content, is addressed by both the examination of a detailed 11 years resource assessment hindcast by the model, and subsequently the extractable levels of energy are estimated. The dataset produced

from this work is freely available. Apart from the findings concerning wave energy, it can also be used to establish extreme events and probabilities at shallow water locations where our knowledge is limited, and no extensive analysis can be performed, often the data and span for a robust analysis are limited and/or absent.

In addition, adaptation of wave energy to other environments is assessed, with promising results concerning less energetic seas. This supports the argument that applicability of wave energy converters is not be only limited to oceanic coastlines, but can have significant benefits to the overall considerations for combination of renewables.

Long-term energy performance by wave converters, and capacity factors are comparable with established technologies. The author believes that if correct steps are taken, financial considerations for wave energy will be enhanced and accelerate their applications.

Evaluating energy production based on coupling of long-term high resolution wave information and wave converters can provide significant reductions of uncertainty. Moreover, site characterisation is done based on various indices, and produce detailed consideration on financial and energy production. The added value lays within the fact that additional locations, are sited in areas of immediate deployment interest.

- What are the economic limitation, considerations and payback period? Are current measures sufficient to provide a boost of the industry?
- How does the environment change in the shallow water regions? What effects does it have on the incoming energy flux reduction and the extreme events?
- Is wave energy a viable option for different regions that are not as energetic as the UK? What would the level of energy contribution be to the local grids?

1.2 Contribution to Knowledge

The need for this work arises from the rapid developments and targets set by the wave energy industry and government bodies. Although, but not limited to, the results offer additional knowledge to the marine offshore community from the resource assessment undertaken especially at coastal locations. That has not been performed before with wave model SWAN for the regions under considerations and for this time length. The output will be useful for the assessment of wave climate, energy, extreme values considerations, and wave modelling performance. The selection and/or modification of different physical parameters in the spectral model, is a difficult process and although the corresponding results may seem to agree with experimental data, the modelling community always needs to consider the computational resources spent for the delivery of results. The specific contributions from this research are:

- Improved wave resource estimations for Scotland and the Mediterranean Sea using a high resolution spectral model.

- Validated a high-resolution (temporal and spatial) dataset for these areas, with provision of expanding data for future research.
- A methodological study illustrating the limitations and performance of the numerical model with customizable physical terms. Adaptation of physical parameters that may lead to improved results.
- Build and improve on the existing knowledge of resource estimation, expand to shallow and coastal location with high confidence.
- Produce a high-resolution long-term homogeneous dataset, that assist the investigation of wave conditions and energy resource at different environments by full incorporations of all model terms responsible for estimates of the wave resource.
- Examine the variability of waves (i.e. intra-annual variation for wave heights) and subsequently wave resource, taking into account of locations with increased interest for wave energy deployments.
- Use the long-term sea states for wave energy extraction of specific wave energy converters. This coupling allows the examination of the performance by multiple devices, in several areas that are of interest but are lacking information.
- Examine the statistical behaviour and extremes of shallow water locations. Previous studies suggests that similar approaches often might not be feasible, due to absence of detailed suitable data.
- Assess the performance of various probability distribution models to inspect if it can be used as a substitute to represent measured data by wave buoys buoys.
- Examine feasibility of wave energy converters in various areas, with different characteristics.
- Examine the economic viability and performance based on wave energy production data.
- Provide with additional information on the extreme environments expected, which will improve our understanding of, especially, coastal locations.
- Establish the proven energy performance, production, utilization rates, for various WECs, underlining their potentials.

1.3 Thesis outline

This thesis comprises of eight Chapters and four Appendices. The structure and general information on each chapter are as follows:

Chapter 1: This chapter introduces the motivation and scope of the doctoral thesis, providing an overview of the question and considerations taken for this body of work.

Chapter 2: This chapter presents the current status of wave energy in comparison with other renewable technologies. Identifies the barriers and potentials that wave energy can provide concerning the regional and global renewable production. Barriers associated for wave energy

and generally for renewable energy devices, are expressed along with considerations on how to minimize such effects. The later part of the literature review focuses on wave theory, wave models that are in existence and can be used to provide resource and climate analysis. Numerical and physical assumptions, limitations, considerations are presented alongside reasons for the selection of the specific spectral model. Finally alterations to key source terms are included with an analysis on the expected results based on the adaptive wave theory in the models.

Chapter 3: Presents the wave model and the versions of SWAN 40.91ABC and 41.01A used throughout the thesis. It's structure, details on the construction of input source material for the initiation of a proper morel are discussed, with considerations and obstacles when an fully operational model is attempted. Finally, considerations on the activation sequence and usage of several options are presented for every part of the model set-up.

Chapter 4: Presents previous scientific studies concerning the limitations and reasons for wave model performance. Predominately wave model have reported under-performance due to the resolution of wind inputs. Thus different datasets of wind input were employed to assess the performance and validity of the model. Wind products are comprised by high temporal, spatial resolutions, and are open source datasets. The results dissemination showed that there are comparable differences depending on the dataset, with increase scattering and reduction of biases. Moreover, the study offered a good examination on the accuracy of wind products themselves, since it is common practice to assess wind products by wind driven wave models. Finally, the optimal dataset for application throughout the thesis chapters concerning the UK and Scotland was based on this performance.

The second study presented in the chapter, offers insight to considerations, limitations and suggestions to overcome the incorrect performance of the model in rapidly varying depths. Though this is not common in Scotland where the orography is smoother, when depths with fast gradients are explored, SWAN violates the stability criteria and although the process produces no errors in the subsequent files, the way to identify the reason and correct it are presented.

The third study explores the effects of Discrete Interaction Approximations (DIA) and frequency alteration on a hindcast. Both the physical output, computational time and storage are addressed. The tunable DIA coefficient proves to be extremely volatile but it affects significantly the results produced. On the other hand, the frequency interval has an effect on the hindcast spectrum. Both those outcomes were taken under consideration when the resource assessment was performed, since often times the wave modeller is required to make assumption on the initial state of the model.

The final study in this chapter examines the hindcast effects and computational requirements of two different mesh lengths for the same area, with identical inputs and how this mesh alterations reduces the result on a smaller mesh. This fact can be attributed to the reduction of boundary fetch on one side that reduces computations.

Chapter 5: A detailed model is run for 11 years at the Scottish and North Sea region. The inputs used, resolution of winds and bathymetry, boundaries preparation and physical processes are presented. Interest is given to the selection of shallow water locations that other models cannot hindcast. In addition, several points compared are dispersed to better assess the performance throughout the region. The customized models proves highly skilled in shallow water areas, while several considerations concerning specific sites are addressed. It is obvious that the input is not the only limitation that the model has, it was proven that the physical aspects of the model itself acts a restriction when extreme wave conditions are present.

Following the set-up process and resources, validation of the model is extensively presented alongside with a multi-model analysis based on data obtained from a public domain project in the same area, exhibiting significant improvements. The author, also compared confidential data for very shallow locations, though they are not applicable for publication and model comparison.

Following validation the homogeneous high temporal resolution dataset is investigated for wave analysis and subsequently energy estimations. Furthermore, the proposal of an additional index is discussed in aid of consideration for future wave site selection and assessments. Several published and literature based wave energy converters are modelled and coupled with the results. Due to nature of the wave energy component, we were able to capture the annual variability on energy production. In addition, we provide robust results on energy considerations for the West, East , deep and shallow water locations, depending on device. Proposing suggested Capacity Factors (CF) that can be used for similar energy comparisons or financial studies.

The last section of this chapter examines the resource assessment and energy applicability of WECs in the Mediterranean and Aegean Seas. For those locations, to the authors knowledge, it is the first time that substantial energy production rates are given for location identified by a resource assessment with a high resolution coastal model. This section also led to the further investigation for the electrical integration, though this is not within the scope of this thesis.

Chapter 6: based on the energy estimation present a thorough an financial analysis for a variety of wave energy converters. Taking into account a detail model of cost benefit approach with and without taxation, and alternating costs, proving the financial feasibility of WECs with minimum assumptions. This leads to the identification of profitability, for various sites and devices around the region.

Chapter 7: It this chapter use of the extensive and detailed dataset produced for various locations, is used for the statistical estimation of extremes and return periods. Moreover the investigation of statistics at shallow locations was imperative as it has been indicated by existing literature and limitations in acquiring long series datasets. Extreme Value Analysis was used to model, disseminate and assess the maxima. Detailed preparation of Generalized Extreme Value

(GEV) and Generalized Pareto Approach (GPD) are presented, along with consideration on the data handling of such long datasets and their reduction. The theory and process steps followed are given with the final return periods. The locations examined are based on the previous chapter and areas of wave energy interest with attention given to shallow water, for which literature has a significant gap.

Chapter 8: Provides some key issues and assumptions concerning the process that was followed throughout this doctoral thesis. Key considerations are discussed and potential barriers that if absent might offer an improvement, with some discussion on the level of improvements expected.

Chapter 9: Provides a brief summary of the overall conclusions by the work, and considerations for future work based on the findings.

Chapter 2

Background and Literature Review

"The past is certain, the future is obscure."

Thales, 640-546 B.C.

2.1 Renewable Wave Energy Integration

Energy is the basis of economic and cultural development of our societies. The industrial revolution allowed for massive steps in the advancements of current societies and their economic prosperity. Though this is true, significant concerns about the impact of man made emissions and climate alterations led to the development of ideas for cleaner technologies. Renewable energy resources are abundant, varying in every location and freely to access but our only barrier will be to properly utilise them.

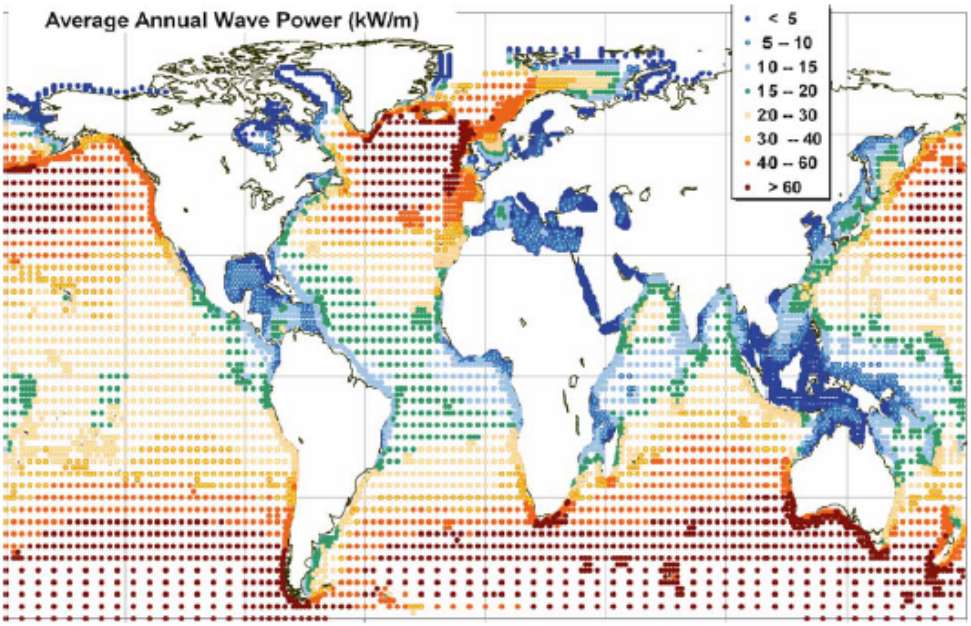

Figure 2.1: Global Annual Average Wave Resource Estimations (Cruz, 2008)

Currently, the two major renewable energy sources that have been commercially developed to full scale are, wind and solar, with comparable costs to conventional power production. Opportunities though exist in the development of an alternative renewable energy production, such as wave energy. The nature of waves is indirectly connected to solar, since waves are directly correlated to wind which is a subsequent product of alternating physical processes by solar radiation. The untapped potential of wave energy has been noted for several decades in the past, and numerous studies have explored and estimated that the available energy content of waves is very high (see Figure 2.1). With almost all countries of the world neighbouring with some sea resource, major opportunities lay for wave energy to actively contribute to the energy mix, though in most cases it has not been considered due to lack of information and infancy of the industry.

This suggests that there is a significant amount of renewable energy that still remains under-utilized. Opportunities from the exploitation of wave energy can add significant contribution to the de-carbonization of current societies. In order to achieve energy independence from conventional power sources every country has to utilize all resources at its disposal. This will ensure the energy diversification, energy security, reduction of energy poverty, economic and scientific advancements which will ultimately lead to a more sustainable and efficient way of living.

2.1.1 Barriers and Opportunities

Though it is sensible to attempt utilizing all the available resources at our disposal, wave energy remains still in its infancy, not due to technological restrictions but by economic and inherent problems that are associated with renewable energy. Technological research in the development of devices and wave energy converters (WEC) that operate with different technology principals is continuing throughout the years, with numerous alternative WEC technologies operating with different principles (Cruz, 2008).

Necessity for the deployment of various forms of renewable energies has been emphasized in many studies by both academic and governmental bodies, in scope of tackling both climate change and energy security (Carbon Trust and AMEC, 2012; Melo and J.Huckerby, 2012; IEA, 2015; OEE, 2015). The targets set by the European Union (Parliament, 2009) aim to help in the development of alternative approaches of energy production based on optimal configuration of local, national and European resources.

The physical and spatial characteristics of waves offer the opportunity for most countries to exploit their potential, though as in other forms of RE, the penetration is hindered by the variable nature of the resource. Contrast to wind, its base driver for wave generation (Kinsman, 1965), the variability of this resource is less due to the physical properties of the propagating waves, with less volatile changes in energy flux and directional changes. This in combination with the fact that temporal, spatial (grid), interconnectivity aids in the adaptation

of 80-100% RE scenario for energy systems, poses significant opportunities for wave energy to be considered in the increasing mix (European Climate Foundation, 2010; Delucchi and Jacobson, 2011; Schaber *et al.*, 2012a).

Current WEC technologies include several experimental devices close to maturity, with some having been tested in experimental facilities. This has strengthened the confidence in the applicability of wave energy technologies, with some results on production having recently made available (EMEC, 2013; Aquamarine, 2015). Lately the International Energy Agency (IEA) has also included wave energy as an potential pillar for the contribution in achieving increased RE production (see Figure 2.2).

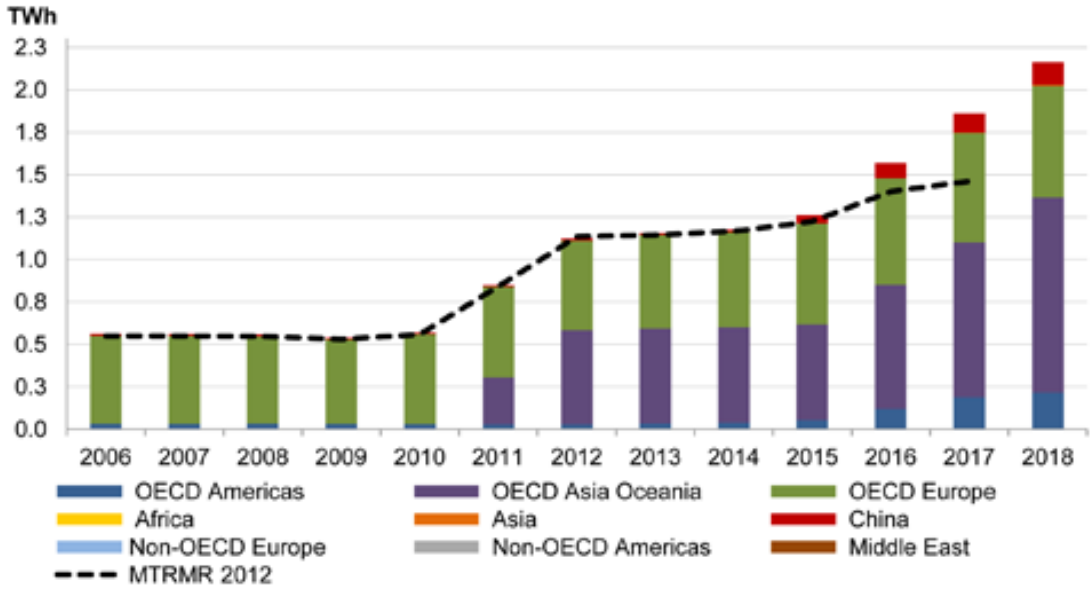

Figure 2.2: Scenarios concerning the production of current ocean power by IEA (IEA, 2015)

Development of the industry has not followed the projections and expected developments (DTI, 2002; Carbon Trust and AMEC, 2012; Melo and J.Huckerby, 2012), while it can be argued that this is due to low financial incentives and promotion schemes throughout the EU. The fact of the matter is that the intermittent nature of another RE resource and lack of objective production information, pose a significant barrier.

The financial and future deployments are dependent on the level of forecast/hindcast and understanding of the environment that WECs are to be operating. As in the case of other renewables understanding the resource and predictability of trends, poses a continuous hurdle to overcome. These reasons may seem to act as a technical and financial obstacle, though this is far from true.

Techno-economic analysis in combination with projection and cost to benefits assessments where multiple RE technology are used, have highlighted that increase of RE in the energy mix will ultimately lead to the reduction of infrastructure and lower electricity prices. Which

will not depend on fluctuation by either market or geopolitical events. Currently onshore wind already obtained a electricity generation price equal to conventional plants, while PV are expected to obtain grid parity within the next years (European Climate Foundation, 2010; Delucchi and Jacobson, 2011; Taylor *et al.*, 2006; Giannoulis and Haralambopoulos, 2011; Michalena and Hills, 2012; Krozer, 2013).

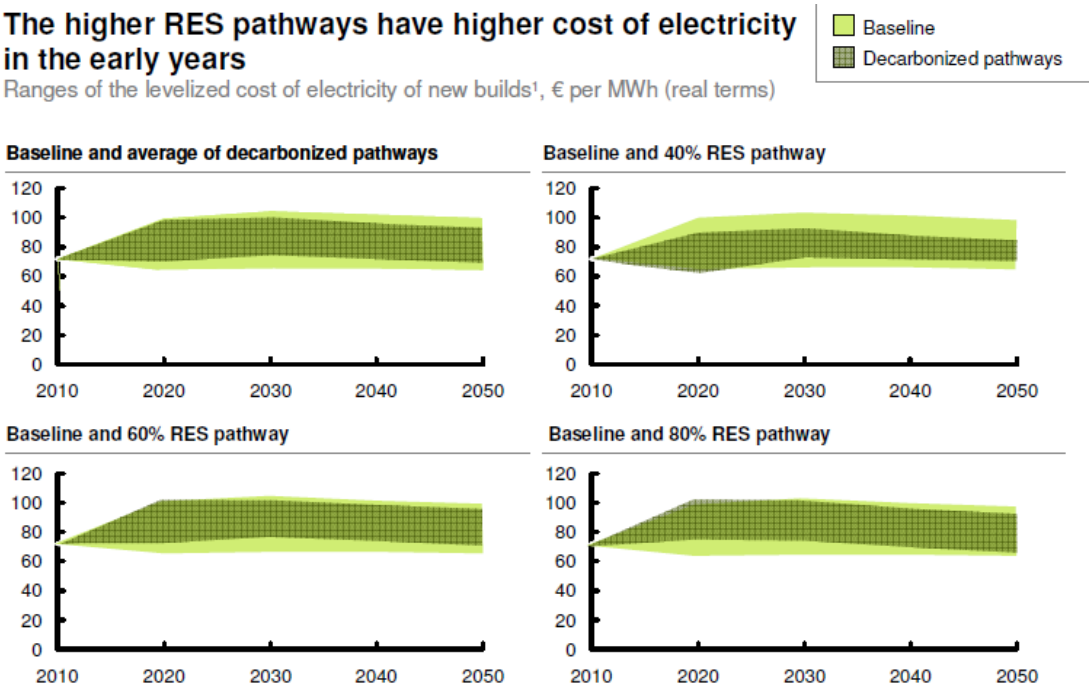

Figure 2.3: Cost of Energy based on the projection by IEA and the World Roadmap for Energy (European Climate Foundation, 2010; IEA, 2015)

In addition, the usage of varied energy mix has been reported to contribute to the reduction of operating hours of conventional power stations, especially in de-centralized non-connected electrical grids, where the cost of energy per MWh is extremely high (Zafirakis *et al.*, 2013). This reduction is both proven in current technologies and is backed by projection scenarios, although still the technical issues concerning reserve capacities and base load exist (Lund, 2006).

Amongst the proposed solutions for adaptation of RE technologies, is the interconnection of all EU electrical grids (Schaber *et al.*, 2012a; De Decker and Woyte, 2013) especially of offshore sites. The exploration of innovative storage technologies (Lund, 2006; Kaldellis, 2010; Connolly *et al.*, 2012; Hedegaard and Meibom, 2012) and the combination of RE devices that will complement each other in terms of temporal production (Fusco *et al.*, 2010; Cradden and Sarantis, 2010; Stoutenburg *et al.*, 2010; Delucchi and Jacobson, 2011).

The first two approaches entail the highest necessity for investments, especially the interconnection of the EU grids. This will add to the ability of the countries to install more RE

technology and take advantage of local resources, with most significant resource situated at offshore for wind, wave and tidal. With the interconnection providing a wider level for base loads, ensuring lower RE fluctuations production, able to satisfy mean and peak demands. The latter options are currently feasible but a certain level of trust for the production of wave devices has to be proven. Major issue pointed out is the lack of sufficient information about the wave environment and especially about shallow water locations. Thus hindering its considerations in future energy scenarios to a much greater extent, equal to the availability and possibility of exploitable resource.

Especially in the North region of Europe, significant advancements are made for the establishment of wave energy as a production alternative. Several technical considerations, and proposals exist for resource potential and utilisation (Nobre *et al.*, 2009; Waveplam, 2009; Carbon Trust and AMEC, 2012). Due to the fact that it is next to impossible to obtain long term data for all locations of interest, numerical methods have been developed to deliver necessary data. Current analysis give a good approximation of deep waters and obtainable energy flux, though limitations for long term coastal data are noted. In addition, developments in wave energy are also made in areas that until now were considered less energetic, due to the fact that characteristics at such locations may actually prove better in order for the wave industry to prove its operation and gain reliability (Bozzi *et al.*, 2011b; Vannuchi and Cappietti, 2013; Antonini *et al.*, 2014). Moving ahead with smaller steps, in order to establish a viable model of operation and access financial resources, as in the case of wind (Garrad, 2012).

This necessity for estimating wave resource at coastal locations, is one of the important components that will help bridge and reduce the uncertainty concerning wave power generation. Furthermore, with a properly structured approach the energy and economic benefits of different WECs can indicate the level of readiness to energy contribution and economic return. The representation of a detailed wave resource though is not only limited to the wave industry, several other industries are to benefit such as fisheries, offshore platforms and marine/naval. The identification of trends and intra-annual variability also indicate the altering patterns which are encompassed in the resource.

Furthermore, properly assessing resource and capabilities of devices will aid in the use of potential information that can be used actively in the consideration and promotion of wave energy. By reducing the uncertainty of waves reliability issues can be slowly removed, and raise awareness on the opportunities and contributions of the wave energy field. This adds to the choice of awareness not only of consumers but also of political and regulatory bodies, by proving that the actual capabilities of the marine industry are comparable with those of other RE technologies. Thus the benefits of incorporating WECs in a larger scale will benefit the path towards de-carbonization, energy security, energy independence, sustainable economic growth and emissions reductions, to name a few.

These underlining opportunities show that wave energy is not only applicable or limited to spe-

cific locations, but its benefits can be used for any wave resource sites worldwide. Identifying the energy content is the first step, to assess production and then the economic viability, thus the improvements on wave resource assessments is imperative.

Moving into a de-carbonized future with ultimate goal to tackle climate change without compromising economic and social prosperity will need the fullest exploitation of all our energy resources. Waves are accessible and have the possibility to provide significant energy contribution to any country, though detailed parametrization of their operation is needed. As the structure of energy maps is changing around Europe, due to recent geopolitical events, it is imperative more than ever to move towards a further integration of RE into the electricity mix. Full usage of all available resources will be the only way to attain a secure and prosperous future.

2.2 Characterizing the Wave Resource

Quantifying the potential energy resource of an area is far from a trivial process. While wave measuring buoys, exploration/naval ships, offshore platforms, offer a valuable source of information, they can only provide specific location characteristics. While such information are vital, at the same time they provide limited spatial and temporal information about the available resource. Limiting our understanding and opportunities not allowing us to expand such individual findings to regions or countries.

Estimations of wave resource with higher accuracy covering entire regional or global domain was not always possible. The limitation in our understanding of wave evolution and computational limitations, hindered the investigation of wave energy. Although, wave energy converters have been developing since the 1970's (Cruz, 2008), the verification of various theories concerning waves were limited to localized studies and experimental observations (Miles, 1957; Pierson and Moskowitz, 1964; Kinsman, 1965; Pierson and Stacy, 1973; Hasselmann *et al.*, 1973), which laid the foundation for wave theory to be adapted by numerical models.

It was not until the early 1980's that the development of increase of the computational strength of computers, and initial efforts of K.Hasselmann in 1984 allowed and paved the way for creation of a joint development group concerned with the evolution of numerical wave models. This attempt led to the development of the Wave Modelling Group, which within ten years managed to evolve the application of wave theory from 1^{st} and 2^{nd} to the state-of-the-art 3^{rd} generation (Komen *et al.*, 1994). This rapid developments allowed the long-term hindcast of global regions and have since been used extensively in the fields of wave evaluation, climate change, meteorology, forecasting and many more.

2.2.1 Wave Climate Analysis

In the late 1980's, with computational resources increasing, the WAMDI Group developed a fully functional wave numerical model, the verification of the model allowed examination of previous sea-states (hindcast) at a much larger scale and within areas with our recording mechanisms (WAMDI, 1988). This proved a significant asset to the investigation of climate change factors concerning the wave environments, and allowed to study the effects for different climate scenarios on the wave climate. From this standpoint, many studies have proposed and promoted the use of calibrated numerical wave models for providing information concerning previous years and most importantly, providing information for areas where no recording devices exist (Goda, 2000; Holthuijsen, 2007; Caires *et al.*, 2008; Mackay *et al.*, 2010a,b).

Such an example of analysis was performed by Swail *et al.* (2000), where a numerical wave model was used to examine climate change occurrences. The model used 40 year hindcasts and focused on the North Atlantic region. Initial findings showed that numerical wave models have differences with instruments. Noting that depending on the equipment (data) used for the validation process, differences in the hindcast may occur. Specifically, depending on the type of equipment the under-estimation may be higher i.e. buoy or fixed platform. It was also pointed out that depending on location the results deviated.

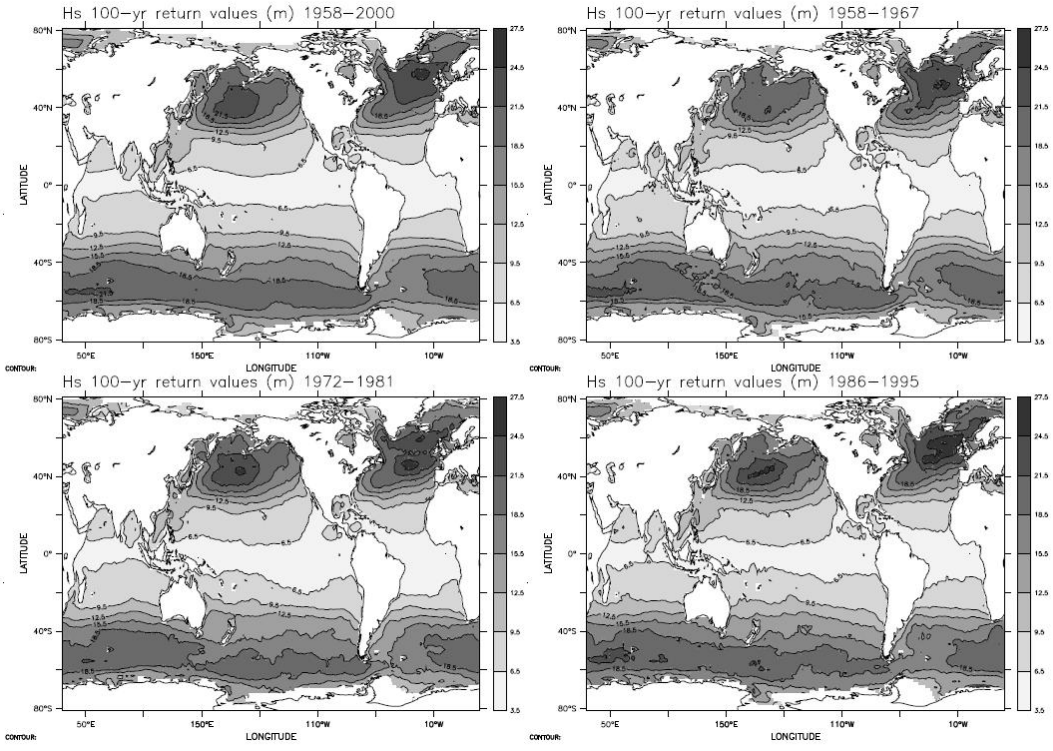

Figure 2.4: Global Return periods as given in Sterl and Caires (2005)

Sterl and Caires (2005) used output from a model and underlined the necessity of numerical

models in climate analysis. The work by Sterl and Caires (2005) allowed for a good representation of extremes on a global scale (see Figure 2.4). In that work several issues were answered and raised, first the estimated wind dataset used was presented and assessed while a full validation, and data assimilation techniques performed at the dataset were examined for accuracy. The confidence obtained by the data allowed for a climatological and extreme value analysis of global positions, with some limitations and deficiencies reported.

Similar work was performed by Young (1999a); Young *et al.* (2012), where results from a long-term model were used, while the first one combined data from measurements by satellites and boys. The results indicated that long-term hindcasts where in good agreement with global altimeter and satellite data, suggesting that satellite and numerical data can be utilized for analysis and model set up. Moreover, a close connection of the wind and wave resource was reported, with wave models being able to provide a testing mechanism for the quality of wind model outputs. Results showed that during the past 25 years it is evident that the wave and wind climate has been changing, with impacts on wave extremes. By not limiting analysis in outdated buoy recordings and measurements, more accurate extreme climate predictions are feasible. The main reason is the limitation of the data length themselves. In addition, the obstacles in climate analysis when using buoys, satellite data and numerical models were discussed in Young (1999b).

Similarly in another study the climate variability in the North-East Atlantic by a 60 year hindcast was examined (Dodet *et al.*, 2010). The authors recognized that in an effort to investigate climate change scenarios, storm severity evolution and pluri-decadal trends, long-term reliable data are needed. The use of a validated model allowed them to expand their findings for a long period of 60 years, covering the Atlantic region and extrapolating points situated off the coast of Spain, Portugal and United Kingdom. Their model was calibrated and validated with buoy historical data, which however showed an under-estimation of -0.19 m in wave height. While the validation allowed expanding the analysis and comparing the long-term hindcasts, their model was limited by the ability to perform the corresponding hindcasts at coastal location (see Figure 2.5). Their configuration involved a numerical model forced by 1-hour winds and 0.5^o mesh resolution.

Amongst the latest most up-to-date long-term data generated for climate change evaluation, is reported in Agarwal (2015). Where a fully customized calibrated model was implemented in the Atlantic to examine historical climate change of the wave resource. The author stressed the need of long-term reliable measurements in order to investigate the potential past and assess the future effects of climate change. This study is one of the lengthiest analysis producing a final hindcast dataset of almost 140 years. The model used several nested meshes to optimize the results, the outter mesh being $1^o x 1^o$, while the inner one had a resolution of $0.25^o x 0.25^o$ This resulted in the construction of an extensive database, which was compared to the climate scenarios from IPCC. The long-term results showed the areas in which climate change and

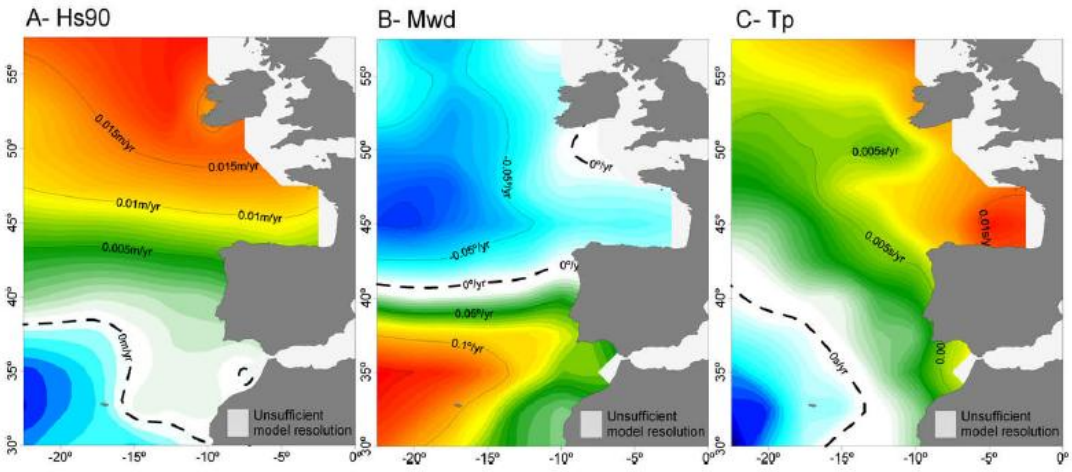

Figure 2.5: Maps from the Analysis of Dodet *et al.* (2010)

wave evolution, throughout decades affects the local resource.

The necessity though of calibrated numerical models is not limited to the science of climate change, many studies involved with extreme events, annual estimations, statistical forecasts and assessment of other models are also reporting their use as a vital component. Two of the most common problems that numerical modelling aids in, are the return period estimation for offshore structures, and wind quality. Starting with the latter, as in case of waves, numerical models for wind dataset generation exist. Although due to the scarcity of offshore mast stations it is very difficult to estimate the accuracy. Combination of wind numerical data, buoys and wind driven wave models allow for the cross-evaluation of two seemingly different physical models (wind and wave).

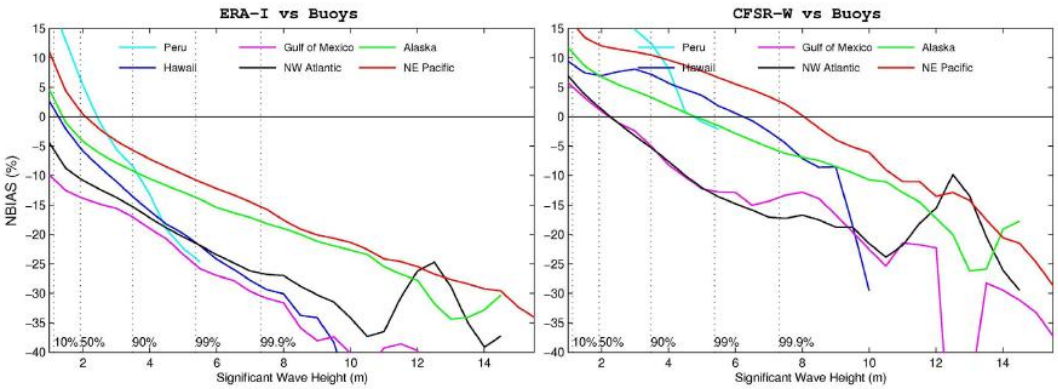

Figure 2.6: Differences between set by Stopa and Cheung (2014)

As in the case of wave models, wind models often exhibit structural code similarities but significant differences in their results. It is important to test the validity of their results, since it has been reported that dataset performance varies in different areas of the world. With results

accuracy being affected by the code set-up and region of primary application. However, exactly the same wind dataset may prove unreliable or with lesser performance for other regions (Caires *et al.*, 2004). This being the case it is important to benchmark both wind and wave models together, since their use is often operational and not limited to hindcasts (Stopa *et al.*, 2013). The recent study of Stopa and Cheung (2014), showed that while the wind re-analyses datasets have improved over the years, their performance and accuracy directly affects the wave models which utilize them. With certain datasets under-performing in specific regions with consistent biases. Previous studies in Southern Europe re-affirmed the same behaviour with different wind products used by a large scale wave model (Bolaños-Sanchez *et al.*, 2007).

Finally, one common application of numerical models, as mentioned previously is the examination of extreme events and return periods. Often, recorded data do not allow the examination of such events due to the limitation in measured recordings. Numerous studies (Tucker, M, 1991; Mathiesen *et al.*, 1994; Goda, 2000; Caires and Sterl, 2005; Holthuijsen, 2007; Young *et al.*, 2012; Agarwal *et al.*, 2013) and recent protocols (Venugopal *et al.*, 2005; van Os *et al.*, 2011; Ingram *et al.*, 2011a; Aarnes *et al.*, 2012; Smith *et al.*, 2013; Smith and Maisondieu, 2014; Larsén *et al.*, 2014) suggest the use of long-term data for valid and robust estimations.

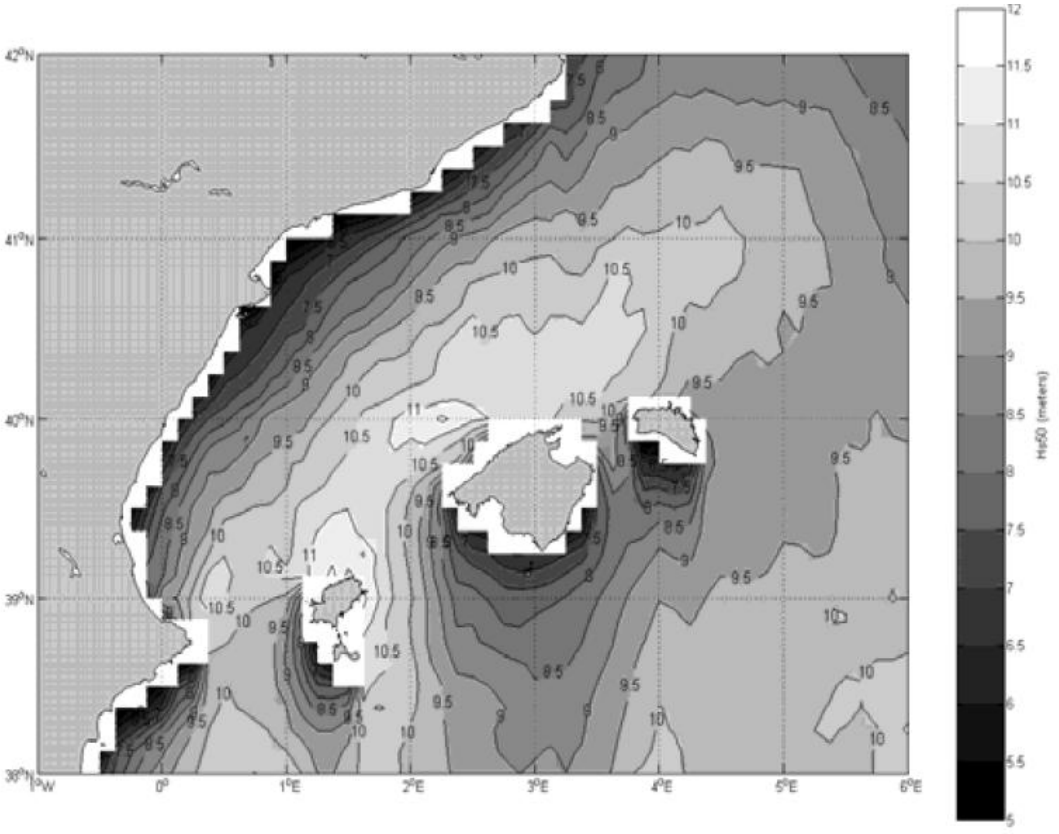

Figure 2.7: Deficiency of large scale model to express useful results for coastal locations Cañellas *et al.* (2007)

In addition, the substantial limitations of ocean scale numerical models is that they are less accurate in resolving the wave propagation in coastal locations, which is a concern that has to be addressed (Caires and Sterl, 2005; Sterl and Caires, 2005; Caires *et al.*, 2008; Cañellas *et al.*, 2007). Cañellas *et al.* (2007) stated that the use of a coastal numerical model is of immediate interest to be used for the evaluation of the wave environment (see Figure 2.7), while Caires *et al.* (2008) examined a limited area in the Petten region (Netherlands) and discussed the available option of numerical models for the production of long-term datasets.

2.2.2 Wave Power Resource Assessment

Expanding on the use of numerical models, their capabilities have influenced the ability to investigate the wave energy potential significantly. Their evolution allowed for a detailed representation of the resource of regions, paving the way for considerations on offshore engineering projects and currently wave energy.

While important wave analysis, in the early years where subjected to namely 2^{nd} generation models (Cruz, 2008; Janssen, 2008). They though hindered by the inability to represent swell and wind sea interaction in an appropriate way, especially at coastal locations. This was due to the fact that second generation models used a parametric approximation for the interaction and contribution of a wave component in the presence of wind seas and swells (Komen *et al.*, 1994; Cavaleri *et al.*, 2007; Janssen, 2008).

While they aided into evolution of the wave modelling sector, they were quickly left behind, as their drawbacks were significant. We shall return to this point in Section 2.3, because it underlines the necessity for a significant part of the research presented within the thesis.

So far resource estimations and long-term hindcasting, have been focused on wave heights, which may indicate energetic environments although it is not adequate for wave energy resource characterisation. Wave energy is comprised by both the wave height, direction and frequency, at which the waves are propagated along the coasts. While for climate and statistical analysis, wave data over hindcast intervals are allowed to have long timesteps between measurements. When we are to investigate wave energy, reducing the recorded time yields us better estimations concerning the variability of the energy flux. While this is desirable, often times modelled output do not specifically examine the coastal resource but rather use coarser models and then assume that the propagated energy flux will not be deviate as much.

Apart from previous studies quantifying the wave resource, dedicated wave energy studies have limited examination and are either global or coarse models based, and limited in time duration and spatial coverage. Fully long-term characterized regions in wave energy terms are limited to some studies. In Cruz (2008) Barstow discusses the evolution of wave energy characterization since the 1990's, while offering some initial limited efforts that were attempted to be developed as the WorldWaves project. The need for at least 10 years of data is underlined in order to allow

for seasonal, year -to-year and annual variability to be included in the assessment. Since year 2000 some efforts have been made in the global characterization for wave energy (Gunn and Stock-Williams, 2012).

Figure 2.8: Early Wave Power estimates by Mollison in 1986, reprint by Cruz (2008)

Amongst the most known is the work performed by Cornett (2008), where a 3^{rd} generation numerical model was utilized for a 10 year period (1997-2006) to provide global wave energy characterization. Up to that point resource assessments were often limited to examination of individual points or buoy locations, thus re-affirming the fact that though climate studies obtain long-term data, energy characterization was absent (Cornett, 2008). The model set-up was based on a wind generated scheme with bathymetry resolution of $1.25^{o}x1^{o}$. Within the study, concerns were expressed about the difficulty of obtaining coastal estimates due to complexity entailed. The work gave significant insights, with reported mean wave energy resource to be highest for South Africa, Chile, New Zealand, Australia, Greenland, Iceland, Ireland, United Kingdom, West Canadian and US coasts. The maximum wave energy reported was approximately 125 kW/m (Southern Hemisphere), while in the North the mean average was around 75 kW/m.

Reguero *et al.* (2012) offered an ocean model with 60 years of calibrated data database, that were then expanded upon wave energy quantifiable that have been used in many energy related studies (Andrés *et al.*, 2014; de Andres *et al.*, 2015). Another important study was produced by Gunn and Stock-Williams (2012), where the outputs from the same global wave numerical model was used to quantify the energy. It also it offered a first time insight to the extractable energy by the coupling of a wave energy converter. The reported global source was 2.1 TW while significant areas are colour-coded, though the set-up of the model provided output quantities

every 3-hours for a 6 year period and utilised a coarse mesh of $0.5^o x 0.5^o$ bathymetry.

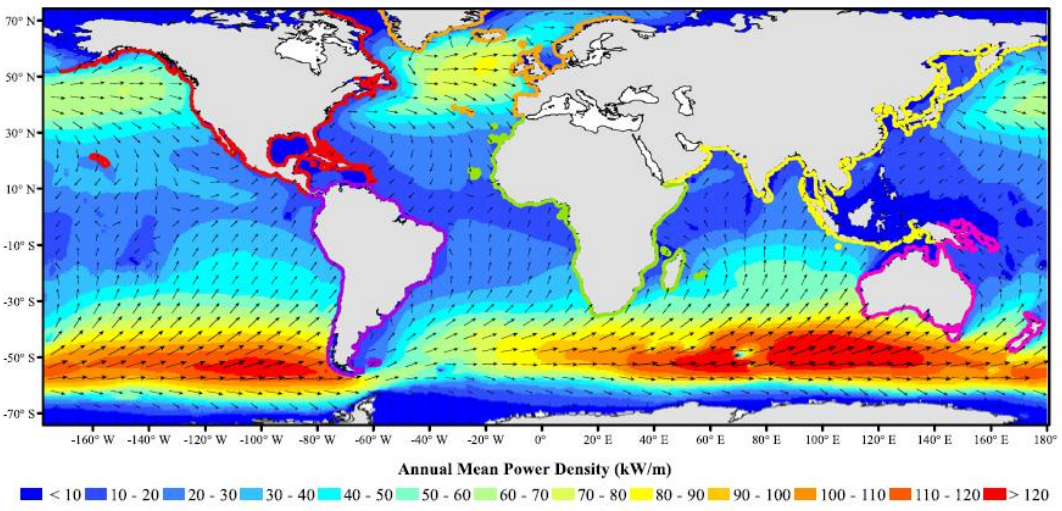

Figure 2.9: Annual mean wave power Gunn and Stock-Williams (2012)

More recently Reguero *et al.* (2015) updated the model Reguero *et al.* (2012), which used a $1.25^o x 1^o$ spatial resolution. This model was presented by the same author, with interest being in wave energy resource assessment. Reguero *et al.* (2015), presented the wave power resources of four locations, this study is the longest dedicated wave power study both spatially and temporally, though using a much coarser resolution. Other studies found in Reguero *et al.* (2015) have been presented here and are limited in time duration for 10 years.

It is obvious that the amount of global studies is limited, with main obstacle being calibration, run-time, and storage requirements. Although, this does not mean that regions have a wider variety of wave energy characterization studies. Focusing in the European region, where wave climate studies are extensive, proper quantification of wave energy is lacking.

More specifically, in the United Kingdom, for Scotland and North Sea the data and knowledge are limited. Though as presented in Section 2.2.1, studies on the climate investigation exist, however they are focused solely on the effects on wave heights and extreme events. Most studies in wave energy have small time duration, coastal representation, and while the numerical modelling techniques appropriate for nearshore locations they are limited in spatial size.

Amongst the most recent long-term ones, is the MERiFIC resource assessment characterization for Cornwall (South West UK) by Smith and Maisondieu (2014), where the wave energy resource was produced for 23 years and was validated extensively. The study used a very fine resolution of 100m x 100m at wave energy locations of interest, which allowed them to fully resolve the coastal and nearshore wave energy content much better that larger models. Note that this study was conducted for the South-West part of England.

A 7-year study was performed by Neill and Hashemi (2013), for the wider United Kingdom,

using a nested scheme approach. The model used was a coastal model, similar to the previous study, with nested meshes at specific limited locations and mostly investigating deep water areas. The model used two set of bathymetry information, for the larger 7 year run the spatial resolution was set at $0.16^o x 0.16^o$, while the limited area nest meshes utilized a $0.04^o x 0.04^o$. The findings didn't only offer a proper characterization of the region, with even the outer meshes (coarser) having better resolution than global models but also investigated the fluctuations of wave energy. This led to the outcome that during winter months had lower performance and higher scattering of values between hindcast and measured locations. This was due to limitations of the numerical model and wind component used (3-hour) provided by the UK MET office, to respond to extreme events as quickly. This wave energy assessment gave meaningful insights and questioned, in good basis the current maps used.

Smaller case studies have also been conducted by Venugopal and Nemalidinne (2015), using a high resolution model with unstructured grid to characterize the North Atlantic and United Kingdom. In this study wave resource calculation was made to Scottish regions where license for the deployment of wave farms was consented. They used a very fine resolution approach to the Isle of Lewis and Orkney regions. The model was validated and came in good agreement with buoy measurements, thus allowing for the coastal characterization of energy, though it was limited to only the year 2010. However their estimation wave power resource agreed with already published information by the Crown Estate.

In addition, two other studies considered modelling the resources for Scottish region and rest of the UK which were based on second generation out-dated models. The first project POLCOMS was commissioned by the Irish authorities (British Oceanographic Data Centre) offered wave height, and current estimations around the West Scottish and Irish coastlines. While the second was produced by ABP MER in 2007 offered wave resource and power characterization along the United Kingdom coastlines, and has been widely adopted and used in the consideration of wave energy deployments (Berr, 2008). Both were hindcasts based on a 2^{nd} generation model, more specifically the wave power resource map model used a frequency distribution of thirteen (13) frequencies and sixteen (16) directional bins separation. Bathymetry resolution utilized a nested approach with the inner mesh having spatial detail of 0.25^o. In addition, the wave power map was limited to 7 years, and low coastal resolution hinders the extrapolation of extreme events or investigation and inclusion of decade trends into the final resource. Some questions and concerns have been raised by Neill and Hashemi (2013), with the above estimation. As its resolution and outdated physical processes posing a significant barrier for the use in coastal areas and also it gave significant over-estimations of power.

Similar approach was taken by Gleizon (2014), with the use of unstructured meshes to resolve the Isle of Lewis wave resource. The model used was able to exhibit an improved representation of the coastal resource, though this was not only limited in duration but area of investigation. The results showed that the application of a wave model in the Scottish coastlines, is a chal-

lenging task with major concerns expressed concerning the assessment by larger models, since they cannot resolve the nearshore interactions. The study duration was limited in 6 months from January to August 2011. A smaller more focused investigation was also performed for limited coastline at the North of Island of Lewis, though the limited data and spatial coverage did not allow for proper representation (Greenwood *et al.*, 2013).

The wave power characterization for Southern Europe has also been not well described in the literature except a few. In contrast to the North Atlantic and upper European countries, the resource available in the area is three times smaller, thus not until the past few years, the interest begun to develop for wave energy. Wave and wind analysis have been carried out over the years for these regions by Soukissian *et al.* (2002); Medatlas Group (2004); Cavaleri and Bertotti (2006); Soukissian *et al.* (2008); Ratsimandresey *et al.* (2008); Bertotti and Cavaleri (2009); Soukissian *et al.* (2012); Mazarakis *et al.* (2012); Karathanasi *et al.* (2015) to name a few. With the exception of Ratsimandresey *et al.* (2008) which looked at hindcasting for 44-year, the other studies were limited up to a decade of data production with resolutions ranging from $0.5^o - 1^o$.

It is easily understood that the area is not extensively studied as the wider North Atlantic and while some resource assessment exist, they are also focused on specific regions. Most studies have concentrated at Italian coastlines, with a third generation oceanic model for 10 years (Liberti *et al.*, 2013), while for the same coastlines a 3 year limited study was conducted using an unstructured mesh numerical model but limited to the Northern Italian region.

For the Western Basin of the Mediterranean, the HIPOCAS project, (Ratsimandresey *et al.*, 2008), constitutes the fullest wave database of information, while most recent studies have attempted wave energy characterization with isolated points of interest from an oceanic larger scale model, which as shown in Figure 2.7 has limitations at coastal zones.

For the Western part of the Mediterranean, attempts have been increasing to divert from just wave and wind assessments to wave resource characterization. Ayat (2013) provided 15 year assessment of the Turkish coastlines via a coastal model, and Zodiatis *et al.* (2014) utilised an oceanic model to assess the wave energy resource variability of the South Eastern basin, Cyprus and Levantine Basin for 10 years.

Finally, summing up wave power assessment for the European region, the Black Sea has recently been investigated initially for its wave and wind resource variability, (Cherneva *et al.*, 2008; Rusu and Ivan, 2010). While the most recent 15 year hindcast for wave power assessment of the area can be found in Akpinar and Kömürcü (2012, 2013).

It is obvious that the level of information concerning wave energy resource assessment is lacking in most parts of Europe, and most importantly for coastal locations where WECs are applicable. The author believes that some of these issues are addressed within this thesis.

2.3 Numerical Wave Models

Investigation of wave evolution and physical interactions led to the creation of numerical models. From the first generation models to the current third generation (Komen *et al.*, 1994; Janssen, 2008), significant advancements have been made in our understanding and knowledge of the mechanics. With advancements in computational capacity, the ability of wave numerical models to offer wave hindcasts and forecasts has greatly improved. Currently investigation and examination of the wave resource, wind wave interactions and forecast of extreme events is predominately performed with the use of spectral models by various institutions and organization around the world coupled with atmospheric models (Janssen, 2008; Athens, 2014).

This thesis uses the SWAN (Simulating Waves Nearshore) wave model. In this section an overview of the available third generation wave models is presented and SWAN wave model is introduced, with explanation about the activation of necessary processes and data required for wave numerical modelling applications. Furthermore, an overview of the available input data and principals for the construction and proper use of a third generation numerical model is presented. A brief overview is given to existing wave models, and the reasons for the selection of SWAN as an appropriate model for this study are elaborated upon.

Wave models can be separated into two distinct categories, oceanic and coastal, depending on the scale. Although most wave models can be applied for both large and small domains, their computational demands and accuracy determine their preferred usage (Janssen, 2008). Classified as oceanic models are WAve Model (WAM) (Komen *et al.*, 1994) and WAVEWATCH III (WW3) (Tolman and development Group, 2014), coastal or shelf-sea models are SWAN (Delft, 2014a), MIKE21 (DHI, 2014) and TOMAWAC (Tomawac, 2014). The majority of wave models are open sourced, although several restrictions are in place, and have continuous development in their processes (Venugopal *et al.*, 2010).

Differences of models lay in the way they resolve the action balance density equation, and source terms available. Nature of the model is also a distinguishable part, with varying options such as deterministic, probabilistic, phase resolving or phase averaged approaches. Their ability to reproduce wave conditions and provide spectral information for shallow or deep water locations, depends on the physical approaches used for solution of the energy density of waves. While commonalities exist in sink and source terms, the solution approach and available options differ within the models.

In this chapter the current 3^{rd} generation models available are presented along with some information and background on current state of operation. The physical aspects of wave theory interactions are presented along with their applicability in wave models, so as to inform the reader for potential alterations that can be examined by the model. Finally, the primary selected wave model used in this thesis (SWAN), is introduced more extensively, considering the physical terms governing its operation, and necessary steps in the preparation of input files

and set-up process for successful application of SWAN.

2.3.1 WAve Model (WAM)

With the introduction of wind interaction theory to wave generation (Miles, 1957), attempt was to incorporate the knowledge of wave theory into numerical models for wave analysis was examined. Miles (1957) theory was the basis for the initial development of 1^{st} and 2^{nd} numerical models but were limited in the interactions and terms that they took into account. They mostly were limited to wind-wave generation without any additional complex non-linear terms accounting in the process.

The first simplistic wave numerical code was developed early in the 1970 (first edition), but in 1984 with rapid development in computer capabilities of mathematical solutions led to the introduction of one of the first third generation model, the WAve Model (WAM) (WAMDI, 1988), developed and enhanced by a team of leading authorities in the field. With previous attempts like the SWAMP project, the introduction of several numerical techniques led to the creation of this advanced model. Initially, hindcasts of previous years extreme events e.g. storm or past wave conditions were examined, with promising results about the overall accuracy of the model (WAMDI, 1988). Currently, this innovative numerical model allows the simulation of a two dimensional wave spectrum resolved in spherical coordinates with consideration on the number of frequencies and directions

WAM introduced initially linear simplified solution for resolving the wave (or density) action equation. Continuous developments allowed the model to simulate two dimensional wave spectra in spherical coordinates, with consideration of a large number of frequencies and directions. Currently the model is operated by various organizations and agencies such as ECMWF. The current version accounts for wind generated seas, propagation, quadruplets (deep non-linear interactions), bottom interaction at deep waters and a simplified modelling of non-linear coastal (triad interactions) (Park, 2008).

WAM has been predominately used for global predictions or oceanic (large areas) simulations, which was the initial interest of the model when it was developed. It offers a wide variety of wave parameters as results, such as wave height, mean-zero crossing period, peak direction etc. (Komen *et al.*, 1994). The governing equations of WAM, as mentioned have laid the foundation for the development of the forthcoming models introduced. This provides the positive ability that its outcomes can be coupled with most existing, nearshore of shelf-sea models, in order to provide the necessary boundary and initial wave field information, with no significant alteration required to the files used.

2.3.2 WaveWatch III

Another suitable wave numerical model is WaveWatchIII (WW3) with its first version developed by Hendrick Tolman (Tolman and development Group, 2014) and currently updated and optimized predominately by the NOAA wave group and oceanic research.

The dominant deep water terms are similar to WAM, though alterations in the way of calculating non-linear interactions by an alternative scheme are offered to the user (Tolman, 2013; Tolman and development Group, 2014) wind-wave generation and some shallow mechanics introduced by the developers, differentiating their solution with comparison to the WAM model.

WW3 offers an extensive manual that guides to the installation process and examples provided. Moreover, several initial proposed test case files are provided based on source codes that are implemented in organization and institutions around the world, providing some insights about the important physical parameters that have to be taken into account depending on the area of implementation (Tolman and development Group, 2014).

2.3.3 MIKE 21

MIKE21 is a wave model developed in Denmark by DHI and is a commercially available software, with application on Window's based configurations (DHI, 2014). The solution of the model considers similar source terms to WAM cycle 4 (Komen *et al.*, 1994) and wind input based on the formulation of Janssen's (Janssen, 1988, 1991).

MIKE21 is a fully spectral model, which can be used in stationary and non-stationary mode. The abilities of the model include, deep and coastal non-linear interactions according to Hasselmann *et al.* (1985). In addition, MIKE21 can also accounts for sentiment transport and current-wave interactions.

This software is highly user friendly with pre and post processing graphical user interface. Unstructured mesh is used for computational grids, which, enhances its calculation of shallow water region. Source terms used account for every component of wave resource, although due to the nature of the software less alterations to significant source terms are allowed in contrast to the openly available source terms (DHI, 2014). The model also requires by the user specific information to such as wind, bathymetry and boundary information. The model is only available under a commercial license (not open sourced)

2.3.4 TOMAWAC

TOMAWAC is a wave model for coastal areas, its capabilities include mostly shallow water mechanics and wind generated waves. TOMAWAC uses a finite element method to resolve the energy density equation in a simplified spectro-angular method. Although focused on coastal areas, only major non-linear interactions are accounted, such as dissipation and refraction from bottom friction and currents.

Complex resource assessments are not advised (Tomawac, 2014) although is mostly suitable for calculations of flows and sentiments transports, since its coupling with TELEMAC provides it this advantage. Availability of the code includes pre-compiled Window's version and a UNIX/LINUX source code, freely available (Tomawac, 2014).

2.3.5 Simulating WAves Nearshore (SWAN)

The above numerical models, offer variety of alternatives, however it has to be stressed that WAM and WW3 are predominately designated for deep Seas and oceanic applications, due to their reduced accuracy in coastal areas. On the other hand, MIKE21 is a skilled model that has the ability to estimate coastal, nearshore and deep water conditions. Though its main limitation is the commercial status, which does not make it accessible to everyone. Finally, TOMAWAC as mentioned is developed for investigating nearshore application, though it accounts for wind-wave generation, limited incorporation of quadruplets interactions hinder its ability to be used in larger domains.

SWAN is a coastal and shelf seas numerical model developed and maintained by the Hydraulics Department at Delft University Delft (2014a). As in the case of WAM and WW3, SWAN is also a phase averaged, numerical model that resolves the energy density equation with the help of Eulerian methods and can account for many physical terms that provide a final solution on the energy density of waves. The use of an Eulerian solution was chosen based on the fact that Lagrangian approach failed to resolve the non-linear components of shallow water mechanics (Delft, 2014b).

The model was developed out of the necessity for nearshore models as indicated after development of the WAM model (WAMDI, 1988). The reason was that although the aforementioned oceanic models WAM and WW3 can assess wave conditions, they are based mostly on explicit numerical schemes that allows them to account linear and non-linear terms up to a specific degree with a certain spatial resolution as limitation. SWAN is a state of the art model with a probabilistic phase average approach that allows both deep water and nearshore water non-linear components to be activated, in spatial mesh resolutions in greater detail that in the case of its oceanic counterparts (Lavidas *et al.*, 2014c). The source code is freely available and can be provided by the Delft team to the user (Delft, 2014a) with user required to install the pre-compiled Window's executable or build in the UNIX system source code.

Both options share the same configurations, as far as the physical coding is concerned, with the user being able to alter and tailor the numerical wave algorithm to its own specifications. Limitations though exist in both distributions, the Windows executable allows only a serial implementation to the user which inherently restricts the speed of computations and amount of available resources to be used e.g. restrictions on the use of memory for larger runs.

On the other hand, option of source code UNIX compilation allows to integrate and utilize much more built in options and potentially use a larger number of cores available. SWAN, in its unlinked form can be compiled to use either serial, Open Multi-Processing (OMP), or an Message Passing Interface (MPI) approach, utilizing more memory and cores to enhance the speed of simulations. In the case of OMP, restriction of cores to be used is up to 8, while in MPI user has to pre-define the numbers of cores to be used, in both cases the flexibility of memory levels to be used per core relies on the user (Delft, 2014a,b).

SWAN is primarily based on the third cycle of WAM formulations for the numerical model solution, hereby known as WAM3, although the user is exposed to many different formulations and options that can be selected. All of the numerical aspects included in wave theory can be altered in accordance to the specifications and experience of the user. This proves particularly useful, in comparison to other software whose ability to change not only the physical scheme but also the numerical and iterative solver is somewhat limited.

2.4 SWAN Considerations and Validation studies

As mentioned in Section 2.3.5, the model allows for nearshore coastal resolution better than its oceanic counterparts. It has been widely used in wave resource examination and is continuously updated and validated. Some of its operational applications have been discussed in Section 2.2.2. Development of the source code and its physical adaptations means that specific terms have to take into account by the wave modeller, if a custom model is to be constructed for an area. In this final section the experimental validation and physical consideration for the SWAN model are presented, in order to assist future considerations when the model is build.

Currently the model is at its 41.01A version, while the studies within the thesis have utilized both versions 40.91ABC and 41.01A, the versions numbers represent added features and additional options that are offered. Starting with Delft (2014b) and Delft University of Technology (2014) many test cases can be found, exhibiting the model performance from validated runs. While in a physical description of the model is presented in an informative way from Booij *et al.* (1999). Considerations on the initial model release and a second part study with verification of the model is presented in Ris *et al.* (1999).

Since then continuous development and constant investigation, predominately of the physical model set-up have been studied. The author feels, such literature study is important for every

wave modeller that is to be involved with SWAN, since they reveal irregular performances and unexpected results that may occur in use of the model. In addition, they allow better understanding between the interactions of wave theory with the spectral model.

From early test case hindcast studies, some behaviours were expressed which could be improved by code customization (Jin and Ji, 2001; Lin *et al.*, 2002), the model was tested under use of fine bathymetry in limited coastal areas, one lake site and a small bay. The output in both cases revealed that the initial models provided a good generation trend, but showed a constant over-estimation of T_{peak} and under-estimation of H_{sig}. Though these initial hindcast results were under-performing, the identification of wave trend generation captured was encouraging.

As the model improved, more source terms and physical processes were added, with further investigation of results. In Rogers *et al.* (2002b) the propagation schemes of SWAN were thoroughly tested in non-stationary runs. The domains were coastal applications with complex coastlines and rapidly changing bathymetries, in order reveal the different propagation schemes accuracy. Currently SWAN can utilize three schemes as selected by the user, and found in Delft (2014b). The schemes are constantly updated and reflect current developments. It was shown that depending on the scale of hindcast, model's size, non-stationary or stationary investigation, mesh resolution and time integration the wave modeller should account and consider different propagating schemes.

The schemes used were the backward space, backward time (BSBT), the second order upwind scheme (SORDUP) and the Stelling and Leenderste (S&L). The propagations schemes were tested for time integration, memory requirement, Courant-Friedrich-Levy (CFL) violation, Garden-Sprinkler effect, and diffusion accuracy of the wave field. Outcomes classified the three schemes according to application, accuracy and associated problems. Following the propagation schemes evaluation the same author Rogers *et al.* (2002a), compared the diffusion from a hindcast wave field with a stable propagation scheme, identifying the significant effects that the diffusion term calibration, has on wind generated seas and whitecaps.

As SWAN was evolving, apart from the propagation schemes more sweeping algorithms and iteration methods were inserted, the high convergence with different options was shown in Zijlema and van der Westhuysen (2005). The so-called sweeping algorithm is one of the main components that affects the hindcast output, as it basically re-calculates and propagates the energy density solutions over the mesh grid points. The scheme in combination with the non-linear interactions tuning, can severely affect the spectral and wave parameters calculated, as shown in Section 4.6.

While consideration on the different propagation and non-linear terms are also included in Young and van Vledder (1993); van Vledder (2000, 2006); Vledder (2012); Rogers and Van Vledder (2013), the comparison of non-linear interactions over new schemes given within those studies, show a detailed comparison and evolution of alternative, between the dominant scheme

which was developed in first 3^{rd} generation models (Hasselmann *et al.*, 1985).

Bottema and van Vledder (2008) tested different configurations over a limited fetch areas with significant deviations. In a personal communication with Professor Van Vledder, it was expressed that the nature of these terms is highly volatile and to a certain extent unknown to us, while certain coefficients seem to work, it has been reported that this is not always the case (van Vledder, 2015).

Interactions of wind generated waves and the non-linearities are also constantly updated in search of coefficients and their tuning, this is also the case of wind interactions and subsequently whitecapping coefficients. Depending on the scheme of wind solution and propagation used the whitecaps should be also re-adjusted. These considerations must account for expected local environments and orography (van der Westhuysen *et al.*, 2007; Siadatmousavi *et al.*, 2011), with whitecapping effects and non-linear triad interactions to be dependent on the location of the hindcast.

The increase and use of higher mesh resolutions also had an effect on the model tuning, with unstructured meshes offering higher spatial representations. This came at the cost of destabilizing the hindcast, leading to spurious hotspots with the propagation criterion often violated, though if correctly used the expected accuracy is increased, (Zijlema, 2010; Dietrich *et al.*, 2012).

This also prompted the retuning of wave model components concerning bottom friction depending on the location, type of orography and terms activated (van Vledder *et al.*, 2010). Wind growth and drag evolution components following the previous study results, expanded the potential options for tunable wind wave interactions (Zijlema *et al.*, 2012). Recently a new parametrization on triad nearshore interactions was proposed, for bathymetry characteristics that increase depth induced breaking and triads Salmon *et al.* (2014).

While SWAN is completely tunable, a good understanding of the effects on source activation, interactions and modelling schemes is essential, to obtain confidence and computational efficiency. Many components have to be considered and tested prior to an extensive hindcast, especially one spanning over few months. The model volatile conditions and wind wave interactions may be poorly resolved at coastal locations, leading to erroneous estimations and hence model parameters must be carefully selected and activated. Asides the technical and scientific manual, the author found extremely helpful the aforementioned studies during the model set-up, while an additional good discussion on wave modelling is also given in Rogers *et al.* (2007); Cavaleri *et al.* (2007); Janssen (2008).

From the above literature it is clear that a spatially finer scale model and temporally longer in duration is needed to provide coastal wave power resource map for Scotland and Southern Europe. This research will produce a detailed map of wave power for Scottish waters and Northern Europe, while it will also attempt to build a basis model for Southern Europe. The

first map will contribute quantification and consideration of wave power in areas of immediate interest in the highly energetic Scottish regions, while the second will develop the basis and consideration for a milder environment, with different characteristics.

It is clear that SWAN is capable of modelling wave resources for nearshore water regions. Its structure offers significant freedom and adaptability of source terms necessary to offer custom solutions and hence used for the research.

2.5 Summary

- The current status concerning energy production and RE is presented.
- Discussion on the barriers and opportunities of renewable energy.
- Introduction of the benefits and reasons that wave energy is hindered.
- Long-term benefits and approaches that are expected to increase RE penetration.
- The reasons that are in need of clarification for wave energy and its potential place amongst future energy considerations and scenarios.
- Relevant studies and historical with up-to-date assessment are provided, as found in literature.
- Problems associated with lack of information concerning wave power assessments are presented.
- It is obvious that in most parts of Europe, there is a significant lack of wave power and coastal information.
- The small number of previous studies is presented and their contributions are underlined.
- The presentation of available numerical wave models and their characteristics.
- Literature review over various studies and validations of the model selected are given.
- Considerations on the evolution of the model's terms, through out its iterations over the years.
- Many studies are cited which may aid in future considerations of a customizable model.

Chapter 3

Implementation of the Wave Model

"Well begun is half done."

Aristotle, 384-322 B.C.

General

This chapter elaborates on how the developed wave theory is introduced in SWAN. The important physical processes that have to be activated for a robust numerical solution are presented, alongside with information on the construction and necessary input for every component.

3.1 Source Terms and Wave Theory

Wave theory and its translation into a working numerical model is presented in terms of the action density balance equation, with an overview of the physics and their importance in the resource analysis. This section provides an insight into state of the art in numerical wave modelling and also acts as reference for the forthcoming chapters. Further, specific parametrisations and improvements are also proposed for the application of SWAN in order to obtain wave resource characterisations of areas chosen. The source term used in SWAN is expressed by

$$S_{tot} = S_{in} + S_{nl3} + S_{nl4} + S_{ds,w} + S_{ds,b} + S_{ds,br} \tag{3.1}$$

where S_{tot} representing the total sum of energy source terms, S_{in} wind input,S_{nl3} triad interaction mostly dominant in shallow water,S_{nl4} quadruplets responsible for wave-wave interactions and energy redistribution amongst wave, $S_{ds,w}$ whitecapping responsible for energy dissipation, $S_{ds,b}$ dissipation bottom friction and $S_{ds,br}$ energy loss by wave breaking (Booij *et al.*, 1999; Delft, 2014b). The terms will be elaborated upon, along with indicative values in the following sections.

Summation of the above terms allows for representation of the wave spectrum in the action balance Equation 3.2, which is responsible for the local generation and propagation of wave groups (C_g) upon relative frequency (σ), direction (θ) in longitude (λ), latitude (ϕ) and in the time domain (t) (Booij *et al.*, 1999). The overall energy density (N) from the action balance is dependent on relative frequency.

$$\frac{\partial N(\sigma;\lambda;\theta;t)}{\partial t} + \frac{\partial C_{g,\lambda} N(\sigma;\lambda;\theta;t)}{\partial \lambda} + \cos\phi^{-1} \cdot \frac{\partial C_{f,\phi} N(\sigma;\lambda;\theta;t)}{\partial \phi} + \frac{\partial C_{f,\theta} N(\sigma;\lambda;\theta;t)}{\partial \theta} + \frac{\partial C_{f,\sigma} N(\sigma;\lambda;\theta;t)}{\partial \sigma} = \frac{S_{tot}(\sigma;\theta;\lambda;\varphi;t)}{\sigma} \tag{3.2}$$

Equation 3.2 represents an Eulerian solution for the spectral density energy balance which is suitable for both deep water and shallow water approaches. The difference is that the deep water approach accounts primarily for wind input, non-linear interactions (deep water interactions) and whitecapping. Whereas the shallow mechanics include a vast array of source terms that affect the wave propagation by triad interactions, bottom friction and even vegetation.

Although recent developments try to incorporate some shallow water mechanics in oceanic models non-linear water terms are not resolved as accurately, depending greatly on the increase of computational requirements and propagation factors (WAMDI, 1988; Cavaleri and Holthuijsen, 1998; Holthuijsen, 2007; Janssen, 2008).

3.1.1 Wind Interactions and Wave Generation

Wave theory has clearly identified that wind was the dominant source term responsible for wave generation, starting with Airy's theory which gave waves a linearised approach, to the seminal work of Miles (1957) on generation of surface waves due to shear flow, and improvements on that quasilinear approach by Janssen (1991). Understanding the complexity of wind on the wave environment has evolved and allowed the development of numerical wave models, leading to hindcast studies (numerical simulation of sea states in the past), and the creation of wave atlases that are used for various purposes, e.g. industrial, marine, naval, climate change (Komen *et al.*, 1994; Cavaleri *et al.*, 2007; Holthuijsen, 2007; Janssen, 2009).

In the work of Miles (1957), wind and sea water were considered inviscid and incompressible, while the latter was also attributed as an irrotational fluid due to the boundary interactions of wind and waves. The development of this assumption allows for the growth of waves with wind interactions at sea level as seen in Figure 3.1.

The major defect of the proposed shear flow wind-wave generation, was the complete absence of turbulent effects of wind, leading to inconsistencies based on potential rapid alterations of the wind profile over the seas. Though for a given, usually, low to moderate wind profile, the

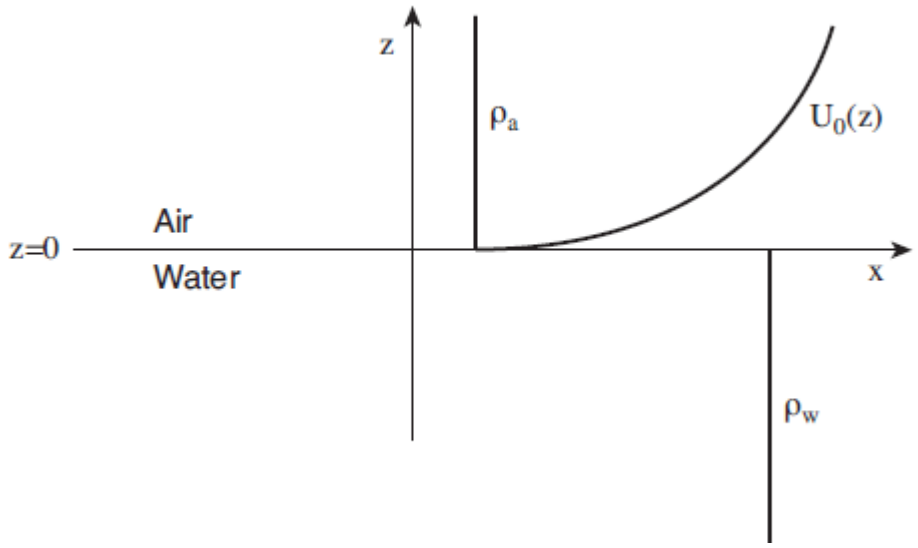

Figure 3.1: Wind and Wave interaction based on an incompressible and inviscid fluid, (Janssen, 2009)

quasilinear approach is sufficient, sudden alterations that occur in the oceans have an effect on the waves generated.

Moreover the interactions of wind and waves are not isolated only by wind acting on waves, but also by momentum being transferred from waves as well. This suggested a limitation on the linear wind-wave theory generation approach. This result disregarded the assumptions for inviscid fluids and introduced the issue of momentum and energy exchanges of wind and wave on the boundary layer of the sea. Leading to the important question for the state of interactions when oceans waves have developed fully, travelling faster or even against the wind direction (Janssen, 1988, 1991, 2009).

In operational numerical wave models several formulations have been adopted, initially the now known as WAM3 formulation, was used. This approach resolves the wind wave generation by solving the energy density (see Equation 3.2), calculating the source terms accounting for deep water interactions (see also Equation 3.1). It considers a linear growth by wind based on a wind friction (wind drag) generation approach. The wind friction coefficient (C_D) implemented, is used to resolve the problem of wind generation, as was calculated initially by Wu (1982) and introduced in the SWAN model. Depending on the wind speed the coefficient C_D (see Equation 3.3), attains different values iteratively according to the wind input range (Komen *et al.*, 1984, 1994).

$$C_D = u_*^2 / U_{10}^2 \tag{3.3}$$

$$C_D = \begin{cases} 1.2875 \times 10^{-3} & U_{10} < 7.5m/s \\ (\beta + 0.065 \times U_{10}) * 10^{-3} & U_{10} > 7.5m/s \end{cases} \tag{3.4}$$

This original WAM3 formulation is used with scaled wind at 10 m, instead of the 5 m that was originally proposed, for lack of wind stress at lower altitudes. This allowed for the formulation of source wind input term to be solved, with $N(\sigma,\theta)$ (often seen as $N(f,\theta)$) representing the energy density in the spectral domain for frequency and direction in Spherical coordinates. With β representing a coefficient of wind generation, which considers the different values of friction velocity (u_*) along the interaction process and $\gamma_\beta = 0.25$ representing the interaction process coefficient (Komen *et al.*, 1984).

$$S_{in} = \beta N(f,\theta) \tag{3.5}$$

$$\beta = max\Big\{0, \gamma_\beta \frac{p_{air}}{p_{water}}(28\frac{u_*}{c_p}cos\theta - 1)\Big\}2\pi f \tag{3.6}$$

In the case of WAM3, the solution of the wind generation coefficient (β) takes a value from 0.8-0.85 (see Equation 3.6), and then substituted in Equations 3.4-3.5. The WAM3 formulation is the favoured solution for most wave models although the use of β within a range of constant values reduces the solution of γ_β values. For this reason a modification with an implicit approach was proposed by Janssen (Janssen, 1988, 1991) which calculates γ_β values allowing a representation of the momentum transfer from the atmospheric boundary in regards to the length roughness of the sea below the wind height. This approach allows for a continuous re-calculation of the γ_β coefficient by accounting for the critical height (μ).

$$\gamma_\beta = \frac{1.2}{k^2}\mu ln^4\mu \tag{3.7}$$

$$\mu = \begin{cases} \frac{gz_e}{c_p^2} exp\left[\frac{kc_p}{|u_* cos(\theta - \theta_{wind})|}\right] & \mu \leq 1 \\ \beta = 0 & \mu \geq 1 \end{cases} \tag{3.8}$$

With friction velocities (u_*), calculated from the Von Karman coefficient, surface length and effective roughness with an iterative way (Janssen, 1988) allowing the U_{10} to be calculated and determined within a range of a spectrum given the initial condition.

$$U_{10} = \frac{u_*}{k} ln\left(\frac{10 + z_e + z_0}{z_e}\right) \tag{3.9}$$

$$z_0 = 0.01\frac{u_*^2}{g} \tag{3.10}$$

$$z_e = \frac{z_0}{\sqrt{\frac{1-\tau_{wave}}{\tau}}} \tag{3.11}$$

where τ_{wave} is the water wave roughness (turbulence), given by the direction and frequency dependant β and density, as calculated by Janssen (1988).

$$\tau_{wave} = p_{water}\int_0^{2\pi}\int_0^{\infty}\sigma\beta N(f,\theta)dfd\theta \tag{3.12}$$

Both formulations account for almost the same physical interactions, while the quasilinear approach proposed by Miles (1957) seems to neglect effects of the air turbulence to the high frequency wave, the alterations and iterative method given by Janssen (1988) and Janssen (1991) have to some extent, improved the modelling technique. In operational numerical wave models the wind input source term is always given by a wind drag estimation, which is associated with the approach used.

The reason for considering wind drag as a primary component, based on wind speed at specific height, is that the inability of wind speed to account for wave surface stress. This led to various research and experimental approaches that proved the presence of surface stress is able to reproduce fetch-limited conditions better (Janssen, 1988, 1991; Komen *et al.*, 1994; Cavaleri *et al.*, 2007).

In this study the application of both terms has been applied although the representation of WAM4 formulation lead to better approximations for fetch limited seas (Lavidas *et al.*, 2014c,a). Additionally, to obtain this approach other physical terms have been implemented, and will be also, elaborated upon in the forthcoming sections of this chapter. Finally, to assist initial wave growth of the hindcasts an empirical expression to avoid evolution of waves below a specified spectrum threshold is also implemented. The wind growth term coefficient (A), reduces the "cold" start running time. Effect of the term is shown in Equation 3.5, which changes by the additional activation of the growth term, for all subsequent analysis this was set at 0.0015.

$$S_{in} = A + \beta N(f,\theta) \tag{3.13}$$

Currently, most operating numerical wave models, to the author's knowledge, use wind speed (zonal) and velocity (meridional) profiles scaled at 10 m, which are then formatted in a single or

multiple files in order to be read by the above mentioned equations and calculate the wind drag. Many databases exist, offering these components at various temporal and spatial resolutions, which will be introduced in Section 4.2.

3.1.2 Spectral Components

To understand effects that the wind scaling calculations have, the notion of the wave spectrum has to be presented. For numerical wave models, the spectrum has primary objective to establish a characterisation of the general ocean waves and not instantaneous observations of the sea surface in time (t). That is the main reason why spectral models such as WAM, WW3 and SWAN are classified as phase-averaged (Booij *et al.*, 1999; Holthuijsen, 2007).

This was made possible by integrating the source terms in a frequency-direction domain known as 2D-spectrum. A spectral approach take into account the fetch (F) which expresses the length of a reference point from a shore line at which there is constant wind blowing (Holthuijsen, 2007; Janssen, 2009).

Although many spectral approaches have been proposed, the basis for the wave spectrum solution can be separated into deep water and shallow water. These classifications are expressed in the form of either the Pierson-Moskowitz (PM) and Joint North Sea Wave Project (JONSWAP) spectrum (Hasselmann *et al.*, 1973; WAMDI, 1988; Komen *et al.*, 1994; Alves *et al.*, 2003; Holthuijsen, 2007). The notion of the spectrum is not limited in regards to exploring wind (or local) sea states but is adopted, because it accounts for the summation of the wave environment acting on an area, including wind generated waves, non-linear interactions, swells originating from distant locations and most processes included in the Equation 3.1. Summation of terms and interactions allows to obtain the solution for the energy density equation.

The basic components of the spectrum are the fetch length and wind speed; at short fetches waves are wind driven and grow rapidly while in the case of larger oceanic fetches. Where the fetch can be considered very large or even infinite, the wave evolution due to wind can be considered constant (Hasselmann *et al.*, 1973; Holthuijsen, 2007).

Pioneering research Hasselmann in the JONSWAP project provide us with the information about the state that significant wave heights (H_{sig}) and peak period (T_{peak}) and their evolution (Hasselmann *et al.*, 1973; Komen *et al.*, 1994; Holthuijsen, 2007).

In the previous Section 3.1.1, the methods of establishing wind drag calculations were presented taking into account wind speeds of 10 m. In the original work of Pierson and Moskowitz (Pierson and Moskowitz, 1964) an anemometer at height of 19.5 was used alongside with a construction of interactions in calculating and determining the timeseries of wave, this led to the factorial determination of H_{sig} and T_{peak}. Although the recorded parameters from the experiment were excluded a correlation in regards to the evolution of the quantities was performed

by Pierson and Moskowitz (Pierson and Moskowitz, 1964; Pierson and Stacy, 1973). This led to the formulation of the so-called PM frequency spectrum (see Equation 3.14).

$$F(f) = \alpha_{PM} g^2 (2\pi)^{-4} f^{-5} exp\left[-1.25\left(\frac{f}{f_m}\right)^4\right] \tag{3.14}$$

$$f_m = \frac{v_{19.5}^{PM} g}{U_{19.5}} \tag{3.15}$$

Using several different wind speeds recorded, Pierson and Moskowitz, presented a similarity theory for wave evolution components that expressed H_{sig} in terms of wind speed (see Equation 3.16). The use of different wind speeds allowed for the examination of wave generation and construction of the PM spectrum, which was derived by an analytical solution of spectral densities $N_{\sigma,\theta}$ over the five samples acquired at the scaled winds of 19.5m (see Equation 3.14).

$$H_{sig} = 0.023 U_{19.5}^2 \tag{3.16}$$

This work managed to represent with some degree of accuracy the wave environment, while underestimations were produced in the calculated wave height with both winds used, at $U_{19.5}$ and U_{10} (Komen *et al.*, 1994; Alves *et al.*, 2003) and the fully developed spectral properties of wave in deep water. The outcome of PM formulation was that in an infinite environment of fetch (oceanic waters) the effect of the bathymetry can be negligible since one can consider depth also as infinite, (Holthuijsen, 2007), allowing direct evaluation of the wave components through simple power laws (seeFigure 3.2). The $\tilde{H}_{mo}$, $\tilde{T}_{peak}$ and $\tilde{F}$ represent the dimensionless significant wave height, peak period and fetch respectively.

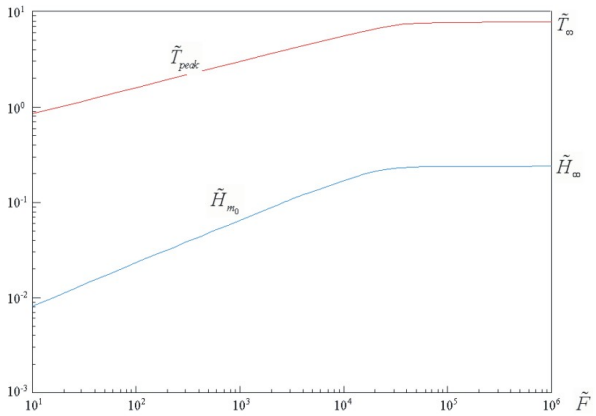

Figure 3.2: Evolution of $\tilde{H}_{mo}$ and $\tilde{T}_{peak}$ as calculated by the power laws derived from the PM spectrum, (Holthuijsen, 2007)

This approach though revealed that under-estimation from those power laws, led to lowering the energy density of locations with finite fetches and non-finite depths. Not all seas are exposed

to similar oceanic conditions, so the necessity for examination in shorter fetches was being considered. In 1973 the JONSWAP team used coastal locations and with the use of several anemometers, exploration ships and wave buoys (see Figure 3.3). They revisited the findings of Pierson-Moskowitz establishing a new parameter factor that exhibits improvement of the spectral properties and thus the estimated energy density of waves (Hasselmann *et al.*, 1973).

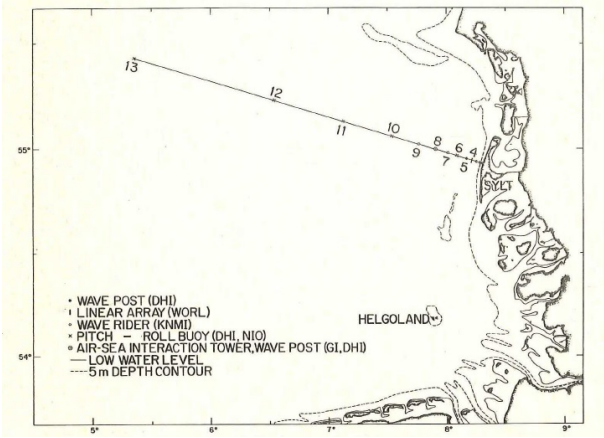

Figure 3.3: JONSWAP experiment location in the coast of Denmark as conducted, (Hasselmann *et al.*, 1973)

Following the exploration of the wind term impact on waves, the conclusion that the u_* performed better than just using an elevated wind speed U_{10} or $U_{19.5}$, although the behaviour of u_* tend to vary according to the interval of winds. The data collected by the JONSWAP project, led to a thorough examination of the local wave resource and wind interactions establishing the fitting of an additional term in the original PM spectrum (see Equation 3.14), known as the "peak enhancement factor" ($\gamma_{JONSWAP}$) (see Equation 3.17) ($f_{peak} = f_m$).

$$\gamma_{JONSWAP} = \left[-\frac{1}{2} \left(\frac{\frac{f}{f_m{}^{-1}}}{\sigma_{peak,param}} \right)^2 \right] \tag{3.17}$$

This factor is used to the non-transition of spectrum values to reach a fully developed state, allowing for the further exploration of other source terms that accounted for removal of energy from the overall density of waves. Nowadays we consider $\gamma_{JONSWAP} = 3.3$ as the mean value for peakedness factor. The final formulation of the JONSWAP has addition of $\gamma_{JONSWAP}$ and the conditional peak-width parameter terms (correction factors), 0.07 and 0.09 for the right and left side of the spectrum respectively, and has to be valid within a specified area of frequencies as seen in Equation 3.18 and Equation 3.19.

$$F_{JONSWAP}f = \alpha_{PM} g^2 (2\pi)^{-4} f^{-5} exp \left[-1.25 \left(\frac{f}{f_m} \right)^4 \right] \gamma_{JONSWAP} \tag{3.18}$$

$$\sigma_{peak,param} = \begin{cases} \sigma_{peak,param} = \sigma_{\alpha} & f \leq f_m \\ \sigma_{peak,param} = \sigma_{\beta} & f > f_m \end{cases} \tag{3.19}$$

The additional enhancement term has allowed the re-scaling of PM spectrum to represent shallower location within fetch-limited condition much better, while the normalization of values decreased under-estimations that original PM had exhibit (see Figure 3.4).

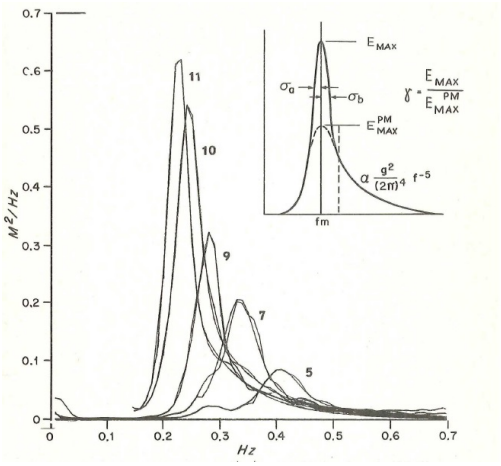

Figure 3.4: JONSWAP spectrum with PM, the evolution is shown in regards to the limited fetch and wind surface stress condition from offshore wind,as taken by (Hasselmann *et al.*, 1973)

Evaluation of the wind components in the spectrum and the overall energy density calculation, although based on experimental approaches, have allowed for the evolution of generation and propagation of waves in numerical models. Due to the nature of hindcasts and resource assessments presented in this thesis the JONSWAP spectrum has been considered as the dominant reason for boundary wave propagation and wave evolution in the model.

3.1.3 Quadruplet Interactions

A ground breaking work was conducted by Hasselmann concerning the interactions of wave-wave components, now known as quadruplet interactions (or non-linear interactions), offering a formulation that can be used to attribute the exchange of frequencies in a spectral domain (Hasselmann, 1961, 1962a,b).

In that study Hasselmann proposed a formulation that explored the transfer of energy from one wave to another when certain resonance conditions are met. This allowed for the exploration of shift in frequencies and subsequent impact on the characteristics of wave height and frequency, leading to a more realistic representation of the wave spectrum components (Hasselmann, 1961; Hasselmann *et al.*, 1973).

These interactions are dominant in deep water conditions, while in shallow water triad (three-wave) interactions come in effect, which constitute an expansion of the quadruplet non-linear (S_{nl4}) and are part of the basic source terms in the total calculations for energy density in waves (see Equation 3.1).

Resonance between two wave components is reached, when two travelling wave groups match in frequency and wave numbers then the components resonate and exchange energies and frequencies (Hasselmann, 1961; Holthuijsen, 2007), see Figure 3.5 and Equation 3.20 -3.21.

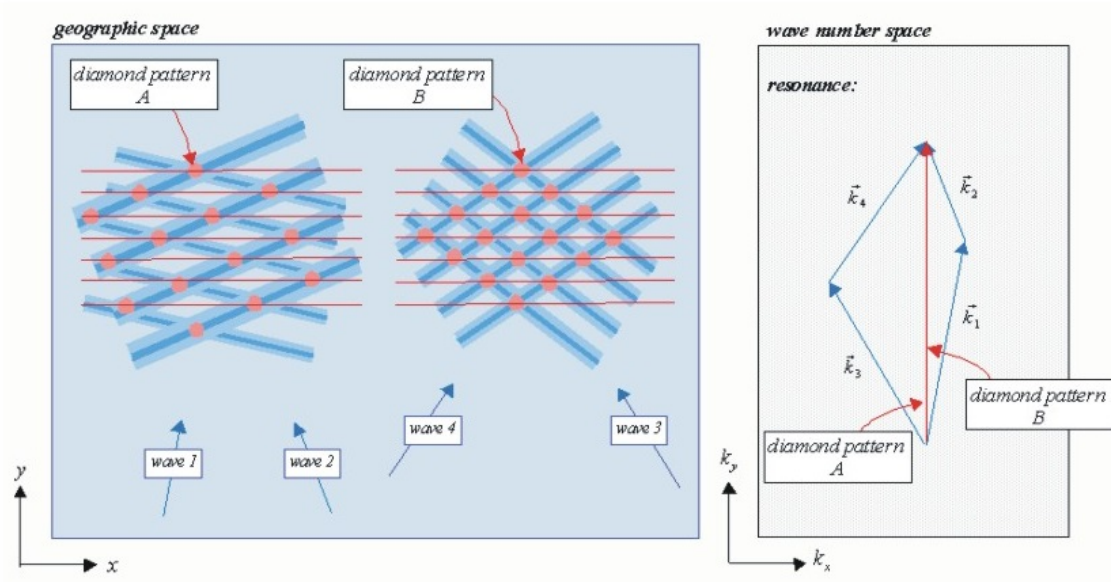

Figure 3.5: Quadruplet interactions between wave components that satisfy the resonance conditions by Holthuijsen (2007)

The non-linear or quadruplet terms S_{nl4} affect the frequency distribution and wave parameters such as T_{peak} and H_{sig} (Janssen, 2009; Holthuijsen, 2007; Cavaleri *et al.*, 2007; Komen *et al.*, 1994). The interactions of wind generated wave resource, incoming swells and local area characteristics are known to affect the frequency and wave form, with quadruplets being responsible for the transfer of energy between frequencies on the spectral peak to both lower and higher, with the dislocation towards higher frequencies being governed by frequency downshifting due to the S_{in} and whitecapping component ($S_{ds,w}$) (Rogers and Van Vledder, 2013).

$$k_{nl,1} + k_{nl,2} = k_{nl,3} + k_{nl,4} \tag{3.20}$$

$$\omega_{nl,1} + \omega_{nl,2} = \omega_{nl,3} + \omega_{nl,4} \tag{3.21}$$

$$\omega^2_{nl,1,2,3,4} = g k_{nl,1,2,3,4} tanh(k_{nl,1,2,3,4} h) \tag{3.22}$$

When resonance occurs, a formulation describing the event can be constructed based on a Boltzman solution with $F_{1,2,3,4} = F(k_{1,2,3,4})$ representing the energy spectrum in accordance

with the wave number and radian frequency. D is a complex interaction coefficient that determines the energy transfer rate from the three interacting components, (see Equation 3.20, Equation 3.22, Equation 3.24) (Hasselmann, 1962a).

$$\frac{\partial F_4}{\partial t} = \iiint_{-\infty}^{+\infty} \frac{9\pi g^2 D_4 \omega_4}{4\rho^2(\omega_1\omega_2\omega_3\omega_4)} \{D_4\omega_4 F_1F_2F_3 + D_3\omega_3 F_1F_2F_3 - D_2\omega_2 F_2F_3F_4 - D_1\omega_1 F_2F_3F_4\} \delta_{nl}(\omega_1+\omega_2-\omega_3-\omega_4)\delta_{nl}(k_1+k_2-k_3-k_4)d^2k_1d^2k_2d^2k_3 \tag{3.23}$$

$$D_1 = D^{++-}_{k_3,k_4,-k_2} \tag{3.24}$$

$$D_2 = D^{++-}_{k_3,k_4,-k_1} \tag{3.25}$$

$$D_3 = D^{++-}_{k_1,k_2,-k_4} \tag{3.26}$$

$$D_4 = D^{++-}_{k_1,k_2,-k_3} \tag{3.27}$$

This complex coefficient D is responsible for establishing the rate of change in the energy between the k wave groups, with the first three considered as active while the fourth is a resultant or non-active component which represents the receiver of these non-linear energy transfers. The δ_{nl} ensures that in order for the non-linear quadruplet interactions to occur the resonance conditions are met (see Equation 3.20) (Hasselmann, 1962a; Young and van Vledder, 1993).

The work on these non-linear interactions was expanded to actual sea environments (Hasselmann *et al.*, 1973), and established the interactions of wind generated seas and quadruplets. These non-linear interactions are responsible for the shift in spectral values initially from high to low wave numbers, while after the development of the peak, from low wave numbers transitioning to higher ones. This process re-distributes the frequency values to higher regions, leading to energy losses (Komen *et al.*, 1994; Cavaleri *et al.*, 2007).

Although these quadruplet interactions, extend their effects beyond wind generated seas, to swell seas as well. The S_{nl4} contribute in the decay of swell components as they interact with local "young" seas. The effect of the wind input is also important, since the combination of S_{in} performance and the re-distribution due to S_{nl4} will lead, depending on specific terms, to the separation of an existing spectrum in "young" and "old", with the latter representing newly formed swell that is de-attached by the process (Young and van Vledder, 1993).

The losses from these non-linear interactions decrease energy of the wave groups, this shows that the decay time of a swell depends on those non-linear terms, and leads to loss in the spectrum and spreading factor of the wave components in regards to the wind direction (Has-

selmann, 1962b; Hasselmann *et al.*, 1973; Hasselmann, 1974; Young and van Vledder, 1993).

The definition of these interactions and their differences in the solution approach play a significant component in the wave resource calibration and assessment. Estimation of frequency shifting, wave height increase through movement of high to low (or vice versa) and the distinction of swells is a further consideration that has to be accounted for.

Based on this knowledge and effect of non-linear quadruplet interactions on the resource, an iterative computational solution was created that has been adopted by all the active 3^{rd} generation models (Hasselmann *et al.*, 1985; WAMDI, 1988). With the increase of computational capacity these complex set of equations concerning the quadruplets process have been adopted and used in two distinct ways, an explicit solution (pre-determined) and an implicit solution.

3.1.4 Whitecapping

Another strongly non-linear process affecting the wave in deep water depths is the whitecapping or wave breaking at infinite (deep) depths. As in the case of the non-linear quadruplet term, Section 3.1.3, this is a not well understood process and has to be carefully set by the user in order to obtain optimal performance and stability by the simulation.

Whitecapping has been identified as the process that reduces, extracts energy from waves in high depths, shifting the final form of the spectrum. The term is associated with the interactions of quadruplets and non-linear DIA solvers, with correct parametrisation, especially in the case of short fetches and variable wind speeds. Tuning of the parameter is not yet well understood by the wave modelling community although suggestions are made about connection to wind speeds and wave interactions (Holthuijsen, 2007; Cavaleri *et al.*, 2007) (see Figure 3.6).

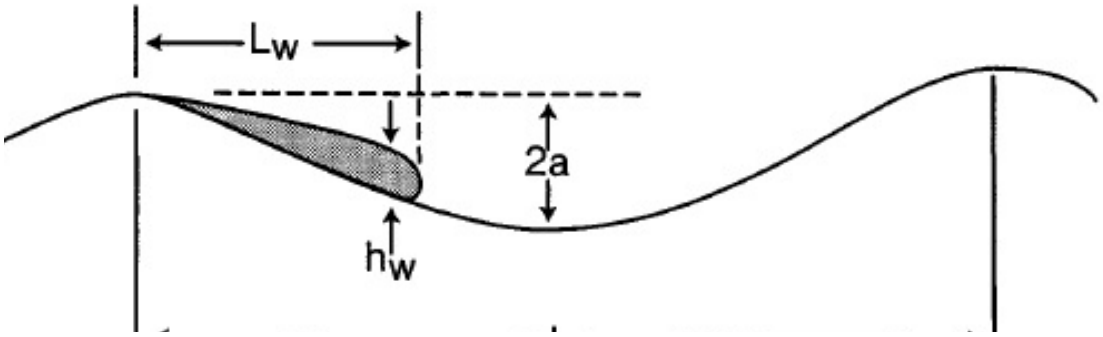

Figure 3.6: The whitecapping effect as it weights down of a sea surface moving up reducing it height by Komen *et al.* (1994)

The pioneering work in the JONSWAP project allowed for the observation and investigation of this phenomenon (Hasselmann *et al.*, 1973). This led to the introduction of whitecapping sink source term ($S_{ds,w}$) optionally activated in third generation wave models. The general term

for the whitecapping calculation was initially given by Hasselmann with the whitecapping coefficient to be completely tunable (see Equation 3.29) (Hasselmann, 1974).

$$S_{ds,w}(f,\theta) = -\mu_{ds,w} k N(\sigma,\theta) \tag{3.28}$$

$$\mu_{ds,w} = C_{ds,w} \left(\frac{\tilde{S}}{\tilde{S}_{PM}} \right)^4 \frac{\tilde{f}}{\tilde{k}} \tag{3.29}$$

The initial adaptation of Equation 3.28 in numerical models, was provided by Komen in the WAM model (Komen *et al.*, 1994). Although, recent developments have contributed to the alteration and tuning of the whitecapping parameter. Since the wind input is crucial to the whitecapping component, calculations are advised to be depended on the selected user scheme for wind generation (Rogers *et al.*, 2002b; Bottema and van Vledder, 2008; Cavaleri, 2009; Dietrich *et al.*, 2011; Pallares *et al.*, 2014).

The process of whitecapping losses are considered as mirror image of the wind induced feedback mechanism that was initially introduced in wind-wave theory. Although, it has been proven that effects of whitecapping over a large numbers of waves is diminished they still affect the final wave component, reducing their magnitude (see Figure 3.7). This is closely related to the wave steepness, local characteristics of the area and averaged over a large number of waves. The summation of losses in energy are small, but effect on the spectral shape and distribution of energy are an important component (Miles, 1957; Hasselmann *et al.*, 1973; Hasselmann, 1974; Holthuijsen, 2007; Dietrich *et al.*, 2011).

The dependence on wind, non-linear interaction and whitecapping have their effect on shifting the spectral shape in the presence of mid-frequencies. The energy losses are negative, while the areas of higher frequencies and the whitecapping effects tend to shift the spectrum towards lower frequencies (see Figure 3.8).

These effects tend to lower or increase the wave height depending on wind speed and the non-linear solver used. The main drawback is our limited knowledge of the whitecapping effect. These effects have to be taken into consideration when a wave resource assessment is performed. The effects of tuning the whitecapping coefficient have been examined by other studies and several configuration have been tried in this thesis, throughout several cases (Rogers *et al.*, 2002b; Ardhuin *et al.*, 2007; Rusu and Guedes Soares, 2009). This led to selecting the whitecapping coefficient that gave the best agreement with recorded and established data.

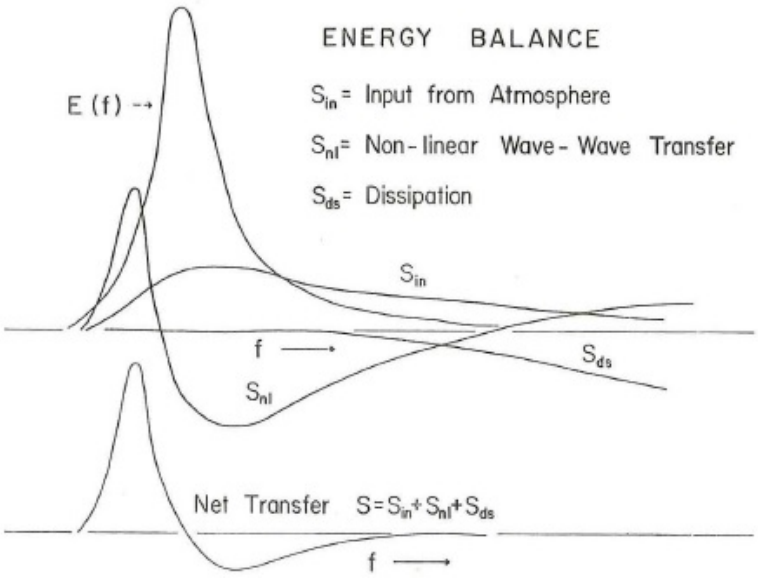

Figure 3.7: Whitecapping effects on the JONSWAP spectrum in shifting the area by Hasselmann *et al.* (1973)

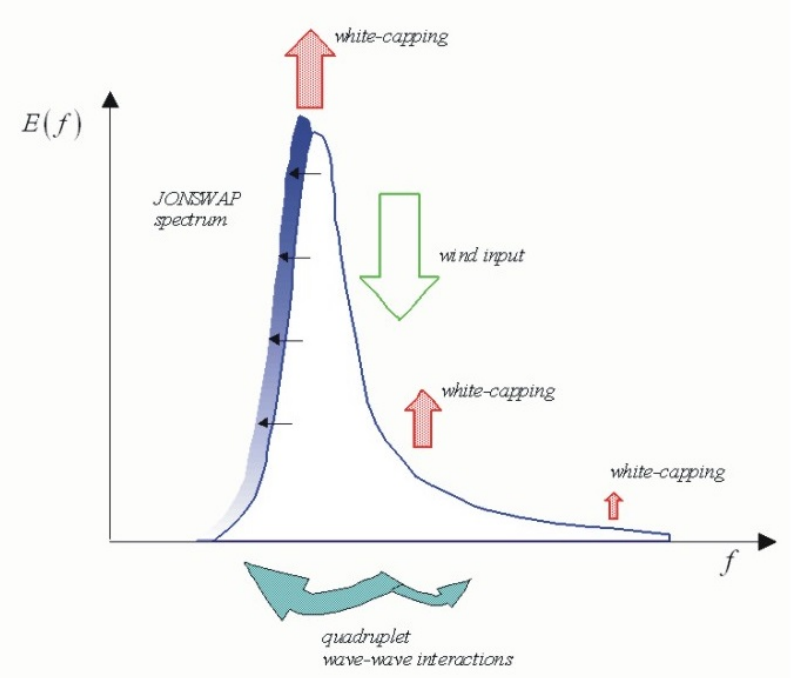

Figure 3.8: Whitecapping effects on the JONSWAP spectrum in shifting the area by Holthuijsen (2007)

3.1.5 Triad Interactions

Triad non-linear interactions constitute an expansion of our knowledge for wave energy redistribution. In contrast to the quadruplet interactions which are dominant in deep to mid-

depth waters, triad interaction are expressed only in shallow water. Their contribution to the spectrum change is more dominant than quadruplets. In reality triad interactions represent the physical shifting in frequency and space of three wave groups, when the corresponding resonance conditions are met. Similar to the case of quadruplets, resonant conditions for triads are limited to only three wave groups, when their frequencies are equal (Holthuijsen, 2007)

$$k_{tr,1} + k_{tr,2} = k_{tr,3} \tag{3.30}$$

$$f_{tr,1} + f_{tr,2} = f_{tr,3} \tag{3.31}$$

Contrary to quadruplets, triad resonance conditions ($\beta_{tr,1,2}$) cannot be dealt by the dispersion relationship, due to the fact that in shallow areas, waves are acting as non dispersive thus they have to be determined by the phase of the three wave components ($\phi_{tr,1,2}$) (Delft, 2014b)

$$\beta_{tr,1,2} = \phi_{tr,1} + \phi_{tr,2} - \phi_{tr,1+tr,2} \tag{3.32}$$

These interactions are responsible for the occurrence and development of a bimodal spectrum shape, when spectra are examined in shallow locations. This is due to the fact that triads move the energy density of waves into higher frequencies, by dislocating dominant lower frequencies, developing "secondary peak". In the case of SWAN triads are resolved with a discrete triad approximation (DTA) (Delft, 2014b).

$$S_{nl3} = \alpha_{EB} 2\pi J^2 \tag{3.33}$$

Where α_{EB} is the proportional triad coefficient which decides the shape of wave components, and J the interaction coefficient between the wave groups.

3.1.6 Bathymetry

In order for SWAN to initiate a wave simulation, a bathymetry mesh has to be prepared. SWAN can employ different types of grids for its simulations, regular (structured grid), unstructured, and curvilinear. The level of resolution of the bathymetry mesh has a direct effect on the wave hindcast, with interactions taking place between depth resolution and several solvers such as triad, bottom interactions and quadruplets.

For the construction of the bathymetry mesh several databases with information on depth at seas exist, currently ETOPO1 (Amante and Eakins, 2014), GEBCO (British Oceanographic Data Centre), and can be utilized to obtain the high accuracy depth profile. Exploration of structured and unstructured meshes was performed in the initial scope of this thesis, the final

mesh form used throughout the thesis is structured with varying resolution depending on size of the investigated area. Both coarser and finer meshes have been used, with nesting for higher spatial resolution hindcast. The author investigated unstructured mesh generation as well, but several drawbacks led to the exclusion of this mesh type for this thesis. The outline for every option is elaborated upon in Section 3.2.4.

3.1.7 Bottom Interactions

In order to fully utilise the SWAN numerical model, the bottom interactions and potential obstacles (optional) can be utilised, though the latter is not an integral component of the source terms. Bottom interactions rely on the spatial resolution provided by the user as discussed. The use of a high bathymetry resolution will allow to enhance the triad solution of interactions, bottom friction, diffraction and refraction terms.

Coastal modelling considerations suggest that bottom friction should be included within the calculation of final S_{tot}, in such areas. This is one of reasons that SWAN performs better, with high resolution meshes interpreted in computational efficient ways, separating it from larger models which due to the spatial resolution usually used tend to not account for bottom friction losses (Komen *et al.*, 1994; Cavaleri *et al.*, 2007).

Bottom friction is not the sole interaction affecting non-linear interactions, additionally breaking and dissipation processes affect the triads which are found in shallower regions. This allows for calculation of interactions between bottom and alteration of wave components. SWAN is able to account for these interactions, though the option is tunable by the user and optional to be considered. The bottom friction formulation in the source code is expressed as:

$$S_{ds,b}(f,\theta) = \frac{-C_b N(f,\theta)\sigma^2}{g^2 sinh^2 kd} \tag{3.34}$$

When investigating coastal and nearshore locations, additional effects are present. In continuation of the bottom interaction section the processes of refraction and diffraction have to be resolved.

When waves approach the shoreline, bathymetry (depth) causes the phase speed of waves to alter their direction this effect is called refraction. In reality it forces the waves to divert from their incoming direction towards shallower areas of the coast due to bottom interactions. This depends on the magnitude of change in wave direction, and will either increase of decrease their height. The refraction effect is attributed to the fact that seas waves and every kind of wave will always turn and travel towards the area with the lower propagation speed (Holthuijsen, 2007).

Diffraction is another process that will change the direction and energy momentum carried by waves. Predominately diffraction occurs in coastal location or in the presence of obstacles, the idea presented is that waves will travel in the "shadowed" area of a coast or an obstacle.

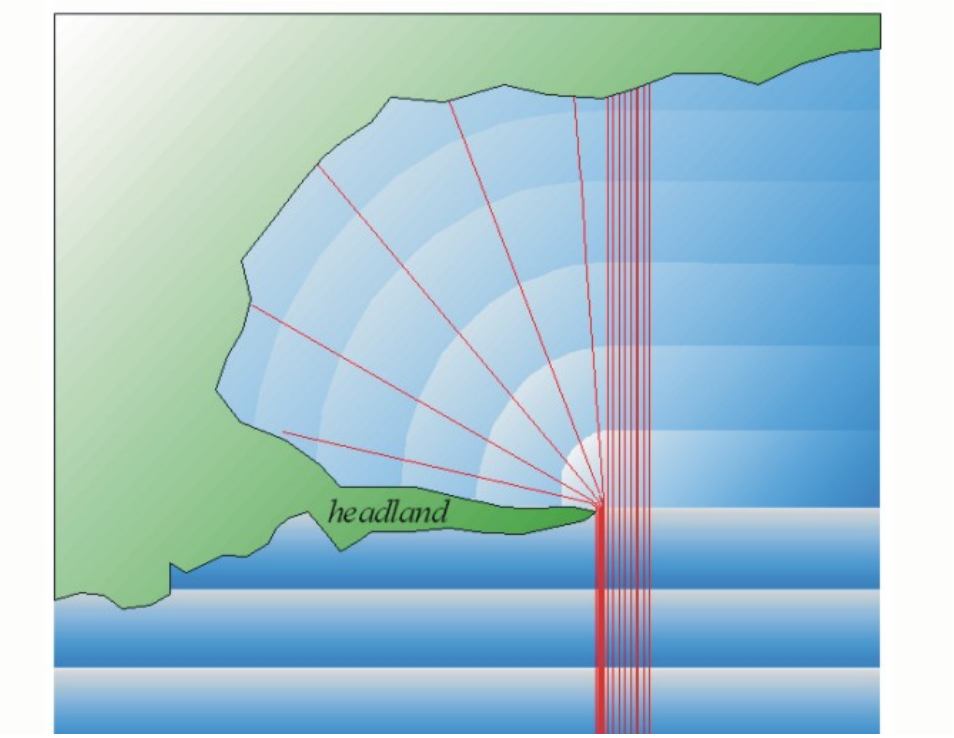

Figure 3.9: Diversion of wave as they approach a coastal location, diffraction and refraction effects by Holthuijsen (2007)

Following the refraction principle of moving to lower propagation areas, this effect is reducing the amplitudes to waves and increases their frequency (Komen *et al.*, 1994; Delft, 2014b). Both properties are user-defined and have been accounted for in the various hindcasts within this thesis.

3.2 Constructing SWAN

This section provides details on the translation and activation of wave theory terms, discussed in Section 3.1. It presents the way they are incorporated in to the SWAN model and how they are activated. Finally, it attempts to provide insightful comments and aid concerning the options available for the construction of input files. The proper structure used ensures the quality of results and confidence in the model.

3.2.1 Activating Wind Fields

Preparation of the file includes both wind components to be used; the file generated has to include for every time step, with U_{10} and V_{10} in a gridded structure. The final form of the wind mesh can be either a regular (structured) grid with a resolution dependent on the spatial properties of the data or an unstructured one. In any case the user, may as well use an interpolated mesh reduction (increase spatial resolution), by linear or non-linear techniques in order to resize and reshape the format of wind.

This option was examined, with a linear interpolation coding sequence, although due to the inconsistencies found in the calibration of the model it was abandoned. SWAN can be provided with the wind input regardless of spatial resolution, as long as the wind components are structured as mentioned, and the computational grid is greater or equal to the examined area.

From this point onwards the wave model will linearly interpolate the wind data and calculate the wind drag and surface stress for every time step. The decision is left with the user to select a spatial and temporal resolution depending on experience, desired solution and speed.

To incorporate correctly the wind file component correctly, the user has to define the mesh with the INPGRID command, providing basic geographical information in spherical or cartesian coordinates. Moreover, the number of meshes which constitute subdivisions of the spatial resolution over length of the file also needs definition. Finally, the starting and finishing timestep of the wind input have to be assigned, along with the time interval of recorded winds.

Following the input command that sets the environment for wind input, the reading sequence must be assigned with the READINP, setting the file name that includes the wind field. The way that wind file is read must be also defined, explicitly mentioning the numbers of header and timestep within the constructed file, followed by definition of the computing language translation format. A example of those sample commands are given below.

INPGRID WIND REGULAR -5.5 29.25 0 81 32 0.5 0.5 NONSTAT start 1 HR end

READINP WIND 1 'fname' 1 1 0 0 FREE
READINP WIND 1 'fname' 1 0 1 0 FREE
READINP WIND 3 'fname' 1 1 0 0 FREE
READINP WIND 3 'fname' 1 0 1 0 FREE

3.2.2 Application of Boundaries and Initial Conditions

The wind input as discussed in Section 3.2.1 is required for the commencement, propagation and evolution of waves within the domain. In Section 3.1.2 effects of wind on the final shape of the energy density and spectrum were presented. SWAN has the ability to operate in a zero initial state and time varying conditions (non-stationary). In order for a correct hindcast to be performed, the location examined has to be taken into account and the selection of a spectrum responsible for the evolution and propagation of wave fields must be selected.

Regardless state of operation, with or without boundaries, the user has to assign a spectrum for wave evolution with the BOUND SHAPE command, this accounts not only for the spectral values applied in the wave components but also the calculations for several other non-linear parameters.

For application of the spectrum that will govern the wave generation and propagation:

BOUND SHAPE JONSWAP 3.3 PEAK DSPR POWER

Next is the application of boundary conditions, if a non zero initial approach is considered wave information must be provided. Boundary data can be spectral from a previous larger or equal SWAN domain, and/or provided by other oceanic models WAM or WW3. These data can either provide only the locations at the edge of the grid or be a part of a larger hindcast usually of coarser resolution.

If the boundary conditions are to be obtained from oceanic models, then two set of commands can be utilised the BOUND2 WAM or BOUND3 WW3, with necessary information about the origins of the grid starting points in cartesian or spherical coordinates and the initial time. Another alternative is using a larger SWAN domain to produce spectral data or boundary information and perform a nested run with BOUND1 NEST and the file that was produced by the previous hindcast. In this case of spectral domains, the user must define the location in the previous hindcast with regards to coordinates of origin, length of effective computations of wave conditions, mesh resolution and starting time for recorded wave components, for this reason the NGRID and NESTOUT command are to be used.

BOUND2 WAM filename FREE Longitude Latitude Time

BOUND3 WW3 filename CLOSED Longitude Latitude Time

Alternatively, the user can provide boundary conditions in a constant way with BOUND CONSTANT and assign the desired data which can be applied to either sides of the domain as a whole, or particular segments, SIDE and SEGMENT command. If not constant values are provided, spectral files can also be utilized.

This requires the user to construct files which will contain the following boundary information varying in time and space. The so-called TPAR file much consists of H_{sig}, T_{peak} or T_z, P_kDir

and D_{spr} with the quantities being time varying or point spectrum data produced by previous simulations at the boundary points.

Major drawbacks with the use of larger hindcast spectral domain for nested runs, is the difficulty of coupling other models, specifically SWAN can perform coupling only in a regular grid option while unstructured meshes are not capable of being used (Delft, 2014a). Additionally, the storage requirements of the spectral data domains pose a restriction in their usage for large time domain hindcast, with their size often times being extremely large.

On the other hand, when a nested run is performed, a larger domain provides the wave environment. This is expected to increase the accuracy of the resolved model based on the assumption that larger domain spectral hindcast provided had been calibrated carefully and accurately.

Spectral point data and TPAR file can substitute the need of nested spectral boundaries, with the first though being restricted to similar storage requirements. Moreover in the case of spectral point data if the boundary conditions are limited (boundary length is small) a low number can decrease accuracy of the hindcast, though the meshes investigated extend over some distances (e.g. in kilometers) then the necessity for more spectral points arise, which are hard to be obtained.

TPAR files are basically spectral output data from larger models, advantage is their low storage demand and the ease of isolating these kind of point even if a previous hindcast is performed and no spectral point were requested to be output. More specifically spectral information can be extracted by a WAM or WW3 domain as long as recorded data comply with the TPAR format, regardless whether these points have been previously predefined by the WAM or WW3 hindcast.

For the hindcasts performed within this thesis, models were run with two dominant configurations, boundary data extracted by the WAM spectral model operated by ECMWF (ECMWF, 2014). Additionally a larger hindcast SWAN run was used which led to a nested run with increased spatial resolution in the domain. The sequence of commands for the proper assignment of both usages are presented below.

SWAN construction for varying spatial and temporal resolution of inputs for TPAR or spectral point data.

BOUNDSPEC SEGMENT XY VAR FILE LEN SPEC/TPAR SEQ

SWAN construction for side boundaries with temporal resolution of inputs for TPAR or spectral point data.

BOUNDSPEC SIDE N/W/S/E CCW VAR FILE LEN SPEC/TPAR SEQ

or

BOUNDSPEC SIDE N/W/S/E CCW CON FILE LEN SPEC/TPAR SEQ

Using a nested grid from a SWAN hindcast

NGRid location -12 54 0 8 7 320 280

NEST filename OUTPUT time 10 MIN

Following these nested output commands the subsequent SWAN hindcast has to call the file produced by the NEST command

BOUND1 NEST filename CLOSED

Finally, to minimize the "cold" starting period of a hindcast the user can use in combination with the inserted boundary and spectral informations, the latest wave conditions recorded by the previous run, finishing a timestep prior to the subsequent initiation. This provides additional information to the hindcast allowing a faster generation of the wave resource.

HOTFILE HOTFILE.hot FREE

INITIAL HOTSTART SINGLE HOTFILE.hot FREE

3.2.3 Non-Linear Terms

The non-linear wave mathematical formulation of wave-wave interactions (see Equation 3.23) allows for the solution on quadruplet interactions and has been adopted as the primary solution by SWAN (Delft, 2014b). The method proposed by (Hasselmann *et al.*, 1985) is known as Discrete Interaction Approximation (DIA), with deficiencies being identified and reported (Tolman, 2013; van Vledder, 2006; Vledder, 2012). Some of the pitfalls in these assumptions include, the over prediction of the wave spreading leading to overestimation of wave direction. Moreover, it has been also underlined that the DIA approach led to underestimations of the overall final energy, and it is valid only for a specific area of spectrum set with the highest spectral values not taken into account (Rogers and Van Vledder, 2013; Bottema and van Vledder, 2008).

In SWAN another solution of the quadruplet and non-linear effects can be resolved by exact computations known as XNL (Rogers and Van Vledder, 2013; van Vledder, 2006; Resio *et al.*, 2001; Delft, 2014a), with the XNL solvers being more computationally demanding. Latest development have presented a Generalized Multiple Discrete Interaction Approximation (GMD) (Tolman, 2013), with optimized terms on the non-linear solving equations. Although the computational requirements and cost are investigated to establish the correlation for accuracy and demands. So far DIA are used in most models (WAMDI, 1988; Delft, 2014a; Tolman and development Group, 2014), since they are considered as good approximations and not as computational expensive as the exact solutions offered, although the option for exact solutions exists in SWAN. Activation of the quadruplets is an optional process that can be activated by the user with approximation coefficients being tunable by the user, depending on the area of investigation.

QUAD iquad lambda Cnl4 Csh1 Csh2 Csh3

QUAD 2 0.25 $3 \cdot 10^7$ 5.5 0.83 -1.25

Evaluation of several schemes of approximations (based on unpublished proposal's by Hasselmann) along with the effects of adaptation on the DIA solvers are investigated in Section 4.6, with considerations not only on the optimal solutions but on the computational demands and time requirements. The activation of whitecapping process is at discretion of the user, throughout the studies in this thesis the importance of whitecapping was recognized from the early stages, thus all of the cases presented have included its activation, with alterations that are discussed in Chapter 4. Depending on the wind scheme chosen as presented in Section 3.1.1, the whitecaps can be activated as:

WCAP WAM3 2.36^{-5} 3.02^{-3} 2 0.5 1

In the case of a WAM4 wind input formulation:

WCAP WAM4 4.5 0.5

WCAP WAM4 4.1 0.5

Following the non-linear terms activation, the final component that is of major importance in shallow modelling assessments is the activation of triads. The α_{EB} and J coefficients are tunable parameters, while activation of the triads is again at discretion of the user. Proportional coefficient, based on (Delft, 2014b), a value of 0.1 has been preferred. To activate the triad interactions responsible in the sequence is:

TRI 0.1 2.5 0.2 0.01

3.2.4 Unstructured Grid

Unstructured grids have been developed in the past years and are used in wave studies. SWAN has the ability to use an unstructured mesh although available software for the creation of an unstructured grid are quite limited. Coupling SWAN with these types of mesh was examined in a small area assessment by Zijlema (2010).

The author initially explored the option of unstructured meshes as a part of the thesis, with the use of some open source numerical models for the generation of unstructured mesh. Most of the open source tools though are not maintained and thus are difficult to be coupled and used with modern versions software increasing difficulty to prepare the mesh.

In distribution of the code for SWAN, the availability of three major unstructured mesh generators is given, two of them are open source EASYMESH and TRIANGLE while a third option of commercial software is available (Delft University of Technology, 2014).

Due to the cost of the commercial software, the author explored the generation of unstructured grids via the open source options. Source codes can be used in a Linux (Terminal environment)

or Windows (MS-DOS environment), although these have to be compiled by the use of type of Linux simulator, usually Cygwin.

As in the example case of SWAN by Zijlema (2010), the TRIANGLE option was initially used. The additional requirements were identified by the author and the successful generation of unstructured meshes was performed (see Figure 3.10). These involved: Items/Software Required to couple the unstructured grid generator to produce a mesh:

1. Active MATLAB 2011 version and older
2. OPNML toolbox for MATLAB
3. BATTRI toolbox for MATLAB,(Bilgili *et al.*, 2006)
4. Maps toolbox for MATLAB, additional component
5. DEV++, compiler in case of Windows
6. Cygwin, compiler in the case of Windows
7. GEODAS
8. BODC coastline extractor
9. Development of propitiatory code in order to manipulate the data

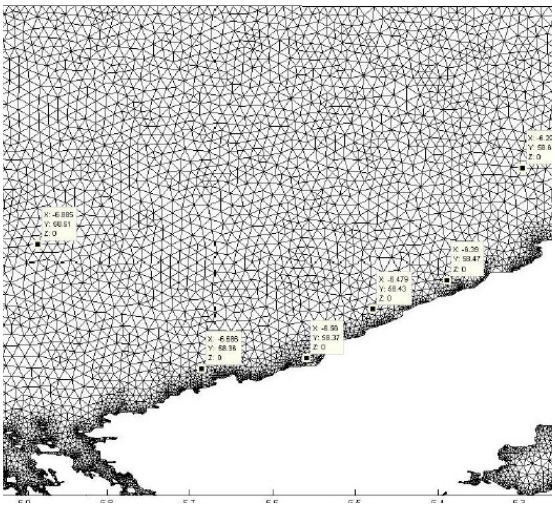

Figure 3.10: Unstructured mesh constructed, zoomed in area

An elaboration on the process itself is not in the scope of this section, though available if requested. To show the drawbacks of the unstructured meshes construction option, a highly resolved mesh was constructed for the Outer Hebrides, and was successfully implemented without boundary information for a hindcast (see Figure 3.11).

The problem appeared when boundaries were applied SWAN failed to initiate, further file manipulation with programming software Python and Matlab were employed to overcome the issue but interpretation of the mesh was halted by SWAN. The reason lays with format of the triangulated locations and their positions at the boundaries. Due to the sensitivity of assignments by the nodes, proper identification of the boundary nodal positions was not possible to

be re-assigned. This led to the existence of "open" boundary which constituted neither sea nor land identified areas. To the authors knowledge coupling SWAN with unstructured mesh can be performed with the commercial software as no issues on the boundary information arise.

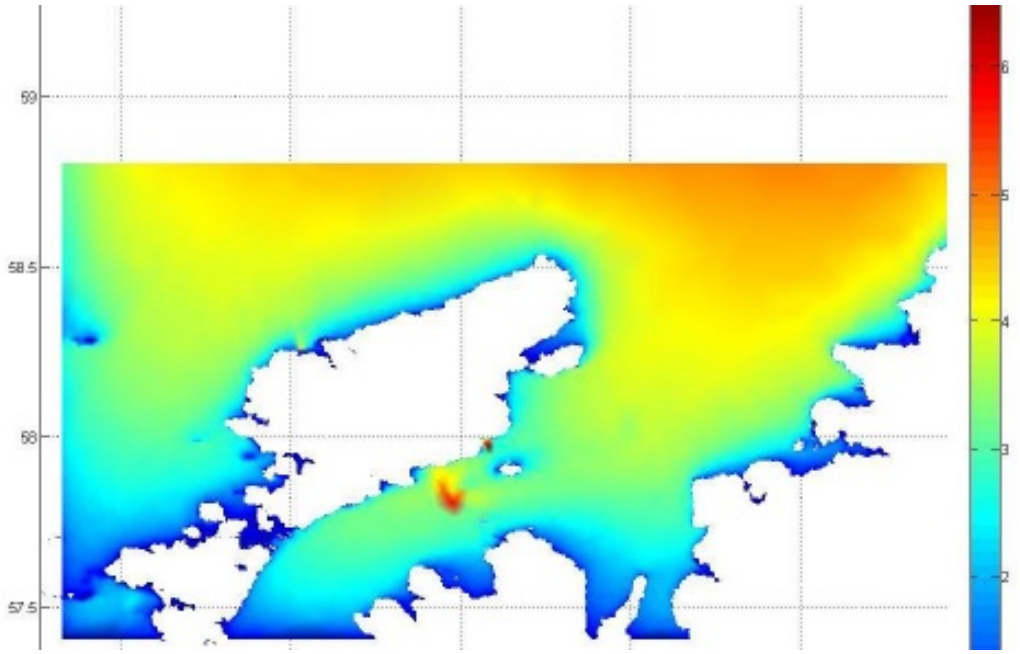

Figure 3.11: Non-stationary H_{sig} results with unstructured grid,

When boundary information are required, see Section 3.2.2, SWAN is unable to determine the location of the boundary file. This is due to the fact the coordinate structure of boundaries on the x and y plane do not follow a regular distribution. Attempts to alleviate the problem of boundary flags assignment was performed with inability of SWAN to determine the correct position of the boundary file, see below:

**Terminating error:SwanBpnlist:list of boundary vertices could not be completed

Moreover, recent studies have shown that the use of unstructured grids with SWAN increases the computational requirements and endanger the stability of the simulation with turning rates not satisfying the CFL criterion more often, leading to break down of the simulation (Dietrich *et al.*, 2012).

3.2.5 Regular Grid

Regular grids are used throughout the published and unpublished work of this thesis. The data were extracted by ETOPO1 with a spatial resolution of 1 arc-minute, the database is an expansion of the previous ETOPO2v2 and ETOPOv5 models (Amante and Eakins, 2014). The database represents oceanic and coastal bathymetry that extend form -90^o to $+90^o$ latitude and -180^o to $+180^o$ longitude.

The best available regional and global data were extracted and processed for the evolution of ETOPO1, from institutes and data sources around the world. Shoreline data were extracted by the Antarctica and NGDC from the Global Shelf-consistent Hierarchical High-resolution Shoreline (GHSS) database. The bathymetry included in the model, utilises data from the Japanese Oceanographic Data Centre (JODC), The Caspian Environment Program (CPE) and the Mediterranean Science Commission (CIESM).

This high resolution database was used to construct the various regular structured meshes employed in this thesis and its various studies. The generation and preparation of the meshes were performed with a developed Matlab code.

After user area selection, several characteristics have to be used as inputs so the source code in SWAN can recognize and match the area, with wind input and other components. The same sequence of commands, as in the wind input case has to be used. Firstly, by establishing the area for which the computations are active INPGRID, and then the command that reads the imported structured bathymetry file, READINP. The modeller has to ensure that the original CGRID command is greater or equal to the coordinates given for the bathymetry in order to ensure all point included.

CGRID REG -10 55 5 5 400 240 CIRCLE 36 0.035 0.5 36

INPGRID BOT REG -10 55 0 400 240 0.025 0.025 EXCEPTION -999

READINP BOT -0.001 'filename' IDLA 3 FREE

Some considerations and potential errors involving the bathymetry resolution and its applicability in the hindcasts are discussed in Chapter 4.

3.2.6 Bottom Friction and Interactions

After the construction of the bathymetry the bottom interactions such as breaking, shoaling, refraction and diffraction are to be activated in order to obtain the highest representation of wave resource at coastal locations.

For the bottom friction original suggestions were made for the applicability and value of the C_b coefficient, with values being taken from 0.001-0.01 m/s, while specific experimental approaches suggested coefficients depending of sea conditions, showed that for swell seas a

value of 0.038 m^2/s^{-3} and for wind seas 0.067 m^2/s^{-3} (Hasselmann *et al.*, 1973; Komen *et al.*, 1994; Booij *et al.*, 1999; van Vledder *et al.*, 2010) are suitable. These proposed coefficients have been applied to wave models, although re-visiting hindcast in various locations revealed that the re-tuning of the factor is to be taken into account for every area investigated. The activation of bottom breaking coefficient is suggested to be adapted when wind seas or fully developed seas are investigated, activation of the bottom friction in SWAN follows the structure of:

BREAK CON

FRIC JONSWAP CON 0.038-0.067 or 0.030-0.038

Moreover SWAN allows, if friction data are available to use two additional expressions based on the Collins or Madsen formulations (Delft, 2014b).

3.3 Summary

In this chapter the construction of several files for the model were presented. Additional options along with tunable values per every major component of the implemented code were also discussed. Information about considerations on tuning the physical approach of significant components such as wind, boundaries, bathymetry information and non-linear interactions were elaborated upon.

- The wave theory incorporation within numerical wave models and their effects in calculating the resource.
- Different theories and the dependence of source terms to improve a hindcast.
- Origins of several coefficients are presented, while their sensitivity in alteration within the code is underlined.

Several obstacles encountered during the thesis were also presented, in the hope that exploration of same options will help avoid similar procedures/mistakes or even improve them. Construction of the specific file formats is a vital component for a successful SWAN initiation, knowledge on the format of data is not always straightforward and clear. The nature of open software codes proves challenging especially since comprehensive information on preparation of the model are often unclear or absent, the author hope this chapter will aid the future implementation of similar studies.

Chapter 4

Numerical Modelling of Wave propagation using SWAN

"Excellence is an art won by training and habituation. We do not act rightly because we have virtue or excellence, but we rather have those because we have acted rightly. We are what we repeatedly do. Excellence, then, is not an act but a habit."

Aristotle, 384-322 B.C.

General

This chapter is focused on the modelling processes that have to be considered for application of the numerical wave model. It discusses parametrisations, and inputs effects of various components within construction of the source code.

Major configuration options are examined, with sensitivity of results varying significantly, underlying the need for considerations when constructing an operational model. Wind input, domain size, bathymetric profiles, propagation scheme and discretisation of frequencies, play an important role in the final outputs of the model.

4.1 Introduction

A successful hindcast/forecast in SWAN model depends on quality of inputs and selection of physical processes, which will impact for assessment of the wave environment. Based on surrounding coastal orography, quality of wind resource input, physical process adjustments and activated terms, wind wave interaction and growth are affected. In this chapter several alterations on the plethora of options for the code are tested and compared with buoy data. In this way the accuracy, pitfalls, and necessary corrections to secure a high level hindcast validation are demonstrated.

The different parameters affecting SWAN, have an effect not only in the accuracy but in the computational requirements of the model, making it more or less computationally expensive. Spatial and temporal variations have an effect on the computational requirements. This may prove useful to future applications of the model for larger or smaller areas. Deviations are bound to exist between models and measured data, since as shown in Section 3.1, our physical understanding of waves is constantly evolving. As discussed, most of the wave theory components are based on approximations and experimental approaches, by a trial and error approach though this does not diminish their significance. Due to the wide range of options available to the user, modeller should understand the effects of each alteration, and its implications in model performance.

This will be further outlined in the following sections, in which the SWAN model was applied to completely different regions, varying from large to small scale and for coarse to high resolved meshes. Different regions will require individual and customized approaches in the modelling, with the choice of physical inputs have a significant effect on the model results.

4.2 Description of Wind Data

Wind is the primary driver for wave generation and thus a proper selection of the wind input is necessary as a poorly source wind input will affect the quality of results. There are several sources for wind datasets, varying in spatial, temporal resolution and area of availability. In the following study wind products from two sources are evaluated, the ERA-Interim Re-Analysis by ECMWF and the CFSR from NCEP/NCAR.

4.2.1 ERA-Interim

The first dataset was extracted from the Re-Analysis product available at ECMWF, ERA-Interim (denoted as ECMWF from now on), is a high level re-analysis package with wind inputs dating back to 1979. The databases also include other wind packages starting as early as 1900.

Since 2010 at ECMWF wind and wave models used have been enhanced and connected via the IFS system, allowing constant feedback and correction of both models. This coupling has produced results with reduced errors, when compared with recording stations (i.e. windmasts, wave buoy and satellites) and past archived datasets (Park, 2008; Richardson *et al.*, 2013; ECMWF, 2014).

Both wind (ECHAM5) and wave (WAM) numerical atmospheric weather models run on two super-computers (CRAY) Cy38r2 for the wind model and Cy33r1 for the wave model. Latter option utilises the IFS coupling system to provide information, in a two-way manner for calibration and improvement assimilation methods. The wave model used at ECMWF is based

on the basic wave kinematic equation and techniques presented in Section 2.3.1. An overview of the modelling process can be found in (Komen *et al.*, 1994; Park, 2008). The improved assimilation techniques show that the current model can provide forecast for up to a 10 day period with promising results, with significant improvements over its previous versions (Richardson *et al.*, 2013; Balmaseda *et al.*, 2013; ECMWF, 2014).

4.2.2 Climate Forecast System Re-Analysis (CFSR)

NCEP provides the Climate Forecast System Re-Analysis data (CFSR), which provide a 31 year wind product spanning from 1979-2010, which is based on the latest Re-Analysis conducted in 2010. This Re-Analysis produced a high temporal and spatial wind product database, as similar to the ECMWF data. Cross-validations and corrections are made by coupling numerical weather model with a wave model (which in this case is the WW3). Moreover, as in the case of several wind products, corrections are made based on interactions and feedback by wave, buoys and satellite data. Validation have shown that the current CFSR dataset has also improved significantly by its previous version the R1 (Rienecker *et al.*, 2011; Stopa and Cheung, 2014; NCAR, 2014).

As in the products provided by ECMWF, various atmospheric and oceanic components are included, with the latter being a result of coupling CFSR to WW3, which is known to perform better with those types of wind products (Stopa and Cheung, 2014; Tolman and development Group, 2014).

4.2.3 Area of Investigation

SWAN was chosen due the fact, that the majority of offshore and marine energy applications focuses in depths not exceeding 150m (Waveplam, 2009; Carbon Trust and AMEC, 2012). Thus a more detailed solution of the nearshore physics is required, something that is not often met at larger scale models. Although approximation on the physical processes are included, SWAN has been validated and shown to work well for nearshore and medium scale models (shelf seas) (Booij *et al.*, 1999).

The area considered for investigation to test different wind products includes Scottish and North Sea regions, see Figure 4.1. The wind data from both ECMWF and CFSR are used as inputs for the numerical wave model. The ECMWF wind dataset employed, has a spatial resolution of 0.125^o and a timestep of 6-hours. On the other hand CFSR data offer a 1-hour temporal resolution while their spatial resolution is 0.5^o. The quantities extracted by both products, are the wind speed U_{10} and V_{10}, this corresponds to the quantities to be recorded at 10m height (ECMWF, 2014; NCAR, 2014).

Use of a detailed coastline and depth bathymetry mesh (see Figure 4.1) enhances simulation of shallow water terms, such as dissipation and triads (see Section 3.1.5 and Section 3.1.7) though

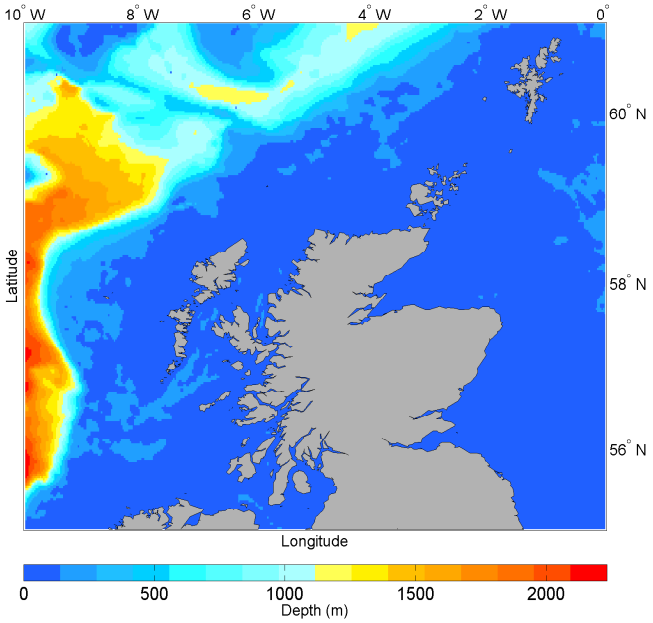

Figure 4.1: Area of investigation, with the colorbar indicating the depth in meters

at the cost of computational demands which are increased. A 15 minute time-step was chosen for both wave models, driven by the different wind products.

The wave climate from the west is exposed to the Atlantic, with its boundaries open to significant amounts of swell and strong winds originating from the West Atlantic front. The wave climate to the North-East coastlines is less exposed to incoming swells, although it is dominated by wind generated seas and lower level of swells from the North. Depending on the influence of location, winds and swells will vary, thus the effect of wind induced waves is crucial.

SWAN requires initial spectral quantities to be assigned and after assessing previous hindcasts in the area. Minimum frequency was set to 0.04 Hz up to 1 Hz with 25 frequency bins and directional resolution per 15^o. In addition, to the wind input wave boundary conditions were extracted from the ECMWF, spectral database, and TPAR files were created for the boundary elements with a timestep of 6-hours. Boundary information were isolated at specified point locations, and in order to correctly present the information, boundaries were broken down into sections of 1^o with corresponding spectral data applied, providing variable conditions along the boundaries.

The wind input term is based on the calculations and theoretical approach of Janssen's exponential growth, which has been incorporated into the WAM 4 distribution with a whitecapping term tuned to 4.1 (Janssen, 1991; Komen *et al.*, 1994). Quadruplet interactions and nearshore triads are activated, terms important which represent the exchange of frequencies between waves and wind, as they propagate from deep to shallow water, thus allowing energy re-distribution (Hasselmann *et al.*, 1985; Holthuijsen, 2007; van der Westhuysen *et al.*, 2007).

Bottom friction and depth interaction are also enabled and their coefficients in this study are set to resemble wind generated seas (0.038 $m^{-2}s^{-3}$) (Zijlema *et al.*, 2012), while vegetation and mud transport were not accounted for, refraction and diffraction terms were also enabled.

Besides the choice of physical terms there are several numerical considerations which affect the computational processes. Primarily these focus on calculations and iteration amounts used in the solvers. Some alterations in the re-computation use of the boundary conditions were used. SWAN re-computes the incoming boundary waves, by setting a higher criterion for estimating the difference between incoming waves and re-computed ones not to exceed 5% .

The mesh generated has a spatial resolution of 0.025^o by 0.025^o and has been extrapolated by the data and procedure presented in 3.2.5, which resulted in a highly resolution mesh (see Figure 4.1).

4.3 Calibrating the model

In order to use the model with high confidence, initial calibrations are required. After the proper construction of input data, the model performance results were assessed and compared with buoy data. Following this initial work, the focus was to find improvements which would lead to a customized solution for the model. This process allowed for an area of customised model, and acquiring knowledge of specific terms that can be applied to certain areas. It must be noted that tuning of the model includes a great amount of sensitivity which may lead to incorrect results.

This section provides a quick overview of the initial tuning of the model, which was the basis of the investigation for the model's implementation. These results provide significant insight into how to assess and tune the model accordingly, while identifying areas that require further investigation and potential tuning (Lavidas *et al.*, 2014a,c).

To assess the model and its capabilities an initial run was performed for March 2010 for the entire computational area, and model parameters were outputed at the CEFAS buoy location West Hebrides (57^o $17,52^{'}$N-7^o $54,84'$W).

A quantitative approach is used to determine the accuracy of the results with buoy measurements, allowing us to expand and investigate the effect of wind inputs. Quantitative techniques for comparing model results such as the bias, root mean error (rms), correlation coefficient (R), Scatter Index (SI) and model performance index (MPI), as well as the distributions obtained. It is favourable to employ multiple benchmarks to assess the performance of the model Ris *et al.* (1999).

$$bias = \sum_{i=1}^{N_i} \frac{1}{N_i}(X_i - Y_i) \tag{4.1}$$

$$rms = \sqrt{\frac{1}{N_i}\sum_{i=1}^{N_i}(X_i - Y_i)^2} \tag{4.2}$$

$$R = \frac{\sum_{i=1}^{N_i}((X_i - \overline{X_i})(Y_i - \overline{Y_i}))}{\sqrt{((\sum_{i=1}^{N_i}((X_i - \overline{X_i})^2)((\sum_{i=1}^{N_i}((Y_i - \overline{Y_i})^2)}} \tag{4.3}$$

$$SI = \frac{rms}{\frac{1}{N_i}\sum_{i=1}^{N_i} Y_i} \tag{4.4}$$

$$MPI = |1 - \frac{rms}{rms_{change}}| \tag{4.5}$$

$$rms_{change} = \sqrt{\frac{Y_i^2}{N_i}} \tag{4.6}$$

where X_i is the simulated wave parameter, Y_i buoy/optimal wave quantity, N_i measurements, the rms_{change} is similar to the use of rms but the data taken into consideration are only the observed. The use of several quantitative indices allows better classification, for example in some cases a good correlation is obtained but a very high bias and a moderate MPI, may prove deficiencies in the model (Ris *et al.*, 1999; Komen *et al.*, 1994).

This initial run which was carried out with default model parameters. The results indicated under-estimations of both wave height and wave period in comparison to measured values from the CEFAS buoy, see Figure 4.2. The model was then tuned and results are reported in Lavidas *et al.* (2014c). The statistical output obtained is given in Table 4.1.

Table 4.1: March 2010, as taken form the calibration/validation process, see (Lavidas *et al.*, 2014c)

	West Hebrides		
	H_{sig} in m	T_{peak} in sec	T_z in sec
MPI	0.96	0.96	0.97
rms	0.31	3.6	1.9
Average Buoy	2.66	10.4	6.63
Average SWAN	2.16	8.2	5.16
Bias	-0.50	-4.2	-1.47
SI	0.31	0.35	0.30

Trend between model and buoy are closely followed although under-estimations by SWAN is evident, see Figure 4.2. The timeseries of H_{sig} from the ECMWF are also included, as seen in

Figure 4.3. It is noticeable that a significant swell component was not identified, at the final days of the hindcast, in comparison with the other wave model provided by ECMWF.

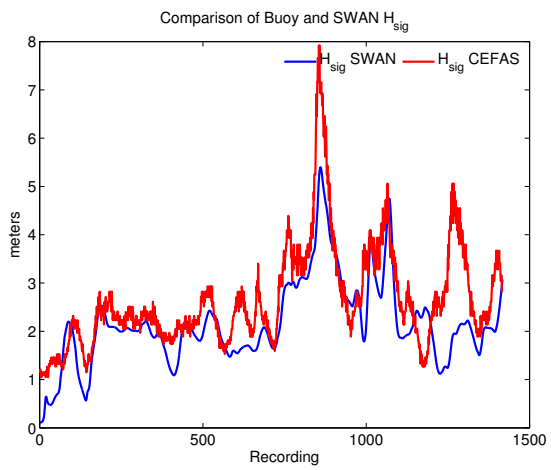

Figure 4.2: H_{sig} West Hebrides (default SWAN)

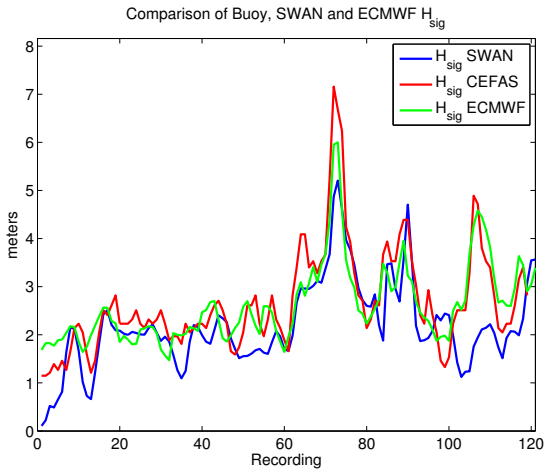

Figure 4.3: Cross comparison H_{sig} at West Hebrides

The behaviour and results of the model are compared with buoy data, see Figure 4.2. While, results comparison of SWAN and WAM model are given in Figure 4.3. Under-estimations of the models can be attributed to several issues such as boundary quality, wind quality (temporal and spatial) resolution etc. (Komen *et al.*, 1994; Cavaleri, 2009). This prompt to further explore of additional custom options and investigation of their effects on the magnitude of parameters in the hindcast. Some of the issues identified in (Lavidas *et al.*, 2014c) with discussion focused on the limitations and potential ways to overcome them. Finer temporal resolutions of the data especially wind and boundaries allow increased accuracy, helping the convergence of the quantities produced and compared with the buoy.

Most errors can also be traced back to the lack of input data sources and their resolution both temporal and spatial. The difficulties in acquiring buoy data for the correlation and comparison is an important issue. Nevertheless even in absence of multiple buoys, generation and approximation of wave fields can be produced by SWAN with high correlations.

In lack of reference points the user has to rely on reducing the overall Scatter Index and bias of the simulation, discrepancies are more often met for wave periods, although this is partially attributed to boundaries, minimum and maximum selection of the frequency bins.

Another factor taken into account is the insertion of boundaries for the computations, unfortunately not many publicly available wave buoys that can provide data for validation exist around the Atlantic, thus the necessity for accessing global wave models is imperative. Freely available data include wind and swell wave heights and it is important to underline that wave periods often provided are not in the appropriate form.

Increasing the temporal resolution of the input wind and boundary conditions allows to simulate

wind generation and wave interaction better, allowing for an increase in hindcast accuracy. Realizing that the default model parameters underestimate the wave height, some of the parameters were then altered until the comparison between model and measurements were deemed satisfactory. Results for H_{sig}, T_p, P_kDir are presented in Figure 4.4.

The model was calibrated for the Scottish area, specifically the North West coastline and Isle of Lewis (Hebrides), the effects of each wind product were examined, (Lavidas *et al.*, 2014a) with initial calibrations per wind products. A further discussion on these effects is presented in Section 4.4, along with additional details on the process.

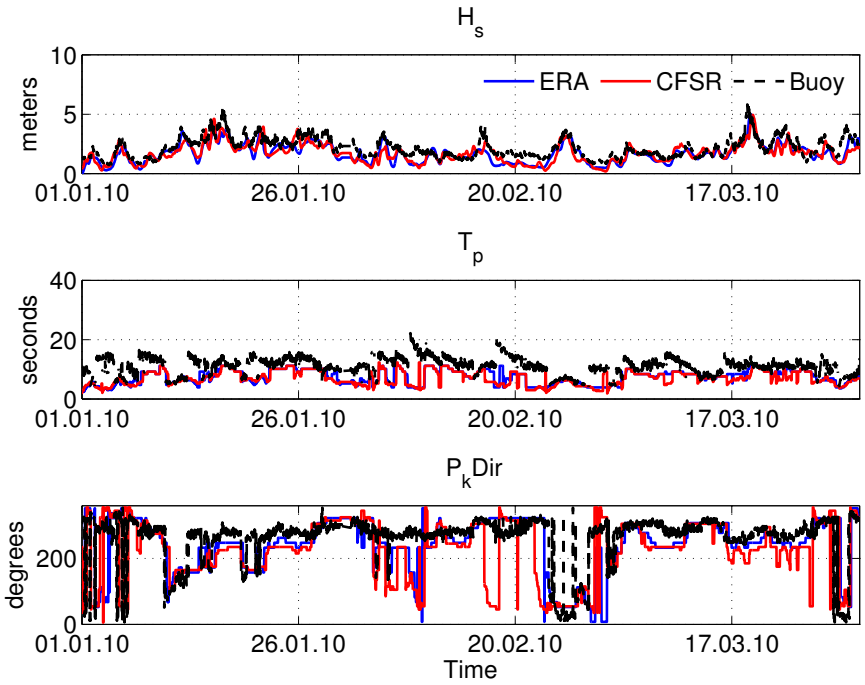

Figure 4.4: Performance of the model at West Hebrides 2010 January-March

In the physical side of the code, SWAN offers several alterations that will affect and alter the outcome but user has to be able to choose the best choice for the area under investigation. Often the most important issues that have to be lowered are the friction parameters and the level for computed accuracy of estimated waves by SWAN.

Alleviation of the first reported limitations led to an improvement for the model and ECMWF driven waves, while another wind product (CFSR) was evaluated in order to reduce potential under-estimations. Improvements in statistics are expressed for the same location, see Table A.1. Model under-estimations is evident in Figure 4.4. A secondary location, BlackStone is also assessed providing further confidence in the model. Even in the case of encapsulated areas such as in the case of BlackStone buoy. The evaluation and validation of both buoy sites are presented in more detail (see Table A.1 and Figure A.1) (Lavidas *et al.*, 2014a).

4.4 Comparing Wind Inputs

Comparisons between various datasets have been carried out and outlined in studies which attempted to quantify the accuracy by new atmospheric models used. In this section the comparison of a large scale calibrated model is implemented in order to establish the performance and optimal wind product for the Scottish and North Sea Area.

The variability of data and the lack of recording wind stations in offshore environments, led researchers to investigate the validity and accuracy levels of the predicted wind by coupling them with large oceanic numerical models (Bidlot *et al.*, 2006). Previous studies have assessed the data information of several re-analysis datasets using existing wind measurements, buoy and numerical models to establish the optimal selection. However, the results were mixed, indicating different level of accuracies and correlation between wind and waves, depending on predominantly the location, i.e. the Northern or South Hemisphere (Caires *et al.*, 2004; Stopa *et al.*, 2013; Stopa and Cheung, 2014).

The use of different wind re-analysis datasets, reveal their numerical accuracy and aids in the selection of the optimal dataset for use in the greater Scottish and UK area. Comparing the performance of different wind products and validating their wave results against buoy measurements; provides improvements not only for confidence in the numerical modelling of wind and waves, but re-affirms the use of wave models for locations with lack or absence of buoys.

With availability and advancements in atmospheric models, the accuracy of winds predictions has improved. Even from initial scopes on the global wind resource, it was obvious that both Hemispheres would show different behaviours. From the two separately investigated cases at the Gulf of Mexico and the wider Mediterranean coast, the quality of winds, reduced the performance, although some characteristics were following recordings, thus it was concluded that the resolutions of the input wind data, alters profile of the hindcast (Cavaleri and Bertotti, 2006; Cavaleri, 2009).

In the work Sterl *et al.* (1998), ECMWF sets were validated against recorded wind and through the use of WAM, in order to assess the wind quality. Application of WAM revealed an underestimation but not a consistent trend, with levels of seasonal variations. The overall performance of the dataset showed improved wind fields, and there were differences in spatial evolution of wave fields. Suggestions were made, as to the improvements of temporal resolution, which perhaps would lead to the increase of accuracy and reduction of biases.

A further re-analysis, extended the use of not only wind input but also included altimeter satellite data coupled (Caires *et al.*, 2004). This was mostly focused on the Atlantic ocean's and predominately at the U.S coastlines, and applying a different numerical wave approach (WW3). The conclusions showed differences from results. Significant deviations between dataset existed and underlined that the use of numerical wave models should be more consistent with

custom tuned parameters. Same locations, showed different biases and scatter indexes, though this was to be expected since the resolution differed. Most importantly the recorded trend was not consistently similar. Several over and underestimations were present for same locations, this led the authors conclusion that the differences within datasets affect significantly the potential wave hindcasts. Thus, selection of the appropriate of a dataset is not a trivial process. Different oceanic locations and global positions require custom approaches.

So far most couplings of these systems are made at an oceanic level and revealed several differences. Global models showed a close connection between swell generation and direction of propagation with the use of different fields (Young, 1999a). The use of coarse oceanic grids provides a broader understanding, but the prediction of wave in near-shore environments, must account the interactions that separate and make SWAN stand out (Booij *et al.*, 1999).

When wave modelling is applied for long periods (e.g. over 10-years) the biases and wind characteristics are smoothed, as they are translated into wave patterns over time, in contrast to shorter hindcast times (Rienecker *et al.*, 2011). This may not affect global models but the quality and assessment of the interactions between wave and wind models is vital, this is the reason that a one-year hindcast is employed. Underestimations often appear, depending on the way the wave kinematic equation in solved by the chosen numerical model.

To alleviate these issues selection of a wind field, is based on the geographical constrains and dependencies in combination with an enhanced numerical wave model. Wind input has an effect on the directionality of waves,spectral shape, frequency exchange, propagation speed and consequently breaking point (Hasselmann *et al.*, 1973; Janssen, 2009).

4.4.1 Assessing the models-performance indices

Buoy measurements are used to assess quality of the simulations and provide us with the necessary data to choose the optimal dataset. Since CFSR and ECMWF have different temporal and spatial resolution it is important to quantify the differences between their results to assess their accuracy, with same numerical physical terms assigned at both wave models, minimizing potential non-similarities in the final results. Hindcasts are compared to recorded wave conditions at specific locations (CEFAS, Center for Environment, 2014).

Four buoys under investigation are located to the West and East of Scotland with details given in Table 4.2. The following section presents the results in terms of West and East of Scotland for four buoys in total. The buoys are located at West Hebrides, Blackstone, Firth of Forth and Moray Firth (CEFAS, Center for Environment, 2014), and are operating for a long period of time providing recording of wave parameters and spectral data at 30 minute intervals.

For these hindcasts the H_{sig}, T_{peak}, T_z are compared with the same recorded values retrieved by the buoys. In the evaluation of the 2010 hindcasts, an annual and seasonal approach is employed for the comparisons.

Table 4.2: Locations of investigation for the wind products comparison

Origin	Coordinates	Location Name
CEFAS	$56^o\ 03,72'$N-$7^o\ 03,41'$W	Blackstone
CEFAS	$57^o\ 17,52'$N-$7^o\ 54,84'$W	West Hebrides
CEFAS	$57^o\ 57,99'$N-$3^o\ 20,01'$E	Moray Firth
CEFAS	$56^o\ 11,28'$N-$2^o\ 30,23'$W	Firth of Forth

Average values of H_{sig}, T_{peak}, T_z for the recorded buoys and the corresponding annual hindcasts results are presented in Table 4.3. It has be noted that buoy recordings have missing data for some time intervals and for this reason a post process stage has been applied, to consider only the recorded data measurements in the comparison.

Table 4.3: Annual indices

	West Hebrides						Blackstone					
	H_{sig} in m		T_{peak} in sec		T_z in sec		H_{sig} in m		T_{peak} in sec		T_z in sec	
	ECMWF	**CFSR**	**ECMWF**	**CFSR**	**ECMWF**	**CFSR**	**ECMWF**	**CFSR**	**ECMWF**	**CFSR**	**ECMWF**	**CFSR**
Average Buoy	2.25	2.25	9.90	9.90	6.23	6.23	2.02	2.02	9.72	9.72	5.96	5.96
Average SWAN	1.93	1.99	10.15	9.93	6.02	5.81	1.93	2.16	9.55	8.99	5.95	5.61
	Firth of Forth						Moray Firth					
	H_{sig} in m		T_{peak} in sec		T_z in sec		H_{sig} in m		T_{peak} in sec		T_z in sec	
Average Buoy	1.14	1.14	7.03	7.03	4.53	4.53	1.12	1.12	7.14	7.14	4.37	4.37
Average SWAN	0.97	1.47	8.08	7.02	5.20	4.6	0.90	1.11	8.08	7.23	4.65	4.40

Corresponding hindcast interval periods are presented for both annual and seasonal data, and it is noticeable that in all cases the generation trend has been followed, see Figure 4.5-4.8. However the CFSR dataset, which offers 1-hour temporal intervals, display larger peaks than the corresponding buoy time-series.

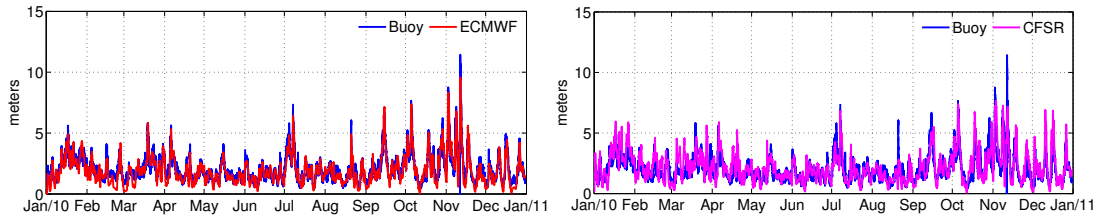

Figure 4.5: Wind product performance for H_{sig} at BlackStone

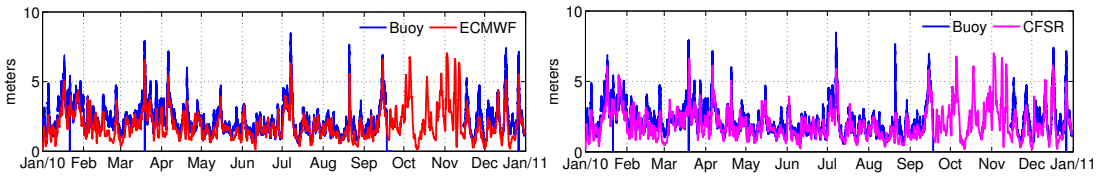

Figure 4.6: Wind product performance for H_{sig} at West Hebrides

Following the annual measurements are separated in seasons and are compared with the recorded time-series, presented throughout Table 4.4-4.7. This allows examination of performance and

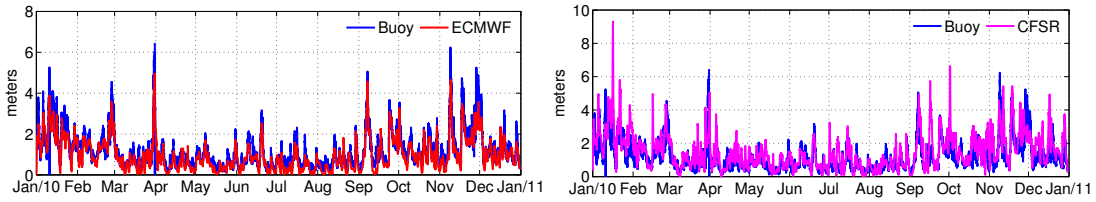

Figure 4.7: Wind product performance for H_{sig} at Firth of Forth

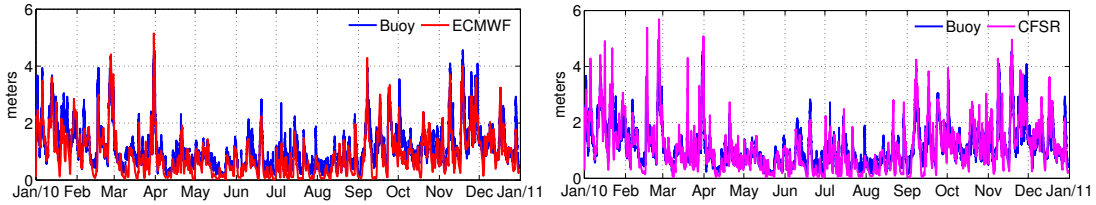

Figure 4.8: Wind product performance for H_{sig} at Moray Firth

effects of the hindcasts on distributions of wave parameters, as expected summer months have lower waves thus the wave parameters are reduced for the summer season. Performance of wave hindcasts allows not only evaluation of the numerical wave model but also the effects that wind products have on the assessments. For a more detailed representation of wave parameters, a seasonal break is used. After post processing the buoy time-series and extracting the non operational intervals, a comparison is possible, for four seasonal steps considered. From January 1^{st} until April 1^{st} is denoted as Season 1, April 1^{st} to July 1^{st} as Season 2, July 1^{st} to October 1^{st} as Season 3 and by October 1^{st} until December 31^{st} as Season 4.

As mentioned from the two datasets used, CFSR have the highest temporal resolution with 1-hour intervals, this improves the wind resolution on wave leading to higher peaks of H_{sig} and replicating the swift change in direction due to winds much better. The ECMWF data matched closely with the measurements the performance indices indicated that the overall mean values annual hindcast favours the ECMWF product.

4.4.2 Impact of wind input from different datasets

Performance indices for the hindcast results and buoys, based on the different data products employed, see Table 4.4-4.7. Results are given for every buoy based on the local characteristics (depths, coastlines, position) that affect the model performance. First buoy to be considered and analysed, was the Blackstone buoy, located West of the Scottish coastline near the Isle of Lewis at 97 meters depth and operational from March 2009 until present (CEFAS, Center for Environment, 2014).

Results for wave parameters used to characterise the performance of BlackStone are presented in Table 4.4 and Figure A.2, this buoy's location is intermediate to shallow waters. This means

Table 4.4: Blackstone Seasonal Indices

	Blackstone											
	Season 1						Season 2					
	H_{sig}		T_{peak}		T_z		H_{sig}		T_{peak}		T_z	
	ECMWF	**CFSR**	**ECMWF**	**CFSR**	**ECMWF**	**CFSR**	**ECMWF**	**CFSR**	**ECMWF**	**CFSR**	**ECMWF**	**CFSR**
Correlation	0.96	0.93	0.93	0.96	0.97	0.96	0.96	0.93	0.95	0.94	0.97	0.96
Average Buoy	2.15	2.15	10.47	10.47	6.24	6.24	1.64	1.64	9.71	9.71	5.94	5.94
Average SWAN	1.97	2.39	9.94	8.87	6.10	5.40	1.56	1.81	9.58	9.16	6.08	5.68
Bias	-0.18	0.24	-0.53	-1.6	-0.13	-0.83	-0.08	0.17	-0.13	-0.54	0.14	-0.26
rms	0.51	0.92	3.54	4.25	1.34	1.45	0.35	0.62	2.45	2.8	1.04	1.28
SI	0.24	0.42	0.33	0.40	0.21	0.23	0.21	0.38	0.25	0.28	0.17	0.21
MPI	0.96	0.96	0.84	0.84	0.90	0.90	0.97	0.97	0.85	0.85	0.91	0.91
	Season 3						Season 4					
	H_{sig}		T_{peak}		T_z		H_{sig}		T_{peak}		T_z	
	ECMWF	**CFSR**	**ECMWF**	**CFSR**	**ECMWF**	**CFSR**	**ECMWF**	**CFSR**	**ECMWF**	**CFSR**	**ECMWF**	**CFSR**
Correlation	0.96	0.93	0.95	0.94	0.96	0.95	0.96	0.93	0.92	0.91	0.96	0.95
Average Buoy	1.90	1.90	8.90	8.90	5.59	5.59	2.39	2.39	9.78	9.78	6.07	6.07
Average SWAN	1.90	1.85	8.92	8.86	5.77	5.76	2.30	2.59	9.75	9.06	5.84	5.59
Bias	0.00	-0.05	0.02	-0.04	0.18	0.17	-0.09	0.20	-0.03	-0.72	-0.23	-0.48
rms	0.38	0.66	2.28	2.49	1.16	1.31	0.53	0.94	3.54	3.75	1.28	1.48
SI	0.19	0.34	0.25	0.28	0.20	0.23	0.22	0.39	0.36	0.38	0.21	0.24
MPI	0.97	0.97	0.86	0.86	0.91	0.91	0.96	0.96	0.85	0.85	0.91	0.91

that non-linear interactions play a significant role in the alteration of the wave field, for which the physics have been activated accordingly.

The comparison performed according to seasons makes it easier to identify the variation and apply improvements, for time limited periods of hindcast or forecast. The correlation coefficient (R) and Model Performance Index (MPI) are high for both models, the temporal improvement (i.e. CFSR data with 1 hour time-step) shows no alteration on the numerical solver of SWAN; in fact the ECMWF dataset produce a slightly higher performance. Moreover, the model operation is constant throughout the year with all season's being resolved.

As expected seasons 1 and 4 (autumn to winter) have the highest average range of H_{sig}, (see Table 4.4). The input of the ECMWF winds present underestimation for all seasons, although the bias is relatively small, while Season 3 presents no bias. The situation is different though for the CFSR wind data driven waves, for duration of the year increased temporal resolution of the dataset led to higher peaks and overestimations, as it can be seen by the rms indices, leading to a higher Scatter Index (SI). Although, this was expected when volatility of wave resource is at its peak, during winter months and based on the knowledge that numerical wave models have restrictions on extreme wave height this is bound to produce overall mean under-estimations. The driving winds shows the same results for the "less" energetic summer seasons.

Although wave periods T_z and T_{peak}, exhibit high MPI coefficients, both models tend to slightly underestimate the periods for winter and autumn, i.e for season 3. In contrast to the CFSR behaviour, ECMWF driven waves are overestimating the spring and summer months, season 3. No significant differences though exist in all the quantities and the overall performance can be classified as accurate.

An increased temporal resolution provides gustiness in the wave model, with the CFSR data attaining higher peaks leading to overestimations, while ECMWF driven data present lower

differences with the recorded data and significantly lower SIs.

The Hebrides buoy is also located along the West Scottish coastline, specifically the South part of the Island of Lewis, at 100 meters depth and operational since 2009 (CEFAS, Center for Environment, 2014). Both West Hebrides and Blackstone are located in the exposed Atlantic side of the area, where large waves and significant amounts of swells are present. The complexity of the area may not be the depth but effect that the wind has on the wave environment. Moving from very deep water to shallow, the linear behaviour of waves quickly transforms into a non-linear activity with triad interactions being responsible for frequency exchange as depths reduces. The energetic wind resource of the area constantly affects the directionality of waves, with gustiness but also providing an additional source of local "young" seas generation, which is combined with swells.

Table 4.5: West Hebrides Seasons Indices

-	West Hebrides											
	Season 1						**Season 2**					
	H_{sig}		T_{peak}		T_z		H_{sig}		T_{peak}		T_z	
	ECMWF	**CFSR**	**ECMWF**	**CFSR**	**ECMWF**	**CFSR**	**ECMWF**	**CFSR**	**ECMWF**	**CFSR**	**ECMWF**	**CFSR**
Correlation	0.95	0.95	0.94	0.93	0.96	0.96	0.95	0.95	0.96	0.95	0.96	0.96
Average Buoy	2.69	2.69	10.89	10.89	6.83	6.83	1.98	1.98	9.89	9.89	6.21	6.21
Average SWAN	2.04	2.20	10.72	10.54	6.23	5.71	1.63	1.73	10.06	9.71	6.14	5.93
Bias	-0.65	-0.49	-0.17	-0.35	0.60	-1.12	-0.35	-0.25	0.17	-0.18	-0.07	-0.28
rms	0.88	0.86	3.58	3.71	1.55	1.83	0.54	0.54	2.05	2.35	1.01	1.25
SI	0.32	0.32	0.32	0.34	0.22	0.26	0.27	0.27	0.20	0.23	0.16	0.20
MPI	0.95	0.95	0.83	0.83	0.89	0.89	0.97	0.97	0.85	0.85	0.90	0.90
	Season 3						**Season 4**					
	H_{sig}		T_{peak}		T_z		H_{sig}		T_{peak}		T_z	
	ECMWF	**CFSR**	**ECMWF**	**CFSR**	**ECMWF**	**CFSR**	**ECMWF**	**CFSR**	**ECMWF**	**CFSR**	**ECMWF**	**CFSR**
Correlation	0.96	0.96	0.96	0.96	0.91	0.91	0.96	0.95	0.95	0.94	0.96	0.95
Average Buoy	1.99	1.99	8.59	8.59	5.53	5.53	2.38	2.38	10.30	10.30	6.34	6.34
Average SWAN	1.71	1.69	9.19	8.21	5.72	5.78	2.23	2.30	10.62	10.27	5.98	5.83
Bias	-0.28	-0.30	-0.27	0.38	0.59	0.25	-0.15	-0.08	0.32	-0.03	-0.36	-0.51
rms	0.59	0.79	0.71	5.21	2.96	1.84	0.61	0.61	2.44	2.6	1.12	1.25
SI	0.30	0.42	0.35	0.31	0.34	0.33	0.25	0.25	0.23	0.25	0.17	0.19
MPI	0.96	0.96	0.86	0.84	0.86	0.91	0.96	0.95	0.84	0.84	0.90	0.90

The combination of high winds and incoming swells at such shallow depths requires a detailed re-presentation of non-linearity for the area. The highest average values of H_{sig} were recorded during winter months, similar to Blackstone. The performances are high for both models, although the increased temporal resolution offers smaller biases for the CFSR data and similar SIs and rms, see Table 4.5 and Figure 4.6.

The results for seasonal periods have more diverse alterations (see Table 4.5). The correlation with measured wave data for both models is high for the summer and spring months (Seasons 2-3). Similar results with closely followed biases and rms, though the ECMWF has slightly better performance attributed to the improved spatial resolution of the dataset. During Winter months (Seasons 1 and 4) so different performance. For Season 1, both models underestimate the T_{peak}, however CFSR shows underestimates and presents higher rms differences for all parameters. Similar performance is seen for T_z with CFSR driven waves presenting constant lower values.

The Moray Firth buoy, is located at 54 meters depth and has been active since 2008 (CEFAS, Center for Environment, 2014). It is located in a intermediate to shallow water region, with non-linear interactions dominant in the environment. Location of the buoy is at the North-East of Scotland, in the Moray Firth gulf. The area is exposed to swell originating from the North side, while the East and West boundaries are dry points (land masses). Subsequently, the swell component is not as strong as for the previous locations, although the area introduces several shallow water mechanics of diffraction, diffusion, depth breaking, triads, that have a significant effect on waves, thus pointing that SWAN is suitable and can be adjusted for such areas.

Table 4.6: Moray Firth Seasons 1-2 Indices

	Moray Firth											
	Season 1						**Season 1**					
	H_{sig}		T_{peak}		T_z		H_{sig}		T_{peak}		T_z	
	ECMWF	**CFSR**	**ECMWF**	**CFSR**	**ECMWF**	**CFSR**	**ECMWF**	**CFSR**	**ECMWF**	**CFSR**	**ECMWF**	**CFSR**
Correlation	0.94	0.94	0.90	0.90	0.95	0.94	0.90	0.93	0.85	0.85	0.93	0.94
Average Buoy	1.47	1.47	7.96	7.96	4.89	4.89	0.72	0.72	6.58	6.58	3.96	3.96
Average SWAN	1.25	1.53	8.41	7.49	5.08	4.73	0.52	0.62	8.36	7.11	4.54	4.14
Bias	-0.22	0.04	0.44	-0.47	0.19	-0.16	-0.20	-0.10	1.78	0.53	0.58	0.18
rms	0.49	0.54	3.52	3.45	1.42	1.42	0.32	0.28	3.99	3.58	1.50	1.30
SI	0.33	0.36	0.44	0.43	0.29	0.29	0.44	0.38	0.60	0.54	0.37	0.33
MPI	0.97	0.97	0.87	0.87	0.92	0.92	0.98	0.98	0.90	0.90	0.94	0.94
	Season 3						**Season 4**					
	H_{sig}		T_{peak}		T_z		H_{sig}		T_{peak}		T_z	
	ECMWF	**CFSR**	**ECMWF**	**CFSR**	**ECMWF**	**CFSR**	**ECMWF**	**CFSR**	**ECMWF**	**CFSR**	**ECMWF**	**CFSR**
Correlation	0.91	0.92	0.86	0.85	0.94	0.94	0.93	0.94	0.89	0.89	0.95	0.95
Average Buoy	0.91	0.91	6.14	6.14	3.99	3.99	1.37	1.37	7.86	7.86	4.63	4.63
Average SWAN	0.67	0.84	7.42	6.71	4.29	4.20	1.17	1.46	8.11	7.59	4.69	4.54
Bias	-0.25	-0.07	1.28	0.56	0.30	0.20	-0.20	0.09	0.25	-0.27	0.06	-0.09
rms	0.42	0.40	3.84	3.64	1.27	1.29	0.44	0.46	3.45	3.59	1.14	1.04
SI	0.45	0.44	0.62	0.59	0.31	0.32	0.31	0.33	0.43	0.45	0.24	0.22
MPI	0.98	0.98	0.90	0.90	0.94	0.94	0.97	0.97	0.88	0.88	0.93	0.93

In this partially "enclosed" environment the generation of waves by the driven models, is again satisfactory with correlation indexes over 0.9, while the model performance MPI is close to unity, resulting in very good model hindcast. Although, the improved temporal resolution of CFSR displays better performances, specifically for H_{sig}, all the seasonal rms errors have very close behaviour, the ECMWF data on the other hand present larger underestimations compared with the CFSR biases (see Figure A.4).

In all cases though the difference is in favour of the CFSR wave driven data which has reduced average biases see (Table 4.6). The T_z period has similar results with correlation factors and MPI high, and correlation of the T_{peak} is above 0.85 for both fields. Peak period T_{peak} though shows that CFSR consistently performs better than ECMWF with both models usually overestimating (see Figure 4.8). Due to the enhanced temporal term the bias presented as almost 50% less than its ECMWF counterparts, while the overall rms and SI indices are in favour of the CFSR.

The final location under consideration the Firth of Forth, the buoy is at 65 meters depth and is located on the outskirts of Edinburgh. The location has similar characteristics as the Moray Firth, with swell originating from the North. Detailed indices are given in Table 4.7 and Figure 4.7.

Table 4.7: Firth of Forth Seasons 1-2 Indices

	Firth of Forth											
	Season 1						**Season 2**					
	H_{sig}		T_{peak}		T_z		H_{sig}		T_{peak}		T_z	
	ECMWF	**CFSR**	**ECMWF**	**CFSR**	**ECMWF**	**CFSR**	**ECMWF**	**CFSR**	**ECMWF**	**CFSR**	**ECMWF**	**CFSR**
Correlation	0.97	0.89	0.94	0.93	0.96	0.95	0.94	0.87	0.89	0.88	0.93	0.94
Average Buoy	1.50	1.50	8.08	8.08	5.16	5.16	0.71	0.91	6.47	6.47	4.05	4.05
Average SWAN	1.32	1.91	8.87	7.78	5.81	5.14	0.60	0.93	7.82	6.51	5.01	4.29
Bias	-0.18	0.41	0.78	-0.30	0.65	0.02	-0.11	0.22	1.35	0.04	0.96	0.24
rms	0.39	1.02	2.88	2.71	1.46	1.38	0.25	0.50	3.47	3.18	1.80	1.28
SI	0.26	0.67	0.35	0.33	0.28	0.26	0.35	0.70	0.53	0.49	0.44	0.31
MPI	0.97	0.97	0.87	0.87	0.92	0.92	0.98	0.98	0.90	0.90	0.93	0.93
	Season 3						**Season 4**					
	H_{sig}		T_{peak}		T_z		H_{sig}		T_{peak}		T_z	
	ECMWF	**CFSR**	**ECMWF**	**CFSR**	**ECMWF**	**CFSR**	**ECMWF**	**CFSR**	**ECMWF**	**CFSR**	**ECMWF**	**CFSR**
Correlation	0.94	0.86	0.90	0.91	0.95	0.95	0.97	0.89	0.91	0.92	0.96	0.96
Average Buoy	0.88	0.88	6.24	6.24	4.11	4.11	1.46	1.46	7.55	7.55	4.79	4.79
Average SWAN	0.71	1.10	6.95	6.11	4.55	4.21	1.24	1.95	8.69	7.67	5.44	4.95
Bias	-0.17	0.22	0.71	-0.13	0.44	0.11	-0.22	0.49	1.14	0.12	0.64	0.16
rms	0.32	0.69	2.99	2.50	1.29	1.14	0.38	0.95	3.34	2.80	1.40	1.01
SI	0.37	0.78	0.47	0.40	0.31	0.27	0.26	0.65	0.44	0.37	0.29	0.21
MPI	0.98	0.98	0.90	0.90	0.93	0.93	0.97	0.97	0.88	0.88	0.92	0.92

This buoy has the smallest recordings of waves, due to its location, with most energy being dissipated and the incoming swells not as strong as in the West part. In contrast with the previous case, Moray Firth, the performance of the CFSR is less than the ECMWF, and the MPI is similar for both models. With ECMWF driven waves presenting less errors and significant lower biases. The H_{sig}, is overestimated for all Seasons with CFSR, while the ECMWF although under-estimating the H_{sig} has a very low bias and is close to the average value, for all cases of seasons the SI of CFSR is under-performs significantly (see Figure A.5).

Subsequently, the period and direction components T_{peak}, and T_z, have a better performance with the CFSR driven field. As in the previous indices explained the higher temporal resolution allows for quicker directional information and at such shallow waters, the temporal effects improve periods measured. The rms period errors are substantially lower with the CFSR while SI is reduced.

Similar behaviour is noticed, with shallow water physical activities increase the scattering throughout the year as more non-linear terms such as diffusion and refraction affect the wave resource, see Figure 4.9-4.10. When separated into seasonal parameters, the comparison improves significantly, since it is focused on individual seasonal blocks, with most under-estimations occurring during winter seasons. Even though in those shallow environments the H_{sig} given by the driven ECMWF winds, SWAN present a smaller annual bias although their maxima values are smaller. Due to their temporal resolution, the CFSR generate a "peakier" environment with more volatile changes in the maximum and minimum parameters.

This can be attributed to the recorded SIs and the overall behaviour of the ECMWF wind product, which is accurate though is constant under-estimations, it leads to less discrepancies. The Blackstone location, which as mentioned, has open boundaries to the Atlantic, shows a distinct difference between the sets, see Figure 4.11-4.12.

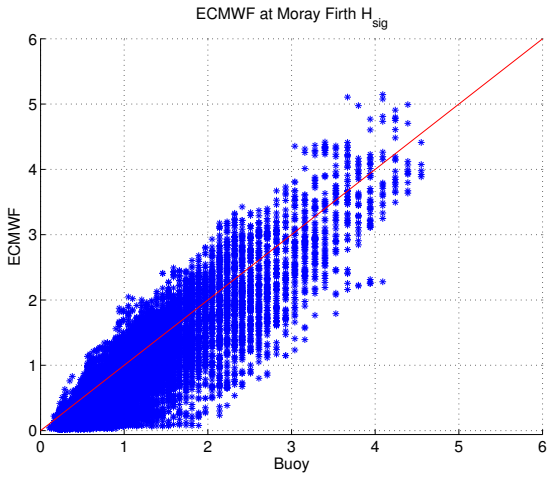

Figure 4.9: Moray Firth ECMWF

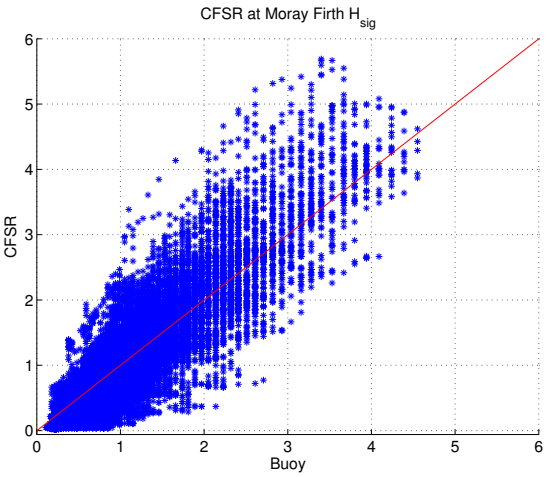

Figure 4.10: Moray Firth CFSR

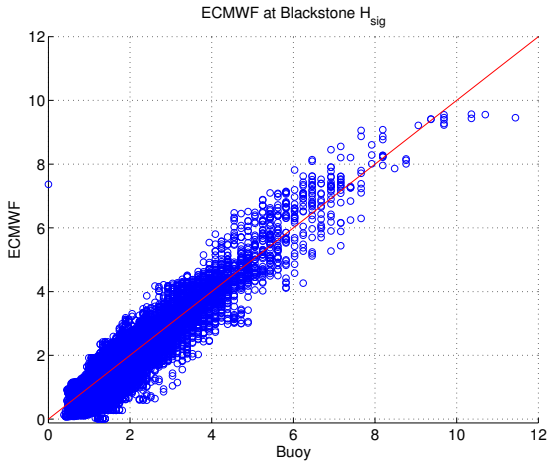

Figure 4.11: BlackStone ECMWF

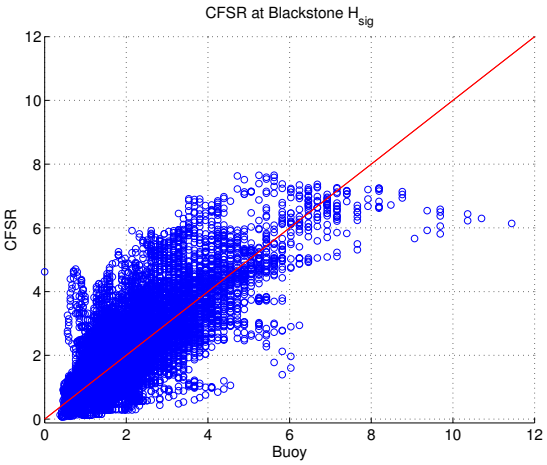

Figure 4.12: BlackStone CFSR

4.4.3 Wind Input Discussions

Two different wind products for use in numerical wave modelling, have been compared. Wind induced waves and wave propagation are strongly dependent on the quality of wind inputs. The use of a customized SWAN code for shallow water areas, allows to further examination of the effects of wind in nearshore applications. The difficulty of having a refined and high correlation of wind and waves at shallow water locations is presented and although SWAN model proves to be a reliable source for re-producing more complex seas, discrepancies are mainly dependent on the quality and behaviour of the wind used.

The area considered is the highly energetic Scottish coastlines, the West presented highest seasonal averages and wave resources, due to exposure at the Atlantic Ocean. East has milder wave characteristics, but the wave resource can still be regarded as energetic, due to its positioning the buoys and most nearshore application have enclosed characteristics with shallow water interactions affecting the resource to much greater extent.

The different winds used, extracted and processed, differ in temporal and spatial resolutions. The wind fields used were based on their optimal characteristics, spatial and temporal. In addition the set up process of SWAN includes additional inputs, bathymetry and boundary conditions which were kept constant throughout the comparison. The interaction of winds and waves, reveal difference in behaviour for each of the datasets. Temporal and spatial resolution is very important for wave resource assessments, thus the selection of a proper wind field would optimise and increase the confidence in hindcast or future forecast waves.

Buoy and hindcast measurements were divided, into four seasons for the year 2010, representing the seasonal changes in the wave fields, as expected all the buoys showed higher accuracies, during season 1 and 4, while season 2 and 3, exhibited a decrease which was much more obvious at the East coastline areas.

Results revealed that for the West coastline area of Scotland (Blackstone and West Hebrides buoys) the ECMWF outperforms its counterpart hindcast of the wave resource, with much smaller biases, lowered rms errors and reduced scattering. Although the 6-hourly ECMWF wind dataset, shows an trend in underestimating the wave resource, H_{sig} consistently was presented with lowered peaks.

The East of Scotland although exposed to high wind resource, has enclosed coastline characteristics, increasing the diffraction and refraction non-linear effects. In the Moray Firth Seasonal hindcast, overall CFSR outperformed the ECMWF waves, the main indexes showed that ECMWF consistently underestimates H_{sig}, while the T_{peak} are slightly overestimated. Both sets present similar *rms* errors with CFSR performing better in the representation of directionality.

The last location examined was the Firth of Forth, which showed different performances in contrast to the other buoys. The seasonal separation of the data, showed that the ECMWF data hindcast, the quantities perform better for season 1-2, while in season 3-4 they had better hindcasts.

Overall for the region of Scotland and North Sea, ECMWF data present better hindcast results, with similar high correlation coefficient given though by the CFSR data as well. In contrast ECMWF wind driven waves exhibit lower differences with recorded wave data, and although H_{sig} is underestimated SI and biases provided, are closer to the desired hindcast results.

In the case of the UK and Scottish coastlines, the preferred wind products seems to be the ECMWF. Though under-estimations appear, the overall scattering and distribution of re-produced data, show a better correlation to the measured values. This does not reduce the performance of CFSR data, while their higher temporal resolution allowed for better simulation of peaks, this behaviour though the performance in shallower locations, and could potentially used for applications which require peak observations.

4.5 Consideration of Bathymetry Interactions

Effects of the wind products quality was examined in the previous section, although the further interactions and potential limitations of the energy propagated within the model domain, have seldom been reported. The principals of wave modelling are considered to be universal, problems arise when applied in areas with different characteristics.

In this section the wave resource potential of a completely different Sea is attempted revealing issues in the applicability of SWAN, in the Mediterranean and Aegean Sea. In contrast with the wave resource of Western Europe, the Mediterranean basin can be considered as an isolated basin with minima wave components incoming from the narrow opening from the West (Straits of Gilbratar) and North East (Black Sea). Furthermore, the depth topography of this basin is constituted by sharp and rapid depth gradients, which affect the propagation of wave within a bathymetric mesh.

At a first glance the Aegean Sea looks like an easily understood environment with major swell components occurring as in open oceans. But the complexity of its bathymetry and presence of various Islands complexes, increases the level of difficulty for accurate wave resource estimations. Sudden depth fluctuations in the bathymetric profile, affect the estimated propagation and wave generation processes, while shallow water effects often result in the significant reduction of wave energy approaching the coastlines (Soukissian and Pospathopoulos, 2006; Korres *et al.*, 2011; Ayat, 2013; Pallares *et al.*, 2014; Veigas *et al.*, 2014).

Similar behaviour of winds was recorded for both previously tested wind products, although the focus was on the interpretation of wave components when energy was transferred from one grid point to the next, leading to alteration of the expected wave spectrum and irregular performance of peak period (T_{peak}).

4.5.1 Nesting and hindcast problems

Due to size of the area under investigation, the Mediterranean Sea, two separated grids were employed, see Figure 4.13. The area for which a thorough resource assessment, Aegean Sea, has a highly resolve bathymetry with 2.75 km by 2.5 km (approximately) spatial resolution, while the greater Mediterranean was chosen as the initial coarse mesh with resolution of 11 km by 10.5 km (approximately) (Amante and Eakins, 2014). As a wind input the CFSR product was chosen to its ability to reproduce higher peak in wave heights, the absence of oceanic swells for the areas under investigation and greater external boundaries, the identification of "extreme" winds is considered (NCAR, 2014).

The Mediterranean area has been assessed by several institutions and research centres, though most of them couple oceanic scale models, with coarser bathymetry and larger temporal resolution winds varying from 3 to 6 hours (Vannuchi and Cappietti, 2013; Hellenic Centre for Marine for Research, 2014; Athens, 2014). To the authors knowledge a highly resolved bathymetry was

first used for the wider Aegean Sea, with a highly temporal wind product for such an extensive validation. The results were in accordance with those of a research centre which performs daily hindcasts for the Aegean area, using the WAM model and wind products by the SKIRON model with 3 hours resolution providing the most up to date forecasts (Athens, 2014).

Several wave buoys were used to validate the model, the number and location of buoys allowed to estimate appropriately shallow and coastal locations where larger models cannot hindcast, due to physics limitations. The process allowed estimation and identification of wave resource for the Aegean Sea and a further study into the applicability and exploitation of waves as a renewable energy resource (see Section 5.3).

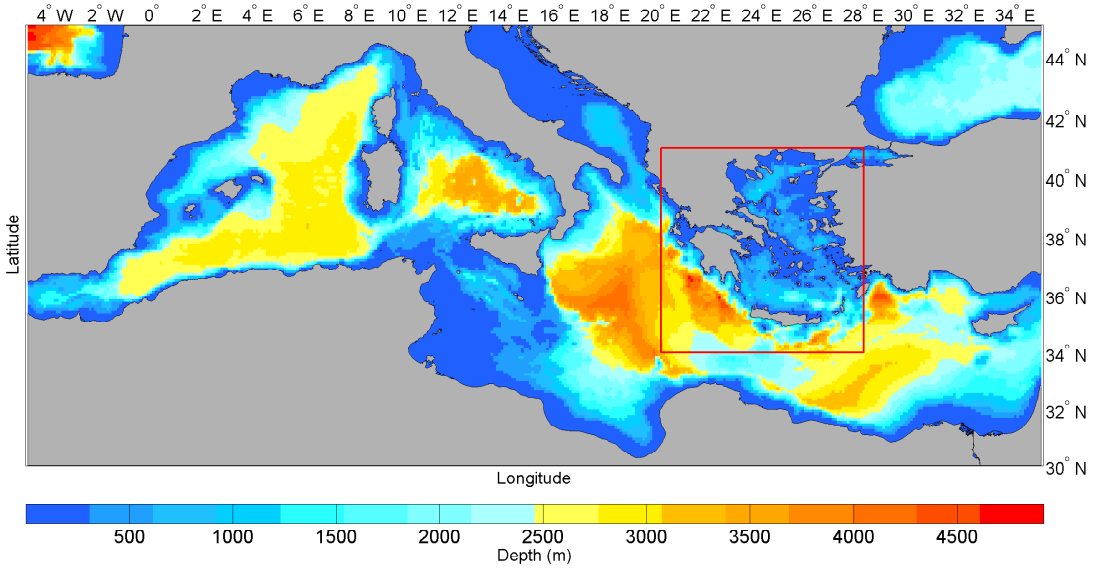

Figure 4.13: The coarse mesh and the subsequent nested Aegean area (B)

Due to the nature of bathymetry for the locations under investigation, model was run with all shallow water parameters active in both coarse and nested hindcast. Frequencies and directions were set within 25 and 24 bins respectively. The wind applied follow the Janssen's expression for exponential growth with a white-capping coefficient of 4.5. Quadruplet interactions are resolved in a semi-implicit way, allowing for additional recalculations per timestep while the bottom friction applied is constant and equal to 0.067 m^2/s^3. Triad interactions for the shallow water regions are fully operational as well as the breaking factor applied in nearshore areas. Finally, the coarse grid offered the boundary and initial condition for the nested, and more resolved Aegean hindcast (Lavidas *et al.*, 2014b).

Although, SWAN terms include enhanced solution for the shallow water terms, it is important for the modeller to take into account the local environment. From the initial screening runs performed, it was discovered that in the Aegean case rapidly changing gradients of the bathymetry led to irregular results and often underestimations (Soukissian and Pospathopoulos, 2006; Bertotti and Cavaleri, 2009; Mazarakis *et al.*, 2012).

With SWAN, the coastal areas are better re-presented, which poses a problem when it comes to choosing the propagation scheme. SWAN relies on solving Equation 3.1 for all of its components in regards with the wind input (as in this case), and separates each solution field into quadrant so that the energy is calculated and then propagated for each side. In all iterations from one geographic grid point to another, the quantities will be recalculated in accordance with new information about propagating energies of wind and waves. Rapidly changing depths of the Aegean, affect the CFL criterion stability. When not met, this results to the occurrence of exploding "hot-spots" in the area, affecting the shape of the peak period . To alleviate this problem the computational timestep and spatial resolution which affect the group velocities, have to be re-examined, with turning rates of frequency and direction have to be re-assigned (Dietrich *et al.*, 2012; Zijlema, 2014).

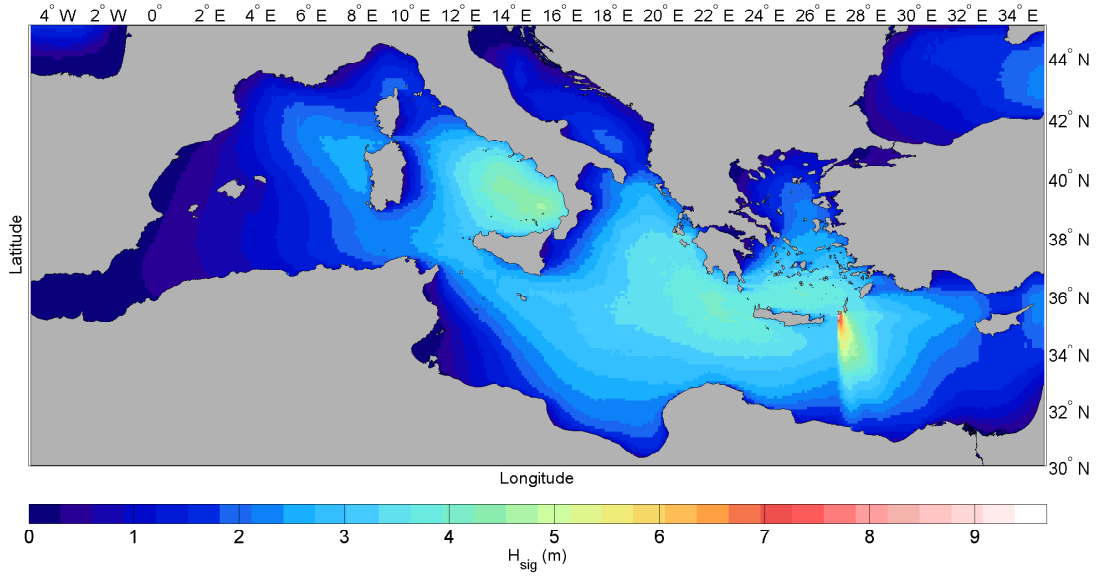

Figure 4.14: Exploding points of energy, affecting the H_{sig} hindcast

The detailed activation of shallow water mechanics and nature of the bathymetry, as activated and examined, affected hindcast output. Aegean "hot-spots" were identified in the East and West area of Crete, the Ionian Sea, Cycladic island complex, the East side of Attica and the various points of the Turkish coastlines (see Figure 4.14). Although Figure 4.15 indicate that the irregular performance of the hindcast, for the Pylos buoy (and with similar behaviour for all the locations), this "explosion" in propagated energy did not affect the output for H_{sig} (see Figure 4.16).

This is shown by the contours which represent only one of the many timesteps recorded with "hot-spots", see Figure 4.14. However not all the data could be included in the present section. The shallow water coastal location displayed an abnormal increase of the significant wave height, which results in "explosion" of waves and subsequently over-estimations on wave energy, see Figure 4.17. Similarly, peak period results clearly show an irregular performance

(see Figure 4.15), which affects the value of the peak period leading to alterations of the spectrum. This led to a shift of the spectrum at higher rates, shifting the tail of frequencies, leading to mis-estimation of wave power potential and disrupting the proper distribution of periods over the area, representing erroneous high frequencies as a norm (Hasselmann *et al.*, 1973; Vledder, 2012).

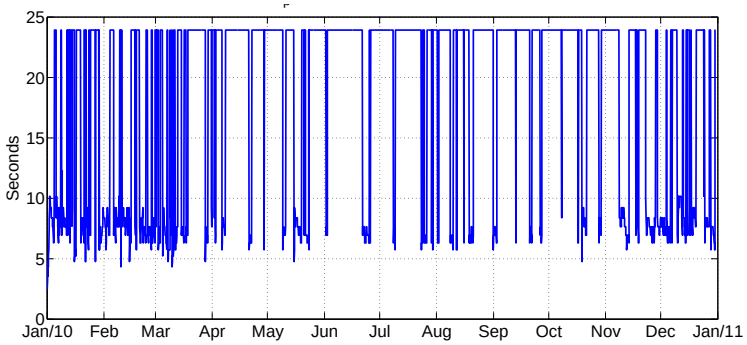

Figure 4.15: Effect on *SWAN* hindcast from the "hot-spots" on T_{peak}

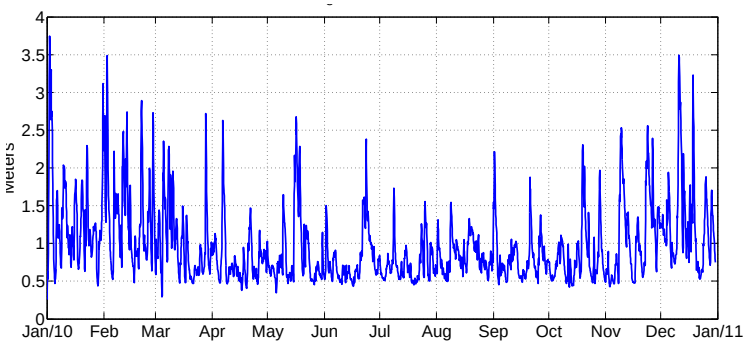

Figure 4.16: Effect on *SWAN* hindcast from the "hot-spots" on H_{sig}

The contours area in Figure 4.17, display the areas affected, sudden depth reduction around the islands affecting proper wave hindcast in the area. This displays the effect of H_{sig} and T_{peak} mis-hindcast and effect on the calculations for wave power, for that specific timestep the area at East of Crete displayed estimated wave power over 800 kW/m at the energy "exploding" area.

As mentioned previously the CFL and re-tuning of the turning rates of frequency and direction had to be investigated. Time-steps for the coarse grid were 3 and 1 hour, both were tested in order to calibrate the model and provide the necessary boundary conditions for the nested run of the fine grid. It is common practice to use a higher time-step for the coarser run (Komen *et al.*, 1994; Holthuijsen, 2007; Janssen, 2009).

In the use of a coarse mesh the resolution proved to be an obstacle, since the spacing was too large to represent shallow water mechanics such as the refraction process, while the representation of the many islands was not evident. In both cases the outcome shows the existence of hot spots in the fields (Rogers *et al.*, 2007), attempted an alternative approach to the problem

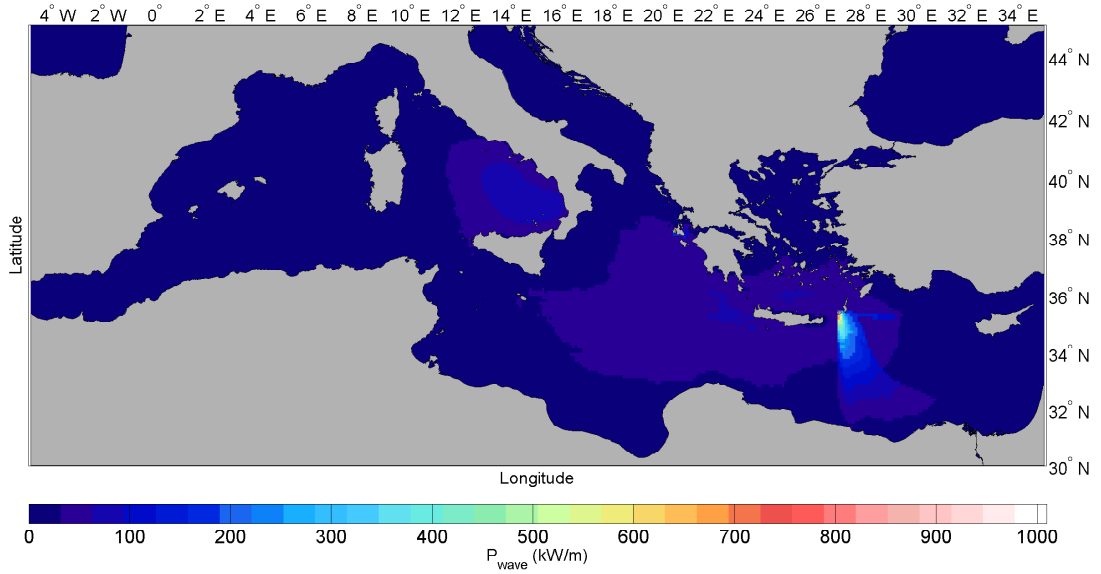

Figure 4.17: Effect on SWAN hindcast from the "hot-spots" on wave power

with a physical calculation on propagation of waves.

The turning rates of frequency (c_σ) and direction (c_θ) allow for the calculated energy which has to be re-calculated at a point, to be considered for the next timestep calculations. The sensitivity of these turning rates are dependent on the timestep set by the modeller and bathymetry gradients dominant in the domain.

$$|c_\sigma| = \alpha_\sigma \cdot \Delta_\sigma \left(\frac{1}{\Delta_t} + \frac{|c_x|}{\Delta_\lambda} + \frac{|c_y|}{\Delta_\phi} \right) \tag{4.7}$$

$$|c_\theta| = \alpha_\theta \cdot \Delta_\theta \left(\frac{1}{\Delta_t} + \frac{|c_x|}{\Delta_\lambda} + \frac{|c_y|}{\Delta_\phi} \right) \tag{4.8}$$

With Δ_t time domain, Δ_θ directional bins and Δ_σ frequency bins that have been set with the *CGRID* command, as mentioned in Chapter 2, within the domain of latitude Δ_ϕ, longitude space Δ_λ and c_x, c_y the propagation velocities, (Dietrich *et al.*, 2012).

The terms are directly connected with the CFL criterion , in case of the applicable implicit solution as proposed by (Hasselmann *et al.*, 1985; Bottema and van Vledder, 2008; Vledder, 2012). Their proper assignment will limit wave energy to shift and/or turn rapidly, in a single timestep calculation.

In addition, several ideal test-cases presented in Dietrich *et al.* (2012) noted that the erroneous assignment of these rates. They led to alleviation of "hot-spots" mainly in the use of highly resolved unstructured meshes, which affects the quality of the results with over-estimating and/or under-estimating.

Although it is not clear which is the optimal value, for our specific location the proposed value is close to unity, from a sensitivity approach the rates were increased from 0.5 to 0.75 and finally to 1. As a consequence, in the case of the Aegean Sea it is suggested that the modeller, if a high spatial resolution is used in a large domain, should consider tuning the turning values to 0.5-0.75, this results in alleviating the "exploding" spectrum originating by the high values of periods as seen in Figure A.6 and Figure A.7. It has to be noted that the turning rates for the CFL criterion are optionally activated.

4.6 Non-Linear Solvers

The non-linear or quadruplet term (S_{nl4}) affects the frequency distribution and wave parameters such as T_{peak} and H_{sig}, (Holthuijsen, 2007; Cavaleri *et al.*, 2007; Janssen, 2009; Komen *et al.*, 1994). The interactions of wind generated wave resource, incoming swells and local area characteristics are known to affect the frequency and wave form, with quadruplets being responsible for the transfer of frequencies on the spectral peak to both lower and higher. The dislocation towards higher frequencies being governed by frequency down-shifting due to the S_{in} and white-capping component ($S_{ds,w}$) (Rogers and Van Vledder, 2013).

Based on the seminal work by (Hasselmann, 1961, 1962a), identification of the non-linear effects were presented, although several assumptions were needed to simplify the mathematical derivation, which paved the way for a solution adopted by numerical wave models. The non-linear effects (S_{nl4}) or wave-wave interactions represent the interaction rates and final energy acquisitions by a non-active wave component (k_4). Initially three wave components are characterized as "active", based on these wave numbers (k_1, k_2, k_3), the interactions and energy of the forth is resolved see Equation 3.23 and Section 3.1.3.

The work of Hasselmann, (Hasselmann, 1961, 1962a,b), was expanded to actual sea environments, and established the interactions of wind generated seas and quadruplets. These non-linear interactions are responsible for the shift in spectral values initially from high to low wave numbers. While after development of the peak distribution shift to low wave numbers, an opposite transition from low frequencies to higher ones also occur. This process re-distributes the frequency values, leading to significant energy losses (Komen *et al.*, 1994; Cavaleri *et al.*, 2007).

These quadruplet interactions extend their effects from wind generated seas, to swell seas as well, with the S_{nl4} playing a role in the decay of swell components as they interact with local "young" seas. Effect of the wind input is also important, since the combination of Sin performance and the re-distribution due to S_{nl4} leads, depending on specific terms, to the separation of an existing spectrum in "young" and "old", with the latter representing newly formed swells that are detached by the process Young and van Vledder (1993).

The losses of these non-linearities decrease the energy of wave groups, showing that the decay time of a swell depends on these non-linear term and leads to the loss in the spectrum and spreading factor of the wave components in regards to the wind direction (Hasselmann, 1962a; Hasselmann *et al.*, 1973; Hasselmann, 1974; Young and van Vledder, 1993).

The non-linear mathematical formulation of wave-wave interactions allowed for the development of an approximate solution, which is now applied in numerical wave models (Hasselmann *et al.*, 1985). This approximation of solution for quadruplet terms was adopted by SWAN (Delft, 2014b), although in their work several other methods of solving Equation 3.1 were developed through Equation 3.23. The method proposed by Hasselmann *et al.* (1985), is known as Discrete Interaction Approximation (DIA), with some deficiencies been identified and reported (Tolman, 2013; van Vledder, 2006; Vledder, 2012). Some of the drawbacks include the overprediction of the wave spreading leading to overestimation of wave direction, while it has been also underlined that the DIA approach lead to underestimations of the overall final energy, and it is valid only for a specific area of spectrum set with the highest spectral values not accounted for (Rogers and Van Vledder, 2013; Bottema and van Vledder, 2008).

In SWAN the quadruplet and non-linear effects can be resolved either via a DIA approach (Hasselmann *et al.*, 1985) or exact computations known as XNL, (Rogers and Van Vledder, 2013; van Vledder, 2006; Resio *et al.*, 2001; Delft, 2014b), with exact solvers being more computational demanding. Latest developments presented a Generalized Multiple Discrete Interaction Approximation (GMD) (Tolman, 2013), with optimized terms on the non-linear solving equations. Although the computational requirements and cost are investigated to establish the correlation for accuracy and demands.

So far DIA are used in most models (WAMDI, 1988; Delft, 2014b; Tolman and development Group, 2014), since they are considered as good approximations and not as computational expensive as the exact solutions offered, although the option for exact solution exists in SWAN. The model resolves the action density equation as sink terms the total of the sink terms is denoted as S_{tot}, see Equation 3.1.

The performance and dependence of the DIA in a fully operational SWAN hindcast in order to establish the optimal way of calibrating the model. The physical alterations and interactions, based on optimal discretisation of frequencies were explored and interesting points were revealed. For the target of obtaining the best set of output by a spectral model, the modeller has to keep in mind the significance and interactions of the DIA with the input source terms. Although improvements may be made in the model by calibrating physical terms to fully understand the effect one must compare the spectrum output as well, with regards to the DIA and frequency.

4.6.1 Tuning the Frequency and Quadruplets

In the field of wave energy, two of the most important terms are the H_{sig} and T_e, with the latter directly correlated to the peak period component T_{peak}. The potential wave resource of an area is determined by the interaction of those two parameters. For this reason, and in order to assess impact of the non-linear solvers, the quantities validated involve the wave height and peak period. The comparison of each output was compared with buoy data as reference. Subsequently the optimal S_{nl4} and frequency resolution approximation is used as a base scenario.

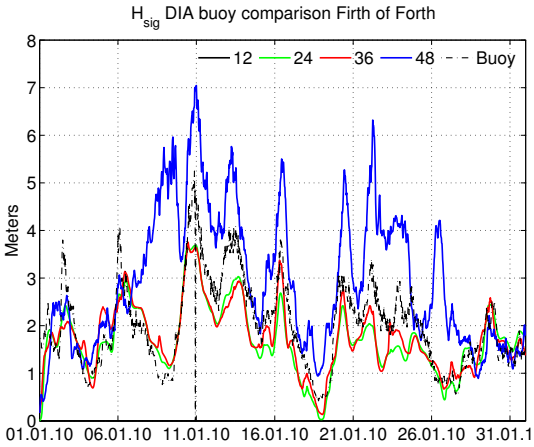

Figure 4.18: Firth of Forth *DIA* effect solver

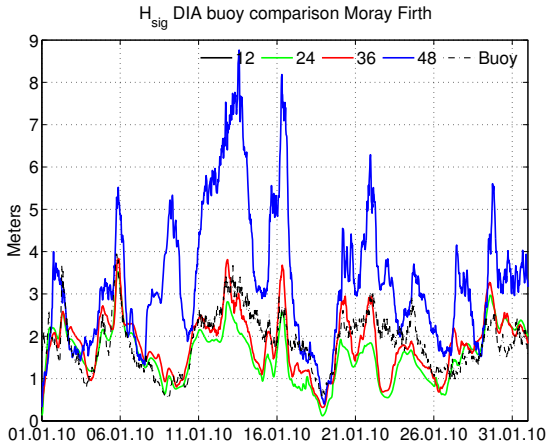

Figure 4.19: Moray Firth *DIA* effect solver

The hindcast was held for a period in 2010 specifically January; this period of winter is amongst the most energetic of the year, which necessitates in evaluating the solver at rapidly varying wind-wave conditions. These volatile conditions tested the non-linear approach by taking them into effect for each case. Spectral information were also assessed in terms of hindcasted spectral components, exhibiting the performance and potential pitfall of frequency dependence. Since higher resolution are favourable when striving to obtain optimal results one has to bear in mind the basic differences and alterations that are produced in comparison with their computational demands.

The directional resolution of the wave field was chosen to be analysed per 15^o, opting for 24 sub-divisions of the 360^o of wave directions, while the frequency resolution is increased by a step of 12 sub-divisions, starting from f_{msc} = 12,24,36,48, with a minimum initiating frequency set as is suggested in (Delft, 2014a). One should expect the highest resulted outputs as frequency increases, since DIA are responsible for the re-distribution of energy calculated in more dimensions though the computational demands should be expected to increase.

Validation for all hindcasts is presented with various statistical indices used in order to assess the performance, see Table 4.8-4.9. The configuration with f_{msc}=12, although completed failed to produce a valid hindcast due to the poor resolution, the f_{msc}=24,36 gave similar results with

Table 4.8: Validation of buoy data to hindcast, with incremental f_{msc}

	Firth of Forth							
	H_{sig}	T_{peak}	H_{sig}	T_{peak}	H_{sig}	T_{peak}	H_{sig}	T_{peak}
	f_{msc}=12		f_{msc}=24		f_{msc}=36		f_{msc}=48	
MPI	0	0	0.94	0.78	0.94	0.78	0.94	0.78
Average buoy	2.02	8.36	2.02	8.36	2.02	8.36	2.02	8.36
Min Buoy	0.42	2.7	0.42	2.7	0.42	2.7	0.42	2.7
Max Buoy	5.25	16	5.25	16	5.25	16	5.25	16
Average *SWAN*	0	0	1.69	8.74	1.76	6.82	2.9 4	5.23
Min *SWAN*	0	0	0.006	2.42	0.13	1.5	0.166	1.24
Max *SWAN*	0	0	3.63	16.34	3.68	14.85	7.04	9.22
Bias	0	0	-0.32	0.38	-0.25	-1.5	0.92	-3.12
rms	0	0	0.58	2.73	0.58	3.29	1.48	3.95
SI	0	0	0.29	0.32	0.28	0.39	0.73	0.47

Table 4.9: Validation of buoy data to hindcast, with incremental f_{msc}

	Moray Firth							
	H_{sig}	T_{peak}	H_{sig}	T_{peak}	H_{sig}	T_{peak}	H_{sig}	T_{peak}
	f_{msc}=12		f_{msc}=24		f_{msc}=36		f_{msc}=48	
MPI	0	0	0.95	0.76	0.95	0.76	0.95	0.76
Average buoy	1.86	8.88	1.86	8.88	1.86	8.88	1.86	8.88
Min Buoy	0.56	3.8	0.56	3.8	0.56	3.8	0.56	3.8
Max Buoy	3.94	17.2	3.94	17.2	3.94	17.2	3.94	17.2
Average *SWAN*	0	0	1.55	8.05	1.82	5.76	3.31	5.1
Min *SWAN*	0	0	0.12	2.42	0.31	1.82	0.32	2
Max *SWAN*	0	0	0.352	14.85	3.83	11.16	8.76	10
Bias	0	0	-0.3	-0.82	-0.04	-3.11	1.44	-3.77
rms	0	0	0.62	2.93	0.53	4.56	1.92	4.86
SI	0	0	0.33	0.33	0.28	0.51	1.03	0.54

the biases and MPI although the maxima values, as resolution increased. Improvements in rms and SI remained in similar terms for the Firth of Forth while the Moray Firth was slightly poorer. Surprisingly the f_{msc}=48 produced the most "extreme" results with significant over-estimations in the terms while the scatter indices were significantly increased, the comparison against the buoy data were examined in Figure 4.18 and 4.19.

By increasing the frequency resolution, the required computational resources also (as expected) increased. Specifically, doubling of the f_{msc} from 24 to 48, resulted in almost double the required time for the solution, making the latter approach most expensive (see Table 4.10).

Table 4.10: Computational requirements of different f_{msc}

	Computational requirements, θ_{mdc}=24 and f_{msc} variable			
	f_{msc}=12	f_{msc}=24	f_{msc}=36	f_{msc}=48
Min/day of simulation	2.74	5.39	7.24	10.14

4.6.2 Frequency Effect on Approximating Spectral Values

Spectral data correspond to the direction and frequency space characteristics of a wave field and the hindcasts also produced spectral information which correspond to the buoys. These informations were transformed to express the true variance of the quantity in (m^2/Hz), allowing a direct comparison with recorded spectral information. Although the buoys record typically less bandwidth of frequencies, the final shape offers an accurate representation of the sea state, such that the hindcast and actual measurements may be compared. The process seemed to operate reasonably well with exceptions of the very coarse (f_{msc}=12) and high (f_{msc}=48) resolutions. The first failed to produce a comprehensive hindcast, while the latter led to a "spike" in the quantities and although the generation trend was the same, output was almost double the measured quantity, see Figure 4.18-4.19 and Table 4.8-4.9.

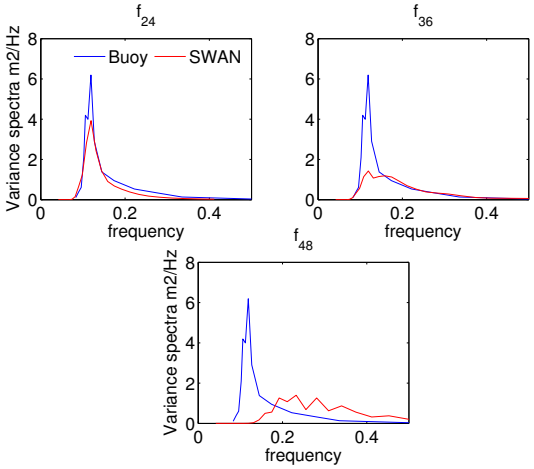

Figure 4.20: 25^{th} Jan. Firth of Forth

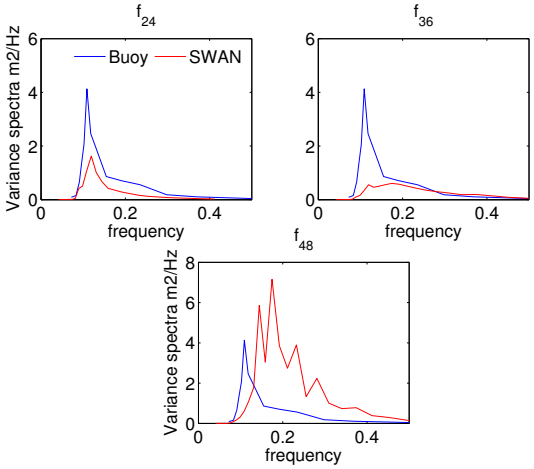

Figure 4.21: 25^{th} Jan. Moray Firth

The increase in resolution of the frequency domain affected the output of the spectra values, for this reason spectral data information from the buoy location are retrieved, two separate days, the 25^{th} of January 2010 and the 1^{st} of February 2010 (see Figure 4.22-4.23).

Examination of the spectrum hindcast data and how they fit on the recorded data showed that the highest resolution of frequency, as in the case of H_{sig}, has produced a high "peak" of variance. On the other hand, for both cases, the division into 24 bins has the closest comparison. Shape is at similar frequencies, with the peak frequency being well recorded although the magnitudes are under-estimating the actual spectrum. For the recordings of 25^{th}, in both cases the f_{msc}=24 shows good agreement in both locations, although the f_{msc}=48 for Moray Firth

places the peak of the spectrum after the actual occurrence and the f_{msc}=36 solution shows the poorest results in both cases (see Figure 4.20-4.21).

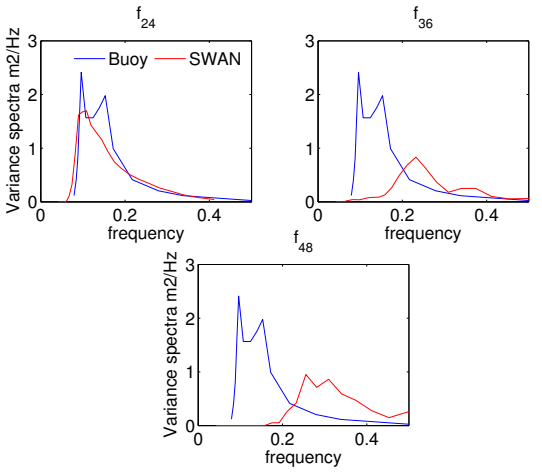

Figure 4.22: 1^{st} Feb. Firth of Forth

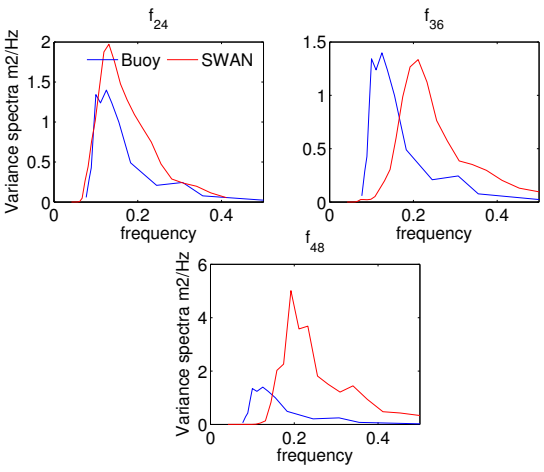

Figure 4.23: 1^{st} Feb. Moray Firth

For the second date under investigation and especially for the Moray Firth f_{msc}=24 results although located similar magnitude are over-estimating, the f_{msc}=36 model matches the recordings in magnitude, although the peak and overall shape is dislocated to higher frequencies. For both locations the high resolution option f_{msc}=48, shows the greatest inconsistencies (see Figure 4.22-4.23). Thus, an increase in the expected bins of frequencies only produces a longer "expected" highest frequency and distorts the comparison. This must be taken into account especially when the hindcast is structured as often times the highest frequency is not typically known.

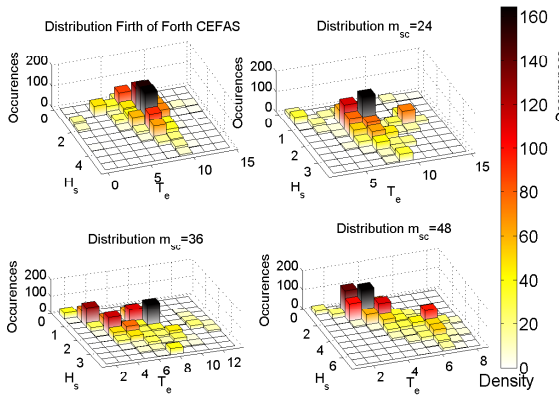

Figure 4.24: Bivariate at Firth of Forth

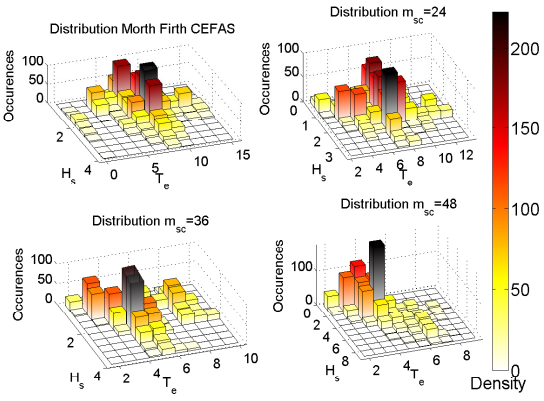

Figure 4.25: Bivariate at Moray Firth

It is imperative not only to assess the statistical indices but also the spectral effects prior to the full application of a model. Such effects may lead to improper coupling of the spectral components with other models and/or the incorrect use of spectral values as boundaries for a nested model. As mentioned in Equation 3.23, DIA are directly related to the frequency

component by supplying higher resolution as an energy re-distribution results for a higher number of frequencies increases. Although this increase may seem logical in terms of higher resolution output, in fact it forces the re-distribution to take place over a much larger number of frequencies. As stated in van Vledder (2000), the alteration of the frequency component to a higher numbers, distorts the favourable area of frequency discretisation, and DIA favour a 1.1 frequency resolution. Extreme alteration of the (λ_{DIA}) coefficients was performed by Vledder in the previous study which led to the degradation of results.

The higher frequencies show that the wave components, which govern the quadruplet interaction increase, which in turn exhibits instability when it comes to the solver solution. These problems were not reported when the use of the XNL are used van Vledder (2006, 2000); Vledder (2012), though it was underlined that these exact solutions pose a significant computational requirement on the system, by increasing both the computational requirements and run time.

Since numerical models offer hindcast/forecast of seas states for offshore applications, the spectrum irregularities may lead to inaccuracy of any potential analysis that requires the spectral components to be accounted for. Specifically application to wave energy and resource assessments are connected with the elimination of such errors in order to provide reliable estimates.

Wave energy is based on the bivariate distribution of H_{sig} and T_e (see Figure 4.24-Figure 4.25). With the energy period calculated by the spectrum a ration of the negative and zeroth spectral moment (i.e. $T_e = -m_1/m_0$), that is used, for elaborate information on the process (see Section 5.2.4).

As the maximum frequency resolution increase, the numbers of frequencies in the quadruplet interaction also increase, thus the number of wave components that have to be calculated. This leads to significant differences in the spectrum between model and buoy measurement. The lowest resolution failed to produce any substantial results, while the highest resolution of the frequency bins, lead not only to distortions in both phase and magnitude spectrum but also in an abnormal over-estimation of wave parameters (i.e. H_{sig}). The alteration of the shape DIA parameter showed the over/under-estimation can be controlled by reducing the shape of the distribution, by allowing the wave components to reach different angles and resonance conditions.

This section shows that the increase of frequency binning does not always lead to optimal wave output components as the spectrum calculated varies significantly. The DIA solution show a high sensitivity to frequency resolution alterations, often leading to un-expected results. The correlation and examination of both spectrum and wave parameters, must be taken into account in order to establish the best calibration/validation of the numerical model, especially when considering the assignment of an initial lower/higher frequency. The selection of a conservative

approach in the frequency bins, ensures that the results will keep their robustness and although under-estimation may occur more often, the output can be utilised with more confidence. For this reason it is desirable to discretise the frequency resolution from 24 up to 30 bin intervals. Alternatively, the user has to ensure that the if both lower and higher values are assigned, the latter has substantial differentiation from the first.

4.6.3 Tuning the DIA Shape Coefficient

In this section an alternative comparison for the tuning of the shape coefficient (λ_{DIA}) was undertaken, in an attempt to provide comprehensive results for the possibility of calibration of the shape coefficient. Four configurations of quadruplet solving processes are assessed via a explicit solver D2 and explicit D4 per sweep, and fully explicit per iteration D3, with the latter allowing interpolation of the explicit solution at the neighbouring points D4 (Delft, 2014a). The non-linear quadruplet, S_{nl4}, interactions were altered based on the availability of SWAN to resolve per sweep or per iteration, in explicit or implicit way (Delft, 2014b). This led to a significant difference in the solver, since the quadruplet integrals calculated for each wave number, at each iteration or sweep, would carry differences on the final negative lobe of the non-linear term. The shape parameter and weight of the non-linear terms were adjusted to 0.15 and 3.75 times 10^5 respectively, as found in Hasselmann *et al.* (1985); Vledder (2012).

The approach of solution, sweep or iteration affects the SWAN component. Since the model separates the solution in four distinct quadrants, and group velocities in the longitude and latitude direction (c_x,c_y). Due to the nature of the total sink term the overall solution is separated in negative and positive parts. These are solved for every point and after each propagation update to every grid point an update is made to the spectral space. This process is repeated for all time steps, with alternating between sweep or iterational process.

While the iteration process is expected to be more computational demanding, maximum number of iteration can be adjusted to lower or higher levels. The S_{nl4} terms were also calculated in an implicit or explicit manner, for the four sweep approach the interactions are calculated prior to the sweep and then integrated. The other method allows for individual calculation of every interactions and then implicitly integrated to the sweep. Difference between the techniques is necessity of solution to be stored or not, within the memory of computational station. Second approach does not require the solutions to be stored although increase the computational costs of calculation per timestep (Delft, 2014b).

The hindcast is held for the period January-March 2010, this period of winter is amongst the most energetic of the year, thus the necessity for evaluating the solver at rapidly varying wind-wave conditions. These volatile conditions tested the effects on the non-linear approach, taken into effect at every different case. The alterations in distributions of wave components and density distributions are presented with distinct differences for every case.

In the previous section it was noted that the importance of the wave-wave interactions is not solely of interested in wind generated seas, but also in the swell and local seas interactions. These interactions shift and exchange frequencies between high and low areas of the spectrum, with the points located at shallow to mid-water depths, it was expected that the dominant exchange will occur from the low area to highest periods, which will in effect diversify the final Density for every solution proposed.

The assessment of the output give good performance for all indices, see Table A.3-A.2. Computational time requirements are calculated for each solution and the minutes/day(m/day) of simulation by SWAN were 7.72 m/day for *DIA*1, 9.65 m/day *DIA*2, 7.9 6m/day *DIA*3 and 5.94 m/day *DIA*4.

At Moray Firth all the solutions have been correlated with the buoy H_{sig} and T_{peak}, all have followed the trend of waves noticed. In the case of both the parameters compared and all yielded underestimations. By comparing the products for the Moray Firth, it is noticeable that the D4 solution has better average H_{sig} with a lower bias and rms value than its counterparts, though on the other hand the D1 solution offers the smallest deviation in the peak period measurements. The same trend is also noticeable for the peak values of H_{sig} and T_{peak}, with D4 and D3 obtaining the closest values to the buoy maxima.

In the case of Firth of Forth the results show again that D4 H_{sig} has the lowest bias, rms and solution provides the highest recorded H_{sig}. Concerning the period simulated by D1 although T_{peak} exhibit lower bias, its rms values are inferior than D4 approach and similar to D2, D3. The T_{peak} offered by the fourth approach offers the average period in seconds with higher bias. For both locations D2, D3 provided similar behaviour, although the D1 and D4 have a greater discrepancy between them. Furthermore, the times of computation per day of hindcast are presented, and D2 and D3 have the highest times of hindcast, D4 records the lowest while D1 gives a moderate value. Taking into account the results of H_{sig} and T_{peak}, the computational time of lowest with the other solution are compared. Differences of the fourth selection with the first, third and second are 30.13% 62.54% and 34.04% respectively. D4 as given in the comparison of indices has the highest solution closest to the real buoy measurements.

Similar comparison is presented with the peak period parameter for both locations, all the simulated results follow the trend of recorded period, D3 and D2 present similar magnitudes and D1, D4 having the largest differences, with D1 solution presenting a much "peakier" resulting period with minimum periods being higher more than the D1 from 1-2 seconds in the case of Firth of Forth. For the Moray Firth D4 had the highest bias although the rms differences are higher in D2, D3. The D1 approximation again offers a "peakier" performance but this time overall, with its maxima and minima being higher/lower that the D4 solution and had closer correlation with the buoy measurements.

The differences between the approximation are expected to alter the distributions of energy

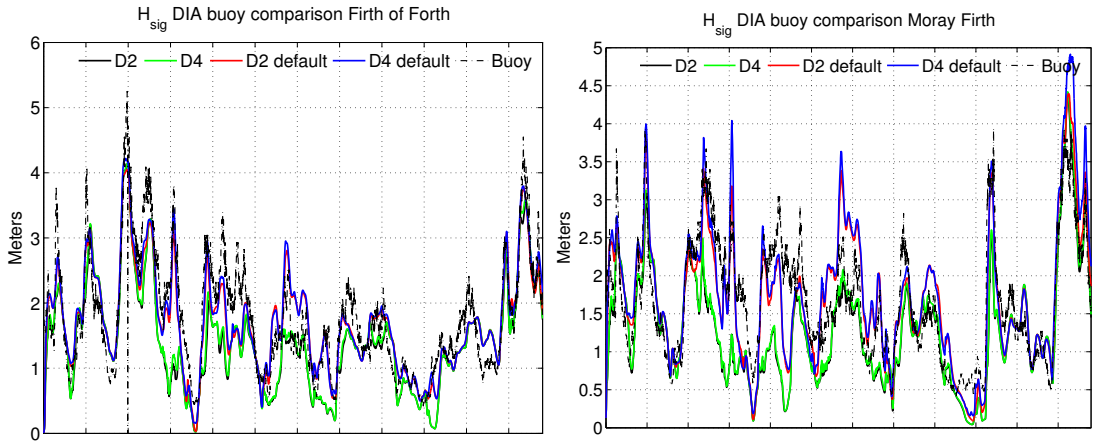

Figure 4.26: Comparison of Default and Hasselmann terms

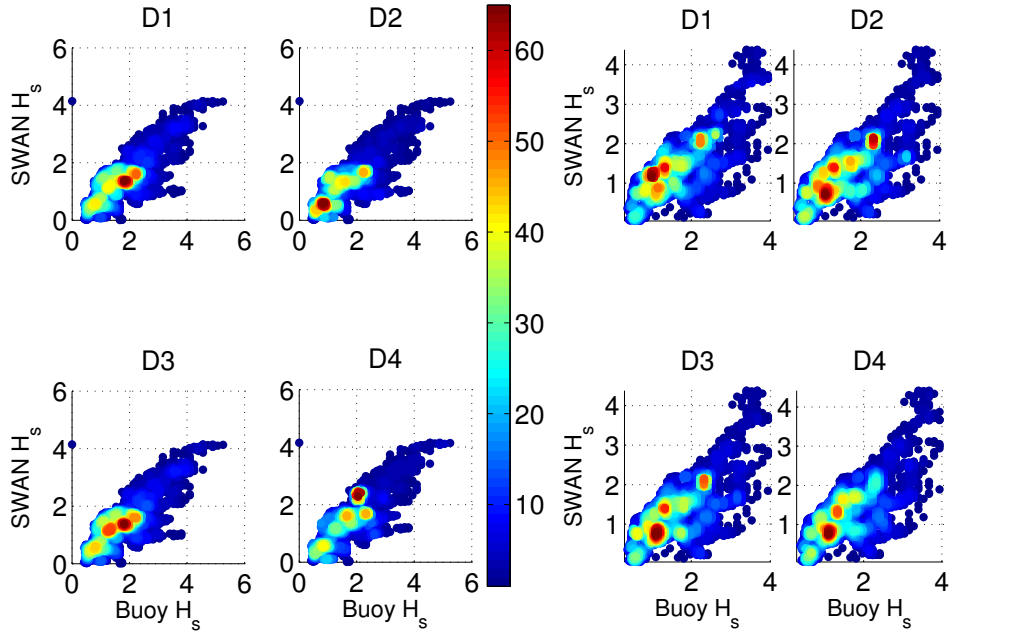

Comparison of *DIA* Firth of Forth

Comparison of *DIA* Moray Firth

Figure 4.27: Comparison of *DIA* (colobar shared)

and shift the spectrum to higher frequencies. Different schemes alter the density distribution of the parameters affecting the spectrum, H_{sig} and T_{peak}, as seen in Figure 4.26-4.27. D2 approximation had the "fullest" simulated H_{sig} residing to a much higher area, while D4 is mostly located at 1.5 meters. Although in the case of the Firth of Forth D4 had more populated areas at higher wave heights. Following the H_{sig}, peak period (T_{peak}) is examined at Moray Firth, D2 and D3 have middle and high range periods populated, leading to lower frequencies and increasing the energy content of the spectrum, while D4 had most populations at the middle areas. In the case of the Firth of Forth, D1 again had more periods residing in higher areas, with D3 being similar in distribution to the D4 solution.

The tunable shape coefficient of the DIA, poses a significant though very unstable parameter for the energy re-distribution, when looking to calibrate the model (personal communication van Vledder (2015)). The study found that the original shape coefficient, λ_{DIA}=0.25, although gave some over-estimations, it performed well enough for the time-series. The unpublished proposal of Hasselmann (discussed in Vledder (2012)), revealed that a reduction of the shape factor reduces the peaks and removes over-estimation, for the area of the East Scottish coastline. A shape coefficient from λ_{DIA}=0.23-0.325, appeared to be adequate for representation of the sea state, consideration has to be given to the initial calibration of the model. By differentiation of DIA component the modeller may reduce or enhance the model accuracy based on location specific physical interactions. This in comparison with the proper designation of the frequency resolution, will ensure the stable operation of the model.

4.7 Length Effects

As mentioned in the previous parts of this Chapter 4, the physical and tunable process can provide results that enhance or deviate from the recorded measurements, leading to erroneous behaviour. In Section 3.2.2, the various choices for boundary application were presented, although as it is seen in this section the effect of the boundaries to the hindcast process is also dependent by the mesh size. Depending on the grid size different boundary approaches may prove to be more accurate.

The non-linear, terms are activated and resolved in a semi-implicit way, while locations under investigation are located in mid and shallow water depths. The bathymetry profile for the wider Scotland and North Sea locations, could be classified as an overall "smooth" area, in contrast to seas like the Mediterranean. Boundary generation, growth and propagation is based on the JONSWAP spectrum , which is appropriate for wind generated fetch limited seas. The direction and frequencies that will represent the sea states are separated into 24 and 25 bins each, while a full 360 degrees circle is considered for the spectral components, with minimum initial frequency set to 0.0418 Hz. Wind wave induced generation and interactions follow the

exponential growth formulation, with power of the high frequency tail been adjusted to a fifth higher order term.

Our main area of interest is the North Sea environment, thus two different sized meshes are employed. The first one is encapsulating the whole Scottish West and East side denoted from now on as mesh A, while the latter one is covering the East Side (wider North Sea) denoted as mesh B. The coordinates of mesh A are 0^o East to 10^o West, 55^o South to 61^o North, the mesh B has the same latitude coordinates while the longitude distance is half with length 0^o East to 5^o West (see Figure 4.28).

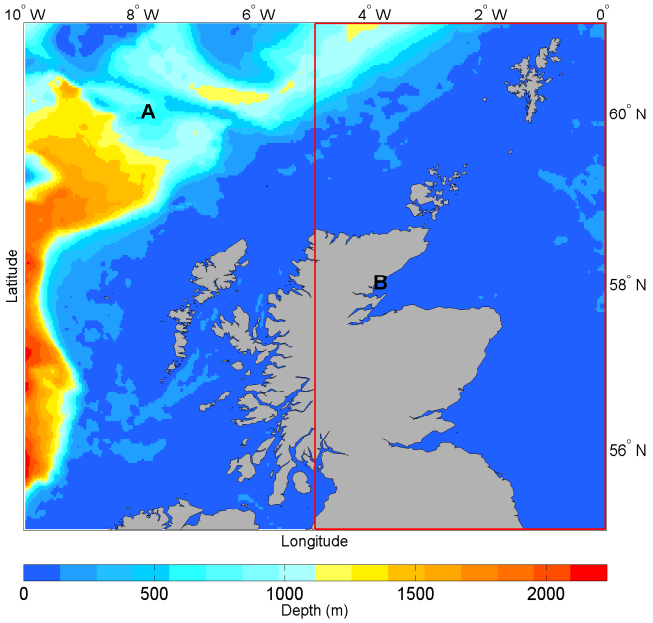

Figure 4.28: Mesh A and mesh B

Both grids have the same boundary information for their common sides, use the same activated physics (bottom friction, triads, quadruplets and linear wave growth), and built with the same spatial resolution as a structured grid of 0.025^o spatial resolution. Boundary data are extracted by ECMWF (ECMWF, 2014) spectral model, with 6-hour temporal resolution and placed at a one degree intervals. Alterations made to the re-computation of boundaries, imposing a stricter rule that limits the re-computation of the boundary information not to deviate from the spectral information. Initial spectral data have a spatial resolution of 0.125^o degrees. Attention was given when the boundary conditions and wind are selected since they are closely connected with underestimations, although the missing of peak quantities has been reported and is to be expected.

The results from both hindcasts were compared against the buoys selected for the calibration and validation. Predominantly buoy's existing in the East of Scotland (North Sea) were considered, for year 2010 the active buoys recording wave data were the Firth of Forth and Moray Firth. The inclusion and proper calibration of the shallow water part of the model, as presented

prior with all components is important since the locale of both buoys are in shallow waters and surrounding land mass affects the directionality and dissipation of the wave resource.

From the statistical indexes it is obvious that both models have similar high behaviour, although the small mesh present slightly higher H_{sig} rms values for the Firth of Forth and smaller average SWAN values in both cases, see Table 4.11.

Table 4.11: Mesh size comparison

	Firth of Forth						Moray Firth					
	Big Mesh			Small Mesh			Big Mesh			Small Mesh		
	H_{sig}	T_{peak}	T_z	H_{sig}	T_{peak}	T_z	H_{sig}	T_{peak}	T_z	H_{sig}	T_{peak}	T_z
Correlation	0.97	0.92	0.96	0.97	0.92	0.96	0.94	0.89	0.96	0.94	0.89	0.95
rms	0.35	3.23	1.52	0.37	3.18	1.45	0.43	3.8	1.37	0.43	3.78	1.37
MPI	0.99	0.94	0.96	0.99	0.94	0.96	0.99	0.94	0.96	0.99	0.94	0.96
Average Buoy	1.14	7.08	4.53	1.14	7.08	4.53	1.12	7.12	4.36	1.12	7.12	4.36
Average *SWAN*	0.97	8.08	5.02	0.94	7.93	5.09	0.90	8.08	4.65	0.89	7.99	4.63
Bias	-0.17	1	0.49	-0.2	0.84	0.56	-0.21	0.95	0.28	0.23	0.86	0.26
SI	0.3	0.45	0.33	0.32	0.44	0.32	0.38	0.53	0.31	0.38	0.53	0.31

Usually a smaller mesh would be employed, for wave resources, although it seems that the mesh A can provide a higher average value reducing the error bounds between simulated and observed (see Figure 4.29). The visual inspection of the results from the meshes is showing that mesh A has a higher tendency to obtain greater values (peaks) and reducing the smaller troughs.

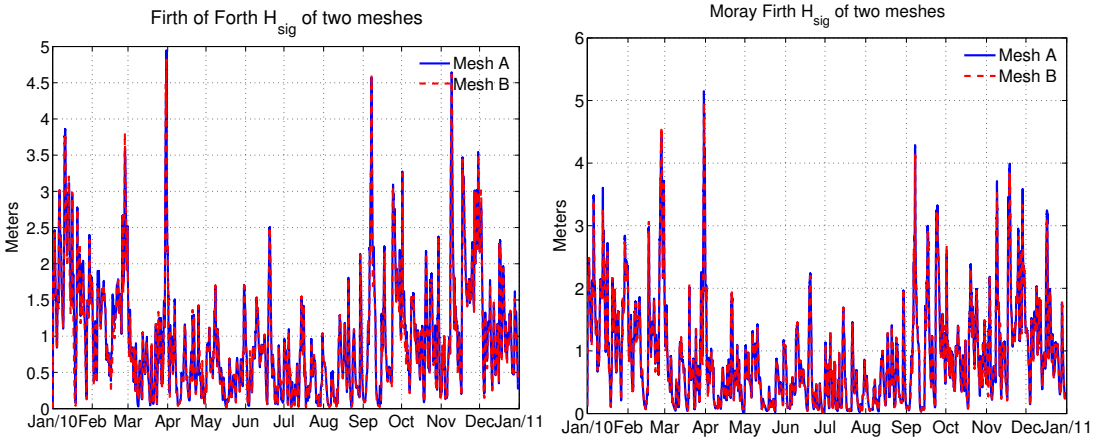

Figure 4.29: Locations H_{sig} comparison

The same behaviour is present in the peak and mean zero crossing periods, with the big mesh allowing the hindcast results to reach higher peaks, see Figure 4.31. It is of major importance not only to assess the quality of the results but also consider the level of performance by the system, and the required time that is expected. It has to be outlined that it is favourable, when considering coastal application to use the optimal performance and cost-effective usage of the available computational resources.

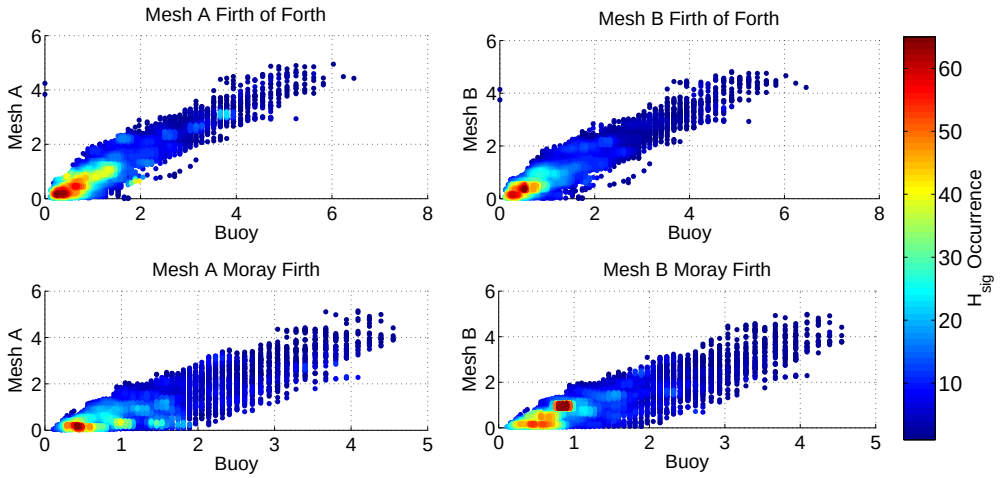

Figure 4.30: Density distribution for different meshes

Both buoys do appear to have a linear fit, but the mesh size seems to alter the characteristics of non-linear solver altering the output hindcast, providing underestimations of the smaller mesh in regards to the bigger one, see Figure 4.30. In the case of unsorted density distribution the Firth of Forth site for mesh A shows a placement of H_{sig} at higher values in comparison with the buoys, while mesh B presents higher under-estimation rates, with the average mean values and bias favouring mesh A. On the other hand, the Moray Firth location shows a placement to higher values for mesh B, though the overall bias has a small difference.

Mesh size plays an important role in the model performance (Delft, 2014b), the extension of the fetch and the possibility of major alterations in the depth gradients may de-stabilize the simulation. In both cases the meshes used are of high resolution, with the East fetch being exactly the same for both options. The non-linear effects though, are approximations used to resolve the complex nature of waves. This is one of the factors, that in combination with the mesh length can have a significant effect on the results (Bottema and van Vledder, 2008; Rogers and Van Vledder, 2013). DIA approach is used in the hindcasts, with a semi-implicit non-linear computation per sweep.

In the work of Bottema and van Vledder (2008), the fetch size was compared with different approximations utilized and compared to a numerical solution for a few timesteps and in one-dimensional simulations, the overall experiment revealed that the careful selection of the non-linear solving approximations enhances or diminishes the solutions. Complex nature of the quadruplets and SWAN selection has been discussed in Section 3.1.3 and Section 4.6.

It was underlined that due to the nature of uncertainty of the non-linear components in their solving the computational time would increase, in our study the overall simulation time can be characterized as almost doubled for the two different meshes. As expected the big mesh required 8.5 min/day and the small mesh had 5.02 min/day, to simulate the sea state. Although

when we are to consider the size and computational timestep, the expected results have discrepancies occurring between the two simulations, see Table 4.11 and Figure 4.29.

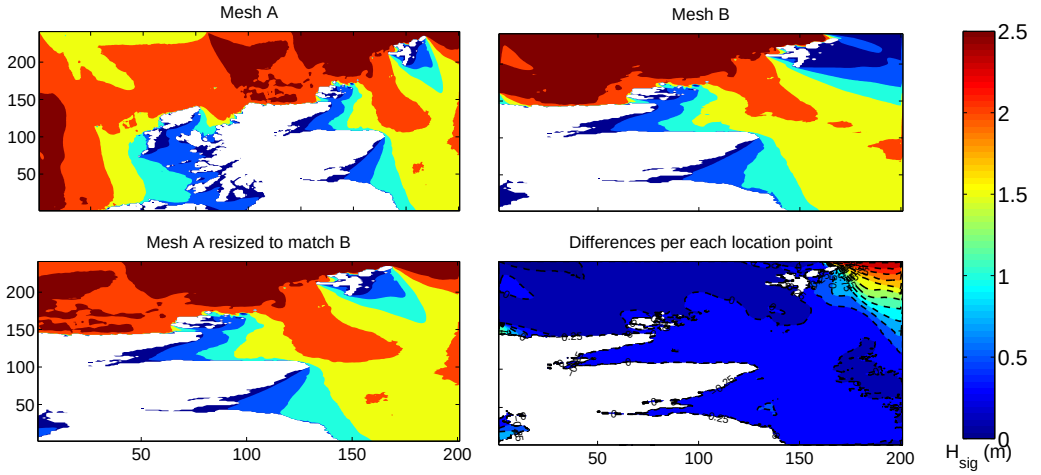

Figure 4.31: Last Computational timestep and differences in area

Differences of hindcast are obvious with the mesh A having a more extended H_{sig} component covering area, while the mesh B presents a smaller sharper contour distribution of wave height, in the North East part, see Figure 4.31. Similar behaviour was recorded for all quantities.

The main focus of this investigation was to examine the performance of a wave resource validation of wind generated seas. Although SWAN is usually utilized for coastal water and nearshore applications its ability to resolved greater meshes in high detail was displayed. The correlation of mesh size, non-linear interactions and appropriate selection of the solver, which was of major importance for the execution of a highly accurate wave resource assessment.

As expected time computations were higher for mesh A, although this decision is not to be taken lightly. The differences in the hindcasts and the distributions of the data are evident, with mesh B having a constant under-performance nearly at all accounts. Has to be underlined that the times of computation are not deterministic and will vary per mesh size and other physical processes that are calibrated, although a fairly accurate representation for the computational requirements is reflected with the reported times.

On the other hand, highest order solution is not the only parameter taken into account the computational requirements were also displayed, aiding to an informative decision for modellers when setting up wave resource models. The computational accuracy and speed of the simulation is of major importance. Time considerations can be helpful for the forecast of resource concerning the offshore industry and especially wave energy developers.

Same boundaries and inputs provided, although mesh A displayed an improvement in the timeseries. With higher peaks both in frequency and wave height, the mean square root error and residuals were smaller for the big mesh leading to less averages. The size though of mesh

B allowed for almost half the time of simulation to be required, thus requiring computational resources for less time. This although can be alleviated by offering higher computational resources in future applications.

Discrepancies between the data can be attributed to the behaviour by numerical model with non-linear and mesh size, that is the reason why specific attention was devoted in setting of the model. To facilitate a proper simulation the CFL criterion has to be ensured at every timestep, but the nature of non-linear interaction and spatial resolution pose one of the most important components for the final spectrum. A higher spatial resolution will provide a potentially better wave representation although that increases the chances that CFL criterion will not be satisfied, leading to an increase of the non-linear energies dissipating by the numerical model. Mesh size will determine the fetch length, which in turn and combination with the resolution will provide the proper shape of the finalized resource.

For this reason, based on application of the model, different considerations on selection of boundary data have to be taken. The area to be investigated is small, then a nested spectral coarse model must first be employed to provide the adequate representation of the boundaries, if though restrictions on computational or time requirements exist the TPAR usage with combination of a larger mesh provide a faster and less expensive solution. Finally, spectral density data can be used but those are often large in size and pose several difficulties in implementation.

4.8 Summary

In this chapter the impact of different wind input, bathymetry and various numerical schemes were used on the resulting wave parameters evaluated. A summary of key points are given below to assess model performance:

- Presentation and identification of wind products in literature, alongside with considerations when a wind dataset is to be used for the UK and more specifically the Scottish area.
- Literature focus on winds and how they tent to affect the wave numerical process, it was found that wind products although validated for global domain, are suggested to be investigated for regional applications. This ensure selection of the optimal wind dataset based on location, Hemisphere and potential application.
- Investigation and assessment of two high resolution (both temporal and spatial) wind products.
- Validation indexes and statistical performance of models assessed.
- Identification of most appropriate dataset that can be employed for Scotland and the United Kingdom, based on thorough validation and physical customisation process for coastal waters.

- ECMWF displays minimal biases and lowest scatter indices when used in the area of Scotland. Overall parameters tend to be under-estimated, although in high accordance with the recorded buoy data. More suitable for resource assessments and power estimates.
- Effects on the distribution of wave parameters in comparison with the recorded ones.
- CFSR product entails a higher temporal resolution, hindcast SWAN parameters showed greater peaks and thus more troughs resulting in the PDF alteration towards overall under-estimation. More appropriate for extreme value analysis and structural safety studies.
- For use of smaller domain hindcasts, the use of CFSR is suggested due to its ability to temporally re-produce the wave field providing higher peaks. Direction components of waves, due to their connection with wind direction were better represented with the CFSR data which captured the alterations in direction faster.
- Application of SWAN in multiple locations, use of nested grids with varied spatial resolution.
- Significant implications identified that alter the wave modelling process when areas with rapidly varying bathymetry and complex coastlines are examined.
- Potential problems and ways of approaching a solution was exhibited. More specifically, the Mediterranean and Aegean Sea proved to carry these problems when coastal modelling was applied.
- Alleviation of the problem was proposed by the identification of turning rates and thus improving the wave hindcast.
- Ability of SWAN to perform high resolution wave resource assessment, which can be subsequently expanded in areas with no buoys was shown, due to the high statistical correlation reported by all the different applications.
- Difficulty of non-linear (S_{nl4}) was presented. Considerations of effects on wave hindcasts both in terms of output and computational resources utilised.
- The nature of non-linear (DIA) solvers is inherently problematic and incomplete. All third generation models use these solvers, although a thorough examination allowed to assess their performance and consider optimal range for their coefficients. Both explicit and implicit schemes were assessed.
- DIA sensitivity to frequency and direction bins was examined alongside proposed numerical schemes on shallow water encapsulated locations of the North Sea.
- Effects of an increased frequency resolution, has shown that although the wave parameters are enhanced, the shape and magnitude of the spectrum deviate a lot from measured data.
- The concept of using both the statistical and spectrum properties of the buoy for calibration, revealed that SWAN, as a spectral model shows high level of sensitivity in the frequency resolution due to the DIA term.

- Combination of DIA instability and frequency in SWAN, suggest that favoured designated frequency bins should be kept from f_{msc}=24-36, in order to produce high level data with good spectral values.
- The tunable shape coefficient λ_{DIA}, offers the user flexibility to enhance the model. Although its sensitivity comes with significant restrictions. It is known that in specific part of the world different shape coefficients are used (e.g. in Japan the λ_{DIA}=0.19).
- The tuning of λ_{DIA} , for the Scottish area is suggested to lay with in a range of 0.23-0.25.
- In addition the effects of mesh length, apart from the mesh resolution was examined. Providing some insight on the benefits and drawbacks of using a large or small meshes. Accuracy and computational requirements were also taken into account.

Chapter 5

Resource Assessment

"Give me a lever long enough and a fulcrum on which to place it, and I shall move the world."

Archimedes, 287-212 B.C.

5.1 Introduction

In this chapter a thorough resource assessment and application of the model is presented, providing high resolution results. As discussed in Chapter 4, two different regions with distinct characteristics are investigated; the Scottish coastline, the Mediterranean and Aegean Seas. Characteristics of these areas are completely different with issues reported and resolved as proposed in Chapter 4.

The results are expanded not only for wave conditions and seasonal alterations, but are also investigated for wave energy applications. High resolution modelling offers the chance to identify areas with potential for wave energy in more depth than previous studies. The first study offers a high resolution coastal and deep water hindcast for the North Atlantic area, throughout a long time period and the alterations that have been occurring during the last decade; the investigated period spans from 2004 to 2014. Wave variability in various locations, with energetic areas identified is given. A rigorous validation conducted at various locations and depths, reveal accuracy of the model.

Additionally, some restricted shallow buoy data are utilized to assess locations of a few meters depth, enhancing understanding of the results and model's confidence. Moreover a detailed energy assessment and energy calculations are given by testing representative wave devices. The necessary steps in the resource assessment of coastal areas is presented, with background information.

A complete energy analysis is provided, with the annual energy flux and wave variations affecting the production; in addition robust estimations of the capacity factor (CF) are given by taking into account locations, depths, environmental characteristics and devices, offering a significant pool of information about the actual value of CF and expected performance of each

representative device. This can be used to enhance the more accurate calculations of economics for wave energy and future energy assessments in absence of buoys.

Furthermore, an index is introduced and used to help in the selection of future sites. The combination of energy flux, resource assessment, CF and annual maxima values reveal effect that the resource of a site may have on the expenditure and maintenance of wave converters.

Due to the large amount of data collected for shallow water locations, the strength of results is increased, creating a large database of wave characteristics recorded at high resolution time intervals. This allows for areas and time periods with no measurements to be substituted by the numerical model, with high level of confidence established.

The second study includes a nested, high resolution assessment of the Aegean Sea, which provides the base to establish locations of wave energy potential. Moreover the quantification of production and extraction devices applied in the Aegean is presented, with annual energy assessment and estimated capacity factors for various locations. To the author's knowledge it is the first coupling of wave resource with energy converters in some proposed areas assessing their performance.

5.2 Scottish Coastline Wave Energy Resource Assessment

A high resolution model is applied to the Scottish waters which provided a detailed resource assessment for various locations. The points are selected based on available buoy locations and several of them are chosen to be compared with previous studies in the region.

The model was run on the ECDF cluster, for a period of time presented as below. The overall run time and computer resources are given in detail per year of hindcast.

Table 5.1: Computational resources occupied by SWAN

Year	Cores	Memory	Minutes/Simulation day	Days of year
2004	8	16 G	11.35 min/d	366
2005	8	16 G	11.09 min/d	365
2006	8	16 G	9.48 min/d	365
2007	8	16 G	11.88 min/d	365
2008	8	16 G	10.53 min/d	366
2009	8	16 G	9.67 min/d	365
2010	8	16 G	11.16 min/d	365
2011	8	16 G	11.15 min/d	365
2012	8	16 G	12.05 min/d	366
2013	8	16 G	9.67 min/d	365
2014	8	16 G	15.21 min/d	282

The overall time in computational worth of the hindcast was 31 days (in actual days). The average computational requirements (minutes/day of simulation) vary, see Table 5.1. This

is due to the fact that computational requirements tend to adapt to the available resources. Meaning that although the requested memory allocation was 2GB per core, it wasn't always possible to utilize a full 2GB/core. The final data consisted of approximately 300GB with input and output of parameters produced by hindcasts for the decade.

The data constitute a high resolution database of shelf waters, around Scotland. A detailed spatial resolution was used (0.025^o), offering higher data outputs especially for coastal locations. Although large models are used for day to day operations or similar hindcasts, their resolution is much coarser (ECMWF, 2014). This study constitutes the latest highest spatial resolution for 11 years and the highest resolution wave energy assessment around the waters. The bathymetry was constructed based on data and resources as described in Section 3.2.5. To the author's knowledge and recent literature review, this study contributes to the enhancement of coastal and shelf seas wave environment in the region, based on a model that took into account all the results about performance as presented in Chapter 4.

The wind product chosen to be used for this extensive investigation was the ECMWF dataset. This decision was based on the findings of the author as discussed in Section 4.4, where different wind products were extensively investigated. The selection was taken on the fact that for the area of the UK, ECMWF tend to produce less rms errors and smaller biases. Although as stated previous research shows that different wind products will vary in performance for various locations and areas. The spatial and temporal resolution of the wind product are 0.125^o and 6 hr respectively.

Boundary conditions were extracted by spectral information provided by ECMWF and post-processed accordingly to produce boundary files as presented in Section 3.2.2 (ECMWF, 2014). All Sea sides or wet point boundaries have been assigned with temporally and spatially varying conditions, leading to a large number of files used. The boundary information initiate from 2004 and go up to the ending at the last computational timestep of 2014. The points were isolated from the ECMWF database by a shell script and the conversion and data handling was performed in python. Furthermore, cross-correlation was performed to ensure proper coordinates were extracted. Each point represents a unique set of spectral values applied to each side, with the conditions having an altering and "moving" spatial application within predetermined areas.

The physical components and structure of the model were based on the data obtained by various calibration methods, with parameters chosen, based on acquired knowledge of the models to minimize errors (see Section 4.2-4.6).

Finally, buoy data offer a high level source for comparison. To ensure proper analysis post-processing has been applied to exempt the time-series which have lack of measurements. The missing intervals are thus not taken into account in the comparison.

5.2.1 Data and Resource

For the validation of the model, several locations have been explored, see Table 5.2. Firstly, areas with established recorded buoy measurements as given by the CEFAS were considered (CEFAS, Center for Environment, 2014). In addition, based on the POLCOMS project which used a phase averaged model to characterise the Irish and Scottish coastlines, some points were chosen to be compared with the hindcast output (British Oceanographic Data Centre). The points chosen are at shallow water locations and close to coastlines, where shallow and non-linear interactions are dominant (see Figure 5.1).

Another potential data source for calibration/validation are satellite data. However, due to temporal restriction as indicated by other studies they have not been considered. The fact that recordings have large gaps between passing of the satellites, 10 or 30 days apart, prompted to the decision. Additional limitation of satellites indicate that recordings of wave parameters initiate approximately $20Km$ off any coastline (Komen *et al.*, 1994; Cavaleri and Sclavo, 2006a,b; Young, 1999a; Vinoth and Young, 2011). Even with the inherit problems of buoys and gap in recordings times, their locations especially at near coastal waters offer reliable considerations for this kind of study.

The outputs of this high resolution hindcast, enhance the understanding and quantifies the available wave energy resource for nearshore water locations, where wave devices are expected to be installed. Moreover, it offers a detailed statistical analysis on the variability and difference that are to be expected to occur on wave power and climate.

Table 5.2: Locations of investigation

Origin	Coordinates	Location Name	Start	End	Depth (m)
CEFAS	$56^o\ 03,72'$N-$7^o\ 03,41'$W	Blackstone	10/03/09 11:30	25/05/13 12:30	97
CEFAS	$57^o\ 17,52'$N-$7^o\ 54,84'$W	West Hebrides	23/02/09 16:30	28/05/14 13:30	100
CEFAS	$57^o\ 57,99'$N-$3^o\ 20,01'$E	Moray Firth	29/08/08 10:00	19/05/14 09:00	54
CEFAS	$56^o\ 11,28'$N-$2^o\ 30,23'$W	Firth of Forth	19/08/08 09:00	12/05/14 07:00	65
CEFAS	$58^o\ 86,221'$N-$2^o\ 84,368'$W	Holmsound	-	-	20
POLCOMS1	$55^o\ 4,00'$N-$6^o\ 0,00'$W	Point A	01/04/2005	31/12/2005	110
POLCOMS2	$55^o\ 6,00'$N-$6^o\ 6,00'$W	Point B	01/04/2005	31/12/2005	73
SWAN 1	$58^o\ 3,75'$N-$7^o\ 0,43'$W	Hebrides 1	-	-	68
SWAN 2	$58^o\ 4,292'$N-$6^o\ 19'$W	Hebrides 2	01/01/2012	01/02/2012	55
SWAN 3	$58^o\ 5,00'$N-$6^o\ 7,25'$W	Hebrides 3	-	-	62
SWAN 4	$58^o\ 4,20'$N-$6^o\ 4,00'$W	Point1	-	-	8.75
SWAN 5	$58^o\ 97'$N-$3^o\ 39'$W	Orkney	-	-	22

The CEFAS data constitute a source of good quality recorded wave parameters in the public domain (CEFAS, Center for Environment, 2014). Although great work has been done by the centre, some time gaps in the recordings were seen absent from the buoy measurements due to either a maintenance work or extreme conditions. These missing data have been identified by a preliminary process, filtered and are not taken into account in the time-series comparison.

Data extracted by BODC and the POLCOMS project vary in time availability with most of them

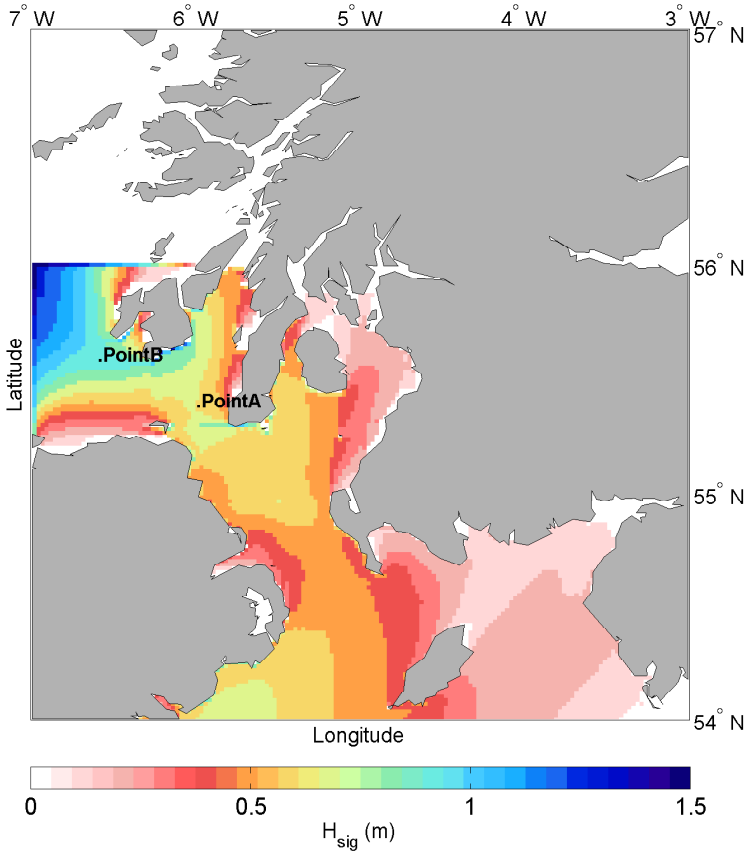

Figure 5.1: Points chosen from comparison from the POLCOMS project

providing some individual months of wave hindcasts within a year (British Oceanographic Data Centre). On the other hand ECMWF data are constantly maintained, providing an excellent source of comparison for wave parameters with the model of the study. This attempt was considered to minimize the absence of annual comparison data and provide a robust analysis on performance of the model, allowing consideration of its use for areas with no recording devices and very shallow waters.

Determination of locations extracted, should be made based on criteria for analysis. Firstly, locations which correspond to measurement points have to be the primarily extracted, to allow a thorough validation. Subsequently, based on the objectives additional locations should represent disperse locations around the domain, with depth consideration of applicability. In this case, since a wave energy assessment is necessary, all additional component are extracted at depths $\leq 150m$, that allows WEC installation. At the same majority, additional locations are placed in different environments i.e. close coastlines (Orkney), open to the Atlantic (Hebrides 1-3, Point1), and to the North Sea, see Table 5.2.

With the previous knowledge and experience, a high resolution mesh was generated and the model was driven by ECMWF winds. After the first year, a "warm" start model was secured so

as to minimise preparation time for the models and obtain real-time data. The domain utilised can be seen in Figure 4.1 at Section 4.2. A calibration run was performed prior to the full usage of the model for high resolution hindcast of the year 2012.

Table 5.3: Calibration of 2012

	West Hebrides			BlackStone			Firth of Forth			Moray Firth		
	H_{sig}	T_{peak}	T_z	H_{sig}	T_{peak}	T_z	H_{sig}	T_{peak}	T_z	H_{sig}	T_{peak}	T_z
Correlation	0.92	0.69	0.78	0.98	0.87	0.89	0.95	0.72	0.83	0.92	0.69	0.78
rms	0.38	3.44	1.01	0.44	2.19	1.11	0.32	2.74	1.04	0.38	3.44	1.01
MPI	0.99	0.94	0.96	0.98	0.92	0.95	0.99	0.94	0.96	0.99	0.94	0.96
Average Buoy	1.1	7.16	4.22	2.5	10.2	6.21	1.02	6.79	4.27	1.1	7.16	4.22
Average *SWAN*	1.04	6.49	4.03	2.54	9.71	5.84	0.95	6.75	4.36	1.04	6.49	4.03
Bias	-0.06	-0.67	-0.18	0.04	-0.48	-0.37	-0.07	-0.04	0.09	-0.06	-0.67	-0.18
SI	0.35	0.48	0.24	0.17	0.21	0.17	0.3	0.40	0.24	0.35	0.48	0.24

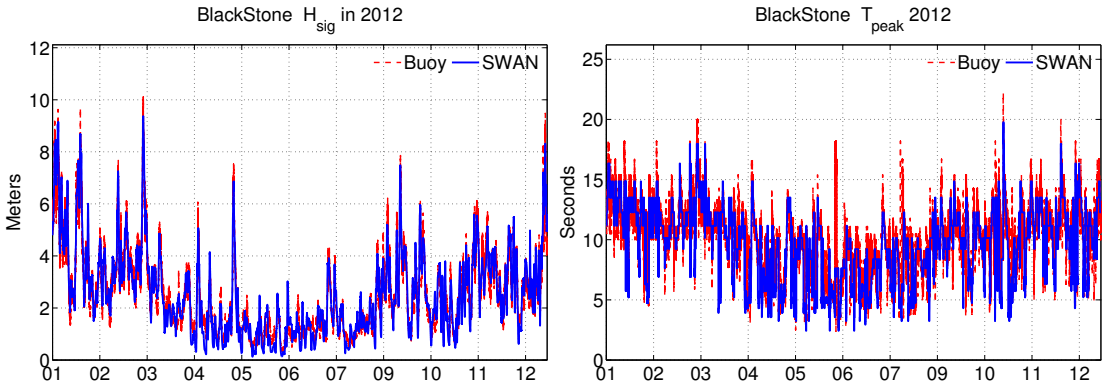

Figure 5.2: 2012 BlackStone location

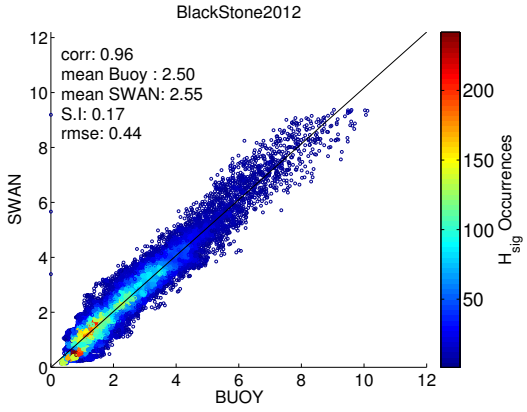

Figure 5.3: H_{sig} scattering and correlation 2012, BlackStone

The calibration hindcast shows the high level of performance of the model, see Table 5.3. The choice was made based on the fact that 2012 was a year that had all buoys active and long recordings. Allowing a full analysis and comparison of not only the annual but also potential seasonal variations. For locations constituting the West coastline of Scotland (West

Hebrides and BlackStone), the H_{sig} biases are very low with the latter buoy providing some over-estimation. The MPI and correlation factors are also satisfactory with constant recorded MPI over 0.9. The rms values are low leading to good agreement and low levels of scattering, see Figure 5.2.

Same behaviour is recorded for the performance of the wave periods, T_{peak} and T_z hindcast, with very low biases and high model agreement. Although it has to be noted that the West Hebrides buoy displays an inconsistency on the qualitative index of the T_{peak}, with a low bias though a high rms value leading to an inconsistent scatter index.

Similar results can be seen in the East side of the mesh, with biases being very low and model performance high. Though a large scattering of T_{peak} is still present. On the other hand mean-zero crossing period was not affected having reduced corresponding indices for a more detailed representation of the trends and scattering of the corresponding buoys and data (see Figure 5.3 and Figure B.2).

This level of performance displays that SWAN provides a good hindcast for the area, although further comparison for the periods (years) that the buoys are active and displayed in the following section. Overall performance as shown allows us to use the 2004-2008 results in confidence even with absence of comparison recordings.

5.2.2 11-year Coastal High Resolution Hindcast

With performance of the model established in Section 5.2.1, and several additional points added into the analysis, a confident resource map and climate analysis of wave parameters is presented. Four major buoy recordings are considered, while at the same time several other interesting locations are presented, see Table 5.2. The scarcity of points and their different characteristics help in solidifying the findings for areas analysed in the forthcoming sections.

Local wave and environment characteristics play an important role not only to the wave resource but also to the statistical parameters describing the sea climate. Inclusion of both mid-depth and very shallow points strengthens the results of SWAN, which is able to characterize locations with depths as low as 8.75m.

The periods with available buoy measurements have been cross validated with the model output, for the corresponding data availability see Table 5.2. A complete validation of the model with data from all available years are given in Appendix B from Table B.1–Table B.6.

For year 2008 the model was compared with only two buoys available, Moray Firth and Firth of Forth; the results presented in Table B.1 display a very low bias for all H_{sig}, with good SI performance. Performance of the model is high for both wave height and mean-zero crossing period, although the T_{peak} performance is within moderate levels. The dominant conditions in these locations are most of the times swell seas that originate from the North and North East

part of the upper boundary. This leads to under-estimation of H_{sig} while the spectral period is also under-estimated (see Figure B.5-B.6)

In year 2009 the recordings available covered the West and East part of the mesh, with the West locations being influenced significantly by locally wind generated waves which in combination with the incoming swells from the Atlantic leading to higher energy sea states. High wave conditions has been re-produced very well by the hindcast, with small values of biases, rms and SI, see Table B.2. These high energy sea states led to a small under-estimation of H_{sig} while the period components have been presented with much lower biases than expected. The Eastern side performance showed a significant improvement over 2008 with both locations having very small differences with measured values. The scattering components for the hindcast, with no correction factors applied, reveal a very good agreement and overall performance (as seen in Figure B.7-Figure B.11).

For the period 2010-2011 comparisons included in exhibit similar behaviour. The hindcasts show that the shallow water mechanics activated with SWAN have the ability to resolve highly energetic seas with very high levels of accuracy, reduced rms, and SI, see Table B.3-B.4. While the average under-estimations can be located for extreme storm events where, it is known that numerical wave models tend to decrease in hindcast accuracy (see Figure B.12).

The hindcasts for periods 2013-2014 present a similar situation with peaks being under-estimated at storm events (see Table B.5-B.6). H_{sig} and T_{peak} as it can be seen by the quantitative comparison and the visual inspection show good level of agreement (see Figure B.21).

Although, SWAN inherently carries some under-estimation levels in its calculations, for factors which have been elaborated in Chapter 4, the proper customization has proved effective in the model output. This allows to expand and consider the results valid for years with no previous data recordings. The statistical indices considered show that the model is able to represent generation and propagation trends of energy, around the coastline. The significant attribute of SWAN is the fact that it can resolve shallow water locations in much greater accuracy that its oceanic counterparts. This means that the confidence levels for the nearshore regions of interest, is enhanced. The local energetic resource offer high levels of incoming energy that are dissipated by bottom and triad-interactions, thus assessing performance of the model in very low depths add confidence on the results.

In addition to the CEFAS buoys data from the Hebrides2 site for the duration of one month were compared with our output, (Vögler and Venugopal, 2012), see Figure 5.4. The correlation of modelled data at 0.96 while the average value of the buoy is 4.45m and 4.84m from SWAN, leading to a positive bias of 0.38m. The high level of correlation lead to a low scatter index of 0.15.

The additional points represent locations for which wave energy extractors can be applied, providing a more robust and full overview of the annual variation that occurs and can be

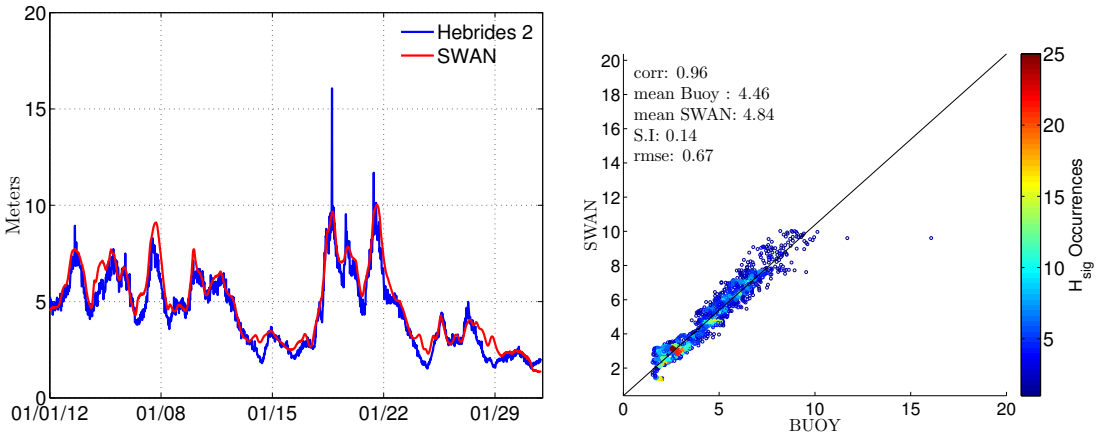

Figure 5.4: Validation of the Hebrides2 location

expected. Through the modelling of nearshore locations, statistical distributions for areas with high level of non-linear interactions will be examined in the next chapter (see Chapter 7), providing better presentation of selection concerning the analysis of such areas. This high-resolution study, has allowed for a detailed re-presentation and generation of high resolution datasets for all major wave parameters, they can be used either for seasonal analysis of energy variability.

As discussed hindcast output varies for each location and depth characteristics (see Table 5.2); the annual fluctuation of H_{sig} and T_{peak} can be seen in Figure 5.5. The hindcast output were utilised to examine the annual variability. As mentioned SWAN under-estimates high wave, though it has a good generation trend and is able to compensate for the missing yearly intervals. The most energetic waters, as expected are located in the West of Scotland, with exception of the West Hebrides point, all the location have a tendency to provide an annual average of 2 meters wave height and good low period intervals average above 10 seconds.

The annual average H_{sig} wave height hindcast exhibit the trend of generation and spatial distribution of wave height, see Figure D.1-D.11. Most energetic sites are located at the West coastlines. Their annual variability also aids in the dissemination of further exploration of potential sites that can be of benefit to the wave energy industry. The annual average H_{sig} is in turn used, to exhibit the percentiles that occur for every year, with an important look into the expected values per location.

The percentiles overview shows the range that H_{sig} is expected to have, conclusions from this can be of aid in the investigation of maxima and median seas. For this reason five different percentiles are presented, the 25^{th}, 75^{th}, 95^{th} and 99^{th}, representing the highest occurring values. Based initially on the 99^{th} percentile, the most commonly found magnitude of incoming waves for the West coasts are on average over 10 meters at deeper waters and 4-5 meters closer to coast. The East part due to its topography and local conditions is dominated by wind

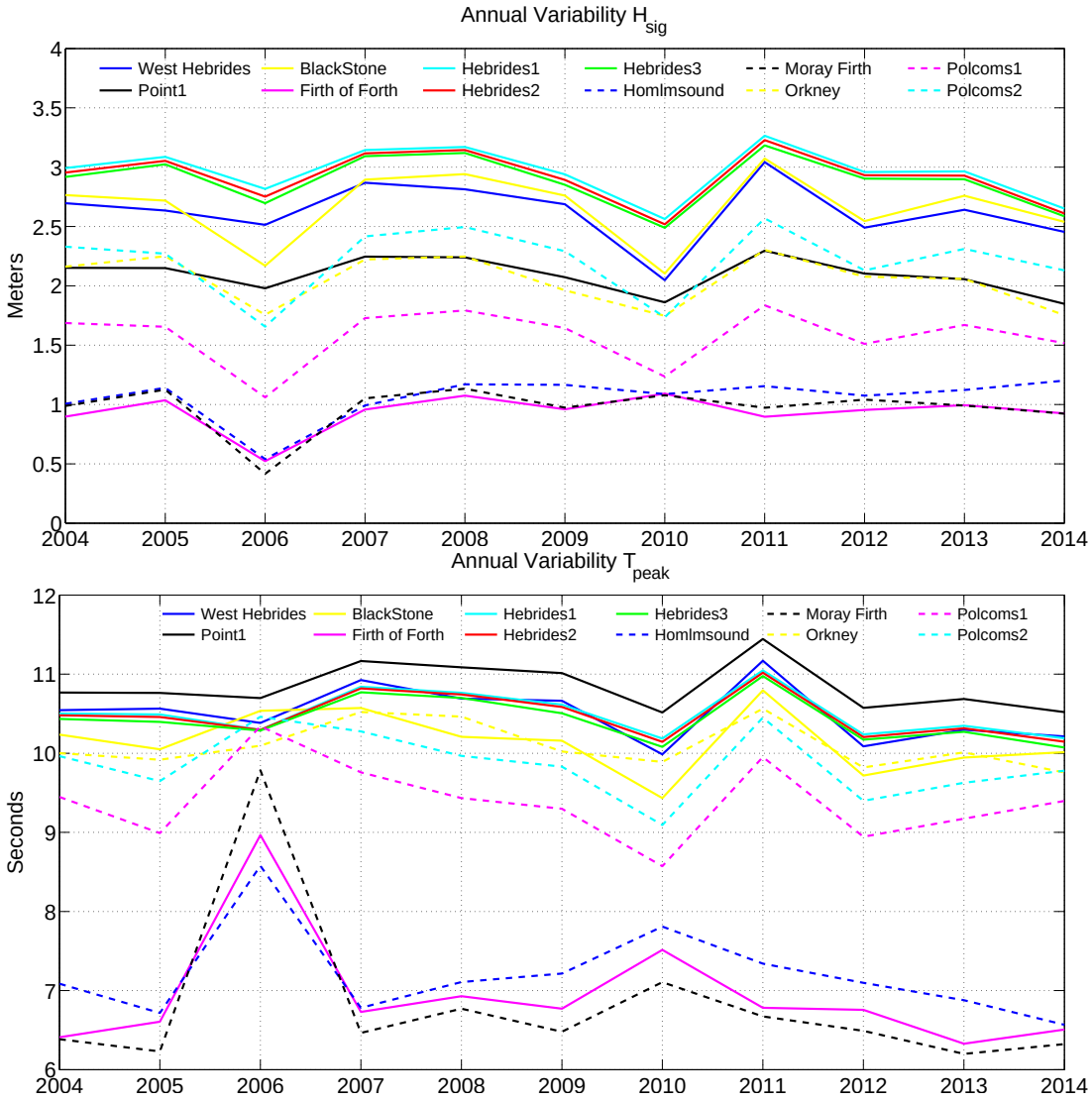

Figure 5.5: Annual Variability of H_{sig} and T_{peak}

generated waves, with some swell components originating from the North boundary. This leads to lower H_{sig} values of 3-4 meters at deep water and 1-2 meters at nearshore locations (see Figure D.23-D.33).

5.2.3 Multi-Model Analysis

Asides buoys used to assess the model, existing knowledge and information from other models are used for comparison. Initially as discussed two locations have been extracted from the POLCOMS project (British Oceanographic Data Centre), see Figure 5.1.

The points and their characteristics represent selection of points being amongst difficult wave field. The surroundings have many coastal areas that affect the performance of wave models as diffraction, refraction and non-linear effects are bound to be dominant which will affect

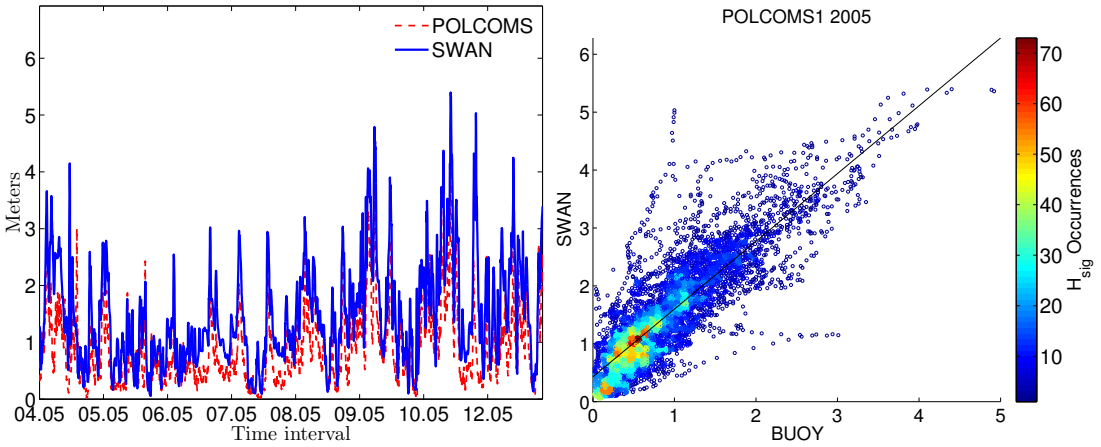

Figure 5.6: Comparison of the POLCOMS1 location

the final resource estimations, see Table 5.2. The POLCOMS project was run by the BODC (British Oceanographic Data Centre). The data are given under permission in the format of a netCDF file. The points thus were extracted by using a bash code that allowed the proper reading and extraction of the corresponding points while their characteristics (i.e. coordinates, variables included) were verified by the use of MatLab and Panoply.

The year selected for the comparison is 2005, the selection was done based on available data duration and the fact that no official recording buoy or other information in the area are available. The hindcast model used in the POLCOMS, is an oceanic model (WAM) and thus its performance in the assigned locations is expected to be inferior to this high resolution hindcast. This comparison is performed to display the potential improvements that derive from this database.

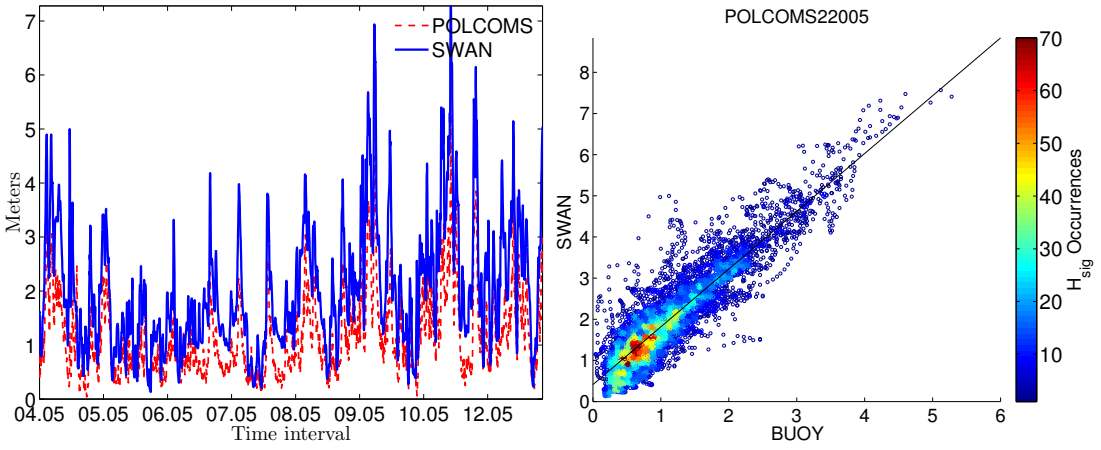

Figure 5.7: Validation of the POLCOMS2 location

Due to the high resolution bathymetry, activation of shallow water mechanics and customiza-

tion of the SWAN code to the broader area was used, and this resulted in improved hindcast. The point of this comparison is to reveal the differences between oceanic and coastal models, and add to the knowledge when selecting an area of interest to be investigated.

Data compared are from April 2005 until January 2006, thus a representative comparison is achieved, not only in terms of location characteristics but seasonal trends as well. The POLCOMS are labelled as buoy (in the scatters) and they are compared statistically to examine the performance and differences between them and the high resolution datasets.

It is noticeable that SWAN displays higher overall peak performance (see Table 5.4), while both of the hindcast values are closely related as displayed by the scatter plots and timeseries, see Figure 5.6-Figure 5.7.

Table 5.4: Performance comparison of SWAN and the POLCOMS output

	H_{sig} in meters	
	Polcoms1	Polcoms2
R	0.92	0.95
rms	0.76	1.05
MPI	0.98	0.98
Average Buoy(Polcoms)	0.89	1.14
Average SWAN	1.47	2.01
Bias	0.58	0.87

Additionally, the author also tried to use the ECMWF ocean database to compare the same output locations for the corresponding comparison. Although as it is noticed in the figure model resolution used by the agency did not allow for a full re-presentation of the area. The spatial resolution of the data downloaded by the ECMWF was 0.125^o, although the area as seen was not resolved by the offered model (see Figure 5.8). This re-affirms the belief that the high coastal resolution can lead to improved results for coastal shallow water locations around Scotland.

5.2.4 Wave Energy potential in coastal areas

The validation process as presented in the previous Section 5.2.1, allows for the detailed examination of the wave energy potential. Wave resource potential is obtained by incorporating recorded or hindcast wave parameters, H_{sig} and T_e, into shallow or deep water resource assessment.

Depending on the areas of investigation and site selection incoming wave energy flux can be examined. Most resource assessment studies perform wave energy estimations based on the deep water formulations of wave generation. The POLCOMS, BODC as well as the BEER-MER (UK Marine Atlas) and other studies are based on calculating the energy flux in deep water (Taylor *et al.*, 2006; Berr, 2008; Cornett, 2008; Carbon Trust and AMEC, 2012; Neill

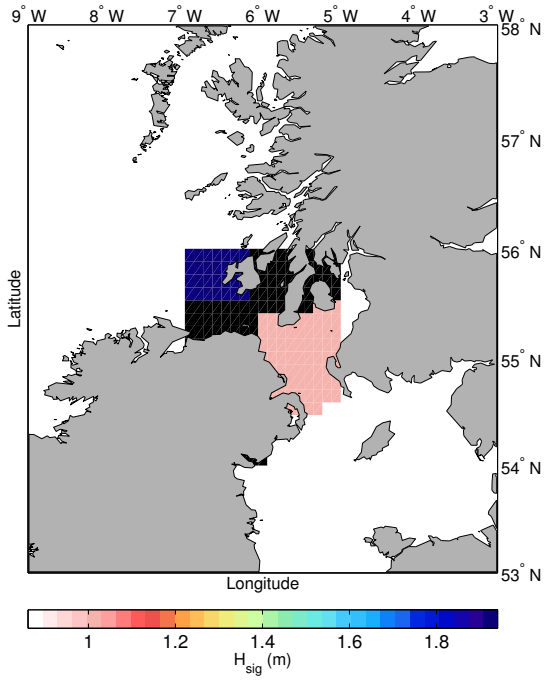

Figure 5.8: H_{sig} by ECMWF corresponding hindcast area (in black no data areas)

and Hashemi, 2013; British Oceanographic Data Centre), have presented the challenges and opportunities that exist within the wave energy sector.

Wave power is derived by the calculation of wave energy flux, which denotes the available resource that is generated and propagated within waves. It corresponds to the notion of available energy flux contained per one unit of crest width, expressed usually in kW/m, estimation of which is not straightforward. In this section the selection of appropriate wave power formulation is presented and used throughout the continuation of several studies included in this thesis.

Starting from a simplistic approach wave energy flux estimations are initially based on linear wave theory, in which depth considerations are taken as having small or no effect. In simple terms wave energy is the summation of kinetic and potential energy per unit surface area of a wave, (Cornett, 2008; Soukissian *et al.*, 2012)

$$E_{wave} = E_{kin} + E_{pot} = \frac{1}{8}\rho g H_{sig}^2 C_g \tag{5.1}$$

$$C_g = \frac{1}{2}\left[1 + \frac{2kh}{\sinh(2kh)}\right]C \tag{5.2}$$

$$C = \frac{\lambda_{wave}}{T} \tag{5.3}$$

$$\lambda_{wave} = T\sqrt{\frac{g}{k}\tanh(kh)} \tag{5.4}$$

The potential energy flux per unit of wave crest (height) depends on the wave group and its celerity (wave group velocity). The relation between wavelength, depth and period is based on the dispersion relationship (see Equation 5.1 - Equation 5.4). Although deep and shallow water interactions in regards to depth alter the estimated energy flux. In deep waters, energy calculations are approached as regular waves with not many variations in frequency and direction (see Equation 5.5).

$$P_{wave} = \frac{\rho g^2 H_{sig}^2 T}{32\pi} \tag{5.5}$$

In the cases of actual sea states and wind seas the situation is much more complex. Waves are a summation of different wave numbers and frequencies interacting in the area, with the power propagated within waves, depending on the energy density travelling with varied frequency and directions. This is expressed by the $2D$ spectrum, $N(\sigma,\theta)$. This reforms the propagated summation of energy as seen in Equation 5.1 (Cornett, 2008; Neill and Hashemi, 2013; Delft, 2014a).

$$P_{wave} = \rho g \int_0^{2\pi}\int_0^{\infty} C_g(\sigma,h)N(\sigma,\theta)d\sigma d\theta \tag{5.6}$$

with

$$C_g(\sigma,h) = \frac{1}{2}\Big[1+\frac{2kh}{\sinh(2kh)}\Big]C \tag{5.7}$$

The fact that several frequencies and directions exist, alters as well the calculation of wave group and velocities, with C as given in Equation 5.2–5.3. However, in this case k is immediately affected by the presence of these quantities, $k(\sigma,\theta)$ (Cornett, 2008).

$$E_{wave} = \frac{1}{16}\rho g H_{sig}^2 C_g(T,h) \tag{5.8}$$

This led to the calculations of wave energy for irregular waves in regards to the period as affected by depth (see Equation 5.8). The period that is required to assess the energy is known as energy period and is extracted by zeroth (m_0) and minus one (m_{-1}) spectral moments. The energy period is calculated as below, while it is also known to be connected with the mean-zero crossing period (T_z) and the peak period (T_{peak}).

$$T_e = \frac{m_{-1}}{m_n} \tag{5.9}$$

with

$$m_n = \int_0^{2\pi} \int_0^{\infty} \sigma^n N(\sigma,\theta) d\sigma d\theta \tag{5.10}$$

The energy period (T_e) is a quantity that is connected with the measured period, although several studies have shown that there is a connection with the periods. Specifically it is assumed that T_e=1.14T_z, and T_e=$\alpha_{wave}T_{peak}$, with the coefficient being dependent on the wave of the spectrum and has values close to unity. Finally the H_{sig} that is introduced to the calculation, entails the overall wave height of combined seas both wind generated and swell originating. The following formula provide the way that the significant wave height is considered (Pierson and Moskowitz, 1964; Cornett, 2008; Berr, 2008; Delft, 2014a)

$$H_{sig} = 4\sqrt{\iint N(\sigma,\theta) d\sigma d\theta} \tag{5.11}$$

Wave energy can also be estimated estimated via H_{sig} and T_e, if only those two parameters are available, see Equation 5.12. However, wave energy is estimated by Equation 5.6, in all cases that are explored in studies within the thesis.

$$P_{wave} = \frac{\rho g^2 H_{sig}^2 T_e}{64\pi} \tag{5.12}$$

Having established the interpretation of wave parameters and their transformation into wave energy, the resource assessment for the examined period is presented. The annual and seasonal power levels are expressed in kW/m, although this is the available resource. Extractable amounts of energy depend on the device used and its characteristics, as they are presented later on. It is noticeable that the West part of Scotland is exposed to high values of wave energy around the coastal regions.

Based on the gridded dataset, the wave power for the duration of the hindcast was quantified. It can be seen that the incoming resource is well above 90kW/m at deeper locations. Western coastlines are exposed to an average resource of $\approx 40-60$ kW/m, while the Eastern side has significantly lower levels $\approx 10-20$ kW/m, see Figure 5.9.

In addition, to an overall picture given above, the resource is also examined in terms of annual means. This allows for the identification of consistent high resource areas, that encompass high levels of H_{sig} and wave power. The annual mean wave power resource (kW/m) of the region can be seen for each year in Appendix D, see Figure D.12–D.22.

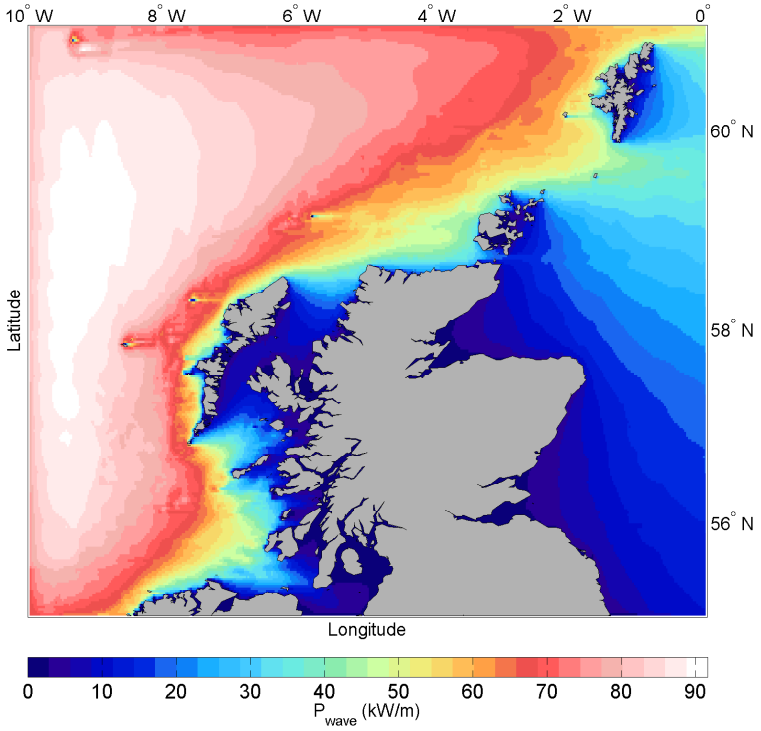

Figure 5.9: Mean wave Power for the region over 11 year hindcast, in kW/m

5.2.5 Annual Variability of Wave Energy

As in the case of H_{sig}, see Section 5.2.2, variability of the wave resource is directly connected to the variation recorded throughout the decade. This means that the alteration of wave energy have to follow predominately change in the distribution of H_{sig}, since the energy calculated is heavily dependent on the square of the wave height.

The evolution of wave energy through the hindcast, allows for inspection of areas with higher energy content. The reasoning behind the examination of the overall timeseries and annual contours, is to offers a high level of understanding about the coastal environment.

In order to better quantify effects of the variability on wave climate, the available wave energy flux as seen in Appendix D, is further inspected in several locations. Application of several devices reveal the utilization factor and production for each site. Coupling of the wave characteristics with wave energy converters, allows us to select an optimal device for a location. In addition, the annual variation that exist can provide information on the potential short-term future performance, as its connected to the variability of the resource.

In this section six devices, representative of the most common technologies are used to estimate energy production. The devices are coupled with the available resource and sea states of the locations, see Figure 5.5. Moreover, selection of sites was also based on their depth characteristics, while the selection of devices is also made in regards to the feasibility of its expected

device in the corresponding depth.

The devices used in the study are representative of several technologies, the Pelamis attenuator, the bottom fixed oscillating flap (resembling Oyster 2), a floating two body heaving converter (resembling WaveBob), WaveStar bottom fixed heave buoy array, WaveDragon an over-topping device and AquaBuoy representing a submerged heave body (Babarit *et al.*, 2012; WaveStar, 2015; Aquamarine, 2015; Hansen and Kramer, 2011; Dalton *et al.*, 2010; Dunnett and Wallace, 2009; Silva *et al.*, 2013; WaveDragon, 2015).

The WECs selected offer a vast array of diversity in application since they represent shallow and deep water appropriate converters. More specifically, due to the nature of construction the Oyster and WaveStar are considered mostly appropriate for shallow water locations while the remaining converters can be classified according to their operational principles. For the technical feasibility of the study, when deep water locations over are examined the Oyster and WaveStar are not taken into account, see Table 5.5–5.6.

Table 5.5: Device classification according to depth

Device	Shallow	Deep	Operational Depths in meters
Bottom Oscillating Flap (Oyster 2)	X		less or equal than 50
WaveStar	X		less or equal than 50
Floating two body heave converter (WaveBob)	X		less or equal than 50
Pelamis		X	over 50
WaveDragon		X	over 50
AquaBuoy	X	X	All

Table 5.6: Locations of Wave Energy Device Application

Name	Depth (m)	Location of point
Blackstone	97	West Scotland
West Hebrides	100	West Scotland
Point 1	8.75	West Scotland
Hebrides 2	55	West Scotland
Holmsound	20	Orkney
Orkney	22	Orkney
Firth of Forth	65	East Scotland

As seen the location depth present a wide array of characteristics from very shallow water of 8.75 m up to mid-depths or approximately 100m. The nearshore locations include the corresponding annual expected production of all devices (e.g. from 8m up to 20m) , while depths over 50m include the two remaining devices. The annual energy yield of each device is calculated based on its power matrix, this allows to additionally calculate the corresponding capacity factor (CF) of the locations. Both quantities allow a significant insight on the opportunities of wave energy and its capabilities.

The variation of H_{sig} affects the energy content to a greater extend, as locations with higher depths seem to have greater recordings of H_{sig}. However, due the nature of shallow locations shoaling, breaking of waves due to bottom friction and non-linear interactions reduce the H_{sig} and decrease the period. With the exception of the locations at the East Scottish coastline, Moray Firth and Firth of Forth, rest locations display high levels of energy content with even the shallowest points record a wave energy potential over 30kW/m.

This of course translates into variability of the bivariate distribution that has to be estimated as investigation on the resource potential and extractable abilities is concerned. The combined distribution of the bivariate sea states, are used with corresponding power matrices to determine energy production.

Starting with the power matrices of the devices presented (see Figure 5.10-Figure 5.15). The nominal production varies per device, for every location under investigation only one wave converter is used, i.e. application of only one device regardless of each nominal capacity. This affects the final energy output, although the capacity factor reveals the span of time that each device is able to operate at each location.

The shallower locations Homlmsound, Orkney and Point 1 are presented with all converters displaying their annual production levels, in terms of the available bivariate sea states given, seeTable 5.7. Following the remaining mid-depth and deep locations compared in production, see Table 5.8.

Table 5.7: Homlmsound, Orkney and Point 1 Annual Variability in Production in GWh for shallow waters

	Homlmsound				Orkney				Point1			
	Oyster	WaveBob	WaveStar	Aquabuoy	Oyster	WaveBob	WaveStar	Aquabuoy	Oyster	WaveBob	WaveStar	Aquabuoy
2004	1.85	0.62	1.09	0.12	4.84	1.61	1.28	0.47	9.77	3.16	0.90	0.68
2005	1.56	0.51	1.18	0.08	3.50	1.22	1.35	0.37	8.66	3.06	0.97	0.59
2006	0.66	0.21	0.28	0.02	3.26	1.16	1.28	0.35	6.52	2.26	1.12	0.41
2007	0.78	0.26	0.91	0.06	3.68	1.29	1.37	0.37	9.74	3.42	0.95	0.51
2008	1.38	0.46	1.12	0.08	4.09	1.44	1.17	0.43	9.84	3.46	0.87	0.55
2009	1.35	0.44	1.06	0.07	3.48	1.23	1.38	0.37	9.16	3.18	0.97	0.66
2010	1.39	0.45	0.86	0.08	3.64	1.27	1.41	0.36	7.66	2.74	1.17	0.61
2011	1.38	0.46	1.21	0.08	3.79	1.35	1.20	0.40	9.76	3.40	0.79	0.47
2012	0.74	0.25	0.78	0.05	4.45	1.57	1.28	0.42	9.01	3.21	0.95	0.60
2013	1.17	0.38	1.01	0.05	2.97	1.04	1.19	0.32	8.57	3.04	0.91	0.57
2014	2.23	0.76	0.81	0.17	3.67	1.28	1.08	0.35	7.53	2.63	1.00	0.49

The proven ability of SWAN, to produce high level hindcasts nearshore, allows to estimate production yields as valid with confidence. The annual variability reveals that in contrast with the sharp deviations in H_{sig}, the final annual production does not deviate as much. In addition, another outcome from this study that helps to disseminate the overall performance of the devices in annual terms, is the capacity factor (CF). The capacity factor (CF) takes into account the nominal rated capacity P_o, the hours in a year (ΔT) and E_o energy produced. Its estimation can be used by the following equation

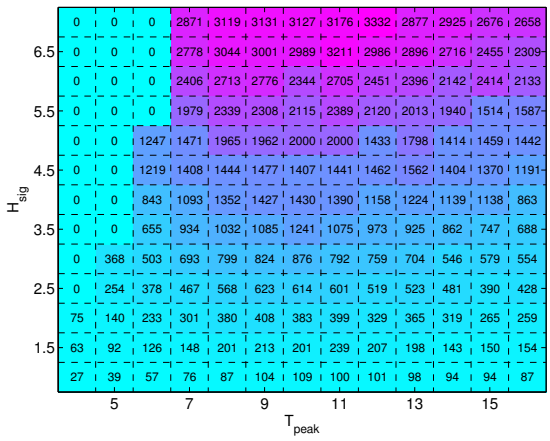

Figure 5.10: BOF Power Matrix

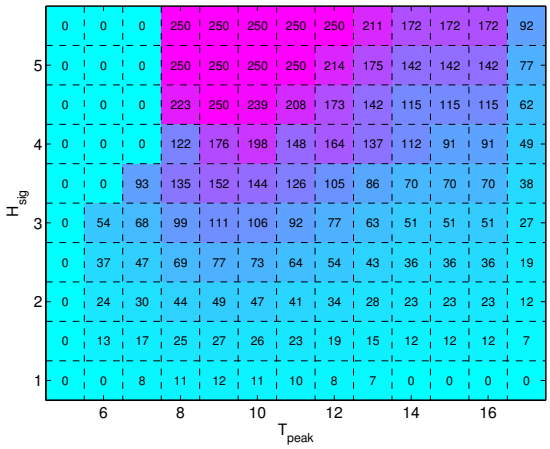

Figure 5.11: AquaBuoy Power Matrix

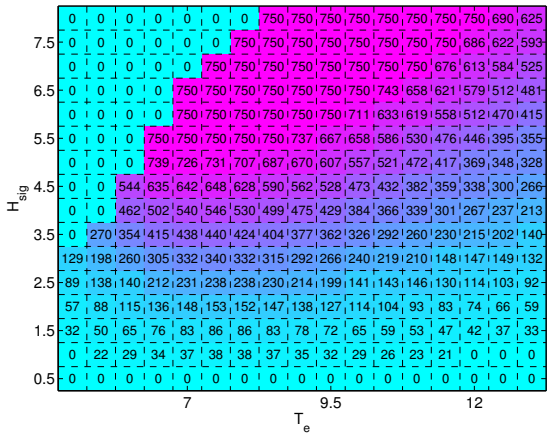

Figure 5.12: Pelamis Power Matrix

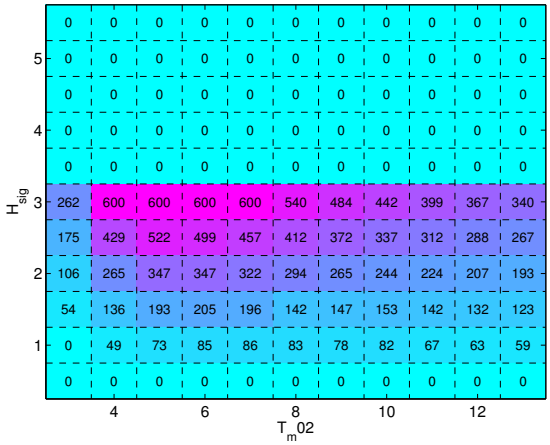

Figure 5.13: WaveStar Power Matrix

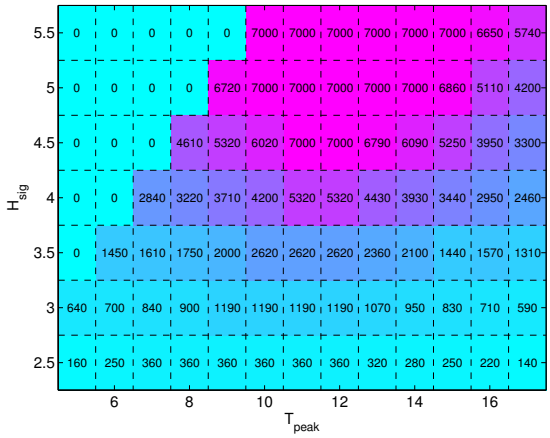

Figure 5.14: WaveDragon Power Matrix

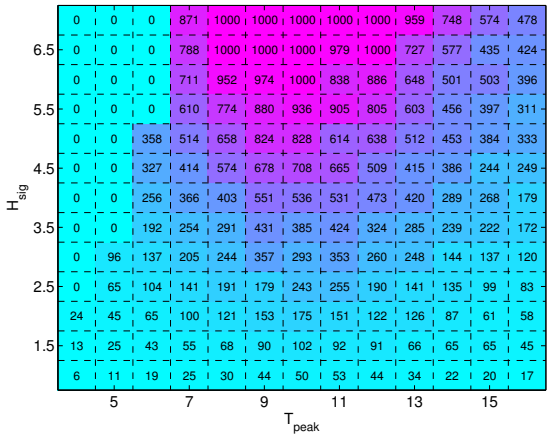

Figure 5.15: WaveBob Power Matrix

Table 5.8: Annual Variability in Production in GWh for deep waters

	BlackStone				West Hebrides			
	Pelamis	Wavebob	WaveDragon	Aquabuoy	Pelamis	Wavebob	WaveDragon	Aquabuoy
2004	1.27	1.41	13.14	0.43	1.92	2.18	19.76	0.57
2005	0.84	0.81	7.10	0.25	1.70	1.88	16.56	0.51
2006	1.07	1.14	20.79	0.33	1.37	1.37	10.59	0.34
2007	1.22	1.27	11.54	0.39	2.19	2.35	19.57	0.57
2008	1.34	1.39	11.99	0.41	2.09	2.23	18.04	0.54
2009	1.36	1.37	11.91	0.41	2.15	2.19	18.05	0.58
2010	0.87	0.77	6.16	0.23	1.40	1.30	10.09	0.36
2011	1.18	1.27	11.22	0.38	2.25	2.45	20.64	0.58
2012	1.36	1.34	11.32	0.39	1.95	1.94	15.57	0.50
2013	1.16	1.16	10.19	0.35	2.09	2.03	16.22	0.52
2014	0.90	0.93	8.35	0.30	1.77	1.93	16.17	0.49
	Hebrides				Firth of Forth			
	Pelamis	Wavebob	WaveDragon	Aquabuoy	Pelamis	Wavebob	WaveDragon	Aquabuoy
2004	1.22	1.68	26.31	0.51	0.63	0.53	2.95	0.09
2005	0.88	1.01	14.56	0.29	0.92	0.74	4.13	0.15
2006	1.02	0.88	7.22	0.26	0.54	0.41	2.20	0.08
2007	1.17	1.11	17.41	0.33	0.58	0.46	3.29	0.13
2008	0.89	0.92	12.94	0.28	0.54	0.43	3.22	0.12
2009	1.17	1.33	17.80	0.39	0.57	0.43	2.77	0.11
2010	1.31	1.08	12.56	0.29	1.11	0.88	5.56	0.22
2011	1.25	1.32	23.36	0.39	0.42	0.30	2.04	0.08
2012	1.24	1.07	17.30	0.32	0.31	0.21	1.45	0.04
2013	0.53	0.63	7.72	0.18	0.59	0.44	3.11	0.11
2014	1.37	1.38	16.09	0.37	0.82	0.68	3.70	0.12

$$E_o = P_o \cdot \Delta T \cdot CF \tag{5.13}$$

with E_o being the annual wave power produced by the coupling of resource with corresponding power matrix. In order to quantify this value, the percentage of occurrences of H_{sig} and wave period (T) must be combined with the power matrix. An indicative bivariate joint distribution for a location provided, see Figure 5.16. The parameter $p_{i,j}$ represents the energy percentage corresponding to the bin assigned. $P_{i,j}$ is the electrical expected output by the same bin as state by the power matrix. The column is denoted j, and the row as i.

Table 5.9: Homlmsound, Orkney and Point 1 Annual Variability in Production in CF

	Homlmsound				Orkney				Point1			
	Oyster	WaveBob	WaveStar	Aquabuoy	Oyster	WaveBob	WaveStar	Aquabuoy	Oyster	WaveBob	WaveStar	Aquabuoy
2004	6.59%	7.03%	20.66%	5.60%	17.28%	18.40%	24.36%	21.42%	34.85%	36.03%	17.09%	31.03%
2005	5.55%	5.81%	22.50%	3.70%	12.47%	13.88%	25.78%	17.08%	30.88%	34.94%	18.43%	26.87%
2006	2.36%	2.37%	5.42%	1.13%	11.64%	13.26%	24.44%	15.77%	23.24%	25.77%	21.24%	18.66%
2007	2.79%	3.00%	17.26%	2.66%	13.14%	14.77%	25.98%	16.96%	34.75%	39.10%	18.14%	23.32%
2008	4.94%	5.26%	21.27%	3.69%	14.59%	16.48%	22.27%	19.46%	35.10%	39.44%	16.47%	25.06%
2009	4.81%	5.04%	20.23%	3.17%	12.43%	14.09%	26.29%	16.98%	32.69%	36.27%	18.50%	30.34%
2010	4.95%	5.15%	16.32%	3.76%	12.97%	14.45%	26.86%	16.59%	27.34%	31.28%	22.32%	27.95%
2011	4.92%	5.26%	22.93%	3.78%	13.52%	15.41%	22.86%	18.47%	34.81%	38.86%	15.10%	21.60%
2012	2.64%	2.84%	14.83%	2.50%	15.87%	17.91%	24.43%	19.12%	32.12%	36.66%	18.12%	27.62%
2013	4.16%	4.34%	19.30%	2.26%	10.59%	11.92%	22.55%	14.81%	30.57%	34.67%	17.39%	25.87%
2014	7.94%	8.70%	15.34%	7.91%	13.08%	14.66%	20.56%	15.82%	26.87%	29.98%	18.95%	22.59%

Table 5.10: Annual Variability in Production in CF for deep waters

	BlackStone				West Hebrides			
	Pelamis	Wavebob	WaveDragon	Aquabuoy	Pelamis	Wavebob	WaveDragon	Aquabuoy
2004	19.26%	16.12%	21.43%	19.83%	29.22%	24.87%	32.22%	26.12%
2005	12.72%	9.20%	11.58%	11.63%	25.87%	21.47%	27.01%	23.23%
2006	16.32%	13.01%	33.91%	15.16%	20.92%	15.62%	17.27%	15.57%
2007	18.61%	14.54%	18.82%	17.71%	33.34%	26.82%	31.92%	25.93%
2008	20.34%	15.89%	19.56%	18.55%	31.87%	25.41%	29.41%	24.50%
2009	20.66%	15.69%	19.42%	18.79%	32.72%	25.01%	29.44%	26.69%
2010	13.18%	8.73%	10.05%	10.41%	21.38%	14.79%	16.46%	16.63%
2011	17.93%	14.48%	18.30%	17.50%	34.30%	27.96%	33.65%	26.61%
2012	20.64%	15.33%	18.46%	17.79%	29.65%	22.10%	25.40%	22.79%
2013	17.60%	13.25%	16.61%	15.92%	31.78%	23.18%	26.46%	23.71%
2014	13.71%	10.62%	13.61%	13.54%	26.95%	22.00%	26.37%	22.32%
	Hebrides				Firth of Forth			
	Pelamis	Wavebob	WaveDragon	Aquabuoy	Pelamis	Wavebob	WaveDragon	Aquabuoy
2004	18.50%	19.15%	42.90%	23.49%	9.65%	6.08%	4.82%	4.02%
2005	13.43%	11.51%	23.75%	13.15%	14.02%	8.39%	6.73%	6.70%
2006	15.56%	9.99%	11.77%	11.92%	8.29%	4.64%	3.59%	3.79%
2007	17.81%	12.65%	28.39%	14.95%	8.79%	5.31%	5.37%	5.75%
2008	13.60%	10.55%	21.10%	12.73%	8.23%	4.93%	5.26%	5.60%
2009	17.76%	15.18%	29.03%	17.86%	8.73%	4.90%	4.51%	4.97%
2010	19.94%	12.32%	20.48%	13.32%	16.85%	10.06%	9.07%	10.14%
2011	19.01%	15.12%	38.10%	17.86%	6.37%	3.41%	3.32%	3.53%
2012	18.83%	12.21%	28.20%	14.70%	4.71%	2.40%	2.36%	2.05%
2013	8.11%	7.22%	12.60%	8.27%	8.99%	5.05%	5.08%	4.88%
2014	20.83%	15.70%	26.24%	16.69%	12.43%	7.81%	6.04%	5.38%

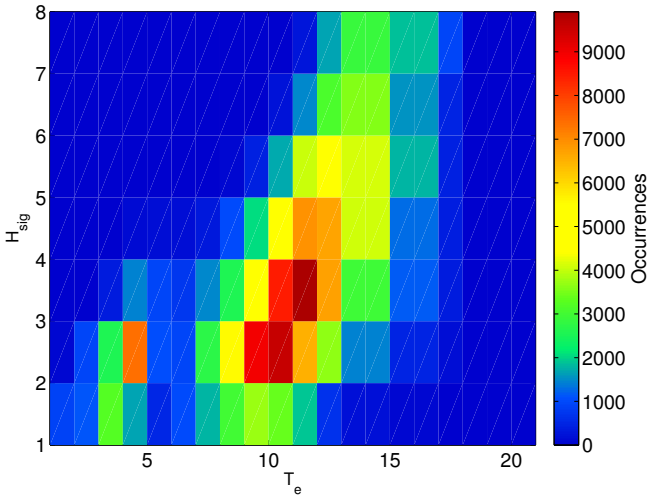

Figure 5.16: Bivariate Distribution at West Hebrides

$$E_o = \frac{1}{100} \cdot \sum_{i=1}^{n_T} \cdot \sum_{i=1}^{n_{H_{sig}}} \cdot p_{i,j} \cdot P_{i,j} \tag{5.14}$$

Notion of the CF from power matrices, although crude since WEC performance is also de-

pendent on directional incident waves, is an extremely helpful term that has been developed and used throughout the years. The term states that according to the produced power, with the device nominal rated capacity and annual time in hours. It is able to provide with a very close to reality approximation of expected production in the absence of information (Manwell *et al.*, 2009; Sathyajith, 2006; Kaldellis, 2011).

This term is used in numerical estimations on energy economics, energy production and provides the basis for a normalization and even comparison of technologies. The CF is dependent on the total energy production within a year and the rated installed capacity, thus smaller the installed capacity with higher production increases the CF. Indicative values in CF per technology are used by institutes, agencies for the aforementioned calculations of energy and economics (Kaldellis, 2011; O'Connor *et al.*, 2013; Bozzi *et al.*, 2011b; Energy Information Administation Agency U.S, 2014). Concerning wave energy, studies have mentioned the use of proposed CF numbers but based on limited amount of data, (Sharkey *et al.*, 2011; O'Connor *et al.*, 2013; Stoutenburg *et al.*, 2010). The nominal installed capacities considered are extracted by the data and the corresponding capacity factors as presented. Note that, electrical losses in the systems are not taken into account since little data exist on the PTO electrical efficiency conversion side.

From the given power matrices the installed capacities of each device are taken into account, with Oyster (approximately 3200 kW), WaveDragon having the highest one (7000kW). In the case of WaveStar, this analysis considers a series of 10 fixed heave buoys with installed capacity of 600kW. The other WECs have a nominal rated capacity ranging from 250kW (Aquabuoy), 750kW (Pelamis) and 1000kW (WaveBob). It has to be noted that in the case of the bottom fixed oscillating flap (Oyster) the nominal is taken as the maxima value presented by its matrix.

CF reveals the temporal usage and productivity of the converters, in a annual time-frame for the given sea-states. For shallow water locations Oyster and WaveBob yielded higher production values due to installed capacities. Interestingly, the AquaBuoy WEC while it has the smallest initial capacity has comparable high operational CF, displaying a versatile performance for all the shallow water location, revealing a promising and cost-effective application.

For mid-depth (intermediate) locations WaveDragon presents overall the greater production levels due to its higher installed capacity. WaveBob and Pelamis have similar yields, while AquaBuoy has the lower energy production. In the examination of their annual CF values WaveDragon attains the highest while (always depending on location), WaveBob and AquaBuoy show high CF rates. It is observed that in all cases WECs yield better performance at shallower locations, due to the compatibility of sea states with their state of operation, that means less occurrence of sea states that will restrict operations (see Table 5.8-5.10).

From the above analysis, the mid-depth locations on the West side of Scotland favour the selection of the WaveDragon and Aquabuoy as an appropriate converters based on the CF,

while the overall highest yield is given by WaveDragon due to its rated capacity. On the contrary for less energetic region of the East coastlines Pelamis presentd higher utilization rated even though the WaveDragon has highest yield on energy production due to rated capacity.

On the other hand selecting an appropriate device for the shallower regions of West Scotland and Orkney proximity areas is a more difficult task. Depending on location all device are within similar ranges, although WaveStar provides higher CF consistently and Oyster yields superior energy production. From the annual utilization point of view though WaveStar outperforms almost at every location, while AquaBuoy due to its range of operation has a much higher CF. Interestingly enough the WaveStar device presents a three times higher CF for the Homlmsound location at which all device are $\approx 5-7\%$. The location itself is a shallow water encapsulated area with finally propagated wave heights being reduced significantly due to non-linear interaction. This can be attributed to the range of converters operation, especially WaveStar, which exhibits more favourable performance for shallower locations and smaller wave heights providing higher production stability.

The annual yields show that even single devices can amount significant contributions in renewable energy, even at shallow water locations obtaining "reduced" wave heights, see Table 5.7-5.8. According to the energy yields, the fixed bottom flap (Oyster resemblance) and WaveDragon due to their higher nominal installed capacity, attain almost twice the amount of energy production, the other WECs which have similar installed capacities spanning from 250kW-1MW, and are able to deliver similar amount of energy throughout the years explored.

Homlmsound and Orkney locations are in similar coordinates and exhibit similar yields, while the location of Point1, situated at Isle of Lewis, shows that even at shallow locations resource of the West Atlantic exposed coastline amounts to deliver twice as much as the two other shallow locations. The mid-depth locations show similar behaviour of performance for both devices, while even the least energetic location at the East Side (Firth of Forth) amount to contribute significant amounts of energy to the overall annual yield (see Table 5.11).

Table 5.11: Overall Mean Annual Production over the 11-year period, in GWh

	Oyster	Pelamis	Wavebob	WaveStar	WaveDragon	Aquabuoy
Homlmsound	1.32	n/a	0.44	0.94	n/a	0.08
Orkney	3.76	n/a	1.32	1.27	n/a	0.38
Point1	8.75	n/a	3.05	0.96	n/a	0.56
BlackStone	n/a	1.14	1.17	n/a	11.25	0.35
West Hebrides	n/a	1.90	1.98	n/a	16.48	0.51
Hebrides 2	n/a	1.10	1.13	n/a	15.75	0.33
Firth of Forth	n/a	0.64	0.50	n/a	3.13	0.11

As stated the yield calculation took into account the nominal installed capacity, in order to have a broader estimation of performance for similar longitudes and latitudes. The CF can act as an index to offer information concerning the decision making and future economic considerations

of wave energy applications. The CF takes into account, all the production information included in the power matrix and sea states. It compares the annual power production providing us with indication that the machine will be operating within a given year. This normalizes the field and reveals the operational situation for any given device at these locations.

The estimation of these capacity factors pose an improvement to the so far perception of wave devices performance. Due to the amount of wave and production data, the CFs given reveal the overall performance of the device and may be used for further exploitation.

From the above tables it is observed that regardless of the annual yield the CF at Orkney favours WaveStar, which although it yielded less than the annual production of the fixed depth flap, it exhibits a higher utilization rate within the year, with least efficient proved to be the heave buoy. Although, the West shallow location Point1 clearly shows that in such highly energetic waters as the one found in the open Atlantic coasts, higher operating devices are to be considered such as WaveBob. On the other hand, WaveStar achieves only 24.22% this performance closely relates to the operational conditions expressed for each device as given by the power matrices (see Figure 5.10-5.15).

For mid-depth (intermediate) locations of the West Scottish coastlines WaveDragon has the highest CF and energy yields. The range of operation at which the AquaBuoy operates allows it to achieve a higher CF from the Pelamis which is three times bigger in rated power. In all three west locations WaveBob and AquaBuoy are the closest in CF rate after the WaveDragon. For the Firth of Forth on the other hand Pelamis proves to be the most favourable device in terms of CF. Though all the devices presented have differences in their rated capacities, extraction of energy and active span of production based on resource, allowed estimated CF to compare them regardless.

Table 5.12: Estimated CF over the 11-year, in %

	Oyster	Pelamis	Wavebob	WaveStar	WaveDragon	Aquabuoy	Mean % Location
Homlmsound	4.70%	n/a	4.98%	17.82%	n/a	3.65%	7.79%
Orkney	13.42%	n/a	15.02%	24.22%	n/a	17.50%	17.54%
Point 1	31.20%	n/a	34.82%	18.34%	n/a	25.54%	27.47%
Mean % Device	16.44%	n/a	18.27%	20.13%	n/a	15.56%	17.60%
BlackStone	n/a	17.36%	13.35%	n/a	18.34%	16.07%	16.28%
West Hebrides	n/a	15.61%	22.66%	n/a	26.87%	23.10%	22.06%
Hebrides 2	n/a	14.45%	12.87%	n/a	25.69%	14.99%	17.00%
Firth of Forth	n/a	12.97%	5.72%	n/a	5.10%	5.16%	7.24%
Mean % Device	n/a	15.10%	13.65%	n/a	19.00%	14.83%	15.65%

The extensive validation of a high-resolution shallow wave model, led to the exploration of mid-depth and very shallow locations. The annual variations in wave parameters affect the bivariate sea states, which will ultimately impact the annual production of each device. Through our examination and coupling of potential device production several capacity factors were found (see Table 5.12) the author believes that there is a comparable behaviour of wave energy to other forms of technology.

The capacity factors calculated have been given to every mid-depth and shallow location, though the author feels that for the West Scottish coastline shallow locations can be characterized by capacity factor of 15-25% (device dependent), the Orkney and North exposed waters by 10-20% (device dependent), though the information concerning activity within the range of operational sea have to be taken into account. In overall locations of small depths in the West exposed Atlantic are expected to improve the renewable generation.

Concerning mid-depth and deep location the performance of WECs led to examine a capacity factor within the range of average 20-30%, though deeper locations are exposed to far more energetic resource they also increase the occurrences of extreme and storm waves, which reduce the operational time of the devices, usually for survivability.

This being the case, from an energy standpoint, shallow locations can be exploited by the four, WaveBob and Oyster with high CF and production, while for deeper locations although the Pelamis and WaveDragon attain high yields and utilisation rates. Surprisingly Aquabuoy, although it has yielded the smallest energy production it has acquired a good level of utilization (CF), and the author feels that this is also a viable candidate, since from an economic point of view it may prove to be less expensive.

Note that these findings are based on the exhibited annual variability in energy production terms. The power matrices used are the so-called "generic" of the corresponding devices. By utilising adjusted device power matrices to the specific bivariate analysis improved results can be expected, with power performance matching resource characteristics better. Although no access to scaled location power matrices were able to be obtained as they are confidential. Furthermore, since most power matrices have been extracted by previous studies the accuracy of the calculations lay within the hydrodynamic and numerical models used for their calibration and calculation, some error bounds concerning the range of error for some devices have been identified in Babarit *et al.* (2012), with ranges of production form -20% to +20% in expected energy production.

Finally, further investigation is proposed to be conducted on the effects, these energy results will have on the capital cost of investments, and potential environmental impacts of each device. This though is not in the scope of this thesis.

5.2.6 Wave Energy Development Index (WEDI)

Resource estimation, energy levels, annual variability of waves, comprise important knowledge in the further exploitation and utilization of ocean energy. Although apart from the quest of most energetic location, several considerations are to be taken also into account. Accessibility, near port location and resource estimations are the drivers for reduction of maintenance and operational cost. The mean annual energy flux variation per location is displayed in Figure 5.17.

The investigation of effects on the cost lead to the adoption of the WEDI index as an informative

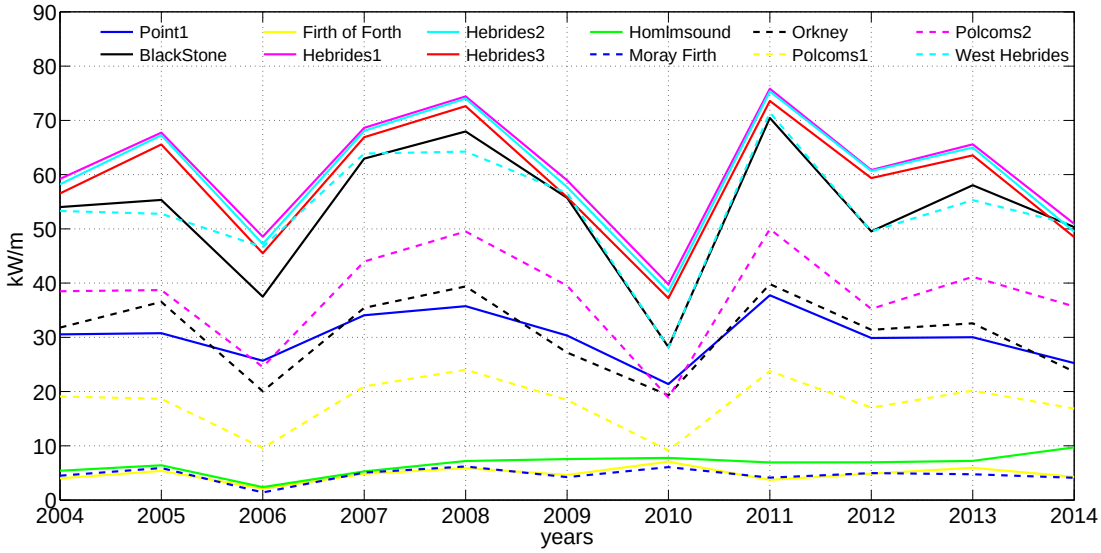

Figure 5.17: Annual Mean Energy Flux Variability

approach (Hagerman, 2001). This index relies on the notion of maximum wave energy flux that is propagated and reaches the potential candidate sites, and this index is directly connected to the maximum values of H_{sig} and T_e that are recorded/hindcasted in the locations. This in turn provides with information about the potential impact of waves on the devices, their moorings and components. The calculation takes into account the extreme values of waves during the SWAN hindcast, leading to the calculation of the highest energy flux. The amount of data allow for a better representation of the decade offshore environment, especially since shallow locations are hindcasted with high confidence, SWAN nearshore water mechanics allowed full representation. Thus special interest is given at the locations that were compared for their energy content and wave converters applicability (see Section 5.2.5).

In overall, a high recorded WEDI leads to an increase in the maintenance and operational costs, with the ability of potential revenues by electricity supply. To further strengthen the notion of optimal selection amongst candidate locations, estimations about the energy flux for the sites are also calculated. This is done to establish performance of the devices and expected increase in cost. The assessment in energy terms allows a direct comparison for the drawbacks and benefits present at each location. The locations and decade indices are provided with maxima of peak energy and significant wave height which present the maxima values of H_{sig} for every location throughout the hindcast years.

WEDI is directly correlated with the extreme energy content of its locations. This is done to stress out the fact that wave energy converters have to operate and "survive" under low and extreme (potential storm conditions). Point 1 has the highest indices, while as expected the East side location present the lowest ones, see Figure 5.18. One has to keep in mind, that the indices is a direct comparison of the individual location and its characteristics, thus actually

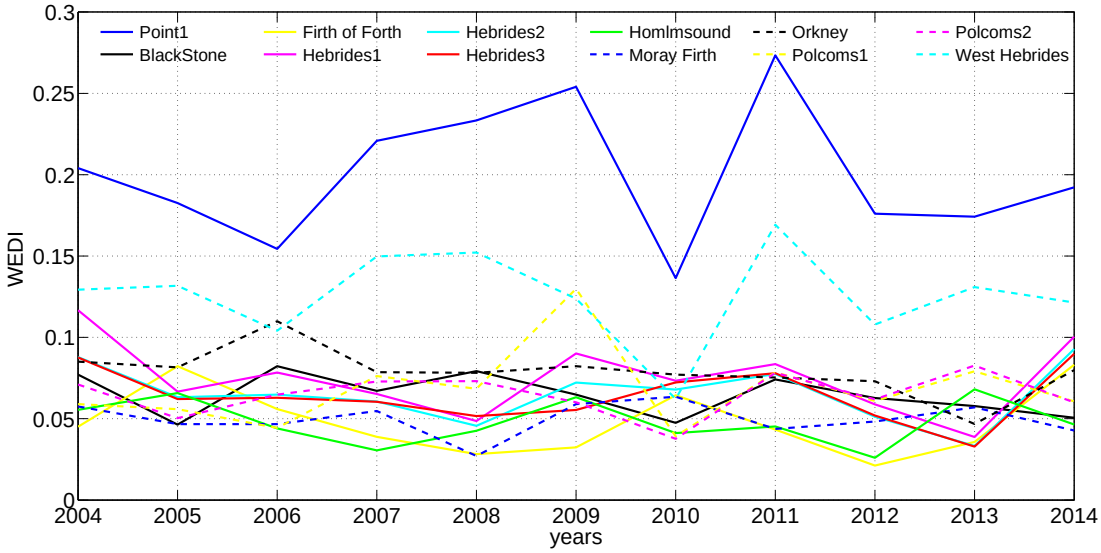

Figure 5.18: Annual WEDI Variability

the most severe weight heights are not occurring at Point1 but at deeper locations, Table 5.6 for depth information.

Since the definition of the index revolves around extreme influx of energy around a location, it is helpful to also consider the annual average wave energy flux as it occurs in every location, The mean energy flux (see Figure 5.19) with the information on production per device and capacity factors as presented in Section 5.2.5, aid to the further dissemination about the locations capabilities. Point1 and West Hebrides present the highest WEDI, while from those two the latter has a better incoming energy flux.

Although this is mainly due to the deeper situation of that area, while the first one is characterised as very shallow environment. In addition (see Table 5.9 and Table 5.10) exhibit the exploitation rates of each device. For the commonly used devices Pelamis and WaveBob, Point1 proves more attractive in terms of energy production capabilities, since a higher CF leads to greater utilisation times annually. This outcome is also validated by the annual electricity production as given in Table 5.7 and Table 5.8.

The combination of the energy production and WEDI, can help us distil the potential location based on a broader context that takes into account the annual production, maxima and energy content. Amongst the most interesting cases that can be expanded for investigation is the Hebrides2 location which present a very high annual energy flux and a significantly low corresponding WEDI, located at mid-depth (see Table 5.2). It share the same wave characteristic environment as the two nearby points Hebrides 1 and 3, with annual CF approximately 20% and amongst the lowest indices.

Combining the knowledge derived by the annual maxima of wave energy and average values, the author feels that several locations can be proposed for further and more thorough inves-

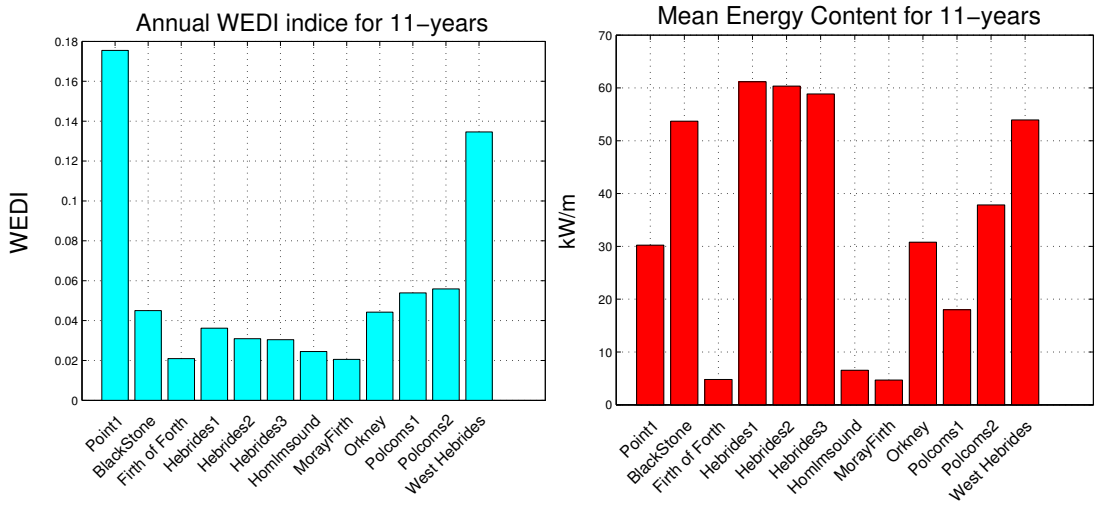

Figure 5.19: WEDI and mean energy content

tigation of renewable wave energy converters, and overview of the WEDI index distribution around the Scottish coastline is presented in Figure 5.20. The locations around the North West side of the Isle of Lewis (Hebrides1, Hebride2, Hebrides3, Point1), Orkney and Polcoms2 locations, are for future investigation by applying specific calibrated wave energy converters alongside with local wave modelling hindcast/forecast systems. Such a future study, shall include optimal size of devices, optimal configuration layout, environmental effects and wave to wave interactions between devices.

The index presented, offers an alternative to the energy and investment criteria for a location, by the approach of taking into account a broader set of factors an informative method for energy assessments site may be implemented. The author expresses the opinion, based on the selection of sites solely on extreme events of maximum energy modelling hindcast may not be a suitable approach. Although, wave modelling offers us the valuable approach in re-creating a high temporal and spatial database of wave events it can not end there. The incorporation of wave energy converters into the results of any modelling process alongside with appropriately selected indices, may prove a helpful for the wave energy industry.

Thus, the presented information do not offer a substitution of existing methods, but rather an additional informative process. In order to fully establish a better representation for wave energy opportunities, high resolution wave data (temporally and spatially) can identify limitations and minimise assumptions. The assessment of energy production behaviours with statistical processes of extreme events is expected to add further knowledge in the selection and calculation of wave energy. This approach is discussed in Chapter 7, where high resolution coastal information are disseminated to optimise the selection of statistical processes and extreme event calculations with application for the general offshore marine community.

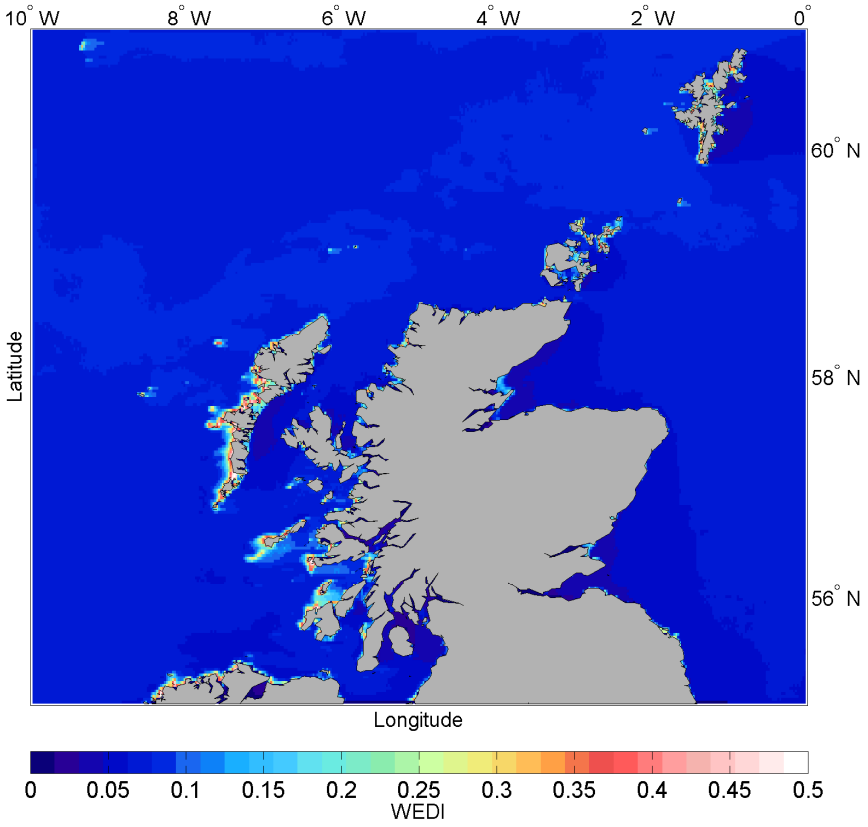

Figure 5.20: WEDI map Scotland

5.3 The Case of the Mediterranean and Aegean Sea Potential

As mentioned in Section 4.5, the Aegean and Mediterranean Seas were investigated in order to examine the resource and explore the opportunities of wave energy potential. After the proper calibration of the model, results revealed several locations that could be used for wave energy deployments in the Greek naval space. Issues concerning the modelling in rapid varying bathymetry areas were discussed in Section 4.5. The initial calibration of the model was based on a tailored solution with the results being presented (Lavidas *et al.*, 2014b).

The domain of the Aegean Sea constitutes a complex and rather unique environment, with many individual islands comprising many points of non grid connected to the main electricity network. This arises the opportunity to explore several small electrical island systems to incorporate wave energy. That would benefit the concerned electricity costs and diversification from the oil based fuels that are used currently in the islands.

This poses a potential contribution to the utilisation of wave energy as a consideration for renewable production. With all islands isolated from the grid and powered by their own individual fossil fuel stations. Potential incorporation of renewable wave energy may alleviate and reduce the imports of electricity of the future necessity for infrastructure. This diversification in

the production of renewables is expected to reduce the need for fossil power plant, the heavily subsidisation of oil transport in the Greek islands and promote the awareness and potential that wave power will have on the system (Kaldellis, 2011; Zafirakis *et al.*, 2013).

The analysis and wave power location identification was performed based on the year 2010, after the alleviation of irregular performance, validation was performed on seven buoy location. The majority of them are located in intermediate waters, although the surrounding orography of most buoys poses a significant challenge. As mentioned, the Aegean Sea is a rather complex area, the vast majority of islands and large coastline enhance non-linear and shallow water interactions, affecting and increase the occurrence of diffraction, refraction and bottom-breaking effects. Many of the buoys are located in encapsulated environments, where the refraction and triad effects are dominant and increasing the complexity for the model consideration. After the validation, all points identified in the areas ,that can be considered as candidates for wave energy were examined.

Both the annual, seasonal averages of wave energy resource were explored in order to establish the initial screening of best areas for wave converters. Following the identification of exemplary sites, the resource potential is given with an investigation of the bivariate seas state and the consideration of two wave devices. The adaptation of two devices is performed, in order to examine the behaviours of the devices in the environments and calculate the average energy output expected, and capacity factor that can be achieved in the Aegean Sea.

5.3.1 Validation and identifying areas of wave resource

The buoy data were obtained by the Hellenic Centre for Marine Research (Hellenic Centre for Marine for Research, 2014), and it consisted with seven buoys active then, their approximate locations as given by the HCMR. In addition the calibration involved the adaptation and identification of the area, based on the data from three buoys, for more information the reader is directed to (Lavidas *et al.*, 2014b) and Appendix B.

Performance of the model, with statistical indices, biases, rms errors, SI indices are given in Table B.7. The time-series obtained are annual, although several periods missing and are excluded by post-processing from the comparison, while some recorded data are affected by "noise" effects, thus caution is advised for these locations.

With an established performance of SWAN, areas with absence of buoys can rely on hindcast data. Locations at shallower waters can be modelled with confidence and a more thorough investigation of wave energy potential is achievable. This is extended to further locations that are taken into account, as seen Table B.7. After the validation process, the model run a hindcast which improved on the indices and especially the period, while at the same time more locations were taken into account, for further examination of the wave energy potential (see Table B.8).

The nature of the Aegean topography, depending on the location leads to underestimation

or overestimation in the biases. Although this kind of performance is expected by numerical models, due to inherit restriction they carry, such as the designated bins interval for frequency and direction. In this case 24 bins are assigned for direction and frequency. This offers a good resolution of the components, requires less computational and storage requirements for calculations of the model. Another consideration was to increase both to 30 though the storage requirements would be much greater. The sudden alterations in the hindcasted data can be attributed to the sudden topography and the shallow water interaction of the Aegean, especially near the sharp island coastlines.

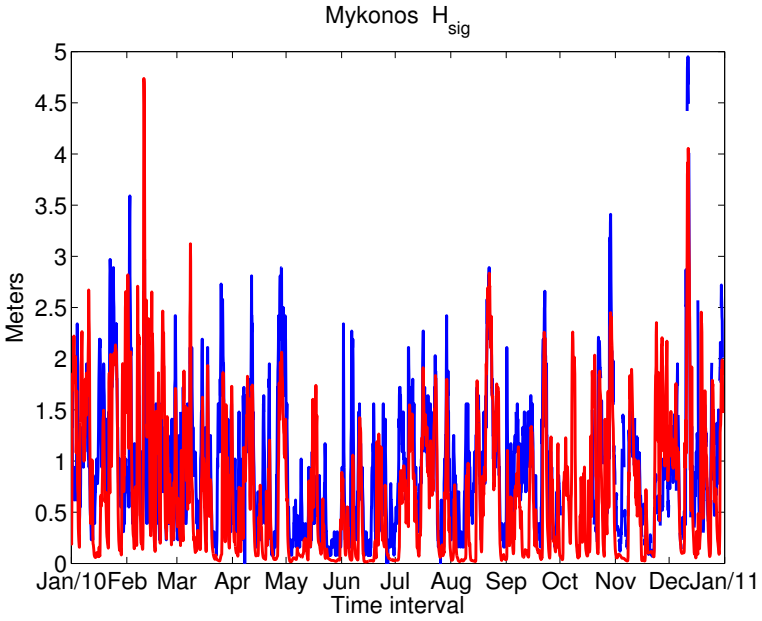

Figure 5.21: Mykonos location hindcast of H_{sig},

The Athos buoy which is located at the Northern part of the Aegean (212m depth), presents the lowest correlation of H_{sig}, this can be attributed to the low levels of available wave height, since the location itself is within an "isolated" environment with many dry (island) points dissipating incoming waves from the South with fetches of North-East and North-West side small in magnitude. The swell size in combination with the rapid changes in bathymetry increase the effects of dissipation, wave breaking and white-capping effects. Although the local wind resource is adequately high in the region.

The Petrokaravo buoy is located in deep water area (211m depth) between the region of Attika and the island of Egina. Location of the buoy is surrounded by land masses (small islands), turning coastlines and the small depths decreasing the wave heights. Here also nearshore water physics are the predominant reason for wave reductions. Coastal tuning applied in SWAN represented accurately the peak and spectral period. Diffraction and refraction of the surrounding dry points, which are at close proximity, redirect and reduce the wave height, as expected.

The Pylos buoy located at the South West corner of Peloponnesus (1681m depth), displays good correlation, with the location exposed in rapid varying winds and swells originating from the West Side of the Mediterranean Sea. Kalamata buoy is set at 340m depth, located at the Messenian Gulf characterised as a highly encapsulated location, the measurements contain a lot of "noisy" recordings thus reducing the validation process and not taken into account. As in the case of Petrokaravo shallow water physics is dominant, the performance of SWAN indicates that further examination is required solely in this area, calibration concerning the nearshore components is imperative, with all parameters offering over-estimations.

Santorini and Mykonos (see Figure 5.21) buoys, are located within the Cycladic complex of islands, with the first located South at the island of Santorini and at depth 314m, while the latter on the North section of Cyclades near Andros and Mykonos at depth 138m. The location are seen by the forthcoming maps, and are amongst the locations exposed to the most volatile resource, interacting with swells from both the North (small swells predominately) from South Aegean and West Mediterranean.

Santorini slightly overestimates the H_{sig} while Mykonos shows a small underestimation in all its quantities. The rms and bias levels though are very small with small deviations. Finally, Lesvos is located at the shoreline of Lesvos, the performance of all indices by SWAN is high, with a good MPI for all measured data, and small deviations.

As mentioned the physical aspect of the Greek sea space offers a complex environment, and the use of coastal water model to obtain and expand our knowledge is imperative. The discrepancies and inconsistencies that appeared can be solved by the localized application of SWAN and a much more detailed bathymetric model of the surrounding area. At this point data less than 0.025^o are not available to the authors. The physical calibration and optimization of SWAN shows that the consistent errors pointed in this hindcast have been alleviated.

Although magnitude of triads, the computational timestep and the turning rates are adjusted, depending on the model resolution to avoid "hot-spots", affecting the hindcast of peak period. For the coarse run, which employs a 0.1^o mesh the CFL criterion was violated, although the initial coarse mesh has higher resolution than most previous studies that have operated similar resource assessments (Soukissian and Pospathopoulos, 2006; Korres *et al.*, 2011; Bertotti and Cavaleri, 2009; Athens, 2014). Selection of the CFSR wind product as input, offers higher peaks thus producing estimations of wave parameters as presented in the Section 4.2.

The annual hourly timeseries are hindcasted for the all buoys' in order to assess the expected levels of incoming wave energy in kW/m. Although the buoys locations are not completely representative for the proposal of wave energy sites, a combination with wave maps, a robust approximation of future energy sites studies can be proposed.

The average annual and seasonal wave power estimations, lead to the proposal of several sites that can be used for further exploitation and consideration of WECs. The annual average wave

power is given in terms of kW/m while an analysis has also been conducted in order to highlight the production variation of the Aegean environment. The classified seasons are Season 1 (January-March), Season 2 (April-June), Season 3 (July-September), Season 4 (October-December), see Figure 5.22.

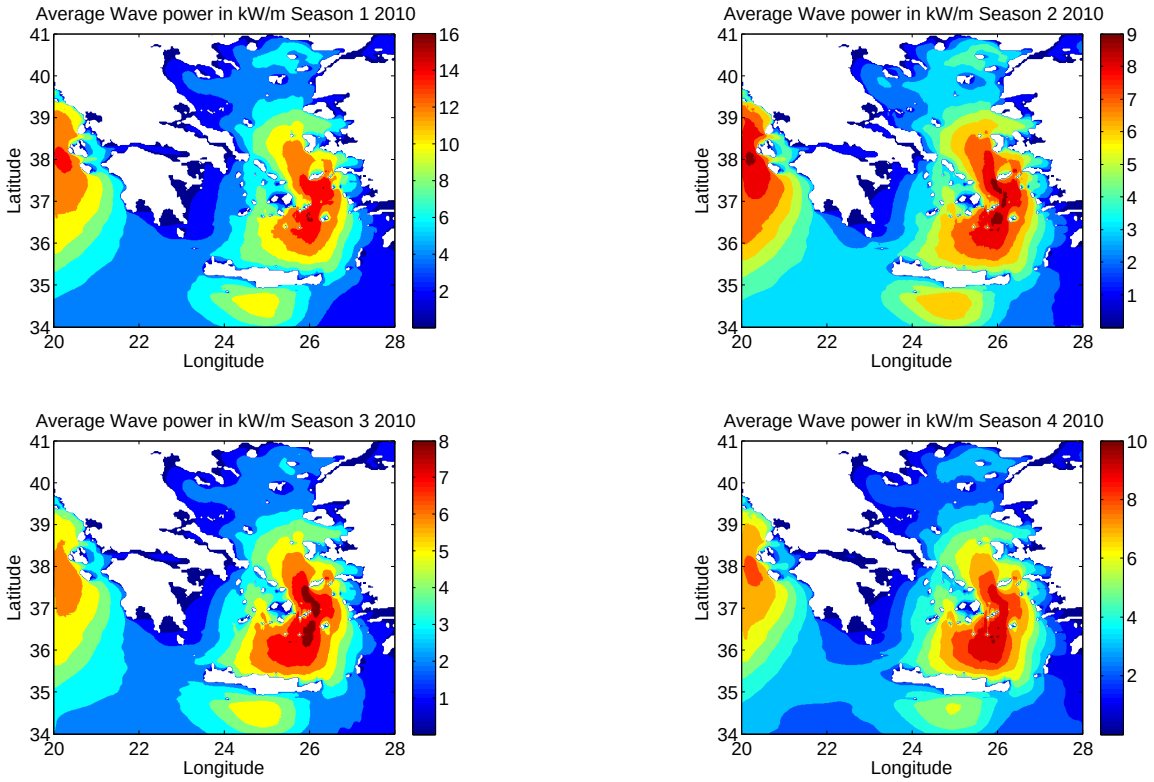

Figure 5.22: Seasonal estimation for wave power in the Aegean,

The most energetic months for waves are the winter and autumn seasons (Season 1 and Season 4) with regards to the timeseries of the individual locations, the most volatile winds are expressed in that time-frame while the highest wave are expected as well (Stopa *et al.*, 2013; Akpinar and Kömürcü, 2013). It is obvious that throughout the seasonal hindcast wave analysis greater amounts of wave power can be located in the Central part of the Aegean, the Cycladic complex, Crete and the Ionian Islands. This poses a potential contribution to the utilisation of wave energy as a consideration for renewable production, since that all islands are isolated from the grid are powered by their own individual fossil fuel stations and a potential incorporation of renewables may alleviate and reduce the imports of electricity of the future necessity for infrastructure. This diversification in the production of renewables is expected to reduce the need for fossil power plant, heavily subsidisation of oil transport in the Greek island and promote the awareness and potential that wave power will have on the system.

Seasonal resource assessment provides information, in order to understand the potential applicability and application of a power device, which provide with the annual estimated power that

can be harnessed. Throughout the seasons, wave resource is concentrated and deemed as high in the same areas, this may be used as a starting point for investigation on the applicability and estimation of wave energy and how it can contribute to the mix, see Figure 5.22.

5.3.2 Wave Power Applicability

In order to assess the energy content of a resource two devices are considered. For this estimation the location with average depth, similar to the allowed depth for the installation of wave devices is noted, while at the same time the identified wave resource areas, as indicated above will be considered. The wave power matrix provides with an indication on available extractable power from a specific technology, based on the average spectral components of the sea-state. This highlights in further detail the selection of sea states dominant in the area and will allow for an overall estimation on the energy content (Fusco *et al.*, 2010; Babarit *et al.*, 2012).

Taking into account the depth variation and available resource, two locations are indicatively chosen for estimation in the contribution of wave power. Each device explored has one WEC installed and the rating of energy production is based on its nominal capacity. This is done in order to quantify the expected production a system like that would have in the Aegean Sea and the potential contribution to the small de-centralised electricity grid of the islands. The two devices used in this assessment are the Pelamis attenuator and WaveBob heave buoy, with both power matrices presented.

Based on the power matrix of the devices, and the hindcast resource for the interval used to validate the model, the expected results allows to assess the extractable energy that can be produced for the Greek territory. The results show that the wave energy converter (WEC) Pelamis is able to produce for the location of Santorini a summation 133.2 MWh, yielding a capacity factor of 11%, while the WaveBob WEC provides 123.9 MWh and a corresponding capacity factor 8%. The Mykonos location exhibits similar behaviour. The Pelamis delivers cumulatively 125 MWh with a capacity factor of 11% while the WaveBob 93.6 MWh has a CF of 7%.

The results indicate that, although the wave resource is not as energetic as in oceanic waters (Cruz, 2008), the Aegean Sea can still utilise WECs to contribute to diversification of the energy mix and enhance renewable energy production. Through the installation of various renewables technologies, groups of island complexes existing in the Aegean can benefit and reduce the intermittent nature of renewables by adopting sources of energy that supplement each other, such as wind and waves (Janssen, 2009; Cradden *et al.*, 2012). Currently many similar studies on small electrical grids, have explored the integration of wave energy into their mix with promising results in areas though that are exposed to the Atlantic ocean (Babarit *et al.*, 2006; Vannuchi and Cappietti, 2013; Veigas *et al.*, 2014; Pallares *et al.*, 2014).

5.4 Summary

In this chapter the application of SWAN models in several location were examined. A high resolution coastal map for Scotland and the North Sea was produced, based on a model applied with customizations for these areas. This led to an improvement of existing maps, in the overall assessments of H_{sig} and P_{wave} annual resource assessments. In order to confidently present the results several outputs were compared with existing buoys and other models. The performance of SWAN improved our perception for nearshore coastal locations, adding to the contribution concerning wave climate in all Scottish coastlines.

Furthermore, coastal water locations were examined, mostly focused in areas of high renewable deployment interest i.e. Orkney, the Hebridean area and the East Side of Scotland. The output maps and annual variability investigation was performed for all existing buoy compared locations, other models and several very nearshore water outputs.

Following the annual variability investigation, the wave energy production perspective is assessed. The necessary information and theory behind wave energy calculations are presented. Coupling of WECs and high-resolution data assessed energy production. Numerous wave converters are subjected to energy production estimations, and capacity factor determination. The sites have been appropriately selected to simulate and follow as close as possible, the interest for wave energy site deployments and nearby validated points. As expected the most energetic area is the West Scottish coastlines, which were extensively examined in terms of production and annual variability.

The coupling and comparison of SWAN with the power matrices, showed the different energy yields by each device. Taking into account the technical characteristics of each device applied them to hindcasted sea-states we managed to investigate the potential of energy extracted per location. This allowed to draw some conclusions for the optimal selection of device based on temporal, spatial and technical features.

In addition, to the energy production cycle investigation, WEDI index was also applied to the maps and locations. This index, in combination with production estimations, can be used to assess the viability in extreme conditions for wave energy deployments, reducing the uncertainty of capital cost in investments and providing a continuous energy delivery.

Apart from the case of Scotland, the model was also applied in a custom way to the Aegean Sea. This led to the identification of wave energy resource areas of interest, and additionally testing the ability in energy production of converters for seas not as energetic as the North Atlantic. To the authors knowledge this was the first attempt in quantifying the wave energy resource production in the area, while it also strengthen the ability in use of the model for adaptation in different areas.

Although the energy content is not as high, it revealed that several opportunities exist for the wave industry even in the case of milder seas. The investigation was prompted by the fact, that

the Aegean is characterized by many island decentralized areas, which depend of conventional production. Apart from the high resolution wave assessment, energy potential of two areas were examined and annual yields and capacity factors determined. Additionally it concluded to findings for further energy investigation in the area, for a more detailed energy analysis in the future at specific locations. The process allowed to develop a numerical SWAN model that is expected to be applied in a larger temporal scale.

Finally, it was shown throughout this Chapter that wave energy modelling, can be utilized in many applications, with climate and offshore studies benefiting already by capabilities of wave modelling. The wave energy community has not fully unlocked the potential of high resolution and increased length numerical modelling.

Chapter 6

Economics for Wave Energy

"No complaint... is more common than that of a scarcity of money.

Adam Smith, 1723-1790 A.D.

6.1 Introduction

Energy performance is a strong indicator on the viability of a renewable technology. Although, several factors may hinder the applicability of a technology. To allow commercialisation and development of a technology, energy analysis must always be accompanied by expected costs. Cost indicators, and financial analysis display the economic capabilities of a technological solution.

While cost of energy (COE) and levelised cost of energy (LCOE), provide comparable results to other technologies. It is not until the economic assessment of payback periods, for the capital expenditure, that solidifies the applicability of technologies. A cost-to-benefit approach allows to estimate the revenue streams and break-even year. In terms of business plans estimating the time for which a technology will repay its expenditure is vital.

In energy application, a robust financial analysis depends on the accurate determination of its energy performance characteristics. Efficiency levels, and production information are extrapolated for the duration of a projects lifetime. From our energy analysis and the long-term determination of production characteristics, the assumptions of financial indicators can be minimised. In addition, to selecting the optimal device for a given resource, the expected energy will determine the financial return.

6.2 Finance of Wave Energy

The energy production capabilities presented in the previous section, revealed that wave energy converters have the potential for large renewable contributions. Although, the economic viability of an wave energy project is the final index that will allow the promotion and further deployment. Economic assessments are directly connected with the disseminated results by an engineering approach. In the previous chapters the coupling of wave modelling and generation capabilities of various devices, alongside with the wave development index provided with a view of factors affecting the economic prospects.

As it will be shown the important results derived from Section 5.2.5 affect directly the assessment of such installations. Since most economic decisions are calculated with potential and approximate values, the robust determination of CF and location characteristics allow for a better representation of the viability and economic potentials by wave energy.

Several studies have examined the integration of renewables and wave energy (Taylor *et al.*, 2006; DTI, 2002), with expected production and cost considerations. Due to the recent interest for wave energy and the reduction of emissions as given by the (Parliament, 2009), studies examining the installation costs and economic performance of wave energy converters have been available for the case of Scotland and several other European countries, (Allan *et al.*, 2011; Mathiesen *et al.*, 2011; Carballo and Iglesias, 2012; Dalton *et al.*, 2010; O'Connor *et al.*, 2013). Providing valuable information about the perspective costs and performance of wave energy, although, most of the studies are limited by their assumptions on the resource availability and device investigation.

The ultimate goal of increased wave energy into the electricity grid is halted by the nature of the resource itself, its variability poses problems similar to other renewables. These uncertainty levels in expected production estimations, increase the cost for capital expenditure, amortization periods, cost of energy, and necessity of infrastructure strengthening the electricity grid (DTI, 2002; Verbruggen *et al.*, 2010; Blanco *et al.*, 2011; Hervás Soriano and Mulatero, 2011; Schaber *et al.*, 2012b; Krozer, 2013).

Though limited data concerning wave energy economics, apart the LCOE of wave devices. So far capital expenditures, maintenance, constructions and variable cost, are based on previous studies and assumptions (Dalton *et al.*, 2010; Allan *et al.*, 2011; Carbon Trust and AMEC, 2012; O'Connor *et al.*, 2013). Reportedly the PTO system of a WEC varies from 1,500,000 £to 3,000,000 £per MW. Though, since no definitive data exist in this part we shall consider an initial capital cost (IC_o), starting from 3,000,000 £/MW since the technologies are in their primary states.

As mentioned in Section 5.2.5 the CF is the main factor for estimating future production estimation which consequently leads to amortization periods, expenditures, revenues and LCOE estimation. Previous studies mentioned which estimated the economic of wave energy projects,

assigned a capacity factor based on correlation to onshore wind regardless of device selected.

The detailed resource and energy assessment per device and location we have chosen to use our own calculated CF. These in turn offer an improved representation of the estimated economic indicators. Moreover, taking into account the severity WEDI index and resource assessment provide in Section 5.2.4, alongside with the contours of wave power potential (see Figure D.12-Figure D.12) and the availability for wave deployment sites as presented by (CrownEstates, 2014). Focus is given at the Isle of Lewis and especially the Point 1 and Orkney locations as shallow, while West Hebrides for a deep water representative (see Table 5.2). With their energy analysis (see Table 5.11) and annual exposure discussed in Section 5.2.6, their estimated capacity factors are used (see Table 5.12).

Based on the findings of energy production of Section 5.2.5 and the underline of the appropriate device selection. The investigation is conducted on the hypothesis that the size of the wave farm is representative of one installed device restricted to its nominal installed capacity as in Section 5.2.4, though (O'Connor *et al.*, 2013) suggests that by the bulk usage on wave energy converters in farm arrays the installation cost might be lowered.

Although, it has to be noted a similar approach on devices increases the uncertainty involved, since the variable costs associated with these installations are not known. A fact that might increase the cost annual operation. For this reason the representative devices are assessed one at a time providing a robust analysis backed up by the wave energy assessment, in hope that this will prove the economic capabilities of such devices with potential reduction in maintenance and operation through farm arrays, as also mentioned in Dalton *et al.* (2010).

6.3 Financial Analysis

The capital expenditure (ICn) is equal to the PTO cost prior to installation (ex-works), in order though to assess the economic performance additional terms have to be taken into account. These correspond to the expenditures on the installation process and annual expenditure on maintenance and operation. These costs vary depending of the specific requirements of each technology, thus in Table 6.1 the costs fluctuate (Kaldellis, 2011; Dalton *et al.*, 2010; O'Connor *et al.*, 2013). In order to keep a uniform approach the shallow water devices WaveStar, Oyster have considered to have no mooring expenditure while a higher foundation (10%), concrete cost(30%). On the other hand, Pelamis, WaveBob and WaveDragon have higher cost associated with moorings and installation processes (see Table 6.2).

All final estimation are based on a cumulative annuity approach, adjusted to current price through inflation (g) taken as 4%, energy escalation (e) 5%, discount rate (r) 10% (suggestion are within a range of 8-12%), (ϕ) is the taxation equivalent to 10 %, while two approaches for the life expectancy are considered 20 and 25 years accordingly.

Table 6.1: Cost Breakdown of wave energy

Components	% of IC_o ("One Off")
Cabling	5%
Mooring	0-15% (Depending on Device)
Concrete	0-30% (Depending on Device)
Installation	3-40% (Depending on Device)
Foundation	0-15% (Depending on Device)
Construction Management	3-5%
Components	% of IC_o (Annual)
Facilities	2-4%
Management	2-4%
Operational Cost (M&O)	2-4%

Table 6.2: Cost Breakdown of Devices

Components	Oyster and WaveStar	Pelamis,WaveBob and WaveDragon
Cabling	5%	5%
Mooring	0%	15%
Concrete	30%	0%
Installation	5%	35%
Foundation	10%	0%
Construction Management	3%	3%
Operational Cost (M&O)	10%	10%

Based on the IC_n and the included installation cost, see Table 6.2, the final CAPEX (IC_o) includes the $inst_{cost}$ works cost.

$$IC_o = ((IC_n \cdot inst_{cost}) + IC_n) \cdot P_o \tag{6.1}$$

In the case of wave energy the Fixed Cost (FC_n) correspond to the necessity in facilities operation, vessels, maintenance, change of small parts and annual management. Each calculation has to account for the return rate of investment and inflation rates at current year (n). Due to lack of information no variable cost have been considered, if more detailed data become available the additional attributes can be also be included.

$$FC_n = m_{cost} \cdot IC_o \cdot \left[\frac{1+g}{1+i} + \left(\frac{1+g}{1+i} \right)^2 + ... + \left(\frac{1+g}{1+i} \right)^n \right] \tag{6.2}$$

This allows us to examine the cost benefit ratio between the years of operation, and corresponding expenditure. No salvage value is included, i.e. potential benefits from recycling after the years of operation. If the value is known then it can be subtracted by the fixed cost at current values, reducing the LCOE.

$$C_n = IC_o + FC_n \tag{6.3}$$

The potential revenues are a combination of the annual estimated energy, and the selling price of electricity (c_o). Expected energy is the installed capacity of the wave farm with the assigned CF, over 8760 hours. In the case of Scotland the selling price of electricity for wave renewable energy, is yet to be determined. The Feed-in-Tariff (FIT) for several countries as well has been expected to range between 200-220 £/MWh for Ireland, (Dalton *et al.*, 2010), while (O'Connor *et al.*, 2013) investigated a FIT of 330 £/MWh for Scotland. In this case a FIT corresponding to 300 £/MWh is chosen as it seems more realistic in comparison to similar past FIT levels of other resources of energy (i.e. solar, wind) in various countries,(Allan *et al.*, 2011; Carballo and Iglesias, 2012; Dalton *et al.*, 2010; Zafirakis *et al.*, 2013). It has to be noted that current schemes for new FIT are to be launched, the so-called Contracts for Difference (CfD), although during the writing of this study no actual values were announced. It is expected that the new FIT will act favourable to the emerging technologies such as wave and tidal and are expected to offer higher rates of return.

$$E_o = P_o \cdot CF \cdot \delta T \tag{6.4}$$

$$R_n = E_o \cdot c_o \cdot \left[\frac{1+e}{1+i} + \left(\frac{1+e}{1+i} \right)^2 + ... + \left(\frac{1+e}{1+i} \right)^n \right] \tag{6.5}$$

In the case of Scotland, there is an additional stream of revenue which are the Renewable Obligation Certificates (ROC). They represent a form of subsidization by the government to promote clean coal and renewable energy technologies, in the form of sell-able certificates. The use of such certificates has been explored and proposed as a balancing force to overcome the high levels of CAPEX required in renewables. These obligations level the issue of non-emitting technologies, which have no negative Greenhouse-Gas-Emissions (GHG) on the environment. Proving a significant driver for the indirect subsidization of such projects (Pepermans *et al.*, 2005; Verma and Kumar, 2013). Studies have pointed out that non-externalities of the environmental cost, are a disadvantage of RE projects, though certificates such as ROCs, and the implemented Emission Trading Scheme balance these deficiencies (Verma and Kumar, 2013; Krozer, 2013).

Thus as additional revenue stream the ROCs selling price is also added, which is awarded for every MWh produced by renewable energy. Currently the UK ROCs system awards 2 certificates per MWh, while additional promises by the Scottish Government have suggested that the number for wave and tidal is to be increased to 5. The value of ROC is dependant on various factors, though several scenarios provide a high value of 50 £/MWh and low values

at 35 £/MWh of certificate exchange (Allan *et al.*, 2011). The ROCs considered to be gained by the produced electricity are based on the 2 ROC/MWh scheme, while as a selling price 40 £/MWh are taken into account.

$$R_{ROC} = E_o \cdot n_{ROC} \cdot c_{ROC} \cdot \left[\frac{1+e}{1+i} + \left(\frac{1+e}{1+i} \right)^2 + ... + \left(\frac{1+e}{1+i} \right)^n \right] \tag{6.6}$$

The amortization point (i.e. "Break Even") can be considered as the gains that are accumulated each year, corresponding to the R_n and C_n, adjusted to current prices. In our case the R_n taken into account have considered two scenarios the case of combined electricity and ROC cash flow stream and the case without ROC.

$$G_n = R_n - C_n \tag{6.7}$$

For the economic evaluation three indices are utilized, two commonly used are NPV and IRR (Kaldellis, 2011), though a third index is used to assess the economic attractiveness of the project, the economic attractive index (n_n^*) (Kaldellis, 2011). The additional index has been used in the following years n_{10}^*,n_{20}^*,n_{25}^*, to provide us with the economic evaluation of the project at various stages. If the value is negative the investment has a non-business attractive behaviour.

$$NPV = G_n = R_n \cdot q \cdot \frac{q^n - 1}{q - 1} - (IC_o + C_n) \tag{6.8}$$

Whereas

$$q = \frac{1+e}{1+i} \tag{6.9}$$

$$n_n^* = \frac{G_n}{IC_o} \tag{6.10}$$

Having set up all the necessary indices, an algorithm was constructed based on the different inputs discussed, the analysis presented takes into account the devices and their corresponding capacity factors as given in Section 5.2.5. At the same time at all scenarios a taxation of 10% has been taken into account to simulate the real life benefits and expenditure of the installations.

Firstly, the most energetic site are considered, Point 1 and then Orkney shallow water locations which has exhibited significant amount of energy flux. In the beginning the return on investment is assessed, following by the LCOE and finally the attractive index for every location.

At negative axis are the devices that failed to produce any benefits during the operations,

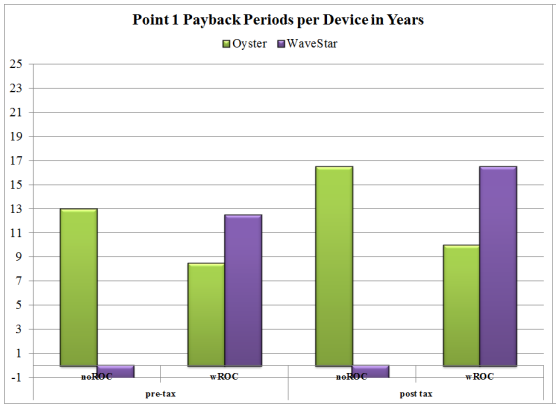

Figure 6.1: Amortization Periods for Point 1

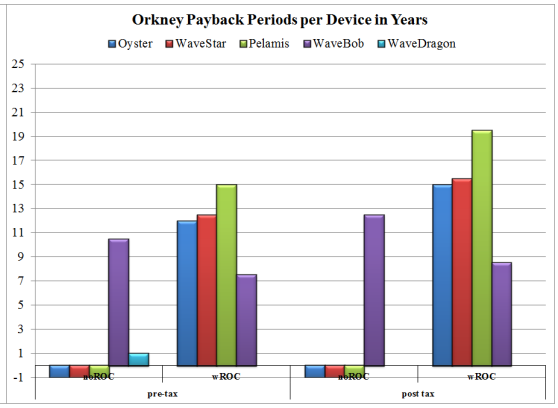

Figure 6.2: Amortization Periods for Orkney

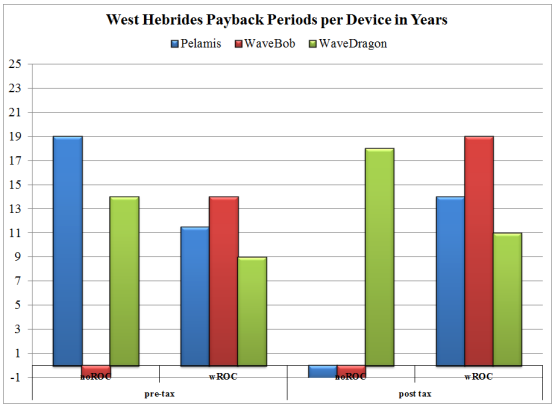

Figure 6.3: Amortization Periods for West Hebrides

see Figure 6.1. The resource of Point1 showed that both devices acquired a high capacity factor, though the existence of ROC's (after tax) lead to a amortisation period of 16.5 years for WaveStar and 10 years for the Oyster. While without tax considerations they drop to 12.5 and 8.5 correspondingly. After taxation, the payback period increases differently for both cases since the revenue stream differs. Several iterations revealed that the tax levels and inflation may be tunable for sensitivity analysis, since they have a great effect on the cumulative cost amortization.

The added value of ROCs, as a form of continuous price subsidization, as a positive effect. With the potential increase from 2 certificates to 5 the cost of the payback period are expected to reduced by almost half, increasing the economic feasibility of the investments.

For the Orkney and West Hebrides the trends of amortisation are the same, with ROCs playing an important role in the revenue stream (see Figure 6.2-Figure 6.3). Devices at Orkney vary in payback period with WaveBob presenting the lowest, while Pelamis has the highest (after tax and ROCs). Similar behaviour is noticed if no taxation is considered. For the West Hebrides, taxation and ROCs combined revenue streams yield payback period for over 10 years for all

devices, while negative performance is taken into account if no ROCs exist. Although, due to the high production capacity of the WaveDragon in this case it is the only device that has a positive payback.

The IRR and attractive indices follow similar levels, with the majority of devices achieving a negative attractiveness. It was surprising, though that the even at these assumptions, the economic behaviour at Point 1 is revealing promising results, yielding the highest IRR. This re-enforces the assumptions that proper economic incentives are able to push the technology of WECs to overcome the associated problems of high RE expenditure.

Table 6.3: Attractive Indices and IRR, post taxation

	No ROC's				ROC's			
Point 1	n^*_{10}	n^*_{20}	n^*_{25}	IRR	n^*_{10}	n^*_{20}	n^*_{25}	IRR
Oyster	-0.54	0.16	0.34	2.22	0.00	0.75	1.03	6.90%
WaveStar	-1.59	-0.30	-0.18	-1.59	-0.34	0.17	0.36	2.34%
	No ROC's				ROC's			
Orkney	n^*_{10}	n^*_{20}	n^*_{25}	IRR	n^*_{10}	n^*_{20}	n^*_{25}	IRR
Pelamis	-0.69	-0.43	-0.33	-2.73	-0.44	0.01	0.17	1.01%
Oyster	-0.59	-0.25	-0.13	-1.19	-0.31	0.23	0.43	2.82%
WaveStar	-0.59	0.25	-0.13	-1.19	-0.31	0.23	0.43	2.82%
WaveDragon	-0.73	-0.49	-0.40	-3.26	-0.48	-0.07	0.09	0.40%
WaveBob	-0.18	0.50	0.68	4.56	0.21	1.12	1.45	9.76%
	No ROC's				ROC's			
West Hebrides	n^*_{10}	n^*_{20}	n^*_{25}	IRR	n^*_{10}	n^*_{20}	n^*_{25}	IRR
Pelamis	-0.68	-0.32	-0.13	-0.62	-0.26	0.14	0.46	3.63%
WaveDragon	-0.39	-0.06	0.21	1.83	-0.04	0.65	0.89	6.65%
WaveBob	-0.76	-0.48	-0.33	-2.15	-0.39	0.05	0.21	1.83%

Similar results of positive and negatives are presented at Table 6.3, it is noticeable though that with the use of various indices, it is observed that the attractive index almost becomes three to four times greater (depending on location) by the addition of ROCs. The assignment of the CF has a direct effect on the IRR, since its affected by expected production levels.

From the results, and in combination with the high resolution assessment, we can confidently assess the economic viability of various sites. It is imperative to enhance our abilities in wave modelling especially for shallow location, with decadal studies. The results allow to propose that the economic viability of WECs is directly connected to the assumptions on taxation and with the revealing of new FIT's. The mean values CF are not expected to change thus the amounts of annual energy can be derived easily. Adding to revenue estimations and ROC and/or ETS additional cash flows that will increase profitability. Normally for established renewable energy installations a IRR within the range of 8-12% provides the basis for a profitable long-term investments, though the attractive index present the favourable or not status of the installation.

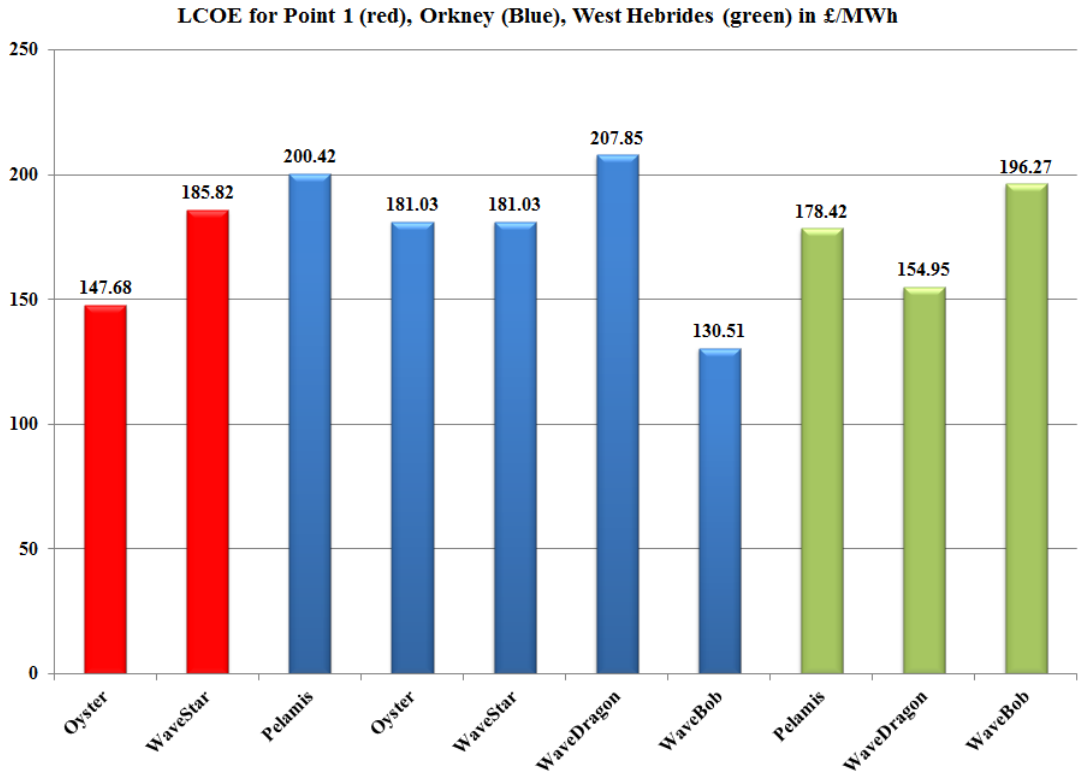

Figure 6.4: LCOE for devices and locations

More specifically, the West Hebrides location yield positive indices for 20 and 25 years. With their positive IRR exhibit promising results for investment considerations. It can also be seen that trend of the attractive index, directly correlated with the expected annual and cumulative gains (see Equation 6.10) reveals that if an investment acquires a close to unity indices then the possibility of having an overall positive and high attractiveness is increased two times. While a index close the medium negative values does not allow a positive performance. Similar trend is identified for the Point 1, while the lowest scores amongst the devices (IRR) are recorded in Orkney. It is interesting to point out that in the Orkney case WaveBob has the best performance, this can be tracked back to the CF calculated since the range of its operation seems to favour the local climate.

Last component of the analysis is the estimation of the levelized cost of energy (LCOE) for the specifics locations and devices, for the duration of the farm life, LCOE has been calculated in current prices per device.

$$LCOE = \sum_{t=0}^{n} \frac{\frac{C_n}{(1+r)^n}}{E_o \cdot n} \tag{6.11}$$

The calculation of the LCOE is shown Figure 6.4, most locations and devices exhibit LCOE as

reported and estimated by various studies (DTI, 2002; Carbon Trust and AMEC, 2012; Dalton *et al.*, 2010; Allan *et al.*, 2011; Carballo and Iglesias, 2012). Although, the proposed ranged of LCOE is within our findings, the ability to simulated and assess for such a long period of time at coastal locations provided the valuable energy performance of the devices. It can be noticed that the LCOE at Point 1, for every device is much more reduced than the expected and recorded values available. This improvement in the calculation of LCOE is the higher CF obtained for shallow water locations. These values underline that the cost of energy per device is not as high as it is calculated.

Though the approach has been conservative, the author would like to stress the fact that data on which the power generation was based were not tuned for specific seas or locations. With a more detailed approach concerning the internal costs, such as salvage values per device, variable costs and actual PTO information can provide a more detailed economic behaviour. Sensitivity analysis indicates that cost of the device per MW (CAPEX) has a significant effect, not only of the payback period but at the LCOE as well. Thus, if the expected financial reduction in capital cost occurs, then the cost of energy will drop significantly. Operation and maintenance are expected to remain at the same levels and have little effect on the costs.

With the future finalization of incentives, more coherent FIT schemes and the activation of the ETS at the European level. The expected gains are to be significant for these technologies, as their capabilities for big amounts of power generation have been outlined.

Finally, as in the case of other RE technologies at the same incubation stage (i.e. solar, wind), the CF and efficiency of WECs is largely greater, than these technologies in similar stages. Thus, the logical assumption would be that by economics of scale, theory of learning rates and experience curves the future cost of WECs shall be decreased significantly. Though in order for that to happen, smaller installation capacity farms need to deployed in order to establish proof-of-concept and performance.

6.4 Summary

In this Chapter 6, the energy analysis results by the high resolution long-term hindcast of the Scotland region, were utilised to assess the economic viability of wave energy. Financial analysis for WECs, due to the immaturity, of the technology have increased uncertainties. One of most obvious, and most significant is the proper estimation of energy production. By utilising the capacity factor database produced in this thesis, we managed to enhance potential estimations of revenue and energy production.

A thorough application of economic viability for the devices allows to see the behaviour of WECs as a business proposal. The difference from previous studies, laid in the fact that CFs used were not extrapolate nor taken as safe assumption. Instead they resulted as coupled outputs

from the energy analysis. Inclusion of detailed CFs allowed us to provide an analysis both pre and post tax, with and without ROCs. The economic indices used revealed that WECs, though at their early stages of development, can amount significant energy and economic returns as an investment. The sensitivity of financial parameters was pointed out, in hope that current developments may provide with additional information on values, the author hopes that this analysis will evolve according to future findings.

Chapter 7

Reducing Wave Energy Uncertainty

"Wisdom outweighs any wealth."

Sophocles, 497-406 B.C.

7.1 Introduction

Generation of highly resolved wave data on multiple location, allows statistical methods to be employed thereby to enhance our understanding of wave patterns. To utilise statistical tools such as probability distribution fittings, extreme value analysis, return periods of various scale, one must have at their disposal data spanning at least a decade. Recording systems such as buoys, although important, are not consistent in the way they provide long-term data time-series.

Extreme waves and storm events may not be captured by a buoy due to either malfunction, physical limitations or retrieval for maintenance processes. As referred in Chapter 2, wave models can provide an excellent resource to fill the gaps of climate factors analysis. Knowledge of climate variability and trends in the ocean environments aids in the planning of many marine applications.

The process of operating a wave numerical model, validating and overcoming potential issues was discussed in the previous Chapters. As shown the results are applicable to a great array of topics, from climate analysis to energy estimations. The use of numerical models has helped in modelling the statistical approach of waves, and the estimation of future extremes at offshore environments.

So far most extreme value analysis and return periods are based on buoy and wave data originating from deep water locations. At which depth interactions have no significant role. Investigating values of shallower locations enhances our understanding on future trends, at areas that interest for offshore applications is increased.

In this Chapter an attempt to individualise the statistical information for locations produced, with the selection of the optimal distribution describing the wave climate of Scotland. Extreme

events are assessed without correcting factors. Although, a process leading to some indicative correction factors for locations is presented, as future reference.

7.2 Correction Factors

The data are corrected for H_{sig} in regards to the recorded buoy measurements, with buoy data are obtained from the post processed data of the (CEFAS, Center for Environment, 2014). Thus no knowledge on their level of accuracy is known. The process of correcting factors from data by numerical models is a continuous development process, though this is usually performed to establish the level of accuracy for the data and potential further assimilation for other smaller nested domains. Common practise is the use of linear corrections, while higher non-parametric techniques can also be applied in expenses of computational resource (Hawkins, 2012; Durrant *et al.*, 2013; Pereira, Belo *et al.*, 2014).

Correction techniques vary widely, from linear to non-parametric with the latter being more time consuming, increase computational demands and usually performed for assimilation (Caires and Sterl, 2005; Sterl and Caires, 2005). A linear correction technique is chosen for the decrease of under-estimations, with pre and post correction factors presented.

The application of linear correction reduces the under-estimations at H_{sig} by shifting lower values to higher ranges. Although, this has an effect on the overall time-series, since the troughs (low waves) are also increased, moving the overall mean value higher. It is important to note that corrections are done for corresponding intervals of buoy data available, the presented correction factors are deemed satisfying only to years with time period coverage greater of 90%, thus these can be used to correct the locations (see Table 5.2). The correction is applied for the active recorded period of buoy measurements.

The SWAN output data from our four locations are utilized, the linear correction method is applied to the buoy data, and the performance statistics of the result (all available buoy years) are included in Table 7.1. By applying corrections to the data, the under-estimations of the annual performance are reduced and some improvements can be seen to the rms and SI of the model. Though it is noticed and as mentioned in previous Sections, that numerical wave models have the tendency to under-estimate peaks and especially of storm events.

Table 7.1: Correction Application

	Linear Correction	rms (pre)	SI(pre)	rms(post)	SI (post)
BlackStone	$H_{sig} = 0.65 \cdot H_{swan} + 3.81$	0.45	0.18	0.42	0.17
West Hebrides	$H_{sig} = 0.65 \cdot H_{swan} + 3.99$	0.68	0.22	0.60	0.19
Firth of Forth	$H_{sig} = 0.39 \cdot H_{swan} + 4.03$	0.32	0.30	0.31	0.30
Moray Firth	$H_{sig} = 0.48 \cdot H_{swan} + 3.91$	0.4	0.37	0.37	0.34

From the correction most benefited locations are in the West area (BlackStone and West Hebries). For both after the linear corrections the SI have decreased by 1% and 3% respectively. On the East Side (Firth of Forth and Moray Firth), major improvements are only seen for the Moray Firth, with reduced rms and SI. This behaviour has been reported in a similar study by Sterl and Caires (2005) with ECMWF ERA-Interim 40 wave and wind dataset in which the rms showed a decrease with SI. In this case the under-estimations of values were minimized but not eradicated.

As noticed by the comparison of the time-series and indices, pre and post correction, the original SWAN timeseries does not deviate much, providing small correction for H_{sig}. The instantaneous biases, i.e. measured vs. hindcast per timestep, are reduced for the high recordings. But one has to account that lower measurements will also be corrected upwards. This may lead to errors in analysis when the wave climate of locations at small depths is considered.

Correction based on buoy or satellite measurements can benefit hindcast locations for that have larger biases. Similar indices can subsequently be used for location in the nearby vicinity, assuming that resource does not change dramatically.

7.3 Extreme Value Analysis

Several engineering applications require the knowledge of statistically derived events, since the ability of forecasts by numerical models is limited to a short-term time-frame (Bidlot *et al.*, 2006; Richardson *et al.*, 2013). The investigation of such expected events improves our understanding of the offshore environment, the construction, survivability of WECs and offshore structures by reducing the uncertainty, and avoiding increases in capital expenses.

The investigation of met-ocean events, helps to characterises the maxima values that may occur with in a year. Extreme Value Analysis (EVA), is an important process which is being used throughout the marine field for the estimation and determination of probabilities of exceedance of parameters such as H_{sig}. Awareness of extreme events and expected return values is vital to the design in offshore industries.

In order to estimate extreme events of 20, 50, 100 or more, sufficient data are necessary. Many previous studies have stressed the necessity of long time-series of wave parameters (Tucker, M, 1991; Carter, 1993; Goda, 2000; Standards, 2000; Dodet *et al.*, 2010; OOP, 2014; Ingram *et al.*, 2011b). Though the existence of such datasets is often quite limited and their reliability at high storm events may be questionable (Tucker, M, 1991; Young, 1999b). These limitations leads to higher uncertainty levels, poor estimations in statistical parameters and reduce the validity of the produced results. Moreover, spatial properties of the available datasets pose an additional major issue, since the quantities differ from deep to shallow and are not the same at

every location, while potential effects of climate parameters pose another obstacle for limited recordings (Ferreira and Soares, 2002; Harrison and Wallace, 2005; Galanis *et al.*, 2012).

For such analysis to be implemented, the existence of long recorded datasets is needed. This poses a problem since most operational buoys usually do not extent so far back (Tucker, M, 1991; Swail *et al.*, 2000; Goda, 2000; Sterl and Caires, 2005; Caires *et al.*, 2008). Suggestions on the length of appropriate datasets propose that the minimum dataset used in the EVA should not be less than 20% of the desired examination time, for example if a 50 year period is investigated at least 10 years of data should be available (Ingram *et al.*, 2011b; Smith *et al.*, 2013).

Substitutes for these drawbacks have been proposed, with the use of satellite data or numerical models, both with having inherit limitations. Satellite observations have a limited temporal domain between their measurements at the same location, from several hours to even days. While use of numerical models, is not to be taken lightly, since a properly set-up and validated model needs to be implemented. Various studies though have examined both options, and used the data for further seasonal and extreme value analysis (Young, 1999b; Swail *et al.*, 2000; Medatlas Group, 2004; Bertotti and Cavaleri, 2012; Young *et al.*, 2012).

The validated output of our model is used for the EVA analysis, in addition to the level of confidence by the validation process, locations at shallow waters and without buoy data are considered. This analysis is not able to be carried out by other oceanic models such as WAM, or WW3, due to their reduced physical solution of shallow water mechanics. The necessity of such studies, has been outlined by previous research which outlined the limitations and the potential differentiation of EVA for shallow locales (Battjes and Groenendijk, 2000; Sterl and Caires, 2005; Caires and Sterl, 2005; Cañellas *et al.*, 2007; Caires *et al.*, 2008; Caires and Gent, 2012).

Starting with the EVA process, all the available recordings obtained are assessed. In contrast to similar studies within the area (Caires and Sterl, 2005; Cañellas *et al.*, 2007; Larsén *et al.*, 2014) most available datasets do not account for coastal locations and have time recording interval of 6-hours or more. With that in mind, with Re-Analysis data, such as the ERA-Interim 40 (Sterl and Caires, 2005) only a handful of studies exist on the use of long series datasets within the European area (Medatlas Group, 2004; Caires and Sterl, 2005; Cañellas *et al.*, 2007; Agarwal *et al.*, 2013; ECMWF, 2014; British Oceanographic Data Centre; Zodiatis *et al.*, 2014; Agarwal, 2015). Limitations entail the use of only oceanic models and long period between recordings (approximately 6-hour). Agarwal (2015) used a highly calibrated oceanic model in the North Atlantic and generated 1-hour output data.

7.3.1 Data Preparation

The data constitute approximately 11-years, with recordings every 30 minutes, leading to a significant large timeseries of wave parameters. Available proposals exist on the use of datasets, some suggest that whole of the dataset is to be used through the so-called total sample or cumulative distribution method. Another approach filtering out the data and acquiring annual maxima values method (AMM), while a third option involves the use of a threshold value in order to utilize a Peak-Over-Threshold (POT) approach.

Another consideration which has to be taken while preparing the data for EVA, is that the values used in the analysis have to be identically independent distributed (i.i.d). Meaning the observations must not affect the successive data and avoid being correlated with the next measurements. This issue of correlation between observations affecting the maximum successive values has been reported for meteorological data that have recordings as close as 3 hours. It was reported that using the whole dataset would yield an over-estimation of return values in the range of 10% in comparison to the POT method, due to influence by lower wave heights (Mathiesen *et al.*, 1994; Goda, 2000).

The option of annual maxima (AMM) refers to reducing the dataset into single maximum recorded values. A variation of the method included the selection of annual maxima and then use a Generalized Extreme Value (GEV) analysis in order to estimate the optimal fitting distribution (Tucker, M, 1991; Goda, 2000; Coles, 2001; Aarnes *et al.*, 2012). Though the AMM is based on sound statistical data and offers a sampling over the data which are i.i.d, it reduces the used data into very small length. Research supports that the AMM, though good enough for a GEV analysis, it requires data of 50 or 100 years or more to be used. If not the AMM may lead to unstable fit of the cumulative density function (CDF) exhibiting poor results. With use of little points storm events identification is reduced, a factor that affects the analysis (Goda, 2000; Holthuijsen, 2007; Vinoth and Young, 2011; Young *et al.*, 2012).

The method for data preparation in this extreme value analysis is the POT, in comparison with the previous method the POT can handle datasets of various temporal duration and lengths. Ensuring the recordings are in i.i.d form, the selection of a threshold can be utilized to isolate maxima occurrences in a pre-defined time domain (i.e. measurement have a minimum hours distance). The pre-requisite of i.i.d ensures that the peaks values used are not correlated and not affect each other. Setting a threshold value, ensures the proper representation of seasonal, annual and even daily behaviour in the wave environments without reducing the final dataset too much as the AMM (Mathiesen *et al.*, 1994; Goda, 2000; Coles, 2001; Caires and Sterl, 2005; van Os *et al.*, 2011; Larsén *et al.*, 2014).

From the size of the data, and literature review the author used the POT analysis as the best option. This ensures that the high level of time recordings will be utilized, offering a better representation of the maximum values occurring at the sites. Higher temporal recordings ensure

that significant storm events will not absent from the dataset. Furthermore, since the dataset has significant higher resolution than previous studies, it is expected that the final sample size includes more data values that have been so far used for similar length hindcasts. Thus the POT method is used in this study to estimate extreme return values.

In order to proceed with reduction of datasets, and perform EVA several steps are required which are:

1. Extract timeseries
2. Filter timeseries, ensuring i.i.d behaviour
3. Set threshold value appropriate selection (u)
4. Filter i.i.d sample with threshold values
5. EVA of new timeseries (GEV,GPD)
6. Evaluation goodness of fit for EVA
7. Evaluation of return period, based on most appropriate fit

The data have been prepared to be i.i.d by filtering and ensuring that the final difference between occurrences is at 3 days. Literature suggest a time frame within 2-4 days to ensure independence (i.i.d) (Mathiesen *et al.*, 1994; Goda, 2000). Following an appropriate threshold is set, the value selected has to be such that it will provide adequate good fit for the EVA while at the same time does not reduce or increase the used data a lot. Suggestion on the selection state that the 93^{th},95^{th} and 98^{th} percentiles/quantiles to be explored. This choice has to taken into account the available data and record its effects of the final data size. Previous attempts utilized 93^{th} percentile which gave a good fit to the investigated values (Caires and Sterl, 2005). Using a 98^{th} percentile, have been reported to lead in reduced final sample significantly and poor fits (Larsén *et al.*, 2014). Large scale datasets have used a 98^{th} Agarwal (2015) and a 99.5^{th} percentile Cañellas *et al.* (2007). The nature and length of our dataset, suggests that the 95^{th} and 98^{th} would lead to increased accuracy of results, though all three options were tested and the sample size was evaluated by a Kolmogorov-Smirnov and a p-value test, which allowed the use of the highest accuracy set.

Locations that are examined are given with the corresponding threshold values for each percentile and the final de-clustered timeseries, see Table 7.2. With focus at shallow water locations, which as mentioned other comparative models cannot operate, see Table 5.2 for depth information.

Table 7.2: Thresholds for Locations

Percentile	BlackStone	Orkney	Homlmsound	Hebrides 2	Firth of Forth
Original size	188,891	188,891	188,891	188,891	188,891
93^{th}	5.39	4.19	2.48	5.54	2.03
Final size	193	187	222	204	234
95^{th}	5.86	4.49	2.72	5.96	2.24
Final size	144	155	173	161	186
98^{th}	7.16	5.17	3.43	7.15	2.83
Final size	86	94	88	78	91

7.3.2 Application of Extreme Value Analysis

Establishing a timeseries that satisfies the consideration of independence, investigation of selecting the most appropriate distribution can be implemented. The filtered values are used to establish an appropriate selection of extreme value analysis and subsequently calculate the possibility of exceedance by return periods. Most commonly two kind of distribution families are utilized for such an analysis the GEV and GPD.

These families of distributions though used widely in EVA and have distinct difference with each other. They can be attributed to the way and the number of parameters calculated for the distributions and selection of best fit. As Longuet-Higgins (1980) stated summation of the wave environment can be characterized by the fitting of a Rayleigh distribution. Though several other attempts have fitted Weibull, Rayleigh and some variations in order to describe the wave distributions (Battjes, 1972; Dean and Dalrymple, 1984; Battjes and Groenendijk, 2000). The existence of the Central Limit Theorem, suggest the mean of a large number of random variables can be considered that has a final distribution of a Gaussian form, regardless of the distributions of each variable (Coles, 2001).

This leads to treat the potential distribution of a large sample as an "unknown" component, which have a sequence of random i.i.d variables M_n, which can be expressed by a common distribution F. This constitutes the recorded events X_n over a time period or observations (n) will comprise the maximum of the distribution M_n over the investigated time period (Coles, 2001; Holick, 2013).

$$\begin{aligned} P_r\{M_n\} &= P_r\{X_1 \leq z, X_2 \leq z, ..., X_n \leq z\} \\ P_r\{M_n\} &= P_r\{\{X_1 \leq z\} \cdot \{X_2 \leq z\} \cdot ..... \cdot \{X_n \leq z\}\} \\ P_r\{M_n\} &= \{F(z)\}^n \end{aligned} \tag{7.1}$$

The problem is that by having a large sample, even the smallest deviation leads to the disruption of a proper fit, with the upper points (z) being easily affected. Overcoming this issue means that

the distribution F is considered as unknown while at the same time the variables are normalized with a linear approach.

$$M_n^* = \frac{M_n - b_n}{\alpha} \tag{7.2}$$

This means that by applying an EVA, our aim is to reduce the de-generation of a distribution over a points (z), stabilizing it with appropriate selection of parameters. The distributions belong to one of three potential families, Gumbel (Type I), Frechet (Type II), Weibull (Type III), as determined by the value of the location parameter (α).

In order to examine the behaviour of the data, the GEV includes all these families of distribution while treating the initial guess as unknown, allowing to fit the data and determine the distribution which best describes our data. Thus $G\{z\}$ can be described by the application of the i.i.d data to a GEV as follows in Equation 7.3.

$$G\{z\} = \begin{cases} exp\left\{-\left[1+\xi\left(\frac{z-\mu}{\sigma}\right)\right]^{\frac{1}{\xi}}\right\} & \xi \neq 0 \\ exp\left\{-exp\left[-\left(\frac{z-\mu}{\sigma}\right)\right]\right\} & \xi = 0 \end{cases} \tag{7.3}$$

Where ξ shape parameter, μ location parameter, σ the scale parameter, with the appropriate distribution based on the derived shape parameter of the block data investigated and the following conditions satisfied.

$$\begin{cases} TypeI & \xi = 0 \\ TypeII & \xi > 0 \\ TypeIII & \xi < 0 \\ -\infty < \mu < \infty \\ -\infty < \xi < \infty \\ \sigma > 0 \end{cases} \tag{7.4}$$

The unification of the families within the GEV, allows for the examination of various dataset with unknown retrieval statistics and the determination the most appropriate behaviour of the tail (i.e. Type I, Type II or Type III). It has to be emphasised that the determination of ξ is dependent on the set and length of data used, as mentioned annual of monthly maxima lead to a smaller array of values examined leading to bias, while very large datasets increase the variance.

The tail of the distribution and its goodness of fit are revealed by the probability plots, K-S test, and the visual inspection of a QQ plot. According to the distribution established by GEV the tail behaviour can be interpreted as: if $\xi > 0$ then the tail is type II decreasing slower in

higher values(i.e. type II represent a " heavier" tail reduction). If $\xi < 0$ then the tail is type III decreasing faster at higher values (i.e. type III represent a " lighter" tail reduction). Finally when $\xi = 0$ then the tail is type I and is referred as a Gumbel exponential.

Considering the above limitations and by properly establishing a distribution describing the data, estimation on the extreme quantiles assists in calculating the return levels (return periods). By estimating return values, information are gained on the annual maximum value that is exceed once a year in every (N) years of investigation and the probability of exceedance at least once during time span of N years.

The return period expressed by the GEV selection can be estimated as the interpretation of the selected family describing the data and the log of the probability.

$$z_p = \begin{cases} \mu - \frac{\sigma}{\xi}\left[1 - \{-log(p)\}^{-\xi}\right] & \xi \neq 0 \\ \mu - \sigma log\{-log(p)\} & \xi = 0 \end{cases} \tag{7.5}$$

With p as seen in Equation 7.6.

For example is the N=100 years described by one distribution (F) from the GEV family then the probability that the z_p is exceed at the duration of one year is 0.01, and the probability of exceedance at least one time during the investigation is given by Equation 7.7

$$p = 1 - 1/N \tag{7.6}$$

$$(1 - z_p)^N = 1 - 1/e \tag{7.7}$$

The example while simple provides the significance and application of EVA and its usage opportunities in the offshore sector, by reducing uncertainties of extreme values.

The other alternative in the EVA examination is the family of distribution described in the Generalized Pareto Distribution (GPD). This alternative was developed to alleviate the issues raised by the use of long examination data in order to acquire better estimation and avoid the pitfalls from the AMM and GEV (Tucker, M, 1991; Goda, 2000; Coles, 2001).

One of the advantages of the GPD is that it can handle larger datasets and associate them with the threshold value, in order to refine the estimated distribution for the location. As in the case of GEV the tails are associated with the location parameter and correspond to Type I, II, III, although depending on the ξ different distribution are fitted to the data. The GPD is characterized and fitted to the threshold providing with the estimated distributions $F\{z\}$ as :

$$F\{z\} = \begin{cases} 1 - \left(1 + \xi \frac{z}{\hat{\sigma}}\right)^{-\frac{1}{\xi}} & \xi \neq 0 \\ 1 - exp\left(-\frac{z}{\hat{\sigma}}\right) & \xi = 0 \end{cases} \tag{7.8}$$

With ξ describing the location parameter and $\hat{\sigma}$ expressing the scale parameter. The GPD has less parameters involved in the calculation. While the following criteria have to be valid in order to estimate the tail Type and appropriate distribution (see Equation 7.9). In the GPD depending on shape parameter, the data are fitted on a generalized Pareto, a special case of Beta, or an exponential.

$$\begin{cases} TypeI & \xi = 0 \\ TypeII & \xi > 0 \\ TypeIII & \xi < 0 \\ z > 0 & \\ \hat{\sigma} > 0 & \\ \sigma > 0 & \\ \left(1 + \xi\left(\frac{z}{\hat{\sigma}}\right)\right) > 0 & \end{cases} \tag{7.9}$$

As in the case of the GEV, having established which distribution describes the sample, an estimation on the return values can be considered. Although, prior to estimation of the actual value one has not only to set the years (N) of investigation but also the rate of threshold (λ_u), according to the notion that a Poisson process is considered. The final reduced dataset, expresses the samples filtered by the POT method of peaks (k), with the n_{years} represent the years of the sample duration. This reveals the cyclic nature of repetition within the dataset.

$$\lambda_u = \frac{k}{n_{years}} \tag{7.10}$$

$$z_p = u + \frac{\hat{\sigma}}{\xi}\left[(N \cdot \lambda_u)^{\xi} - 1\right] \tag{7.11}$$

As in GEV probability plots, CDF, QQ and distribution plots alongside with the p-value indices are used to assess the strength of each solution. For both in this study we use a comparison between GEV, GPD, both using the Maximum Likehood Method (MLM) as presented in Coles (2001). While the distribution and QQ plots assess the goodness-of-fit and act as a diagnostic, higher correlation and the tail behaviour is expressed in the QQ and probability plots respectively, with both ideally desired to have a diagonal straight distribution with most estimated data points along the linear line.

7.3.3 Fitting the Data

The EVA analysis can be performed with various modelling and programming tools, though some deviations may exist for each software in the way of solution. Although Matlab includes a statistical package for the evaluation of EVA, a separate in code has been adopted in this study for the extremes evaluation. Specifically, it was found that a designated Fortran, mex, $C++$ code has been developed by Lund University. The source code is denoted as WAFO- A Matlab Toolbox for Analysis of Random Wave and Loads (Brodtkorb *et al.*, 2010; WAFO-group, 2000) with latest release in 2011.

The additional advanced option of this toolbox, allowed for a faster estimation of EVA and allow for alterations to the functions. Moreover, several additional characteristics include specific distributions developed only for wave analysis, with GPD and GEV having re-written to operate for wave studies. In addition, a more straight forward visual representation in achieved with minor alterations to the code provided, allowing comparable results. Lately several similar attempts have been realized with EVA packages adapted to specific wave analysis, such as ORCA which offer a automated solution and optimized EVA examination (van Os *et al.*, 2011) (under commercial license)

The adapted S-Plus GEV and GPD are used with the MLM and all the datasets are assessed for the different thresholds allowing a comparative analysis for the best dataset and result ot be used for the estimation of the return values. The reduced dataset by different thresholds are utilised to assess the distribution fitting of both GEV and GPD. After finding the best fit distribution extreme values are established.

The different thresholds and their corresponding datasets were subjected goodness-of-fit tests, which lead to the specific investigation of one threshold value. The corresponding EVA are displayed, as expected the GEV provide a poor fit on the tail of the distribution, while the GPD improves it behaviour as the threshold is increased (see Figure 7.1-7.6).

Each set of GEV, GPD, and percentiles fitted to the data have four plots. The first (top right) and fourth (bottom right), provide the fitted reduced timeseries with the probabilities. The second (top left) provides the histogram density plot and the third (bottom left) the QQ plot. For the construction of the density plot, a kernel density function was utilised to estimate the univariate histograms.

The histograms derived by this kernel estimator, are considered "smoothed" histograms, depending only on the bin width and not on the length of the dataset. Allowing a better fit to the theoretical values. The estimated shape of the kernel used an automated smoothed parameter selector. This allows best fit to the data.

The smoothing parameter automatically calculates the bandwidth selection, making sure that it minimizes the mean integrated square error. WAFO offers a selection of automated kernel estimators to improve fit of data. The kernel used is based on an asymptotic mean integrated

square error. It assumes the underlying density is a Gaussian process and provides a smoothing factor as an estimate of the standard deviation by the underlying distribution (Brodtkorb *et al.*, 2010).

The probability and QQ plots are the bottom two plots in each graph. The GEV through CDF (upper left plot of each graph) has a good fit, it shows a significant deviation on calculation of the extreme values, while histogram of the data is given in the upper right plot of each graph. From the examination of estimated shape parameters the GEV shows a Type III (Weibull), on the other hand fitted GPD shows a Pareto distribution with a Type II tail. The QQ plot for all GPD approaches have a better correlation and fit to the extreme analysis in contrast with the corresponding GEV. Although the fitted residuals plot is not linear, still it has an improved fit that the corresponding GEV as well.

In terms of which dataset has the best performance, it is noticed that use of the 95^{th} percentile provides the best fits in both GEV and GPD while the length is sufficient, see Table 7.2, as seen in other studies whereas for example a 20-year dataset was reduced to approximately 300 values (Agarwal, 2015). A further comparison with a K-S test and the comparison of p-values for the dataset generated by the threshold of the 95^{th} percentile, see Table 7.3.

Table 7.3: p-values from the goodness-of-fit test (Kolmogorov-Smirnov (K-S) for the Generalized Extreme Value and Generalized Pareto distribution

	p-value		Shape		Scale		Location	
Name	GEV	GPD	GEV	GPD	GEV	GPD	GEV	GPD
BlackStone	0.54	0.7	-0.15	0.33	0.98	2.54	7.05	0
Hebrides 2	0.2	0.46	-0.32	0.12	0.87	1.98	6.9	0
Homlmsound	0.33	0.53	-0.35	0.13	0.41	0.96	3.16	0
Orkney	0.28	0.59	-0.3	0.23	0.56	1.4	5.11	0
Firth of Forth	0.17	0.40	-0.32	0.08	0.38	0.84	2.6	0

A comparison between the locations, shows that p-values of the GDP perform better than the GEV. This in combination with the best fitting curve (points), show that the GPD can resolve better than the GEV. The p-values are such that the null hypothesis cannot be rejected, indicating that samples originate from the same distribution, for the corresponding GPD. As expected the GPD approach yields better results and statistical fits for the EVA. For this reason the GPD-POT results are utilised in the examination and derivation for the return value analysis.

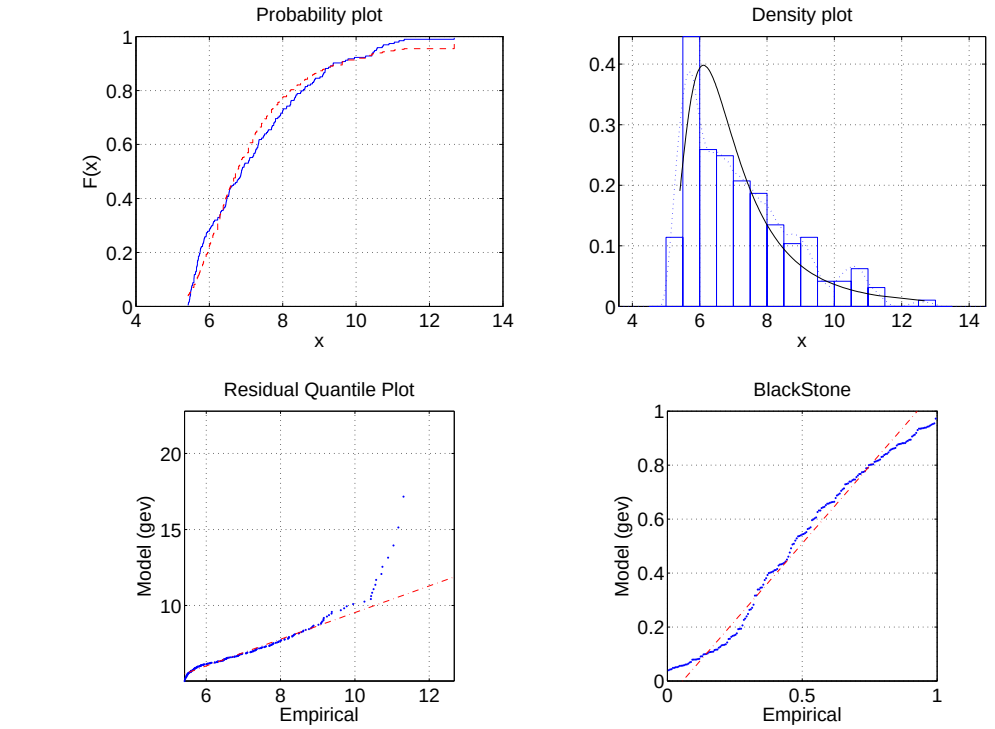

Figure 7.1: GEV at 93^{th} percentile

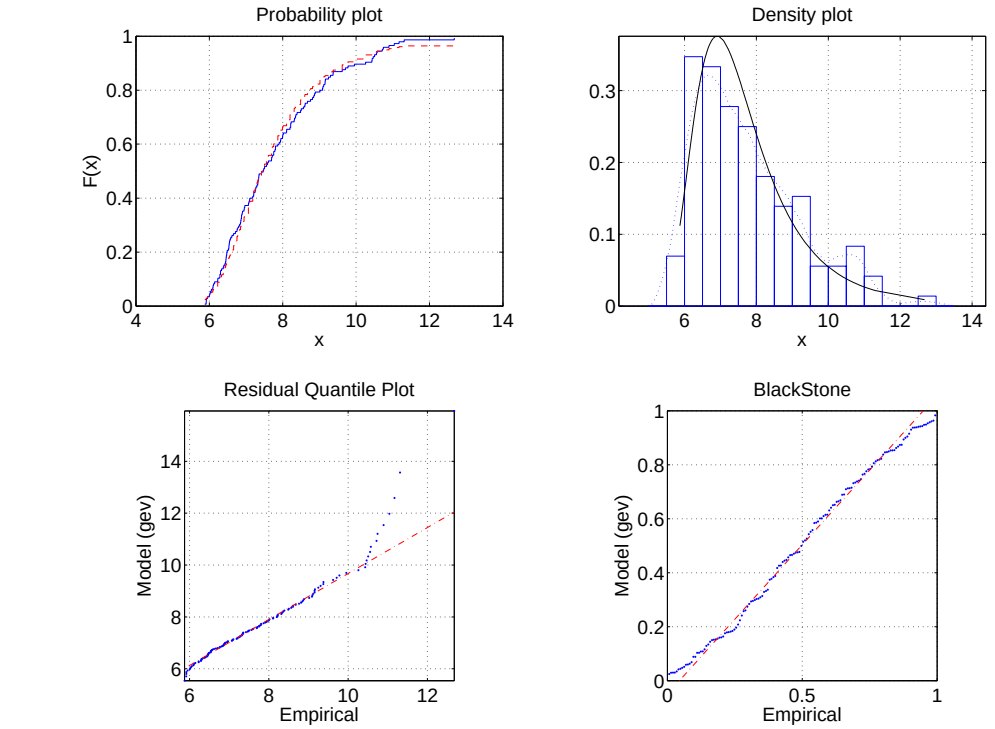

Figure 7.2: GEV at 95^{th} percentile

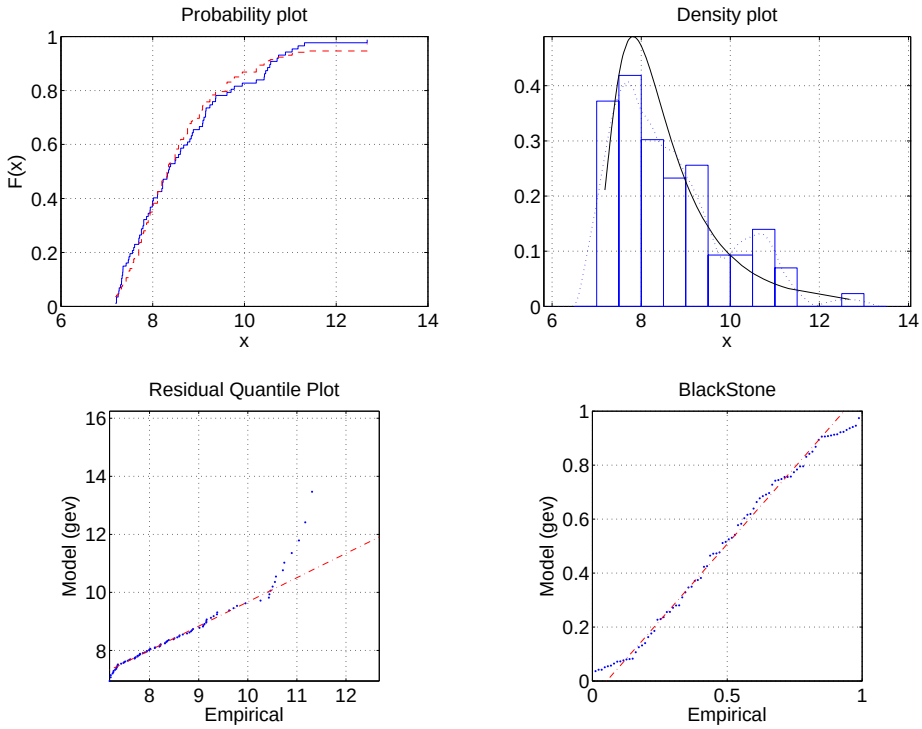

Figure 7.3: GEV at 98^{th} percentile

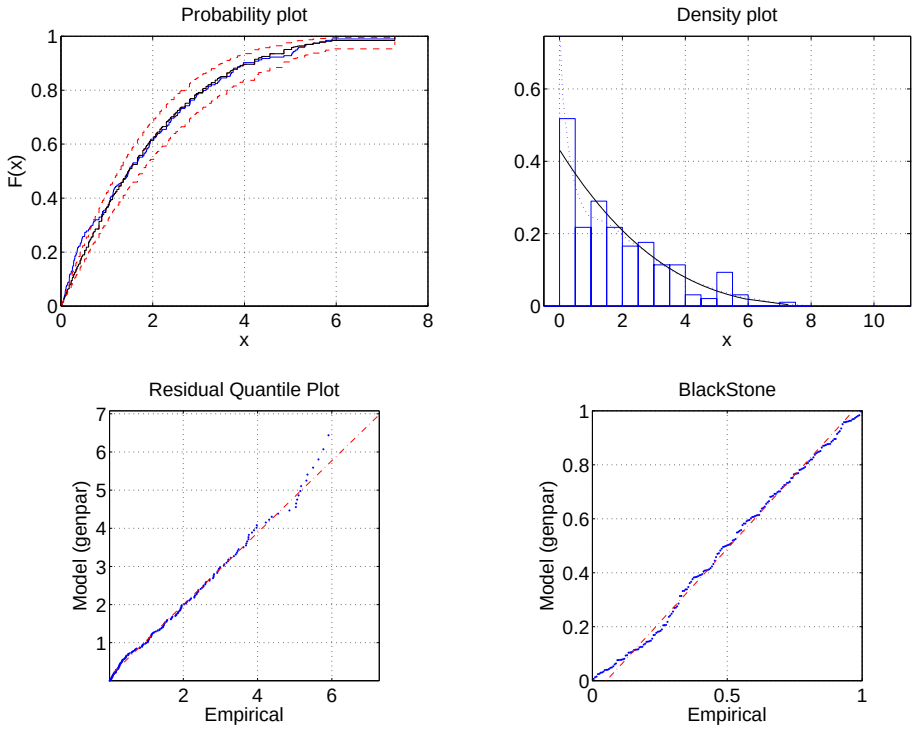

Figure 7.4: GPD at 93^{th} percentile

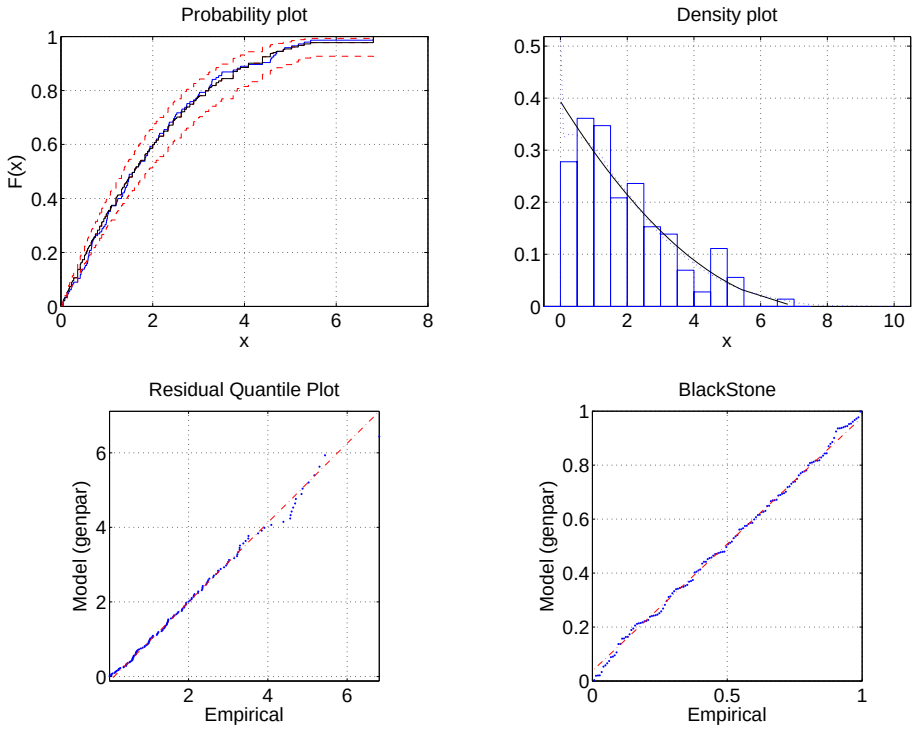

Figure 7.5: GPD at 95^{th} percentile

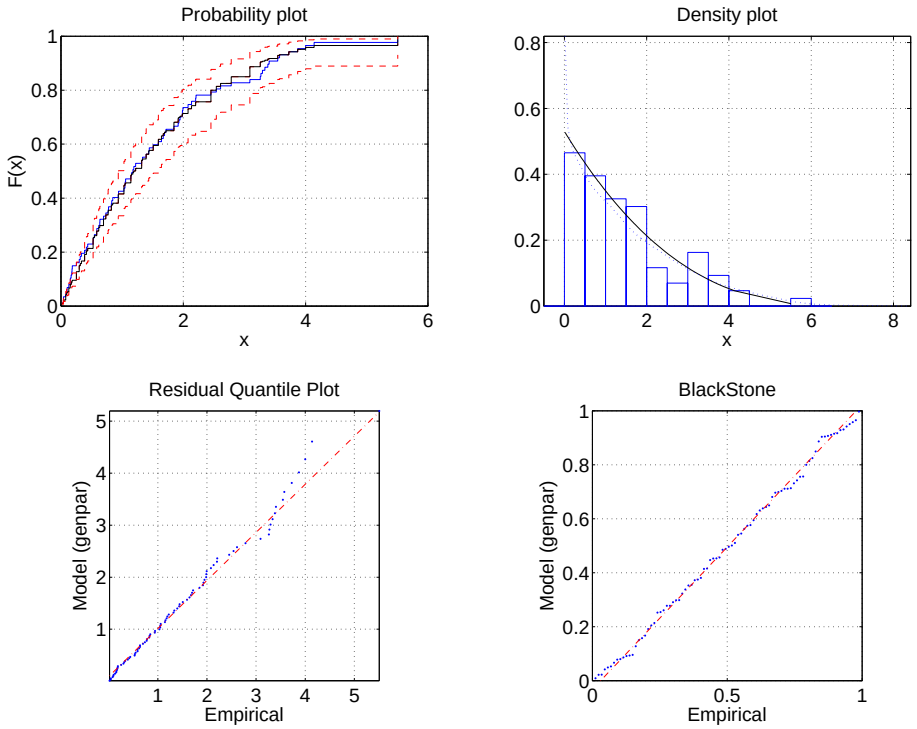

Figure 7.6: GPD at 98^{th} percentile

7.3.4 Estimating Return Periods at Shallow Locations

The return level (return periods) can be calculated by utilizing the fitted GPD parameters of each location and based on the procedure presented Equation 7.8-7.11, and calculate the return periods. Since most wave applications are to be installed in a location for 20 years, it is of significance to examine the return periods for H_{10}, H_{20} years and H_{50} years, keeping in mind that any potential re-powering and re-use of a site might be possible.

The GPD performed better in the analysis, with improved upper tail performance in that the GEV. Due to the amount of data the subset filtered by the 95^{th} shows an overall better performance with linear behaviour. The author would suggest that this set should be considered, though the initial comparison amongst the low 93^{th} and high 98^{th} quantile are presented, see Figure C.1 -C.22.

Table 7.4: Return values for H_{10},H_{20} and H_{50} in meters.

	93^{th}			95^{th}			98^{th}			Max Record
	H_{10}	H_{20}	H_{50}	H_{10}	H_{20}	H_{50}	H_{10}	H_{20}	H_{50}	Dataset Max
BlackStone	14.04	17.9	23.06	15.28	19.7	27.45	11.8	14.2	18.25	12.67
Hebrides2	11.88	13.8	16.57	11.86	13.84	16.74	10.85	12.38	14.57	14.7
Homlmsound	5.86	6.89	8.39	5.71	6.69	8.14	5.4	6.33	7.76	6.6
Orkney	9.96	12.21	15.86	9.21	11.11	14.13	8.07	9.4	11.48	8.8
Firth of Forth	4.97	5.8	6.98	4.76	5.51	6.57	4.32	4.87	5.62	6.4

Return period for each threshold and consequently altered length of dataset, see Table 7.4. Though the scope of the study was not to examine the extreme values for 100 years return period since other studies as cited have already been performed. Through the use of a recent similar study, the Firth of Forth location shows good levels of estimation. More specifically, for the Firth of Forth location, based on the dataset of the 95^{th} percentile. The estimated H_{100} is 10.94 meters, while for the same site Agarwal (2015) reported that depending on sample size and technique the estimated H_{100} are 8.60 and 11.07 meters respectively, using a 15 year dataset reduced based on a 95^{th} and 98^{th} percentile approach.

As stated our main focus is at the locations of immediate interest for the wave industry, areas at the West Side and Orkney islands. It is interesting to note that for all shallow locations, the H_{10} at all sets have similar values, and the same is seen for the H_{20} with some minor reduction in the 98^{th} threshold sets. While the final H_{50} return the highest reduced dataset has the lower estimated value, with the other clustered data having similar values. This trend is followed throughout Homlmsound, Orkney and Hebrides2. Firth of Forth experiences, the lowest resource. Its maximum value of H_{sig} is almost 50% less than the locations on the West. Its final return values are affected by the lower wave heights, reducing the expected extreme levels.

BlackStone is exposed to the harshest waves, while the location of Firth of Forth presents it with a low estimation. The shallower locations exhibit a high magnitude return values,

with maximum values over the dataset being high as well. Interestingly, the depth limitations processes do not allow further development of the wave heights as in the case of BlackStone. Return value is higher than to the maxima of the dataset even in the case of lower chosen threshold. This indicates that the expected return values will have severe effects on offshore structures. Taking into account the proposed datasets, 95^{th}, shallow location present a higher percentage of return values in relation to their maximum values. Though the wave height will be limited by depth breaking, the return value at all shallow location locations is significant, while for deeper water the expected waves are heavily dependent just on the resource size i.e. BlackStone and Firth of Forth.

The fitting of distributions on EVA is not proven, but it is the most appropriate way to estimate probabilities of exceedance. The suggestion that each point will have a different distribution relays heavily on location and local characteristics. Depending on the sensitivity and the goodness-of-fit tests used to assess the proposed estimation. A lower goodness-of-fit as indicated by the QQ plot one may lead different return values, which when taken into account for offshore structures may jeopardise the survivability of increase the cost of the installation. As in accordance with previous research the GPD seems to fit better to the estimated data, although its one of the few times that actual estimations on nearshore locations exist.

Considering the performance and confidence in the wave model as presented in Chapter 5, the estimated return periods are expected to be within realistic estimation levels. SWAN allows a full representation of shallow water non-linear interactions, aiding in the dissemination of results and the generation of datasets for locations with limited approach by other models. A similar approach with the existing dataset can be used, providing with significant level of knowledge concerning the construction phase of WEC or offshore engineering applications.

7.4 Summary

In this Chapter a full use of the hindcast was utilised to establish an EVA and return expected period at shallow water locations. Determination of statistical parameters based on EVA, was performed and a goodness-of-fit test was applied to examine the optimal families of distributions. The ability of SWAN to hindcast shallow water locations is of major interest for the wave industry and re-affirms the position of applicability not only wave energy production, but also the exploration of survivability.

Scaling and manufacturing devices based on statistical indicators from deeper locations showed that the absolute levels of wave heights are significantly reduced mainly due to the physical limitations found at locations. Bottom friction and non-linear wave breaking interactions reduce the incoming wave heights, thus a proper approach indicates, that tailored results to such locations improves the knowledge of construction and survivability. This will enhance design consideration without compromising financial estimates.

For this reason the production of high temporal datasets for long periods of time is crucial. Depending on modelling techniques and reliability of data, based on the validation process. One may choose to increase the statistical estimation by re-scaling the hindcast through use of correction factors. This although hinders some potential over-estimations since the behaviour of linear corrected data inherently increase the troughs, leading to a potential higher return estimate.

Though correction has been applied to the data, due to limited recordings from buoy measurements the level of such technique is not proposed. Some correction can be applied to sets that exhibit major underestimation in capturing storm values. This can be incorporated, if chosen, in an analysis of extremes values. Although, the final corrected values have to be in close correlation with measurements as indicated by the validation process.

Chapter 8

Discussion

"The only true wisdom is in knowing you know nothing."

Socrates, 470-399 B.C.

During the investigation of this doctoral thesis several issues were risen. This section, presents the limitations and considerations encountered, discussing the results and potential improvements that could be taken into account in the future to improve and build upon this body of work.

Starting off, the author would like to advice for the use of open software and source codes, as it is of major importance to the examination and contribution to the scientific community, though these come at a cost of complexity. Initially, it has to be stressed that all the pre-processing, data inputs, coding and source codes, used were tried to be performed using open access format ensuring re-reproducibility of the work.

Any potential work with SWAN and similar packages is advised to be performed in a UNIX environment. Due to the nature of work environment and dependencies it was found that code adaptation and use of packages was essential and ensured better operation. Most of the work (with some minor exceptions) was performed by gaining access to the super-computing facility at the University of Edinburgh (EDDIE), supported by the Edinburgh Computing Data Facilities (ECDF). If an operating model is to be developed for hindcasts and forecasts, access to similar facilities is highly advisable.

Though access was granted, some issues were encountered hindering some applicability. Such facilities, operate in UNIX environments, thus a good understanding of bash and UNIX coding is necessary. The nature of source code requires the user to compile and activate several features manually. Unfortunately, the author tried to utilize the option of netCDF and MPI compilations of the source code, but issues during installation prevent the netCDF package. Such issues may arise depending on the compilers availability within the facilities. Normally is that in such systems the user cannot install its favourable or tailored solutions, but rather to choose amongst existing ones. The problems in installation were presented with the netCDF option, when tried to be activated. The available versions of netCDF packages seemed to have compatibility issues with the SWAN code, which did not allow the proper installation. Thus an OMP solution

without netCDF support was preferred.

Such services also carry some other operative limitations. The storage allocation and run time were both limited to a specific number. More specifically the author was granted access, and is grateful, to the Institute for Energy Systems (IES) marine group which has a cumulative space of 2 TB. This meant that the shared directories were operated amongst other users that require same or even more storage space. Allocated user space for the author was limited to 200GB. This meant that some key consideration on the setting up of the model, and run-time temporal files had to be taken into account. In addition, maximum allowed time of operation for one job had a hard limit of 48 hours, after this threshold the job was automatically cancelled.

Numerical modelling of large time-scales and domains requires a significant time of both computational time, resources, and most importantly storage. Throughout the thesis major parts of the resource assessment were performed using 24 direction and 25 frequency bins, this was selected after careful considerations, benchmarking, and sensitivity analysis. The output and temporary files generated by the numerical models are extremely large and when the distribution of frequencies and directions are increased. Adding significant burden on the storage and run time components. Also the mesh under investigation, both in terms of spatial and temporal terms are very fine, which often led to the exceedance of threshold time.

For smaller domains such as the Aegean Sea, higher number of bins were utilized, but this decision was dependent of the overall mesh size and after additional benchmarking. In addition, the output of spectra files, domain mesh and temporary solution algorithm files were found extremely large. In one of the cases, during the Scottish area calibration, all the components were increased to 36. But due to the 200GB limit mentioned this led to exceeding the available space for the computational solution, leading into a continuous loop and exceedance of the operative limit.

The output files are also of significant size, not only for storage purposes but also for post-processing. Overall the single 11 year hindcast had to be broken in time pieces, carefully adjusted not to exceed the time limit. Due to the requested meshed output the of 3 hours for the whole area, the final size of just these information obtained was approximately 300 GB. Apart from the difficulty of storage, significant barriers were risen when the post-process was applied. Although, initial higher temporal resolution maps (1-hour) were investigated.

Furthermore, preparation of the data is of major concern, as mentioned all data used were public domain, though limited knowledge exists on the generation of appropriate files and their structure when they are to be used for SWAN. The author tried to clarify them for future users in Section 3.2. Major components are the wind products, for which as presented two have been considered. While several more exist and used by the author but not included in this body of work. Size of the final files even for a targeted area often times exceed 2-4 GB per year (depending on size and resolution), thus for the overall 11 year hindcast the storage size was

imperative to be taken into account. As far as the boundary information are concerned, though the use of spectral data has been tested by the author, their storage and size requirements are extremely large leading to a significant drawback. The alternative of high spatial and temporal TPAR files allowed for a very satisfactory representation of the boundary information reducing the size storage requirements, although the data have to be isolated by a spectral field and manipulated accordingly.

All the pre and post-processing was performed at a workstation which unfortunately had significant memory limitations. The hardware used was comprised of a dual core system with just 4 GB of RAM, this meant that the preparation of files was hindered by processing power. For example, after the coding in python for the manipulation of wind files, the conversion into a SWAN compatible mesh would take 2-3 days per year (depending on size of the domain given). For pre-processing, python was found to be more reliable and fast acting as it can manipulate netCDF data faster than Matlab. Similar issues were also present in the post process of the data.

The post-processing was performed using Matlab software on the same workstation, again memory of the operating system and Matlab itself contain restrictions. Meshes for the production of maps are not easily manipulated by Matlab due to the import size of the .mat file. In addition, the calculation time of such files meant significant time for the post process. Alternative options tested were Octave and SciLab, which are similar environments to Matlab, and the author has migrated some of the code into their structure.

Overall constrains are mainly hardware and can be relatively avoided or improved by the upgrading of systems and storage availability, while the open source community offers a wide variety of software alternatives, though with some steep learning curves at first.

Other limitations are not as straightforward and require a significant input by the research and wave community, in order to enhance the results of similar studies. Firstly, the lack of buoy recording has been stressed by the author and previous researchers. Especially the absence of long term data at shallow location proves a significant barrier to the calibration and appropriate calibration/validation of a high resolution model such as SWAN.

Consideration on deployments buoys at shallow waters is important, even if not located at wave energy sites. This will allow further exploration of non-linear components calibration part of SWAN and the better adaptation of the resource assessment. The author is grateful, that he was allowed access to a shallow water buoy in order to compare and calibrate, though the data were restricted and had limited time duration. Suggestions for buoy usage especially at depths of smaller than 10 meters is highly desired.

Moreover, limited data exist on the validity of power matrices, operating costs, maintenance and general wave energy and financial considerations. This leads to increasing the numbers of assumptions when the energy or financial assessment is performed. Major issue of importance is the data and information concerning the installed capacities used by its device alongside a

valid power matrix, losses, levels of mechanical and electrical efficiency. Though the industry is new, the potential of such improvements in both the technical aspects and policy considerations are expected enhance the overall status of wave energy as a noticeable technology in renewable production. As shown in this thesis, the amount of considerations was decreased by the use of a numerical model, which allowed to deliver key estimation that can be used by other fields. Proving that WECs have comparable and even better performance than many established RE technologies. Providing such data will reduce the amount of hypothesis and assumptions in energy production assessments, and is expected improve research concerning WECs.

Finally, a limitation, if considered as such, was the time constrain. The author believes that the SWAN process presented here can be utilized as an operating module in a larger wave forecasting process. Though this entails experience, dedicated facilities and research staff involved. Currently the UK MET, and ECMWF offices perform short term forecasts of high accuracy, though are limited by the models used. A similar process can be implemented and improved upon, providing significant information to the offshore, wave energy and grid operating sectors. The implementation of a weather numerical model such as the Weather Research Forecasting (WRF) Model, can provide with dynamically downscaled temporally and spatially forecast datasets for the Scottish area. Ideally, the model would feed these winds into a larger oceanic such as WAM or WW3, in order to provide boundary data and a inner nested SWAN code of higher spatial resolution. The model would be similarly calibrated for these waters, providing high level of information concerning offshore climate. This entails highly integrated systems and requires a data assimilation techniques to be constructed, though the output will be of benefit to several sectors. Such process will be able to forecast the energy production patterns of WECs reducing the variability levels that transmission operators are concerned with. It will also add to the knowledge of climate trends and improvements in models.

Even if some considerations or problems might have been overlooked, the author hopes this discussion offers some key points about the problems that a future user interested in wave numerical and energy modelling may encounter. Hopefully this page will allow users to set-up and deploy a strategy addressing the issues by adapting to software, hardware and information gathering.

Chapter 9

Conclusions

"Every art and every investigation, and likewise every practical pursuit or undertaking, seems to aim at some good: hence it has been well said that the Good is That at which all things aim."

Aristotle, 384-322 B.C.

In this section an overall view of the key findings are presented in a summary form per chapter. In addition, future work considerations and studies explored, but not included within the thesis. They are presented in hope that further research will utilize them.

Chapter 3 offers a comprehensive step by step process for SWAN: construction of a operating source code, alongside information about the structure of files, sources of obtaining data, construction of various input files, proper formatting, and preferred software that will aid in the construction of inputs.

1. Code explanation and construction
2. Structure of input files for SWAN comparability
3. Suggested Input format and processes

Chapter 4 based on the wave theory and adaptation of the numerical model as presented in the two previous chapter, a detailed examination of a customizable solution of the Scottish area is presented:

1. Wind dataset selection
2. Calibration of wind dataset and SWAN
3. Effects of Wind temporal files to SWAN hindcast

The evaluation of wind products to improve under-estimations by the model, as proposed by literature, findings suggests that increase in temporal resolution is not always favourable. Calibration of a model based on wind input will yield better results. This led to propose an optimal dataset of wind product for Scotland and North Sea based on statistical and numerical comparison of wind driven waves.

1. Quadruplet interaction coefficient
2. Suggested coefficient and width of frequencies

The dependency of non-linear complex quadruplet interactions was also examined. The uncertainty of this term especially makes it extremely difficult to assess and calibrate. The study showed that effects of alterations, have significant effect on hindcast performance and computational time. The DIA coefficient and solution schemes, are amongst the most sensitive terms. A reduction in the coefficient showed a decrease in the hindcast results and computational times. While, the tuning based on scheme affected the estimations in varied manners. From the process, it is favourable to assign the designation of frequencies not only to bins subdivision, but ensure a large difference within minimum and maximum set frequency (almost 4 times bigger). The DIA coefficient is suggested from $0.23 - 0.25$ for the UK region. While, the D2 scheme has the best performance and less computational demands.

1. Nested domain processes with SWAN
2. Sensitivity to rapid changing bathymetry
3. Coefficient proposed range for alleviating CFL violation

Application of the model in a nested way, was also studied and unveiled, issues concerning rapidly changing depths. It showed the weakness of SWAN in some areas, the process of identification and problem alleviation. In the case of such areas, two main components are important. First, the proper assignment of the computational timestep (especially in large scale coarse studies). The computation time has to be adjusted based on the mesh, and wind product temporal resolution. In addition, areas with quick depth changes it is suggested that the user activates and re-tunes the turning rates for frequency and direction with a coefficient within the range of $0.5 - 1$.

1. Consideration of mesh size and effects on computing resource

Finally, considerations on the mesh length dependence and quality of hindcast was explored, applying quantitative and qualitative methods to assess the correlation, differences and time requirements. Length of mesh size has an effect on hindcast, with DIA and fetch size contributing to differences. In the absence full coarse spectral meshes for nesting, the mesh size should also be subjected to calibration in order to ensure optimal performance. While, differences are small it is important to note that SWAN is not as efficient for large domains, thus careful mesh size has to be considered.

Chapter 5 dealt with implementation of the model for a high-resolution resource assessment dataset and energy analysis:

1. Developed of a high resolution wave hindcast database
2. Validation of database
3. Qualitative and Quantitative metrics
4. Statistical behaviour of wave resource
5. Wave power resource assessment for 11 years and variability analysis

The model is calibrated, run and extensively validated with publicly available buoy data, shallow water propitiatory data, and with the results by two other models leading to a multi-model

comparison. The results provide confidence about the level of hindcast and in combination with the validation indices, the datasets and maps produced offer a significant improvements to the wave climate and energy resource estimation for the area.

To date it is the only nearshore model that satisfies the temporal duration needed, according to international standards. Moreover, in contrast to other models applied in the area, all complex nearshore activated terms were tuned and used, providing for the first time a high-resolution wave power assessment. Aiding significant information to the existent growing number in wave energy.

1. Impact of maximum power levels to survivability (WEDI index)
2. Energy analysis coupled with high-resolution data and representative WEC
3. Optimal selection of WEC based on resource, depth, and power production
4. Estimated annual power per device and location
5. Proper representation of capacity factors and energy production

The use of such a detailed dataset, allowed to examine the energy content and compare several different WECs and their performance over a long period of time. Allowing robust estimation of energy findings, production and utilization rates. At the same time an additional index for wave energy consideration is presented, taking into account wave resource interactions and reducing the chances for failure of WECs.

Such energy results, and detail examination of coupled converters has never been done for the Scottish coasts. Interest is situated at locations which are coastal and of immediate interest to the wave energy community. The analysis compared different locations and WECs allowing to establish robust results on most appropriate type of device, based on range of operation and metocean characteristics. Such a database for CF and energy production, over such a period of time was absent for Scotland. It actively addresses issues associated with expected energy performance and provides guidelines on wave energy quantification.

1. WEC adaptation to milder environments
2. WEC energy production opportunities at milder seas

Finally the author, was interested in exploring the possibility of adaptation of WECs to milder seas and assess their energy performance, results showed promising energy production that can add to countries energy mix. Proving that wave energy is not only to be considered for energetic waters, milder seas offer the advantage of smaller lower extremes and increase survivability which may benefit the emerging industry to build confidence in operation as well, through adaptation of devices to the areas is suggested.

Chapter 6 utilised energy results and proposed parameters obtained by energy, coupling for a detailed financial analysis comprising:

- Detailed structure economic analysis of WEC
- Cost to Benefit Analysis

- Expected revenues and additional certificates for wave energy
- Amortization periods for different region and WECs
- Levelised Cost of Energy at different areas and WECs

The economic model took into account all major components comprising a WEC installation, confidence is increased due to the use of a robust energy evaluation proving that the utilization rates is comparable with existing more mature RE devices. Financial findings provide payback and LCOE estimations with smaller assumption margins. Taxation rates, FITs, and ROCs have been adjusted according to sources available in literature. The outcome shows clearly, that WEC are a viable financial technology option even at early stages of commercialization where CAPEX is expected high. The outcome exhibits that as the learning rates are increased the cost is expected to fall, as was the case for other industries.

Chapter 7 explored and attempted to improve the knowledge of extreme value analysis for the climate, and offshore community: The ability of obtaining high resolution, long duration data, allows to examine the probabilities of exceedance. Such results can be taken into account for the construction of marine structures, naval activities and design consideration of WECs' to minimize cost and/or increase the survivability.

1. Correction factors
2. Limitation of existing wave databases
3. Presented Extreme return values
4. Application of GEV, GPD-POT method
5. Considered and applied of multiple thresholds
6. Estimated wave return period for 10,20 and 50 years

Previously attempts are cited stressing the fact that coastal analysis of extremes is missing, the application and process of the analysis steps and appropriate manipulation of datasets are presented. Finally, the return period of exceedance for wave height are given for 10,20 and 50 years. These times were chosen based on the fact that WEC are to be operative for up to 20 years, and that other studies with longer available datasets have explored the 100 year return, though they were hindered by the inability of their models to hindcast the coastal locations.

Chapter 8 present some keys issues regarding the obstacles encountered, the limitation and potential improvements of our dataset are explored. The Chapter ends with consideration of software, hardware and calibration processes of the model.

Finally, Chapter 9 presents an overview of the findings and discusses future work.

9.1 Future Work

Majority of the work, allowed the author to understand and look in more depth the connection between high level hindcasts and their applicability in the engineering world. This doctoral thesis, also explored several other ideas that were not able to be fully developed and included in the overall result.

The ability to produce validated data, increases the potential areas that the results can be utilized for future research and expand upon. The model can be used as an operating forecasting model with data assimilation and interconnection to a larger oceanic and wind model. A tri-way coupling will be increased by combination and exchange of continuous data information for models correction. Though similar techniques are in place the inclusion of a shallow water model has not yet been incorporated. A step like this will contribute to deterministically reduce the uncertainty bounds of wave energy with forecasts, concentrating one or two days in advance at a very highly resolved temporal space.

To improve the performance of numerical wave models, satellite data can be combined with data assimilation techniques to enhance performance and minimise discrepancies. In a data assimilation option, satellites are amongst the best options since they can include recordings over large domains. That can be used to a determine a corrective process for whole domains.

Having established WECs performance in energetic environment, future work includes assessing the wave climate and energy potential in other areas. More specifically, the author would like to explore the long-term wave power resource, applicability and adaptability of WECs in the Mediterranean region. Quantifying the resource and energy levels, will not only assist academic cases, but is to also provide arguments concerning benefits at milder environments. Application of WECs in low resource environments, may not hinder but in fact accelerate proof-of-concept and reliability for the wave energy industry.

Another alternative is to utilize this coupling of SWAN and WECs production to produce minute data and assess the operating energy characteristics i.e. voltage and current quality fluctuations delivered to the grid, assessing the impacts of WECs energy incorporation. The hindcast datasets can also be utilised to optimize the sitting of WECs based on hydrodynamic principals and compare the wave-to-wire performance over a very long period of time, introducing wave climate variability into the calculations.

Furthermore, asides the power quality assessment, a temporal cross-correlation of renewable production can be also investigated. More specifically, wind and wave power production for co-located and/or non co-located turbines, is expected to contribute to variability considerations. Utilising, high resource assessment (wind & wave), power production of both technologies can be estimated at very high spatial and temporal resolution. Subsequently, any potential cross-correlation can indicate the level of dependence, and complementary production by the selected devices. For example wind can be considered as base RE, and the cross correlation by WEC

can provide the complementing hours of non-wind production.

The same process of energy calculation can be coupled with a storage medium of bulk scale storage to achieve mechanical reduction of WEC variability, such option can be adjusted by similar studies found in the wind industry. Moreover, the nature of WECs can additionally be considered for modular desalination and hybrid stations to de-centralized systems, reducing the cost of energy in such highly energy demanding processes.

Finally, climate studies and offshore marine activities can also benefit, by introducing coastal hindcasts. Thus, the barrier of data availability can be alleviated. A more detailed examination of intra-annual, decade and century can be achieved providing knowledge on the statistical behaviour of waves. Overcoming the barrier stated by previous studies of significant deficiencies in shallow water environments.

Appendix A

Application of Numerical Modelling

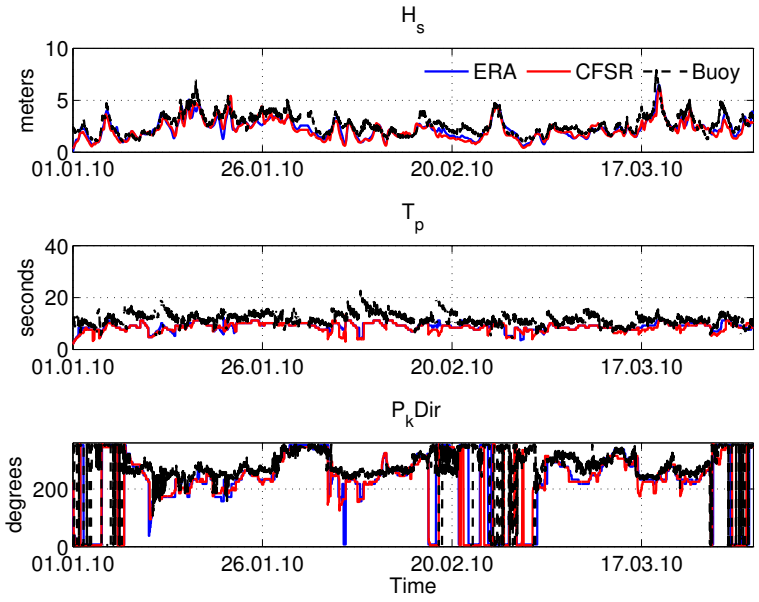

Figure A.1: Performance of the model at BlackStone 2010 January-March

Table A.1: January-March 2010, as taken form the calibration/validation process, see (Lavidas *et al.*, 2014a)

	West Hebrides				BlackStone			
	H_{sig} in m		T_{peak} in sec		H_{sig} in m		T_{peak} in sec	
	ECMWF	CFSR	ECMWF	CFSR	ECMWF	CFSR	ECMWF	CFSR
R	0.97	0.97	0.94	0.94	0.96	0.98	0.92	0.92
rms	0.70	0.79	3.65	3.77	0.69	0.74	4.28	4.56
Average Buoy	2.69	2.69	10.89	10.89	2.15	2.15	10.46	10.46
Average SWAN	2.27	2.17	10.62	10.19	1.70	1.70	8.94	8.44
Bias	-0.42	-0.52	-0.26	-0.70	-0.44	-0.44	-1.52	-2.08
SI	0.26	0.29	0.33	0.34	0.32	0.34	0.40	0.43
OPI	0.29	0.33	0.30	0.31	0.37	0.40	0.40	0.42
MPI	0.95	0.95	0.83	0.83	0.96	0.96	0.83	0.83

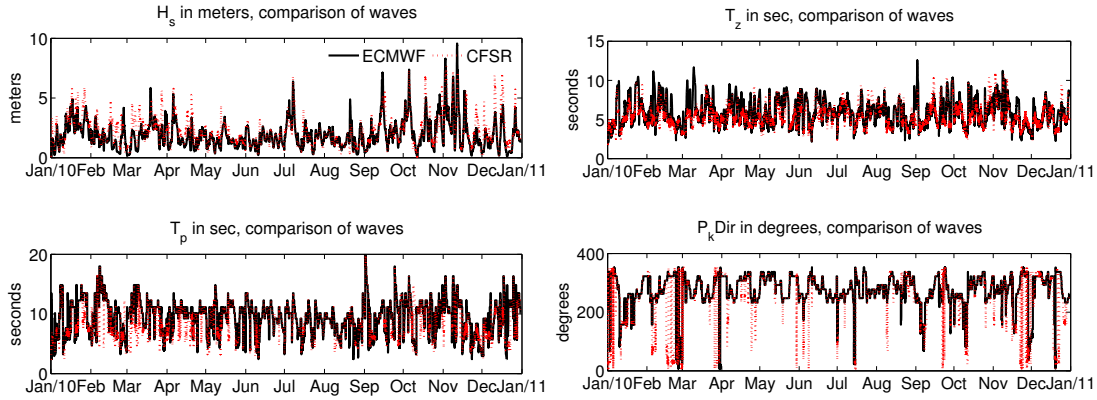

Figure A.2: Comparison of time-series H_{sig} and T_{peak} at Blackstone

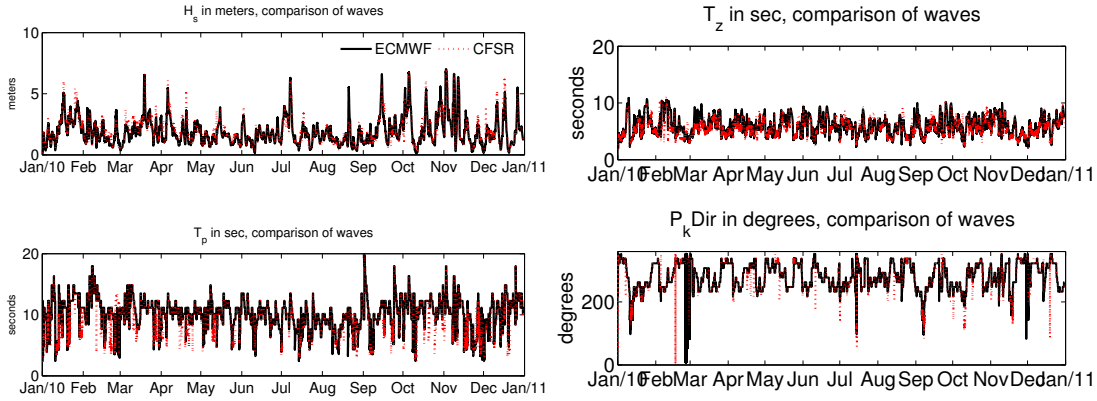

Figure A.3: Comparison of time-series at West Hebrides

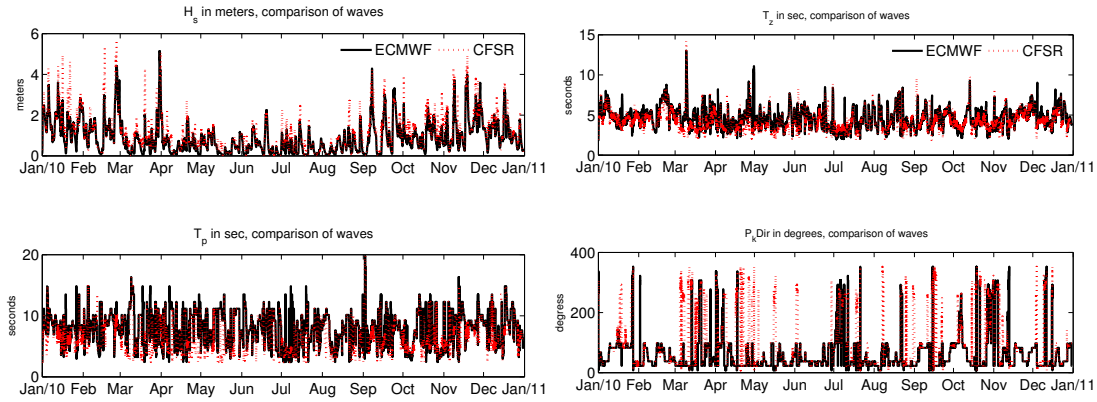

Figure A.4: Comparison of time-series at Moray Firth

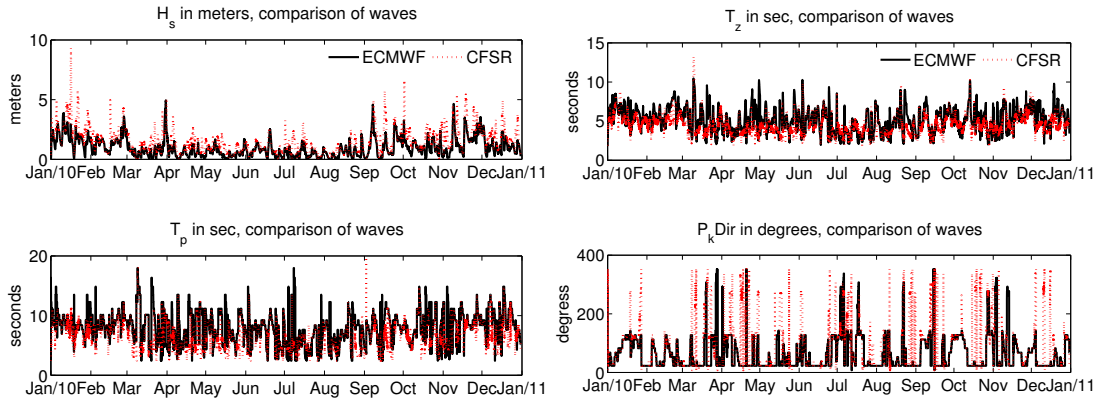

Figure A.5: Comparison of time-series at Firth of Forth

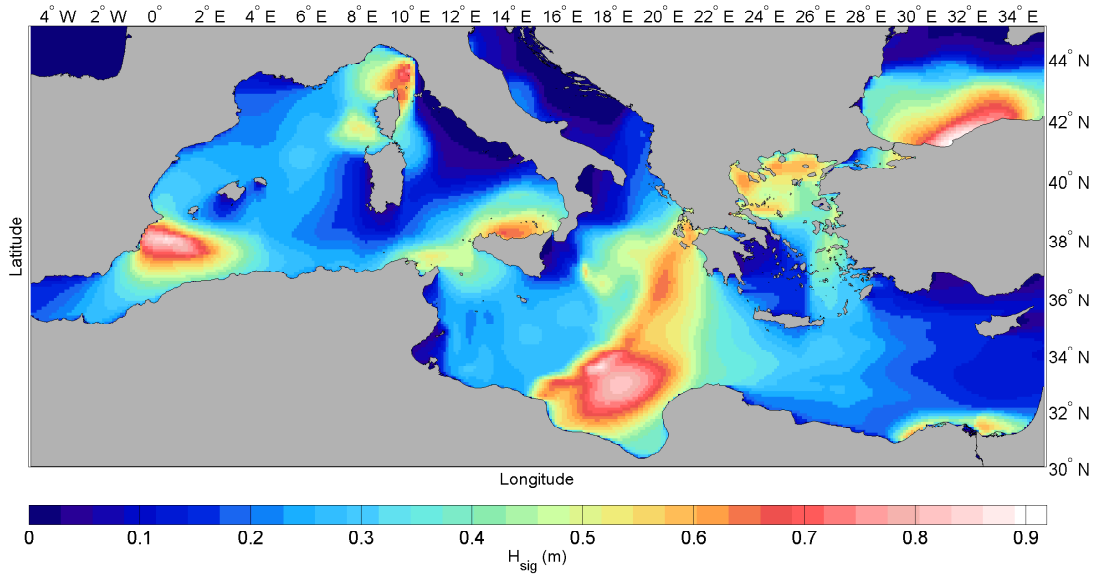

Figure A.6: Alleviated performance for the Mediterranean

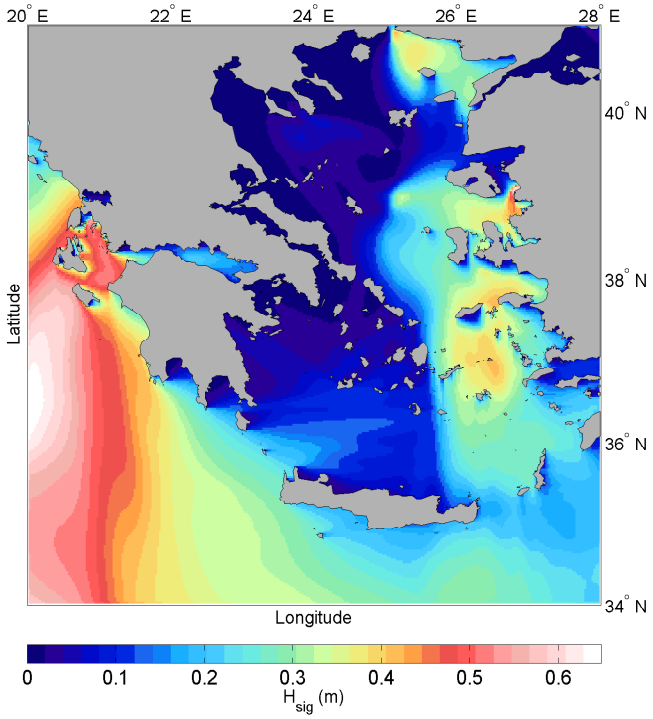

Figure A.7: Alleviated performance for the Aegean Area

Table A.2: Moray Firth tuning of the λ_{DIA} coefficient

	$\lambda_{DIA}=D_1$							
	Average Buoy	**Average SWAN**	**Bias**	*rmse*	**Max buoy**	**Max SWAN**	**Min. buoy**	**Min. SWAN**
H_{sig}	1.68	1.28	-0.4	0.71	3.94	4.38	0.38	0.043
T_{peak}	8.18	6.8	-1.37	4.15	17.20	16.3	2.6	2.42
	$\lambda_{DIA}=D_2$							
H_{sig}	1.67	1.28	-0.39	0.71	3.94	4.38	0.38	0.043
T_{peak}	8.16	6.79	-1.78	4.15	17.20	17.9	2.6	2.42
	$\lambda_{DIA}=D_3$							
H_{sig}	1.67	1.28	-0.40	0.71	3.94	4.38	0.38	0.043
T_{peak}	8.16	6.80	-1.38	4.16	17.20	17.97	2.6	2.42
	$\lambda_{DIA}=D_4$							
H_{sig}	1.67	1.31	-0.36	0.69	3.94	4.41	0.38	0.044
T_{peak}	8.16	6.64	-1.52	4.05	17.20	14.85	2.6	2.42

Table A.3: Firth of Forth tuning of the λ_{DIA} coefficient

	$\lambda_{DIA}=D_1$							
	Average Buoy	**Average SWAN**	**Bias**	*rmse*	**Max buoy**	**Max SWAN**	**Min. buoy**	**Min. SWAN**
H_{sig}	1.77	1.41	-0.36	0.64	5.25	4.14	0.042	0.06
T_{peak}	8.12	7.87	-0.25	3.09	16	16.34	2.7	2.42
	$\lambda_{DIA}=D_2$							
H_{sig}	1.77	1.41	-0.36	0.64	5.25	4.14	0.042	0.06
T_{peak}	8.11	7.86	-0.25	3.09	16	16.34	2.7	2.42
	$\lambda_{DIA}=D_3$							
H_{sig}	1.77	1.41	-0.36	0.64	5.25	4.14	0.042	0.063
T_{peak}	8.11	7.86	-0.25	3.09	16	16.34	2.7	2.42
	$\lambda_{DIA}=D_4$							
H_{sig}	1.77	1.43	-0.34	0.61	5.25	4.15	0.042	0.06
T_{peak}	8.11	7.85	-0.26	3.07	16	16.34	2.7	2.42

Appendix B

Resource Assessment

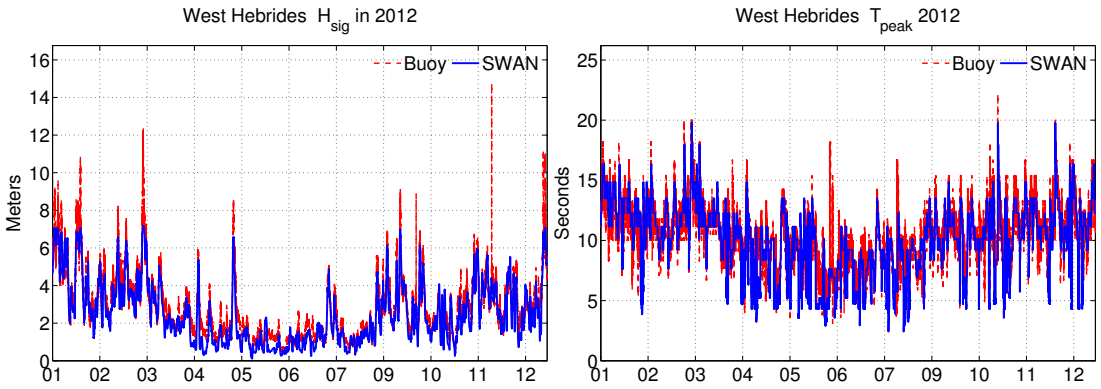

Figure B.1: Hindcast*2012*, West Hebrides

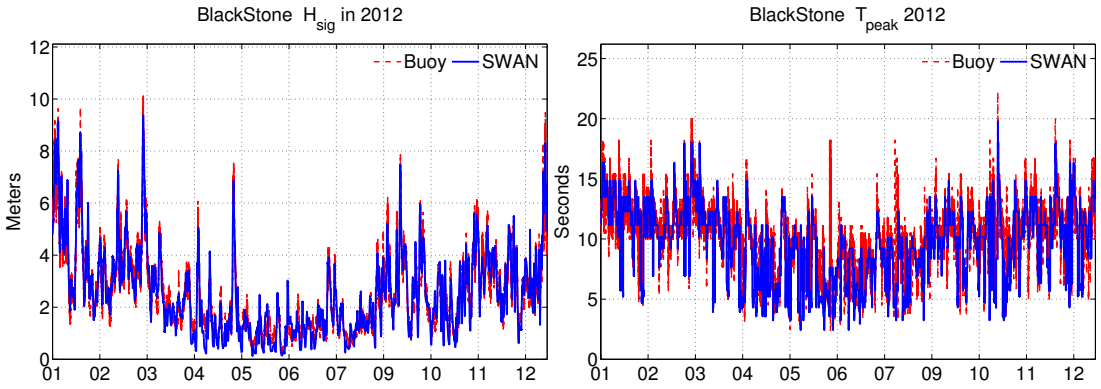

Figure B.2: Hindcast *2012* at the BlackStone location

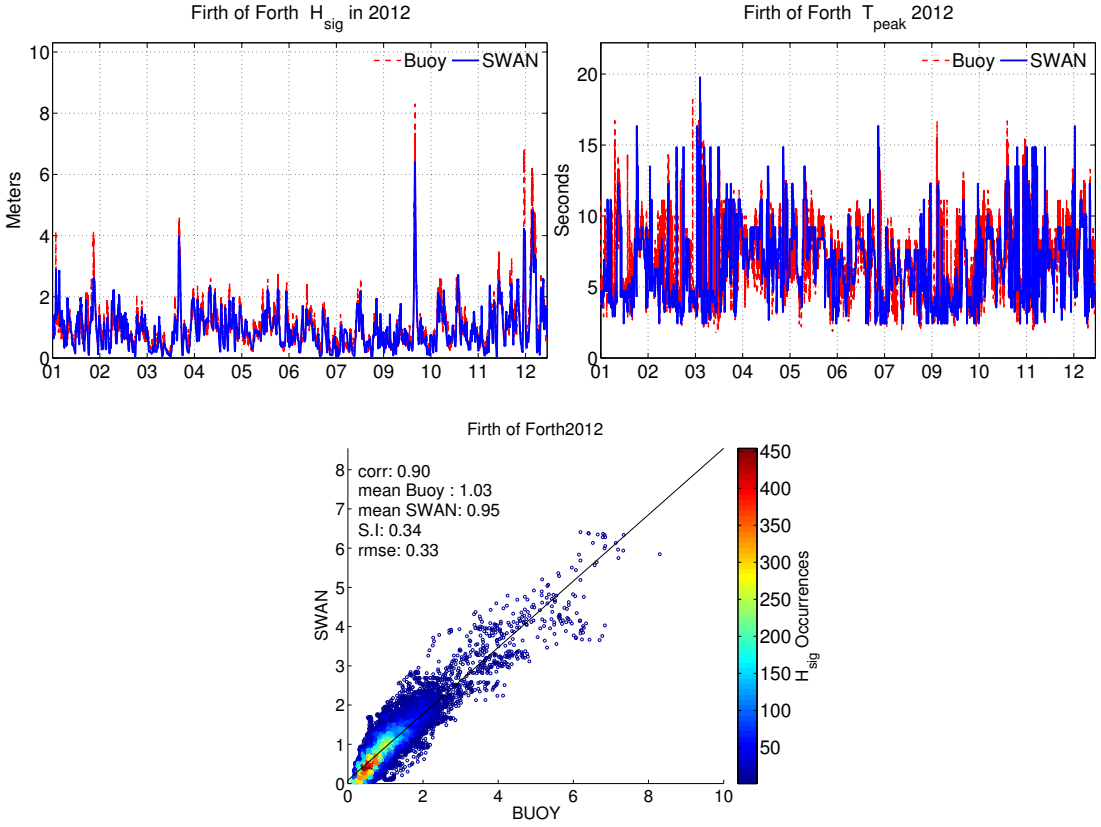

Figure B.3: Hindcast *2012* at the Firth of Forth

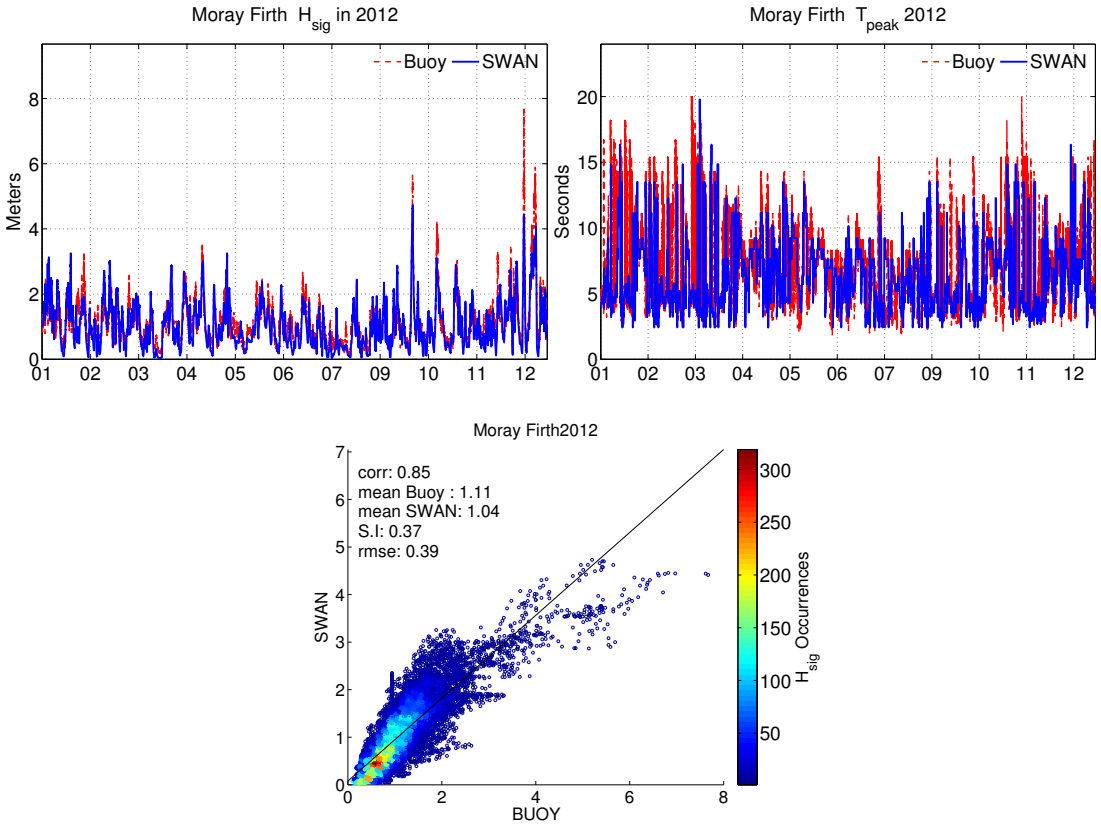

Figure B.4: Hindcast *2012* at the Firth of Forth

Table B.1: Hindcast 2008

	Firth of Forth			Moray Firth		
	H_{sig}	T_{peak}	T_z	H_{sig}	T_{peak}	T_z
Correlation	0.94	0.76	0.81	0.92	0.78	0.73
rms	0.33	2.88	1.11	0.43	3.41	1.23
MPI	0.98	0.91	0.94	0.98	0.89	0.94
Average Buoy	1.08	6.98	4.24	1.23	7.86	4.34
Average *SWAN*	1.09	6.86	4.32	1.24	6.96	4.20
Bias	0.01	-0.1	0.07	0.01	-0.89	-0.14
SI	0.31	0.41	0.26	0.35	0.43	0.28

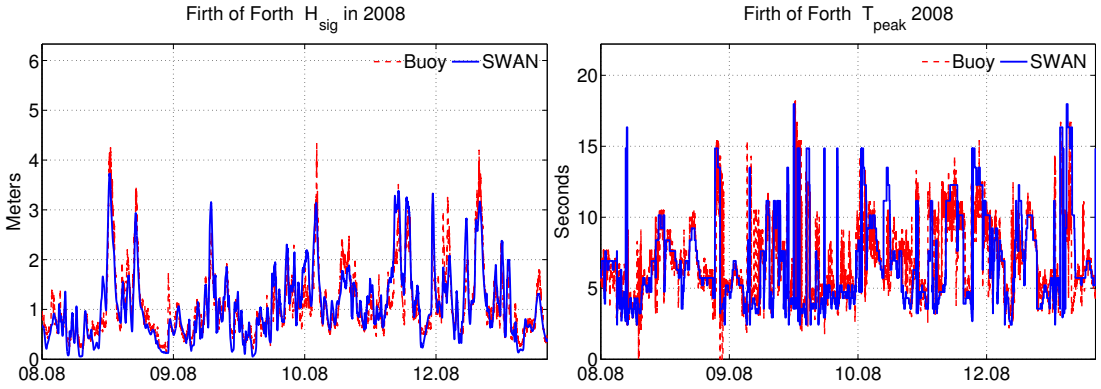

Figure B.5: Hindcast *2008* at the Firth of Forth

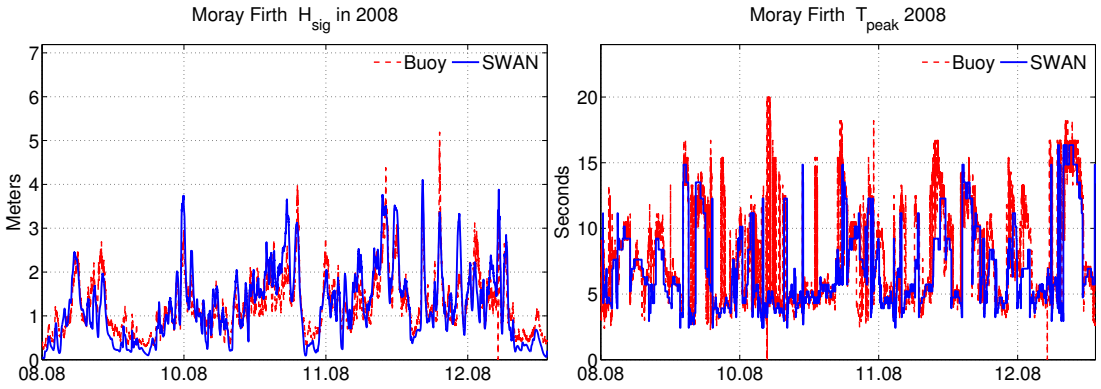

Figure B.6: Hindcast *2008* at the Moray Firth location

Table B.2: Hindcast 2009

	West Hebrides			BlackStone			Firth of Forth			Moray Firth		
	H_{sig}	T_{peak}	T_z	H_{sig}	T_{peak}	T_z	H_{sig}	T_{peak}	T_z	H_{sig}	T_{peak}	T_z
Correlation	0.96	0.85	0.85	0.97	0.83	0.89	0.94	0.74	0.81	0.91	0.73	0.79
rms	0.62	2.02	1.34	0.44	2.33	1.09	0.3	2.73	1.09	0.38	3.24	1.02
MPI	0.97	0.91	0.94	0.97	0.91	0.94	0.99	0.94	0.96	0.99	0.94	0.96
Average Buoy	2.8	10.46	6.51	2.41	9.99	6.08	1.01	6.77	4.22	1.07	7.05	4.18
Average *SWAN*	2.5	10.24	5.87	2.5	9.66	5.89	0.95	6.77	4.29	0.97	6.47	3.97
Bias	-0.29	-0.22	-0.63	0.09	-0.32	-0.19	-0.05	0	0.06	-0.1	-0.57	-0.2
SI	0.22	0.19	0.2	0.18	0.23	0.18	0.3	0.4	0.25	0.35	0.45	0.24

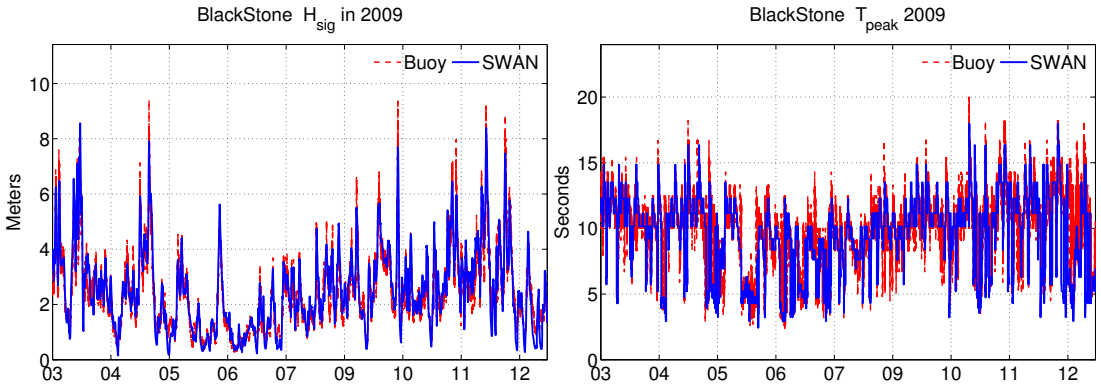

Figure B.7: Hindcast *2009* at the BlackStone

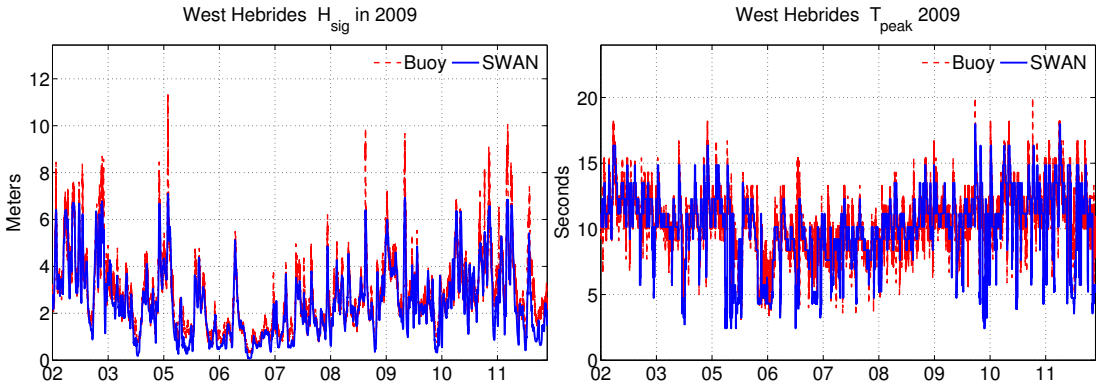

Figure B.8: Hindcast *2009* at the West Hebrides

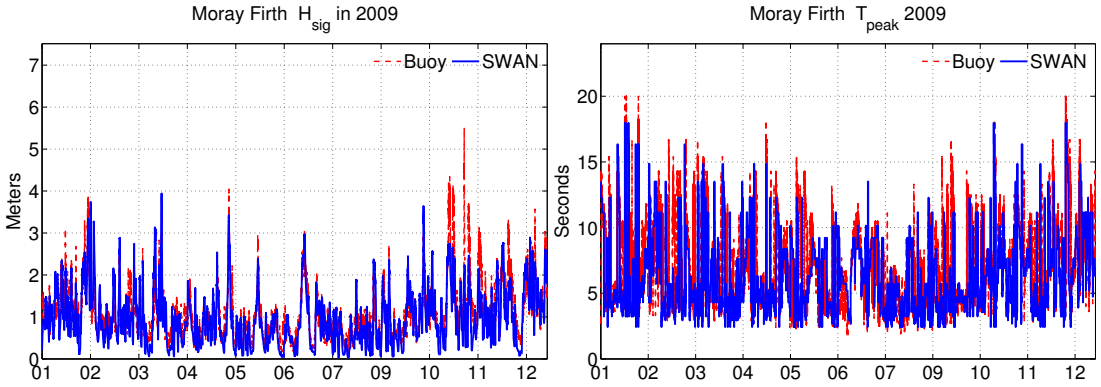

Figure B.9: Hindcast *2009* at the Moray Firth location

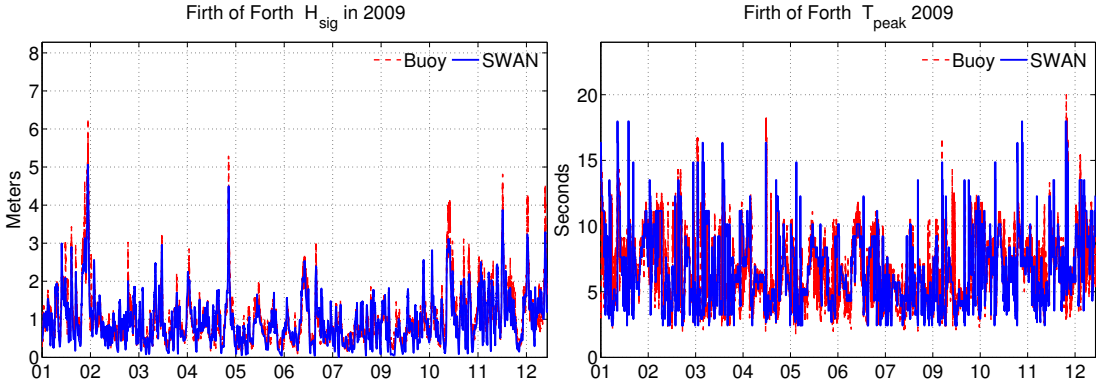

Figure B.10: Hindcast *2009* at the Firth of Forth location

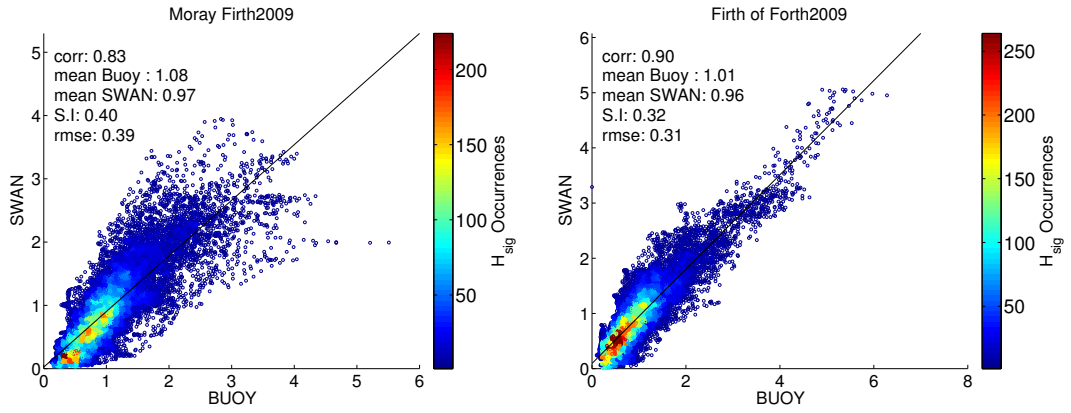

Figure B.11: Hindcast *2009* Scatter and accuracy representation

Table B.3: Hindcast 2010

	West Hebrides			BlackStone			Firth of Forth			Moray Firth		
	H_{sig}	T_{peak}	T_z	H_{sig}	T_{peak}	T_z	H_{sig}	T_{peak}	T_z	H_{sig}	T_{peak}	T_z
Correlation	0.87	0.78	0.8	0.96	0.79	0.85	0.96	0.754	0.81	0.94	0.69	0.77
rms	0.84	2.46	1.44	0.44	2.56	1.17	0.32	2.64	1.18	0.37	3.2	1.13
MPI	0.98	0.91	0.95	0.98	0.92	0.95	0.99	0.94	0.96	0.99	0.94	0.96
Average Buoy	2.38	10.62	6.38	2.05	9.96	5.97	1.15	7.11	4.54	1.13	7.37	4.37
Average *SWAN*	2.04	9.98	5.69	2.1	9.43	5.69	1.09	7.51	4.75	1.07	7.1	4.28
Bias	-0.33	-0.64	-0.68	0.05	-0.53	-0.28	-0.05	0.39	0.21	-0.05	-0.26	-0.08
SI	0.35	0.23	0.22	0.21	0.25	0.19	0.28	0.37	0.26	0.33	0.43	0.25

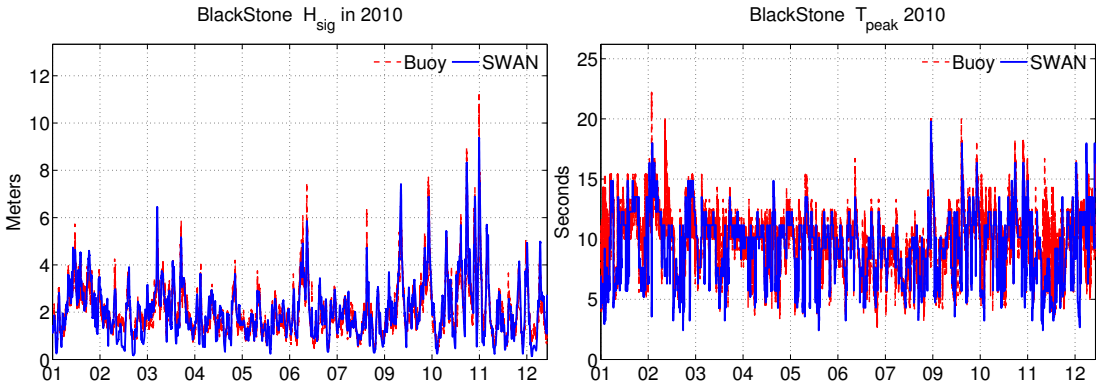

Figure B.12: Hindcast *2010* Blackstone

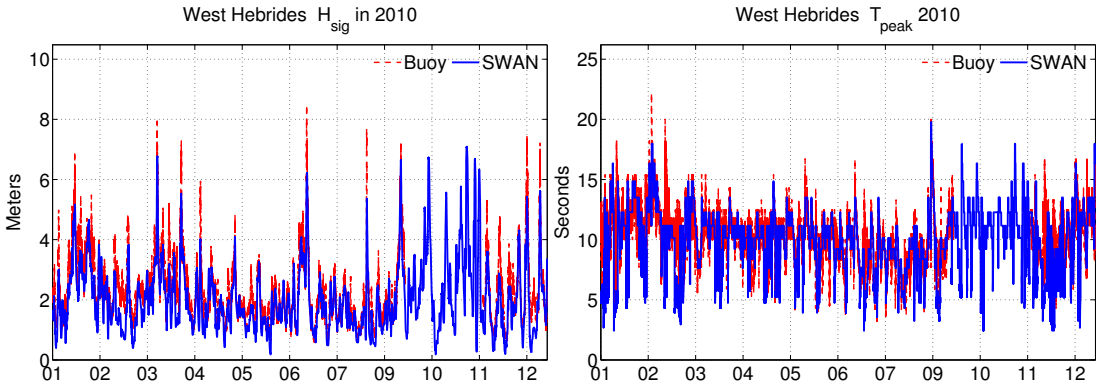

Figure B.13: Hindcast *2010* West Hebrides

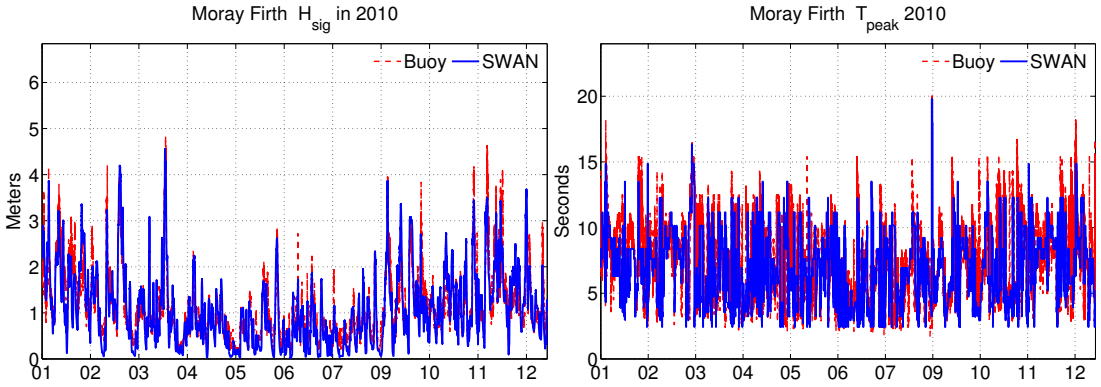

Figure B.14: Hindcast *2010* Moray Firth

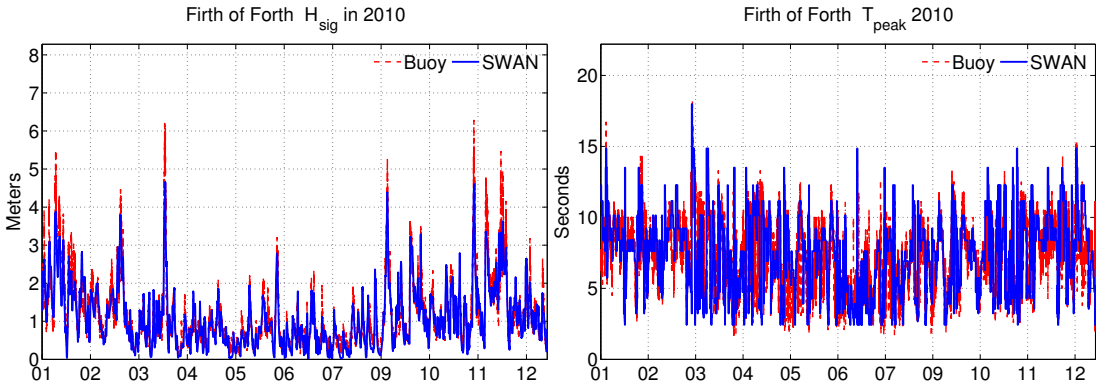

Figure B.15: Hindcast *2010* Firth of Forth

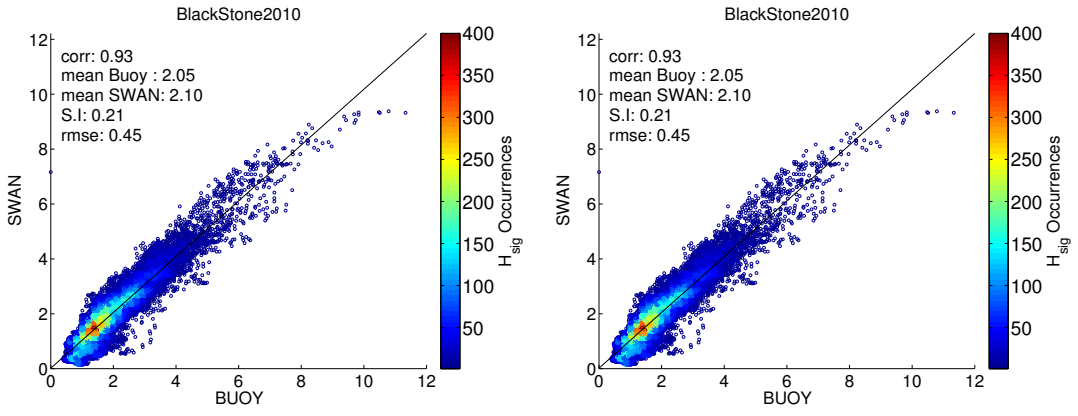

Figure B.16: Hindcast *2010* Scatter and accuracy representation Blackstone Firth of Forth

Table B.4: Hindcast 2011

	West Hebrides			BlackStone			Firth of Forth			Moray Firth		
	H_{sig}	T_{peak}	T_z	H_{sig}	T_{peak}	T_z	H_{sig}	T_{peak}	T_z	H_{sig}	T_{peak}	T_z
Correlation	0.96	0.89	0.85	0.98	0.89	0.9	0.92	0.68	0.75	0.87	0.71	0.7
rms	0.69	1.78	1.4	0.47	1.88	1.1	0.32	3.4	1.19	0.47	3.95	1.4
MPI	0.97	0.91	0.94	0.97	0.91	0.94	0.99	0.95	0.96	0.99	0.94	0.97
Average Buoy	3.33	11.17	7.04	2.95	10.88	6.74	0.9	6.36	4	0.98	6.93	3.9
Average *SWAN*	3.04	11.16	6.27	3.07	10.79	6.52	0.89	6.78	4.17	0.97	6.67	3.87
Bias	-0.28	-0.001	-0.76	0.11	-0.09	-0.21	-0.01	0.42	0.17	-0.01	-0.26	-0.02
SI	0.2	0.16	0.19	0.15	0.17	0.16	0.35	0.53	0.29	0.44	0.57	0.36

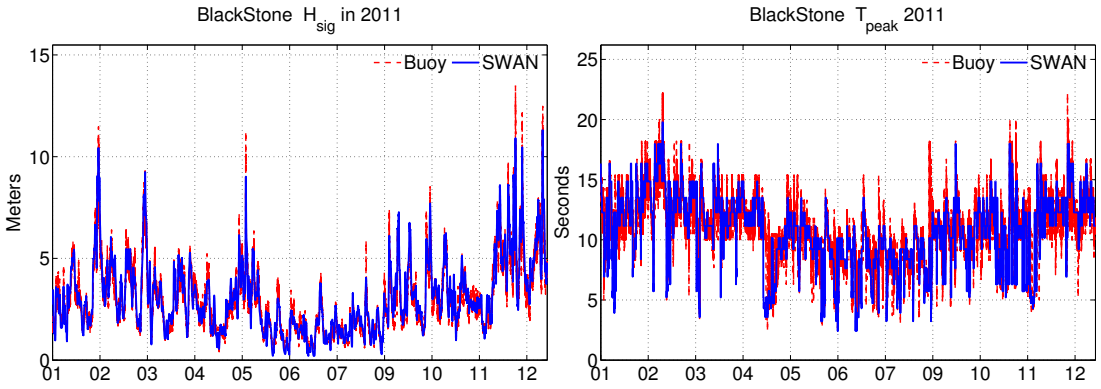

Figure B.17: Hindcast *2011* BlackStone

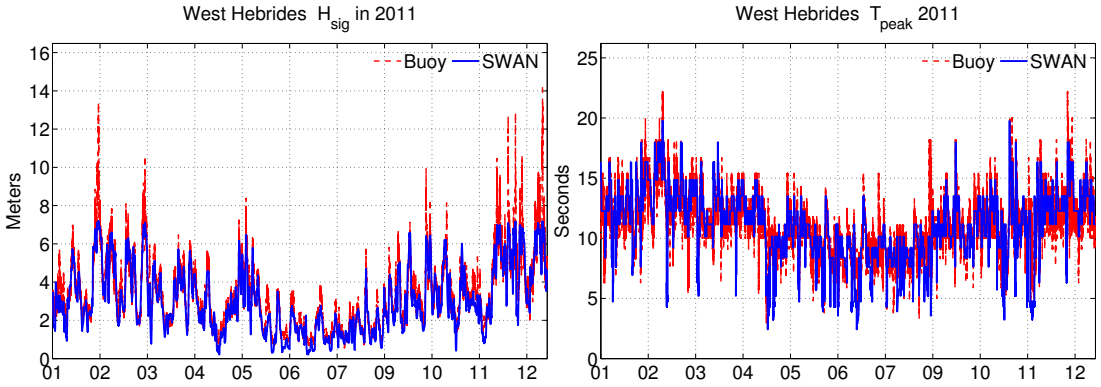

Figure B.18: Hindcast *2011* West Hebrides

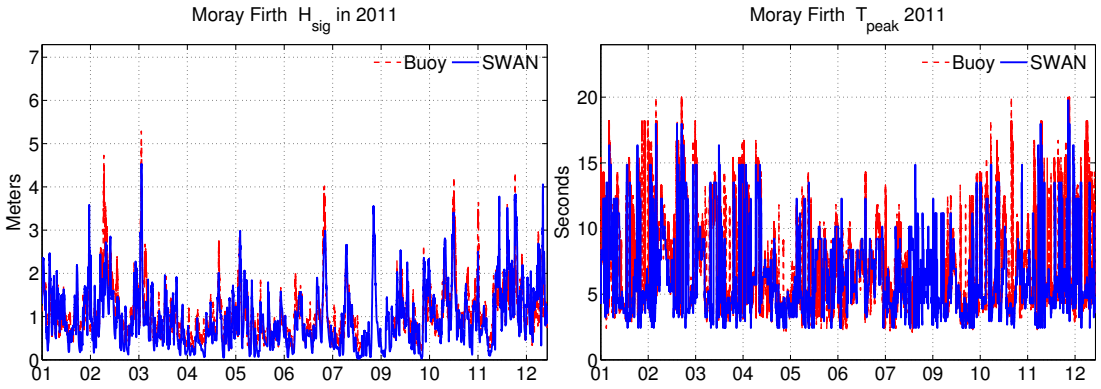

Figure B.19: Hindcast *2011* Moray Firth

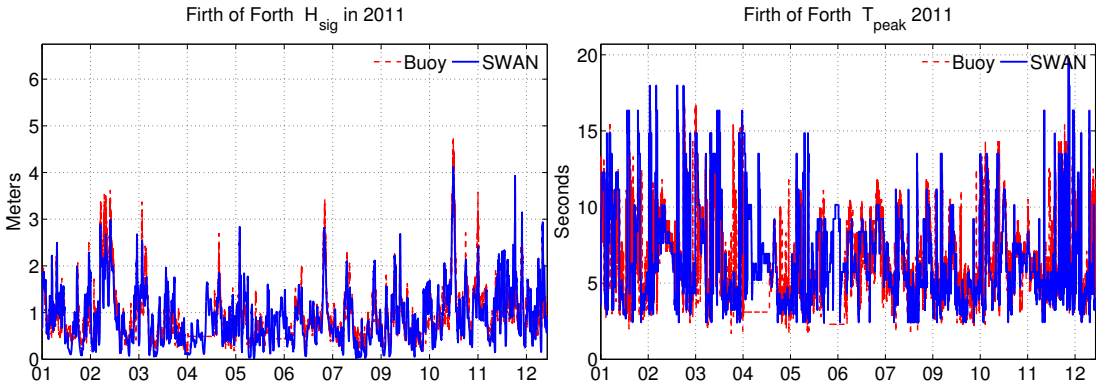

Figure B.20: Hindcast *2011* Firth of Forth

Table B.5: Hindcast 2013

	West Hebrides			BlackStone			Firth of Forth			Moray Firth		
	H_{sig}	T_{peak}	T_z	H_{sig}	T_{peak}	T_z	H_{sig}	T_{peak}	T_z	H_{sig}	T_{peak}	T_z
Correlation	0.97	0.86	0.85	0.97	0.87	0.9	0.96	0.72	0.86	0.94	0.69	0.8
rms	0.73	2.17	1.44	0.48	2.47	1.14	0.31	2.79	0.89	0.36	3.4	0.96
MPI	0.977	0.91	0.94	0.96	0.87	0.92	0.99	0.95	0.96	0.99	0.94	0.96
Average Buoy	3.01	10.92	6.77	2.76	10.8	6.46	1.05	6.41	4.17	1.05	6.82	4.11
Average *SWAN*	2.64	10.29	5.95	2.83	10.08	5.93	0.99	6.32	4.1	0.99	6.19	3.82
Bias	-0.36	-0.6	-0.81	0.06	-0.7	-0.52	-0.06	-0.08	-0.07	-0.06	-0.62	-0.28
SI	0.24	0.19	0.21	0.17	0.22	0.17	0.3	0.43	0.2	0.34	0.5	0.23

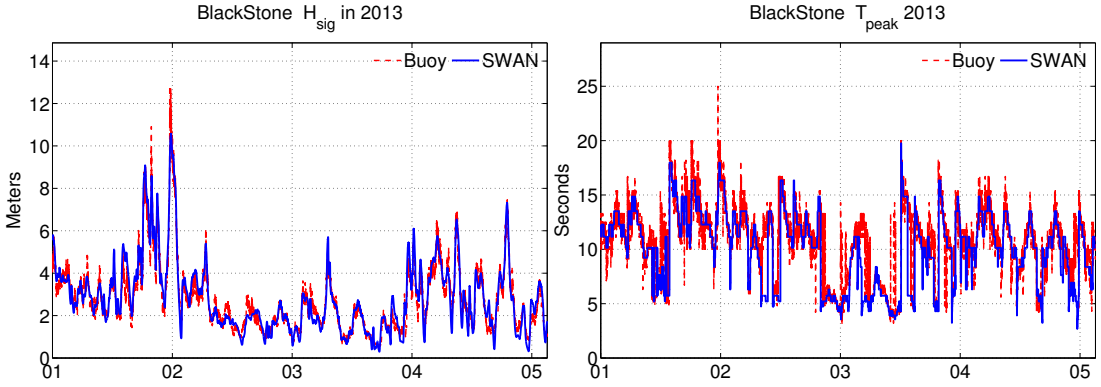

Figure B.21: Hindcast *2013* BlackStone

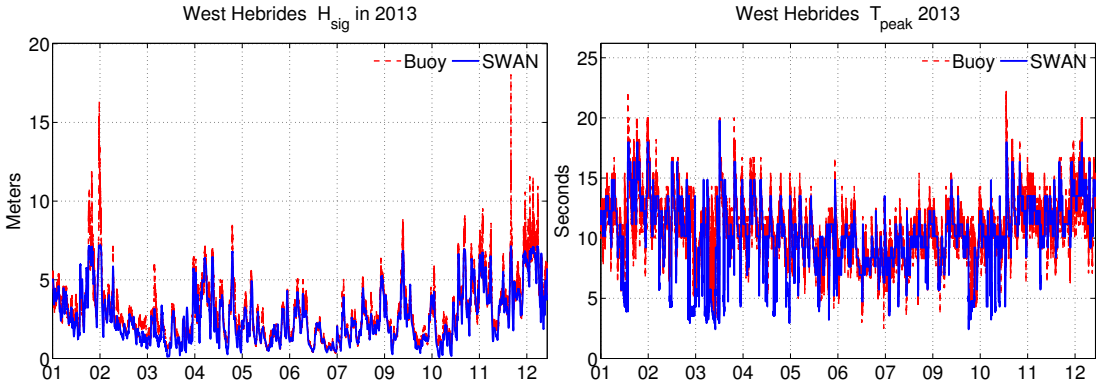

Figure B.22: Hindcast *2013* West Hebrides

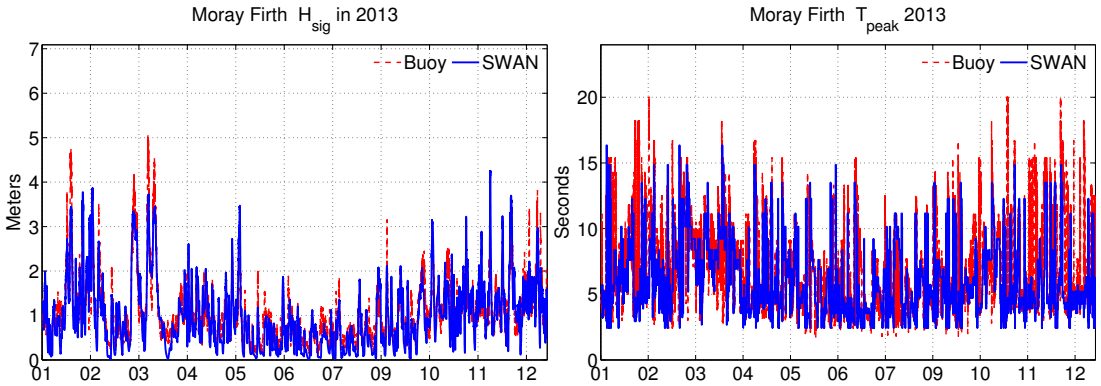

Figure B.23: Hindcast *2013* Moray Firth

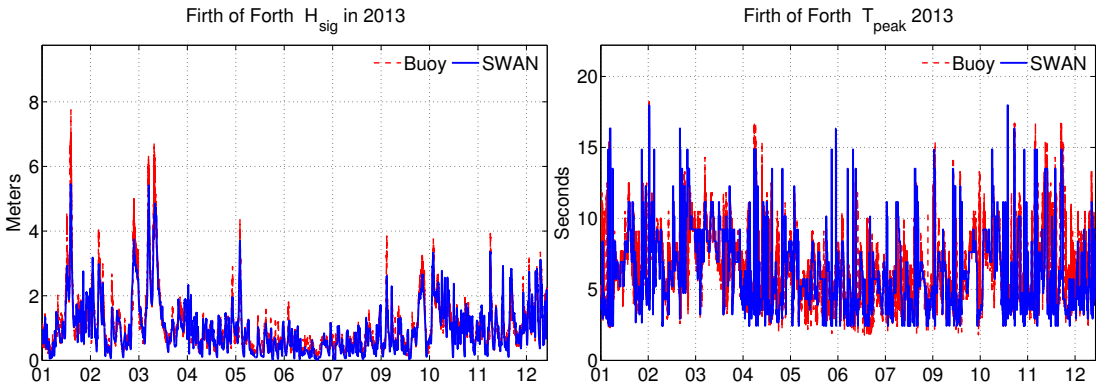

Figure B.24: Hindcast *2013* Firth of Forth

Table B.6: Hindcast 2014

	West Hebrides			Firth of Forth			Moray Firth		
	H_{sig}	T_{peak}	T_z	H_{sig}	T_{peak}	T_z	H_{sig}	T_{peak}	T_z
Correlation	0.96	0.85	0.83	0.95	0.68	0.84	0.92	0.74	0.81
rms	0.75	2.21	1.65	0.37	2.82	1.03	0.5	3.34	1.16
MPI	0.95	0.85	0.91	0.98	0.9	0.94	0.98	0.9	0.94
Average Buoy	3.52	12.03	7.45	1.32	7.17	4.61	1.36	7.43	4.53
Average *SWAN*	3.21	11.49	6.42	1.18	6.85	4.39	1.15	6.56	3.96
Bias	-0.31	-0.54	-1.02	-0.14	-0.32	-0.22	-0.21	-0.86	-0.56
SI	0.2	0.18	0.22	0.28	0.39	0.22	0.37	0.45	0.25

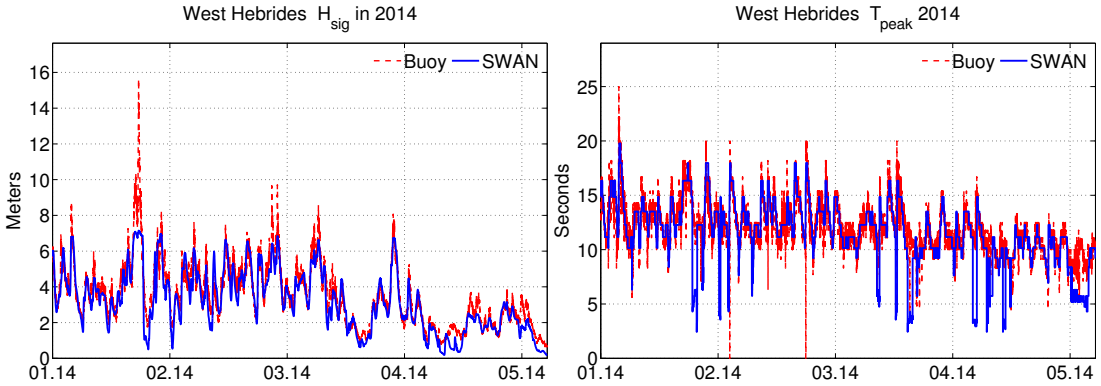

Figure B.25: Hindcast *2014* West Hebrides

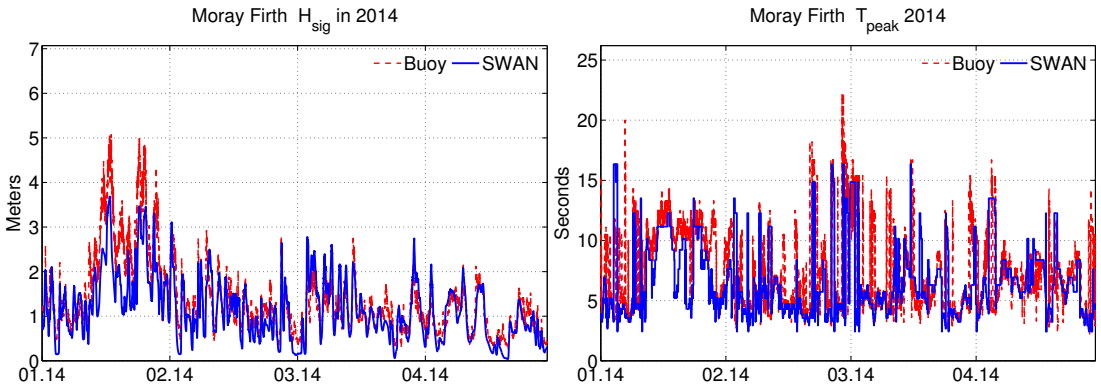

Figure B.26: Hindcast *2014* Moray Firth

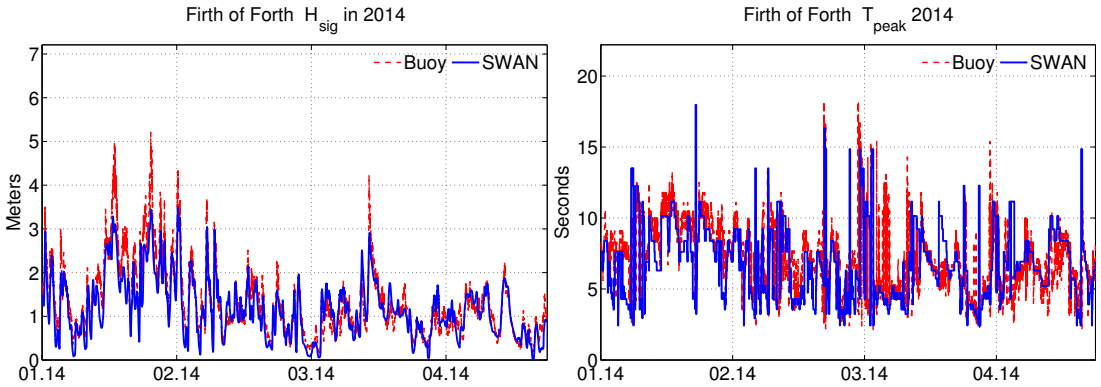

Figure B.27: Hindcast *2014* Firth of Forth

Table B.7: H_{sig} at locations in Aegean during the calibration process

	Athos			Pylos			Petrokaravo		
	H_{sig}	T_{peak}	T_z	H_{sig}	T_{peak}	T_z	H_{sig}	T_{peak}	T_z
Correlation	0.77	0.91	0.95	0.93	0.96	0.97	0.88	0.88	0.96
rms	0.75	2.04	3.21	0.53	1.44	0.87	0.33	2.25	0.87
Average buoy	0.81	4.59	3.75	0.99	5.59	4.23	0.55	4.35	3.23
Average *SWAN*	0.39	4.28	3.29	0.66	5.48	4.12	0.29	4.98	3.5
Bias	-0.41	-0.31	-0.46	-0.33	-0.11	-0.11	-0.26	0.63	0.27
MPI	0.98	0.89	0.91	0.97	0.88	0.91	0.96	0.78	0.82

Table B.8: Validation of Aegean

	Petrokaravo			Athos			Pylos			Santorini			Mykonos			Lesvos		
	H_{sig}	T_{peak}	T_z	H_{sig}	T_{peak}	T_z	H_{sig}	T_{peak}	T_z	H_{sig}	T_{peak}	T_z	H_{sig}	T_{peak}	T_z	H_{sig}	T_{peak}	T_z
Bias	-0.26	0.89	0.65	-0.41	0.02	-0.11	-0.25	-0.07	0.00	0.11	0.46	0.83	-0.19	-0.12	-0.11	-0.22	0.16	0.06
Average Buoy	0.51	4.3	3.22	0.81	4.86	3.86	1.01	5.92	4.4	0.92	5.05	3.77	0.9	4.85	3.6	0.76	4.59	3.56
Average *SWAN*	0.25	5.19	3.87	0.39	4.88	3.75	0.76	5.84	4.4	1.03	5.51	4	0.71	4.73	3.49	0.54	4.75	3.6
rms	0.22	1.52	0.72	0.74	1.91	1.19	0.46	1.35	0.78	0.73	1.67	0.23	0.58	1.72	0.8	0.52	1.52	0.94
MPI	0.90	0.92	0.94	0.98	0.9	0.92	0.98	0.89	0.91	0.92	0.9	0.93	0.98	0.91	0.93	0.98	0.91	0.93

Appendix C

Reducing Wave Energy Uncertainty

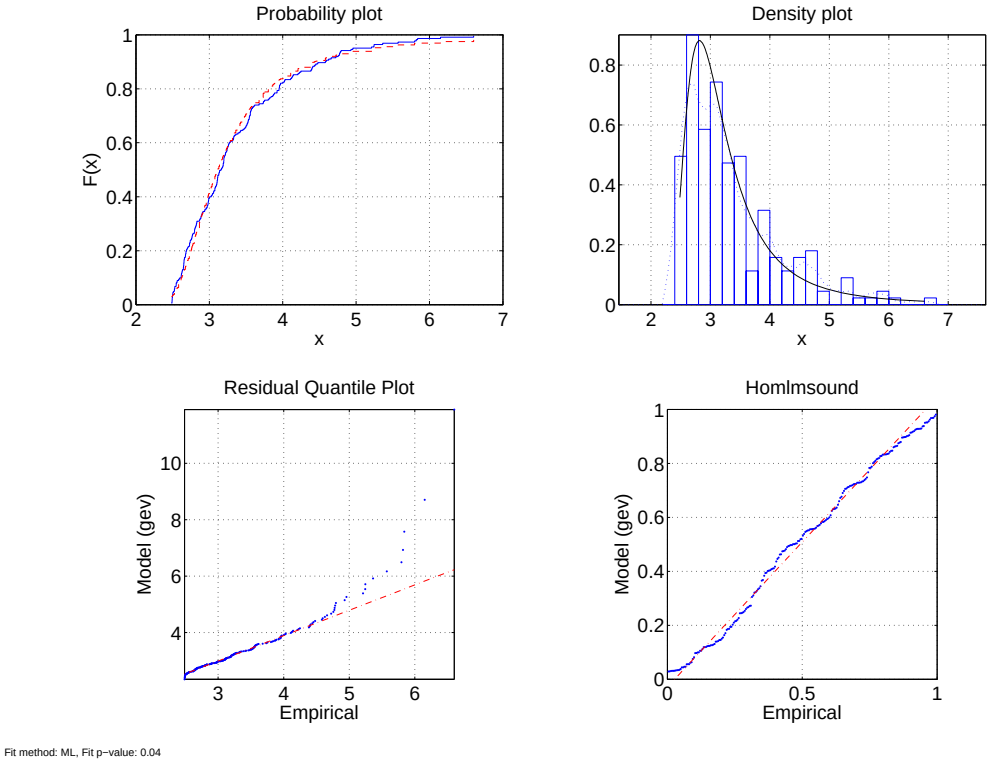

Figure C.1: GEV at 93^{th} percentile

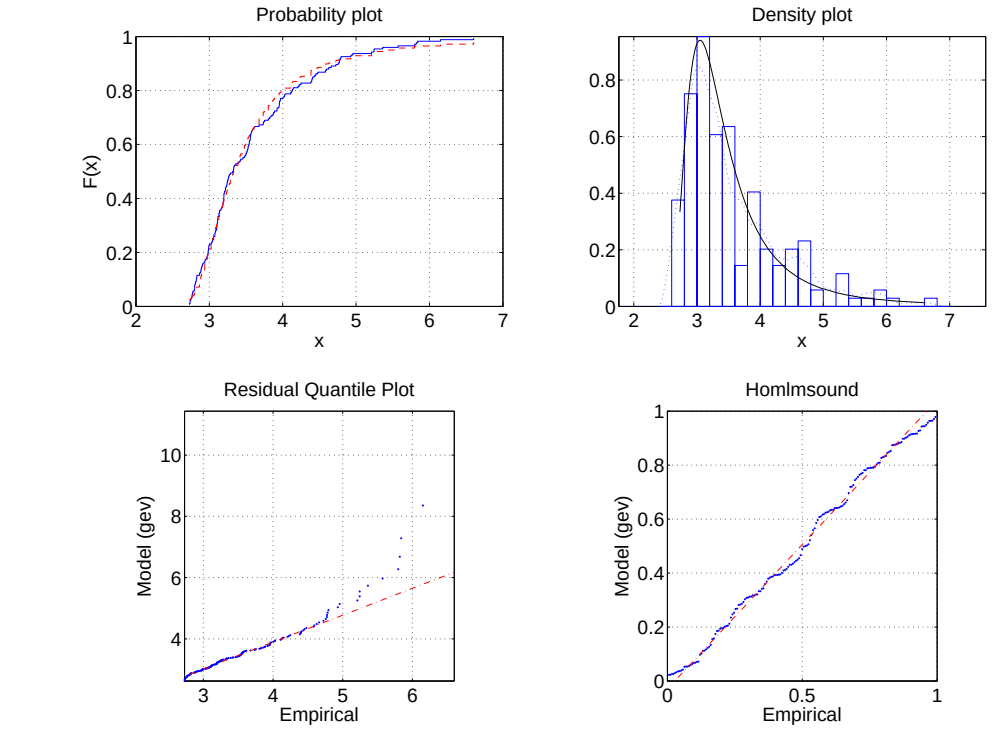

Figure C.2: GEV at 95^{th} percentile

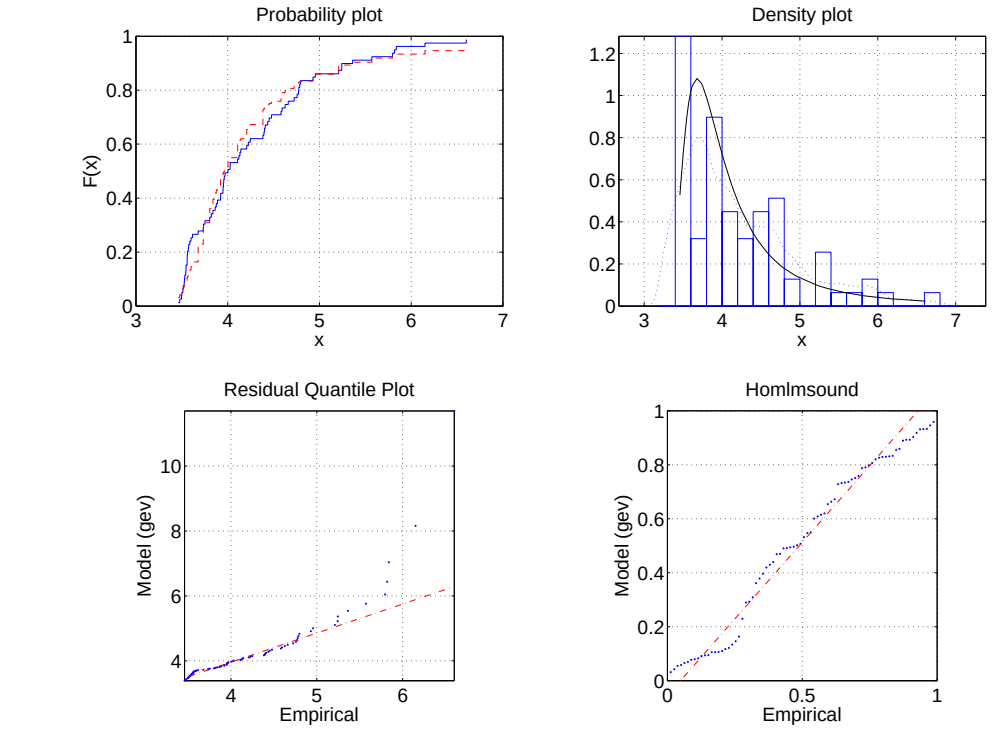

Figure C.3: GEV at 98^{th} percentile

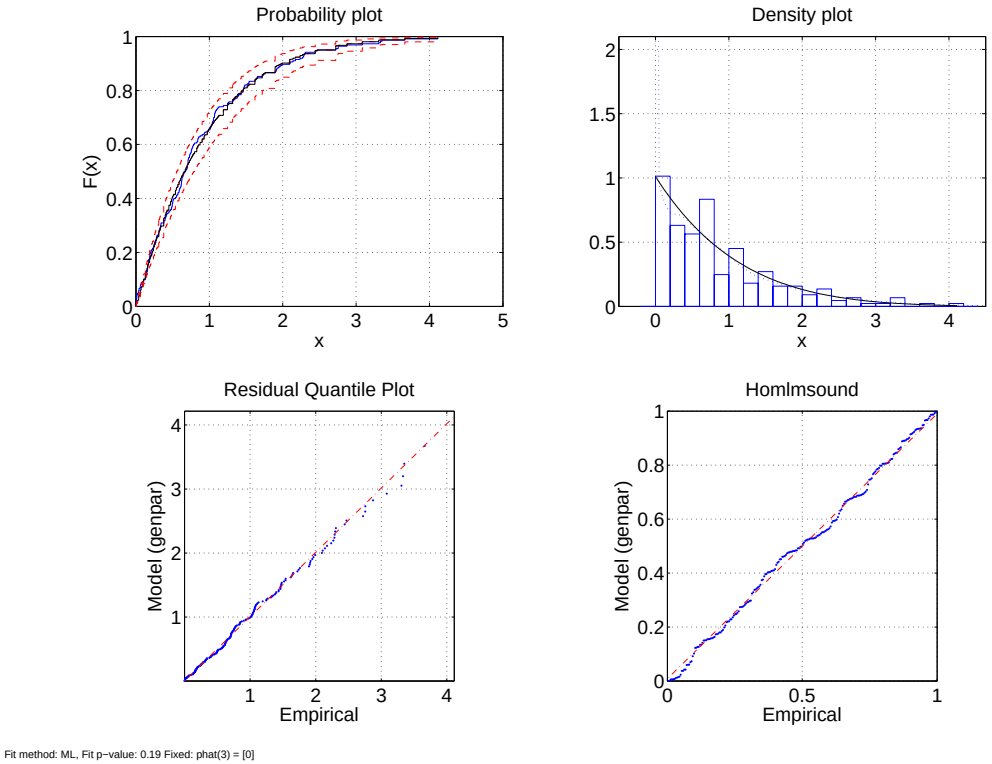

Figure C.4: GPD at 93^{th} percentile

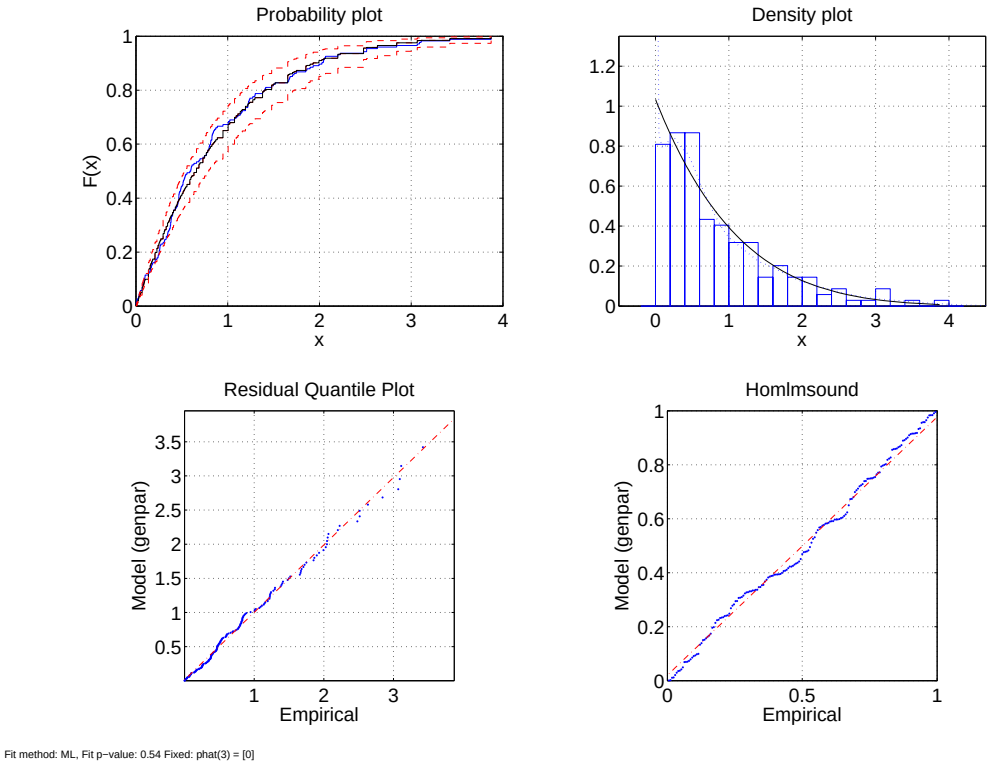

Figure C.5: GPD at 95^{th} percentile

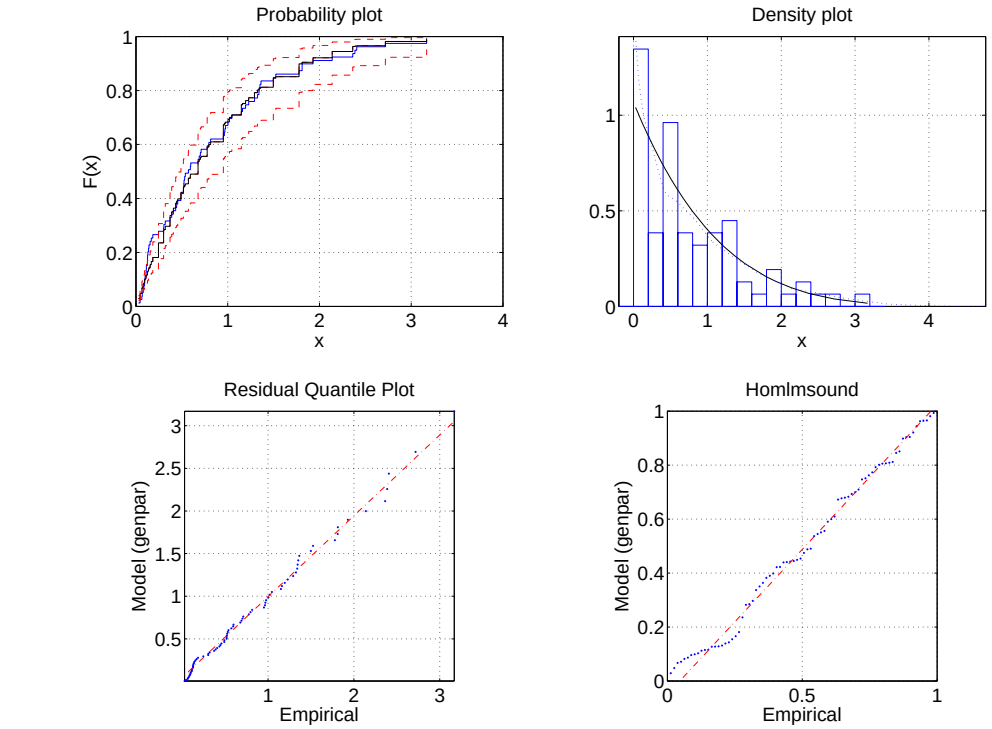

Figure C.6: GPD at 98^{th} percentile

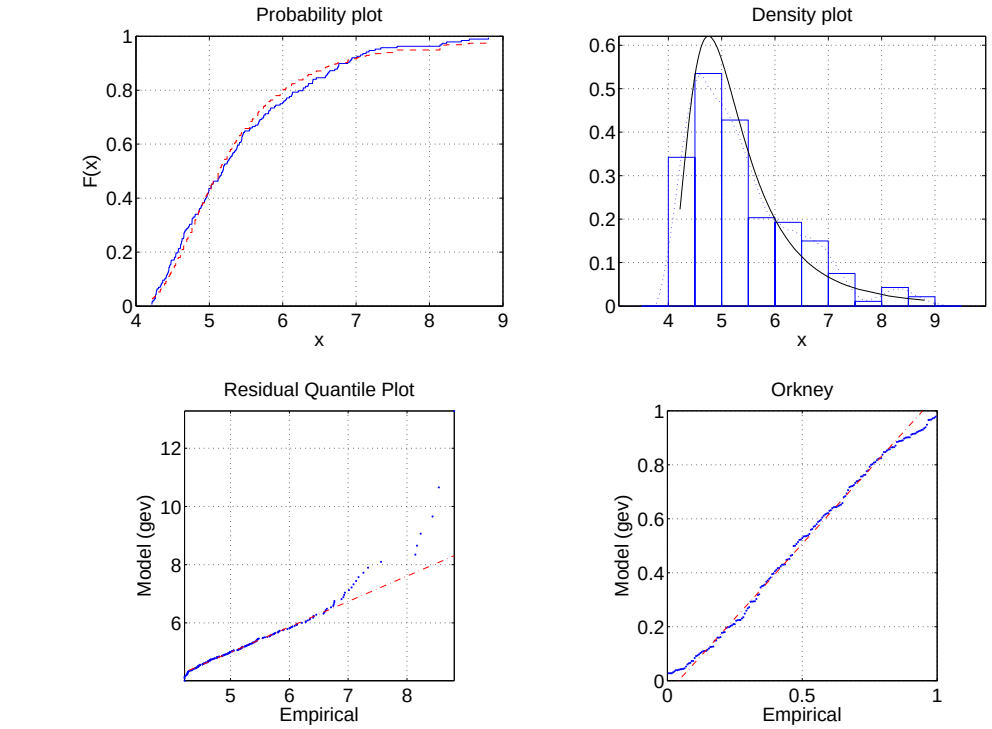

Figure C.7: GEV at 93^{th} percentile

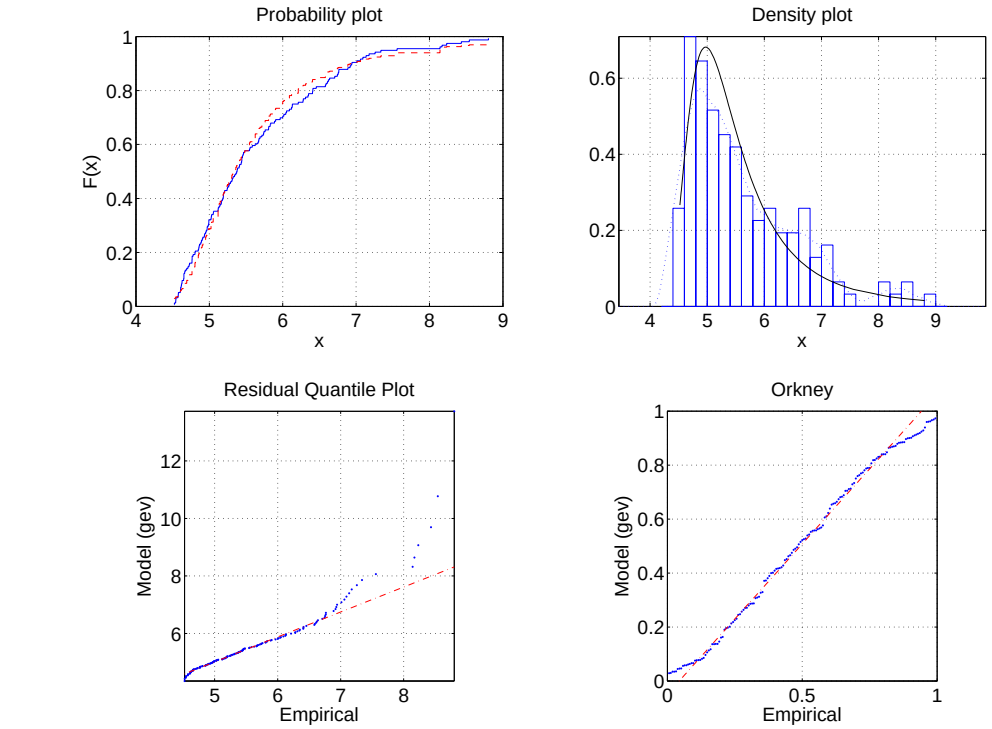

Figure C.8: GEV at 95^{th} percentile

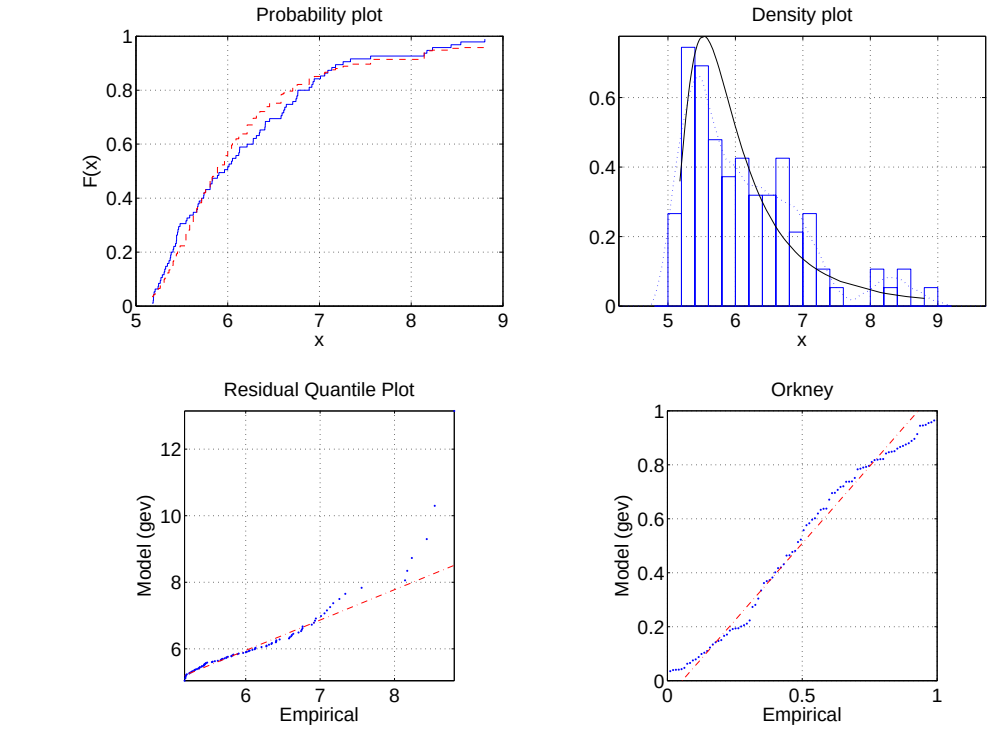

Figure C.9: GEV at 98^{th} percentile

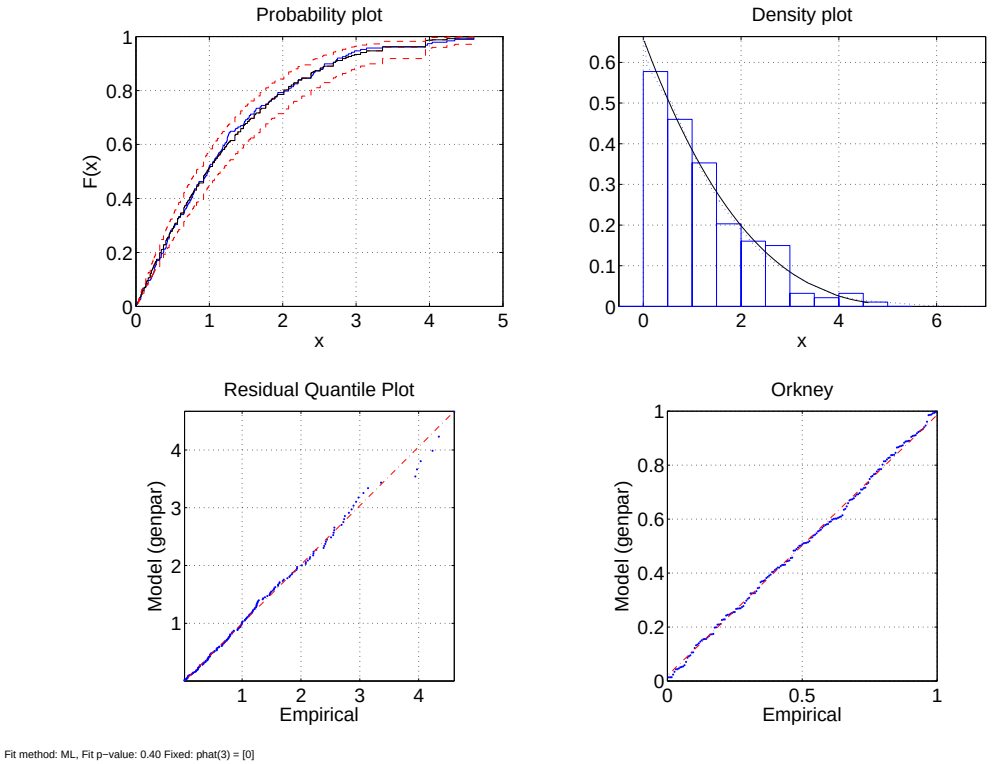

Figure C.10: GPD at 93^{th} percentile

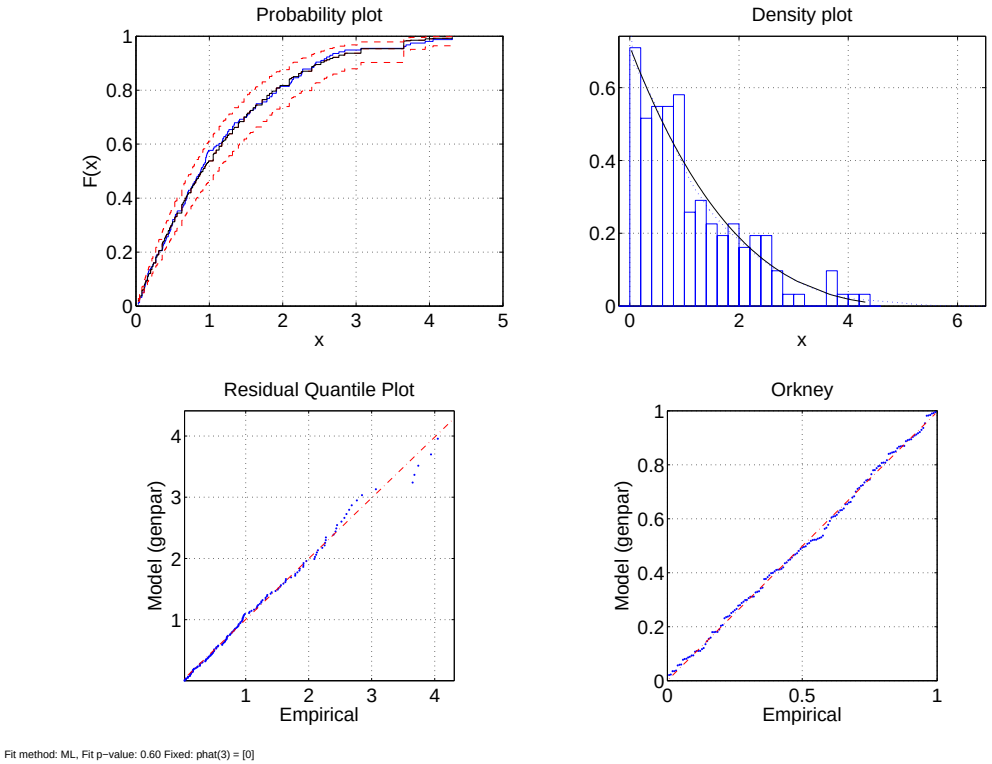

Figure C.11: GPD at 95^{th} percentile

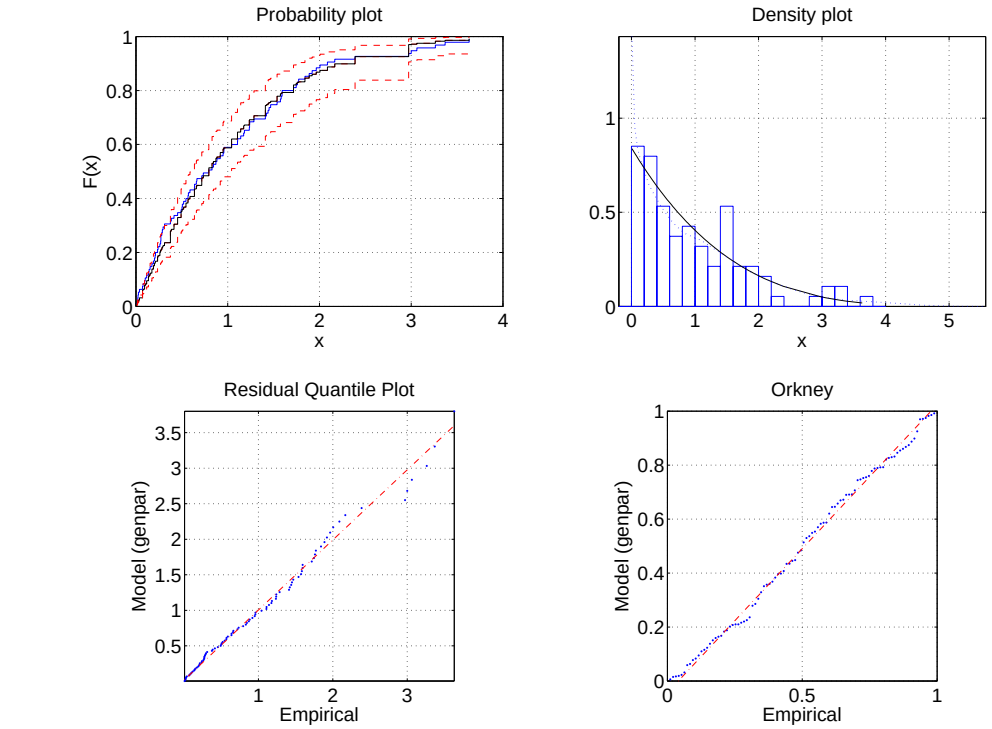

Figure C.12: GPD at 98^{th} percentile

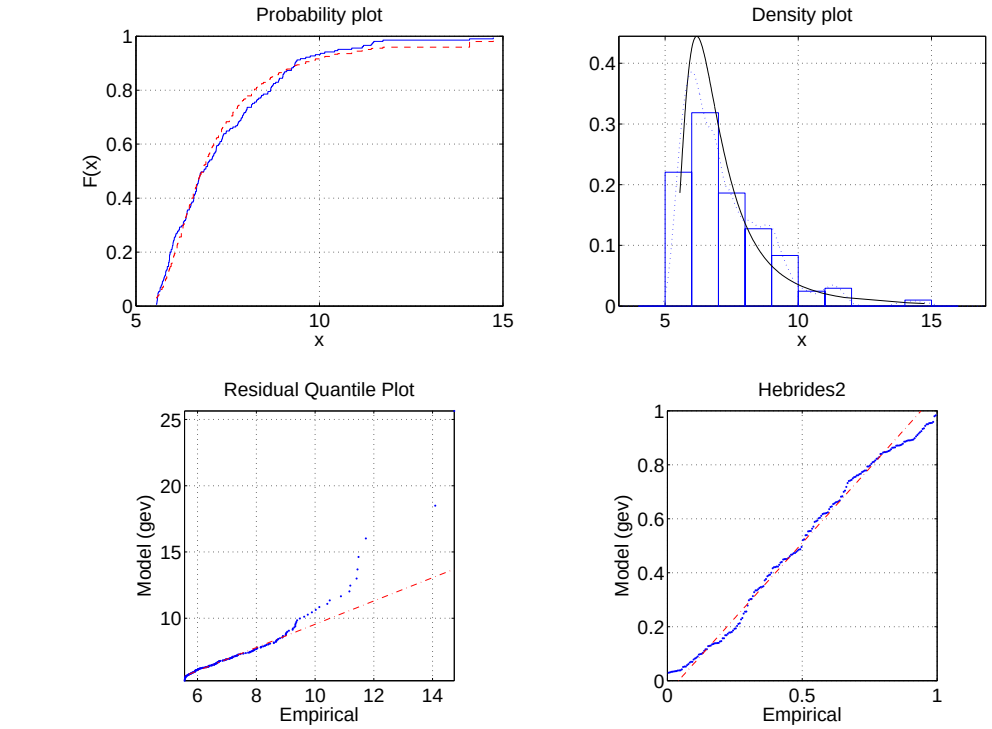

Figure C.13: GEV at 93^{th} percentile

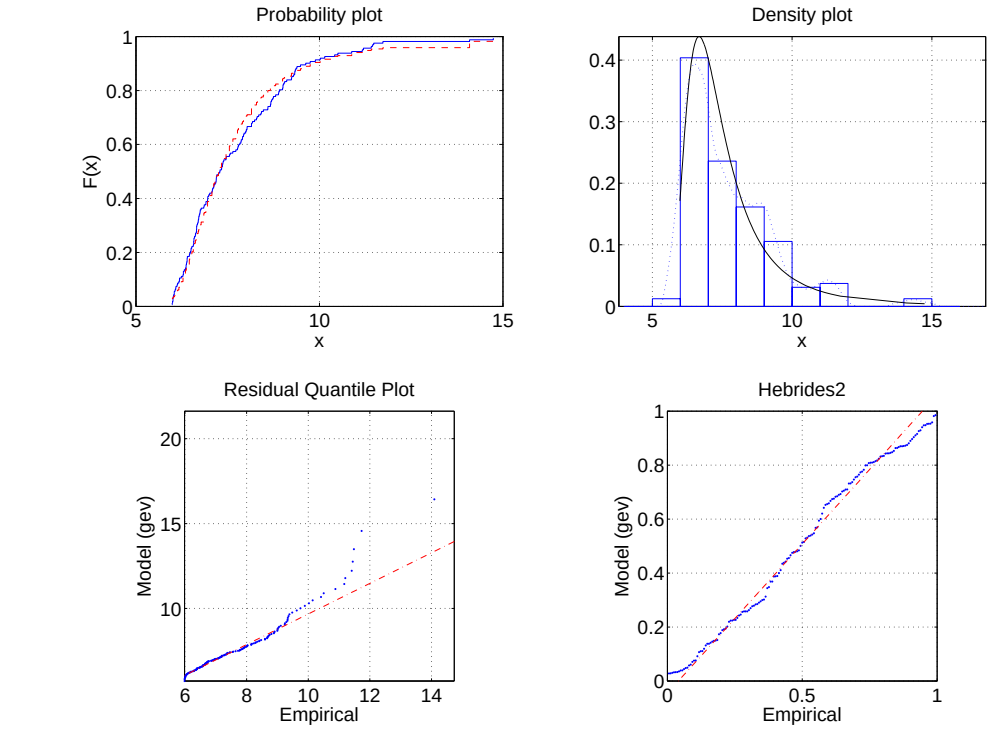

Figure C.14: GEV at 95^{th} percentile

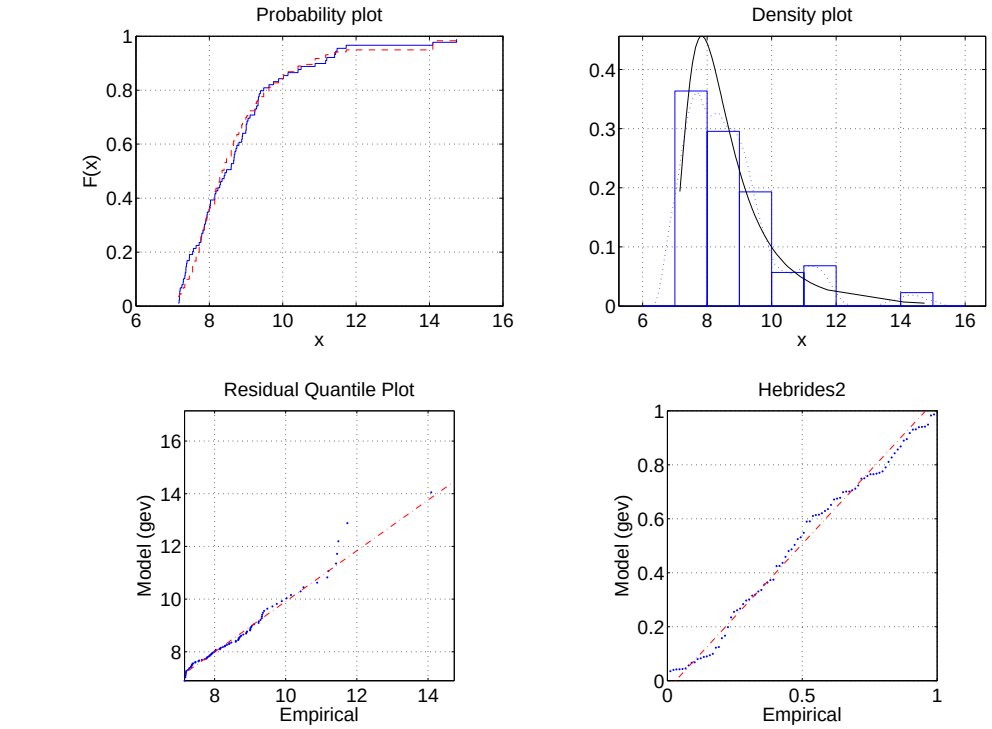

Figure C.15: GEV at 98^{th} percentile

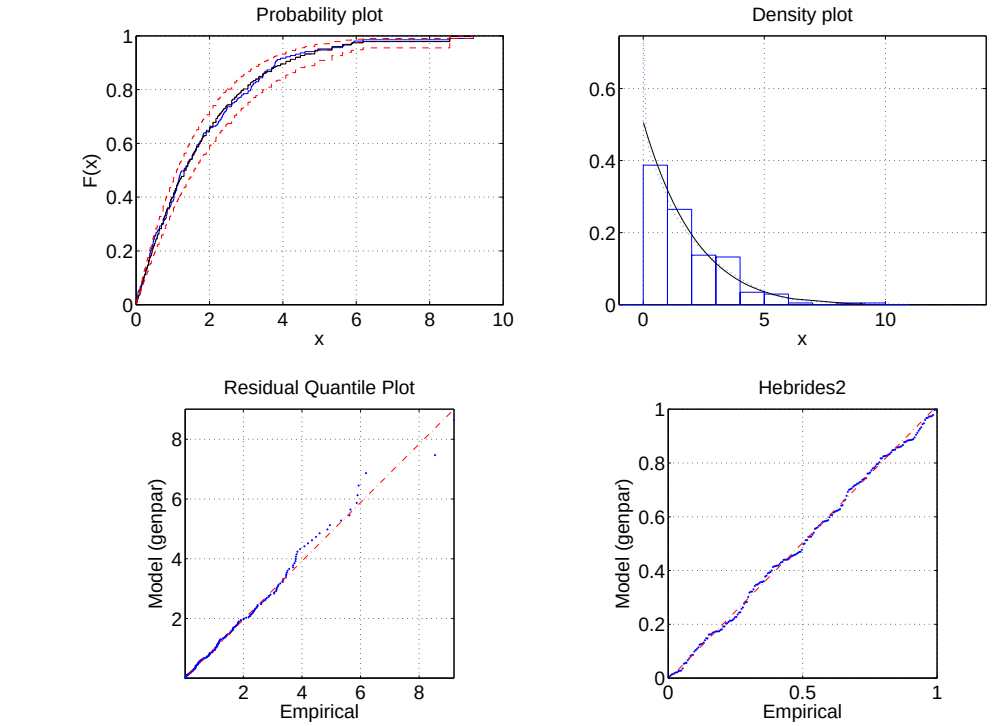

Figure C.16: GPD at 93^{th} percentile

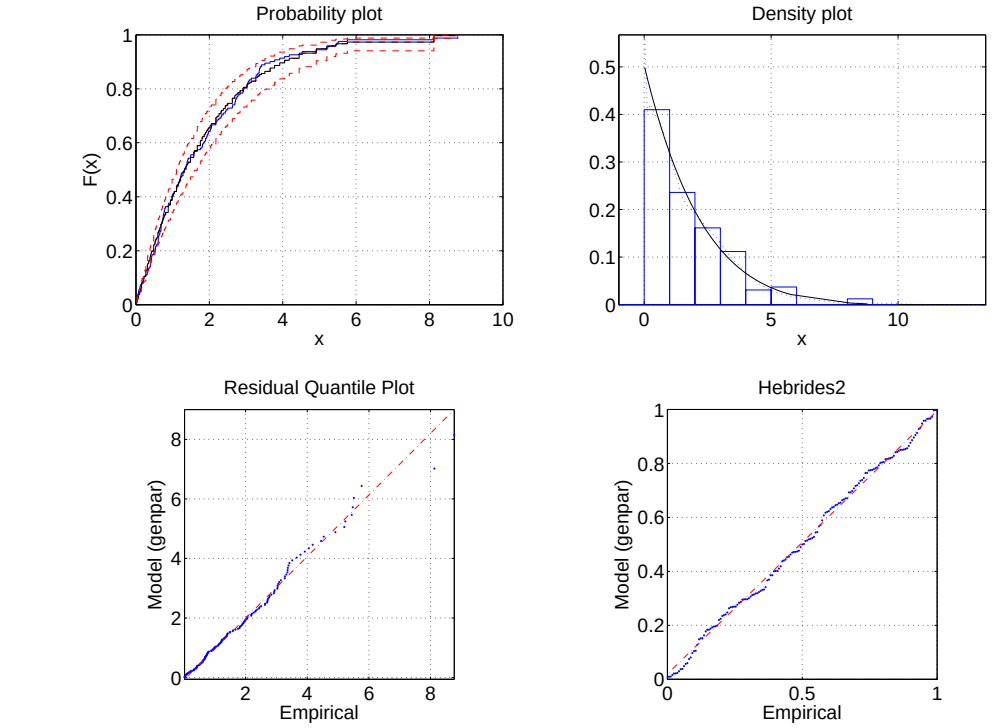

Figure C.17: GPD at 95^{th} percentile

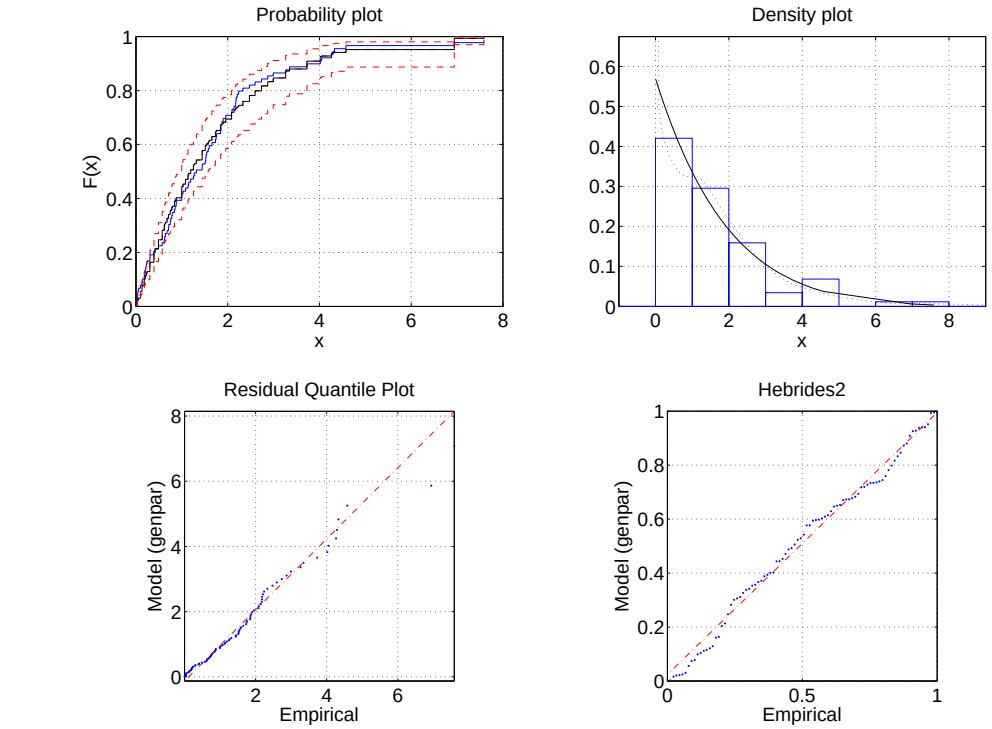

Figure C.18: GPD at 98^{th} percentile

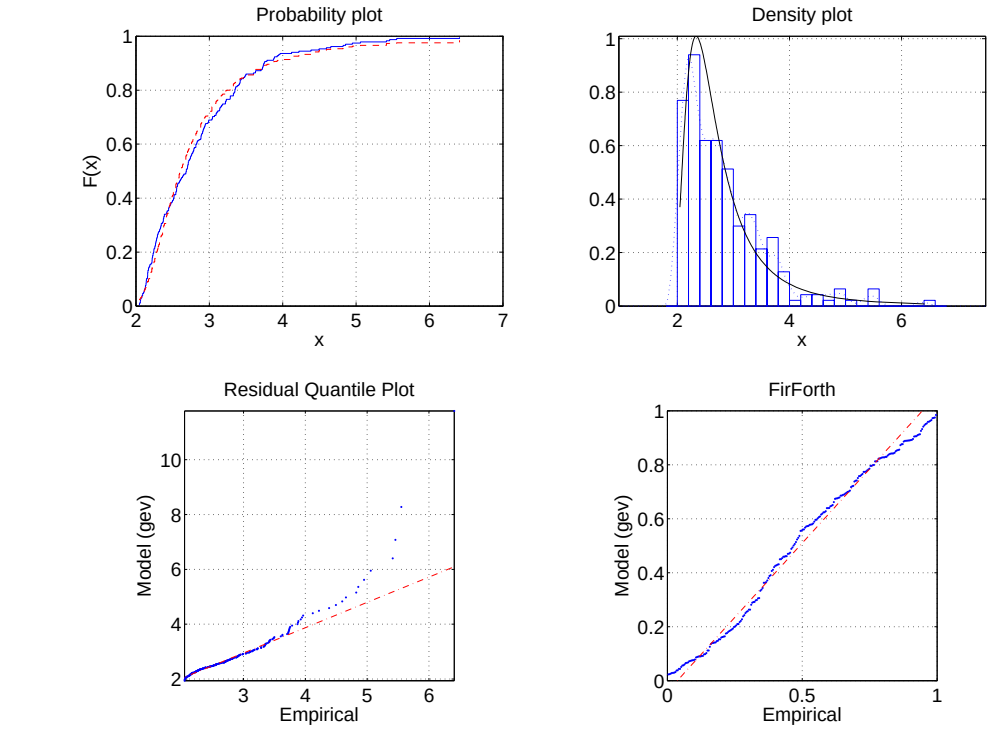

Figure C.19: GEV at 93^{th} percentile

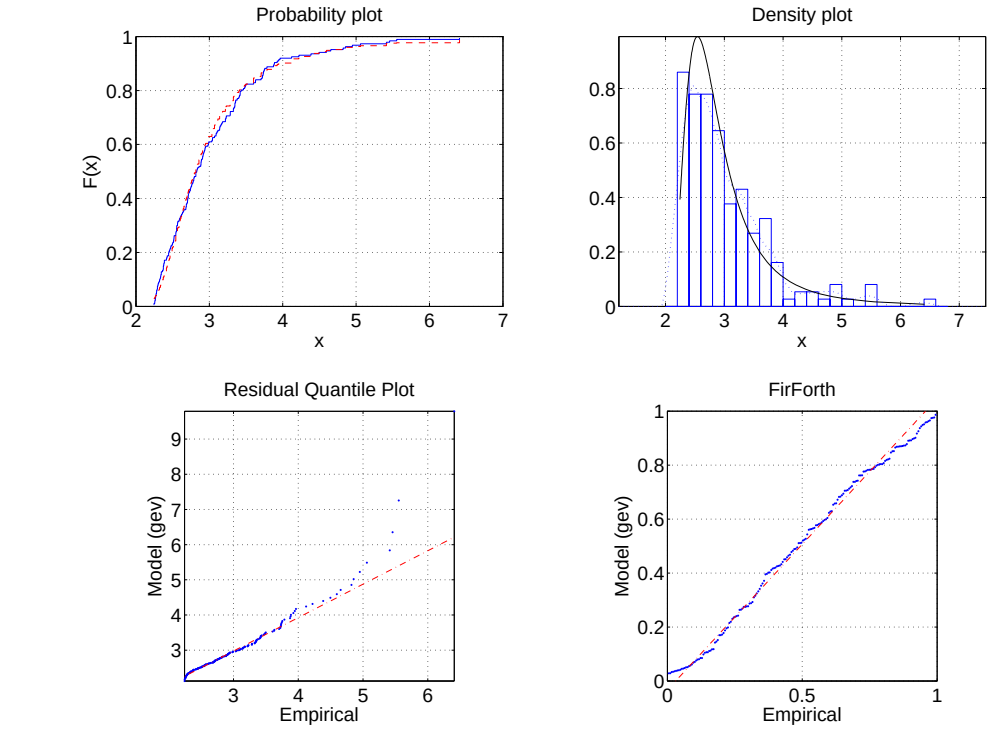

Figure C.20: GEV at 95^{th} percentile

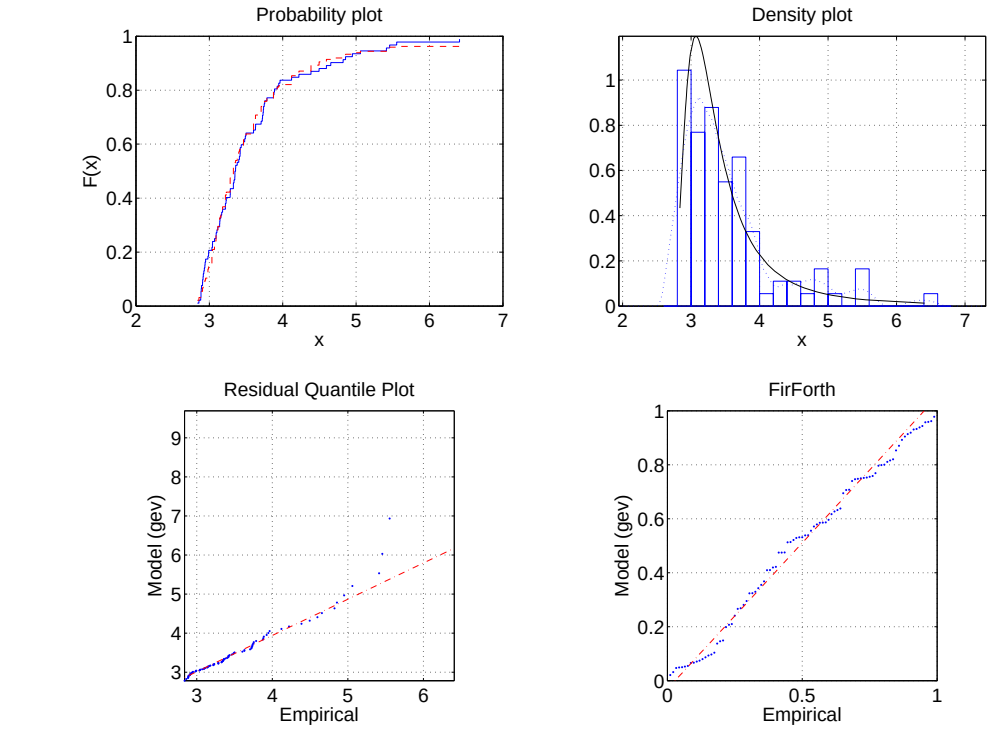

Figure C.21: GEV at 98^{th} percentile

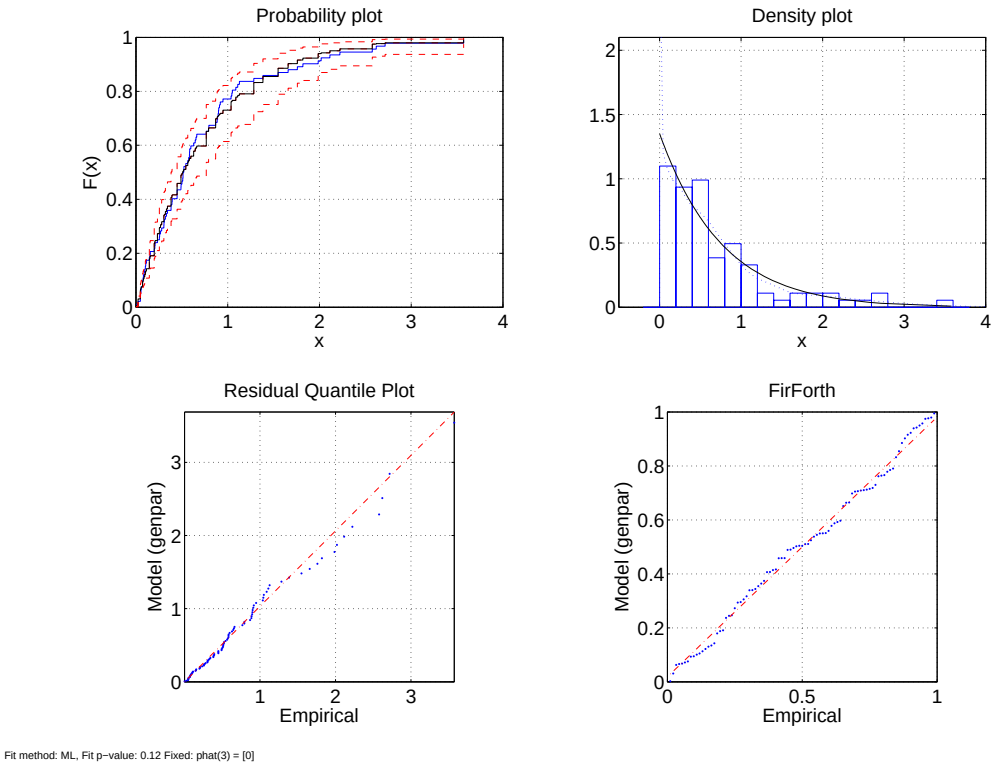

Figure C.22: GPD at 98^{th} percentile

Appendix D

Maps

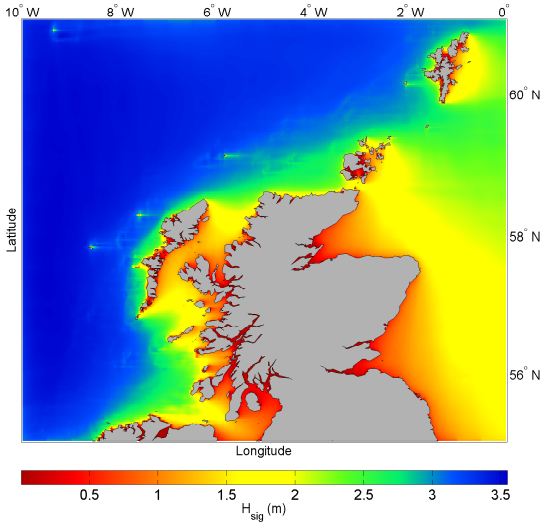

Figure D.1: Annual Average H_{sig} 2004

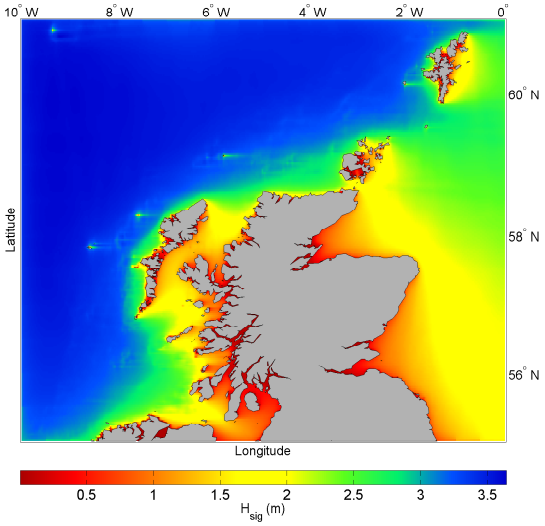

Figure D.2: Annual Average H_{sig} 2005

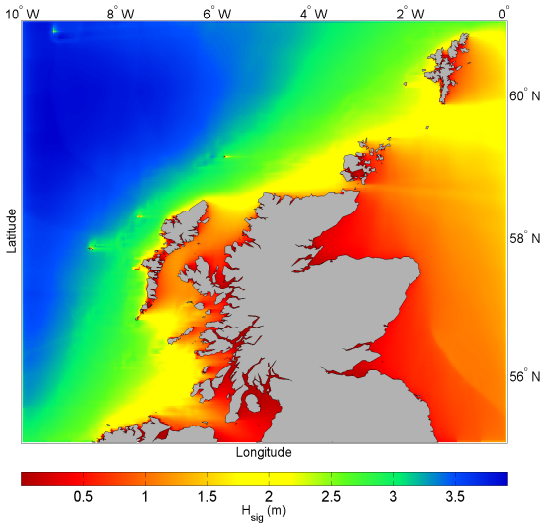

Figure D.3: Annual Average H_{sig} 2006

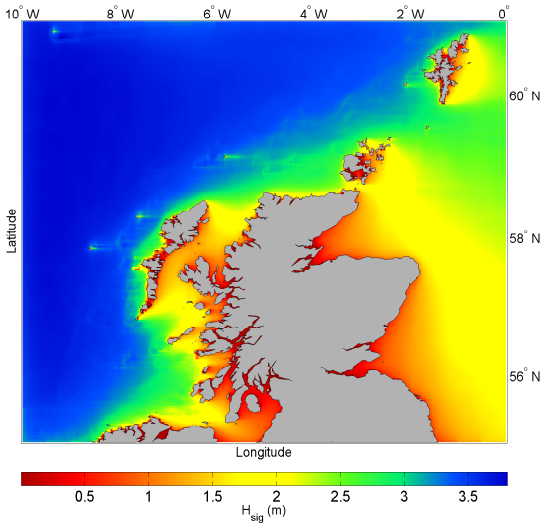

Figure D.4: Annual Average H_{sig} 2007

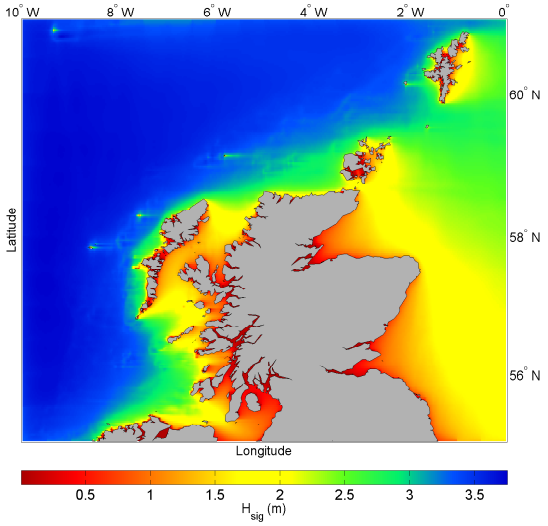

Figure D.5: Annual Average H_{sig} 2008

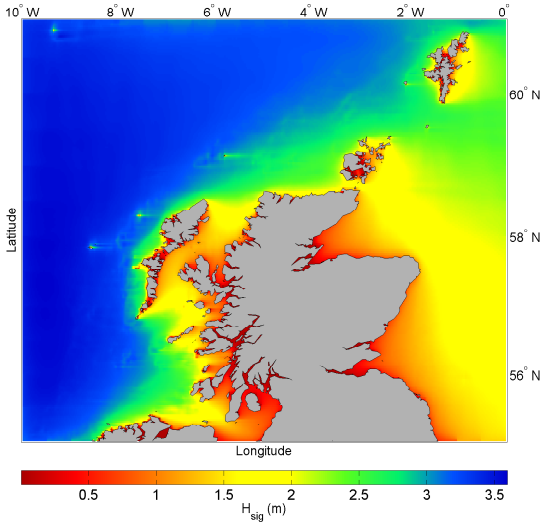

Figure D.6: Annual Average H_{sig} 2009

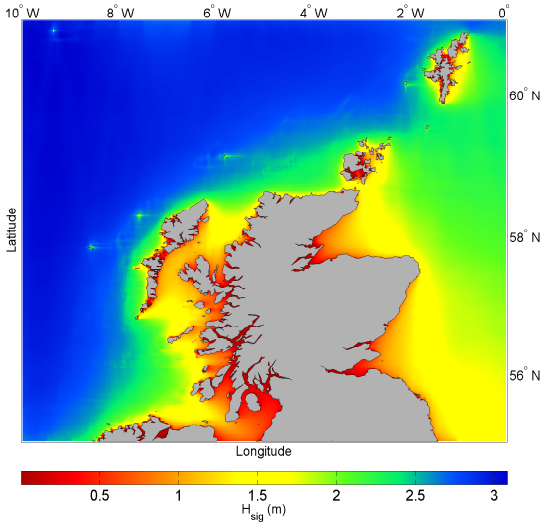

Figure D.7: Annual Average H_{sig} 2010

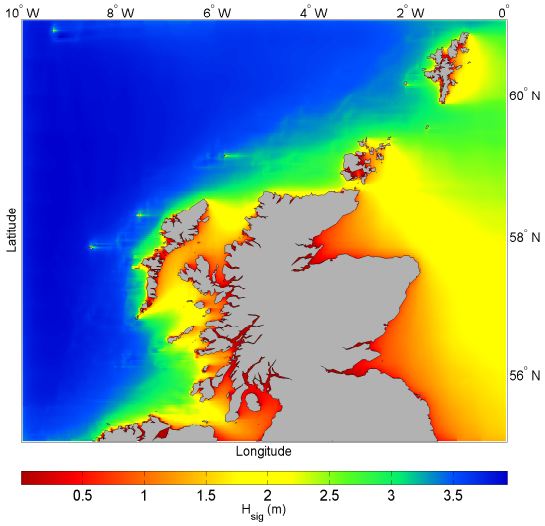

Figure D.8: Annual Average H_{sig} 2011

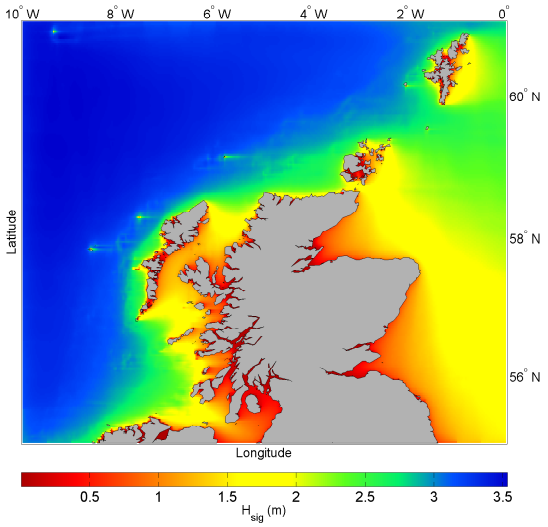

Figure D.9: Annual Average H_{sig} 2012

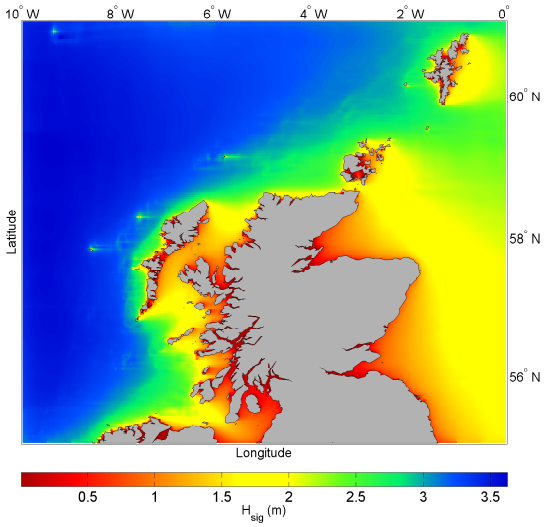

Figure D.10: Annual Average H_{sig} 2013

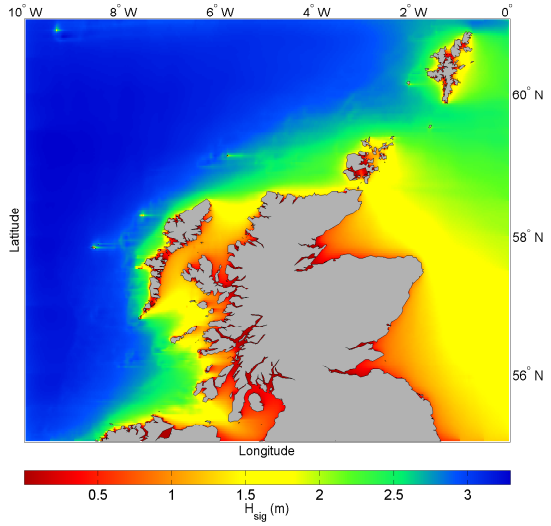

Figure D.11: Annual Average H_{sig} 2014

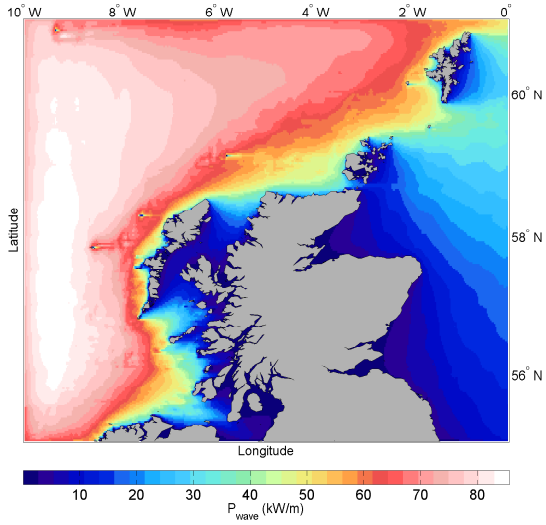

Figure D.12: Annual Average P_{wave} 2004

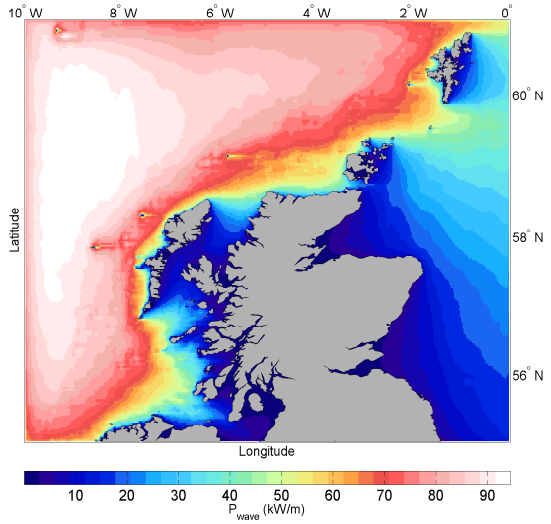

Figure D.13: Annual Average P_{wave} 2005

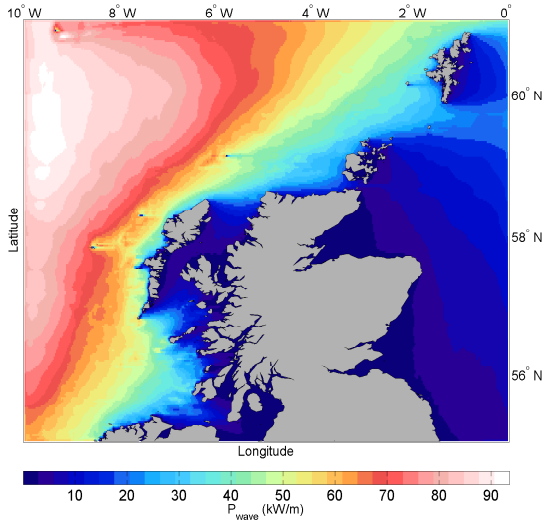

Figure D.14: Annual Average P_{wave} 2006

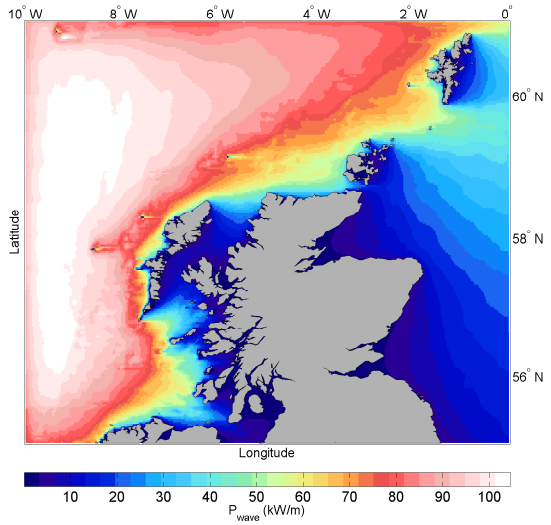

Figure D.15: Annual Average P_{wave} 2007

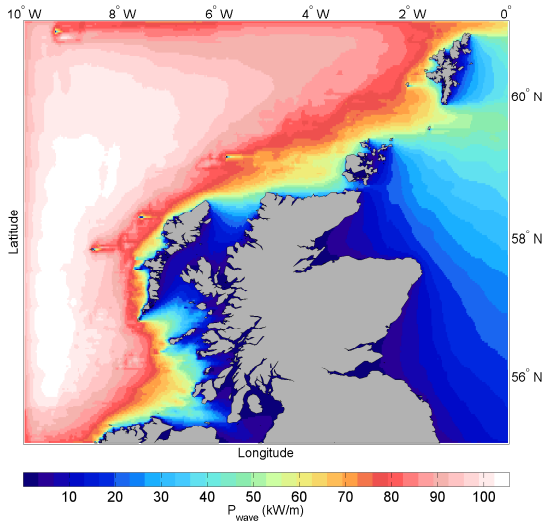

Figure D.16: Annual Average P_{wave} 2008

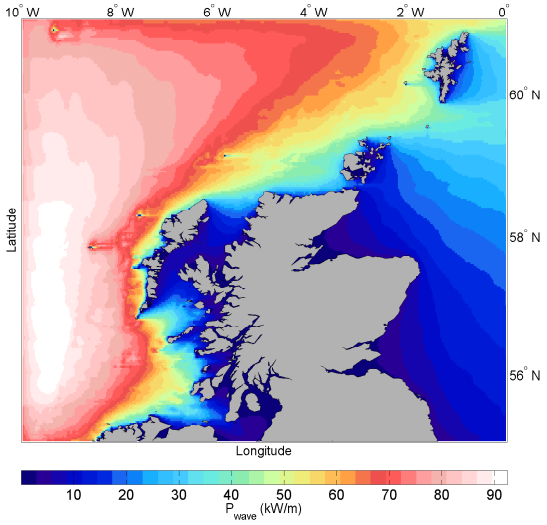

Figure D.17: Annual Average P_{wave} 2009

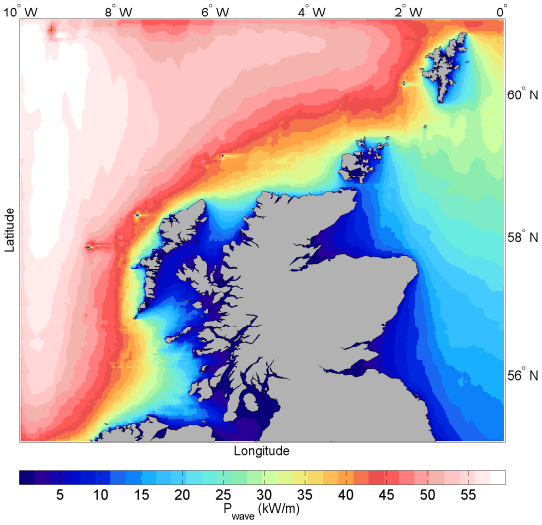

Figure D.18: Annual Average P_{wave} 2010

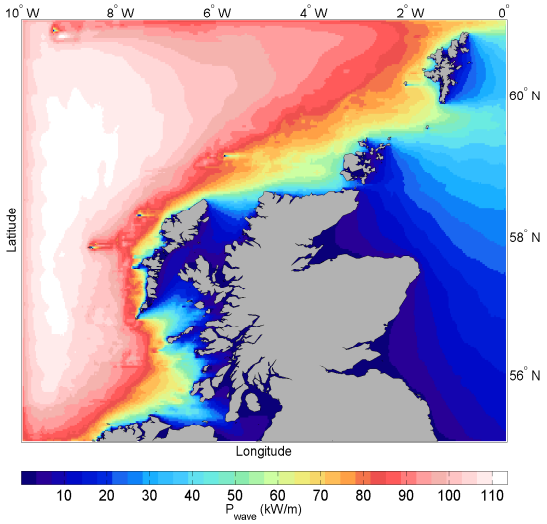

Figure D.19: Annual Average P_{wave} 2011

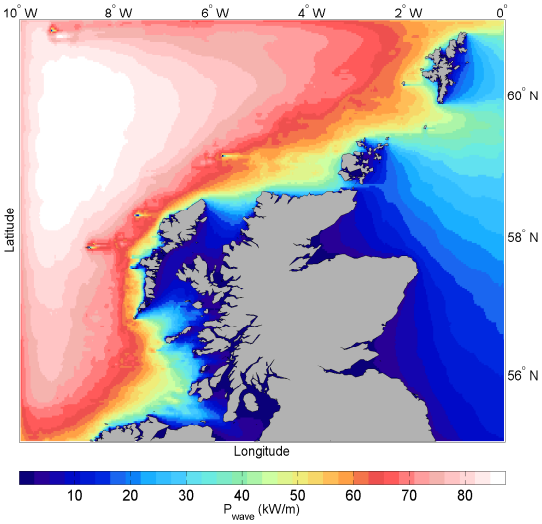

Figure D.20: Annual Average P_{wave} 2012

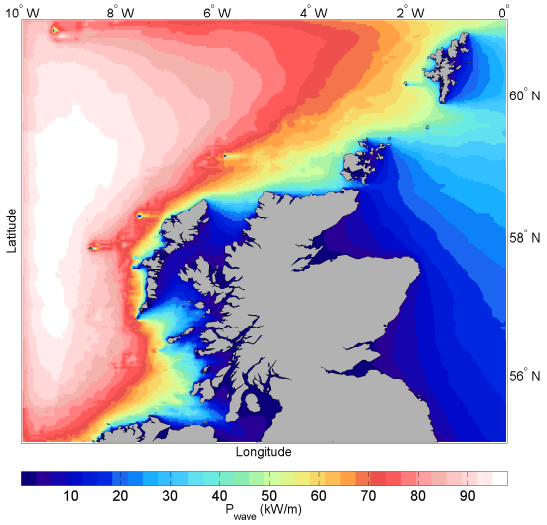

Figure D.21: Annual Average P_{wave} 2013

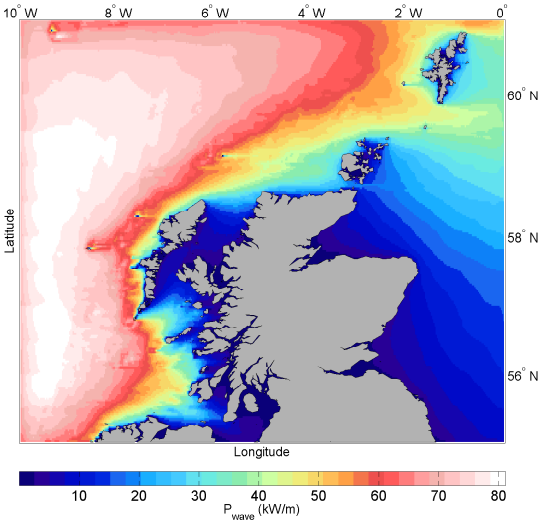

Figure D.22: Annual Average P_{wave} 2014

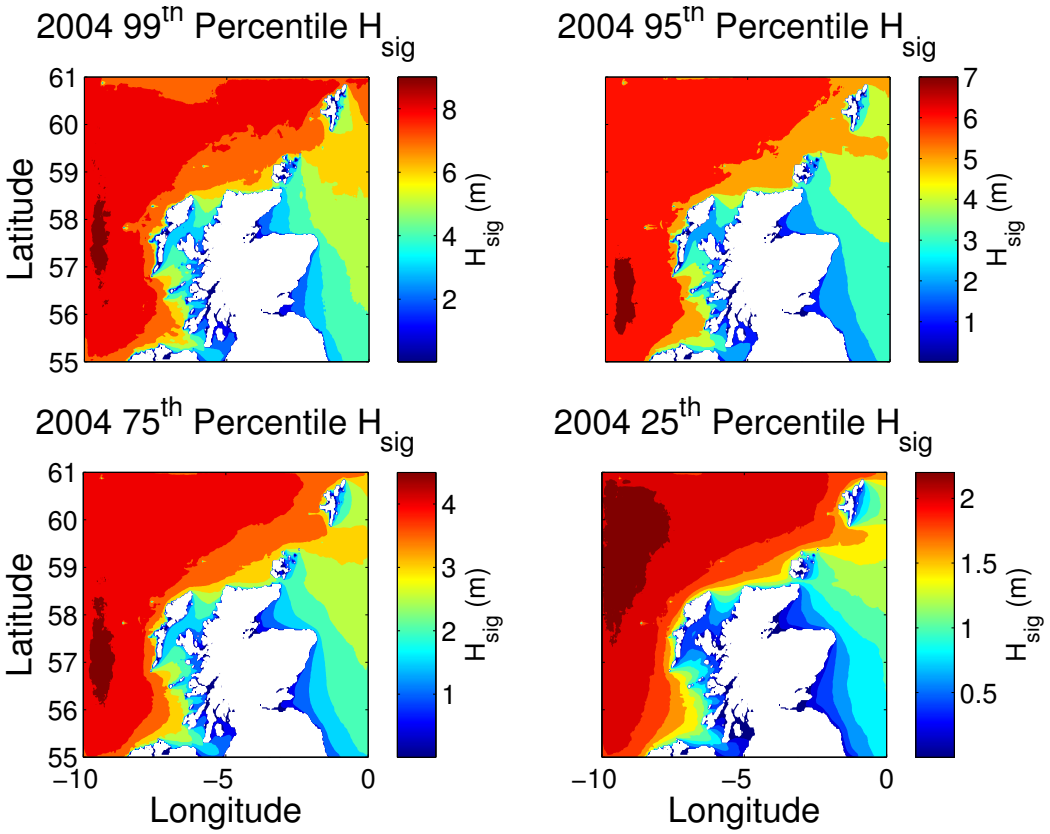

Figure D.23: Annual percentiles 2004

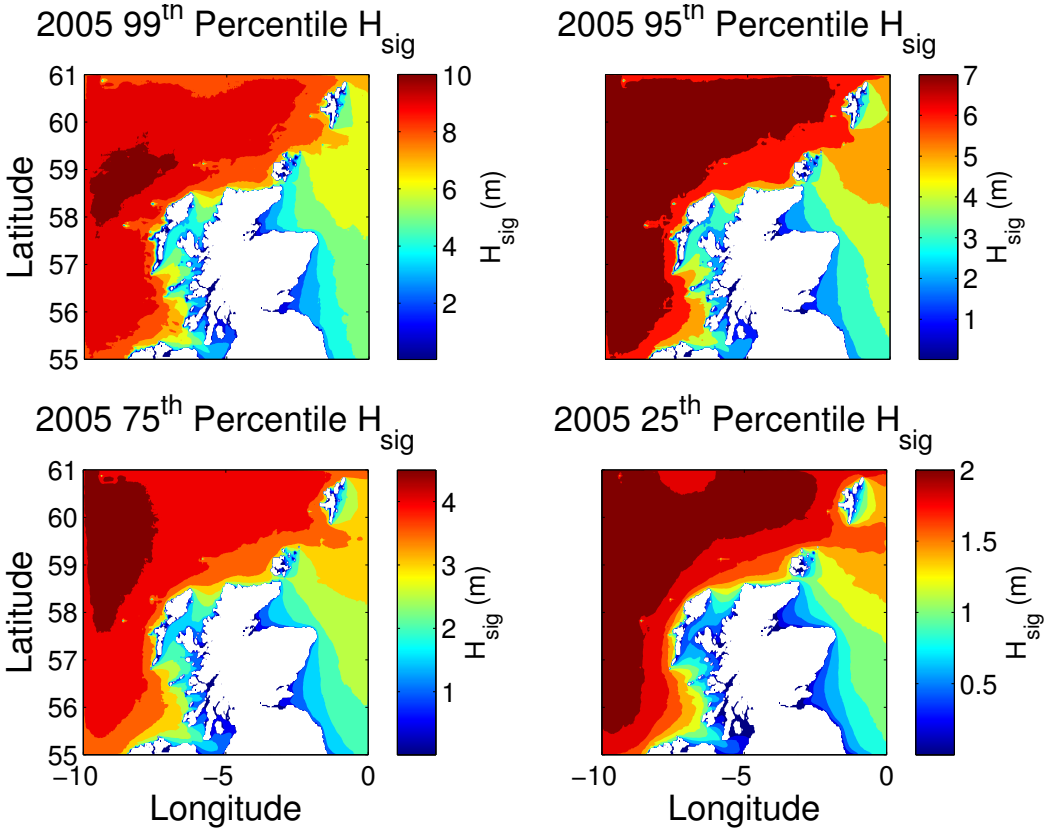

Figure D.24: Annual percentiles 2005

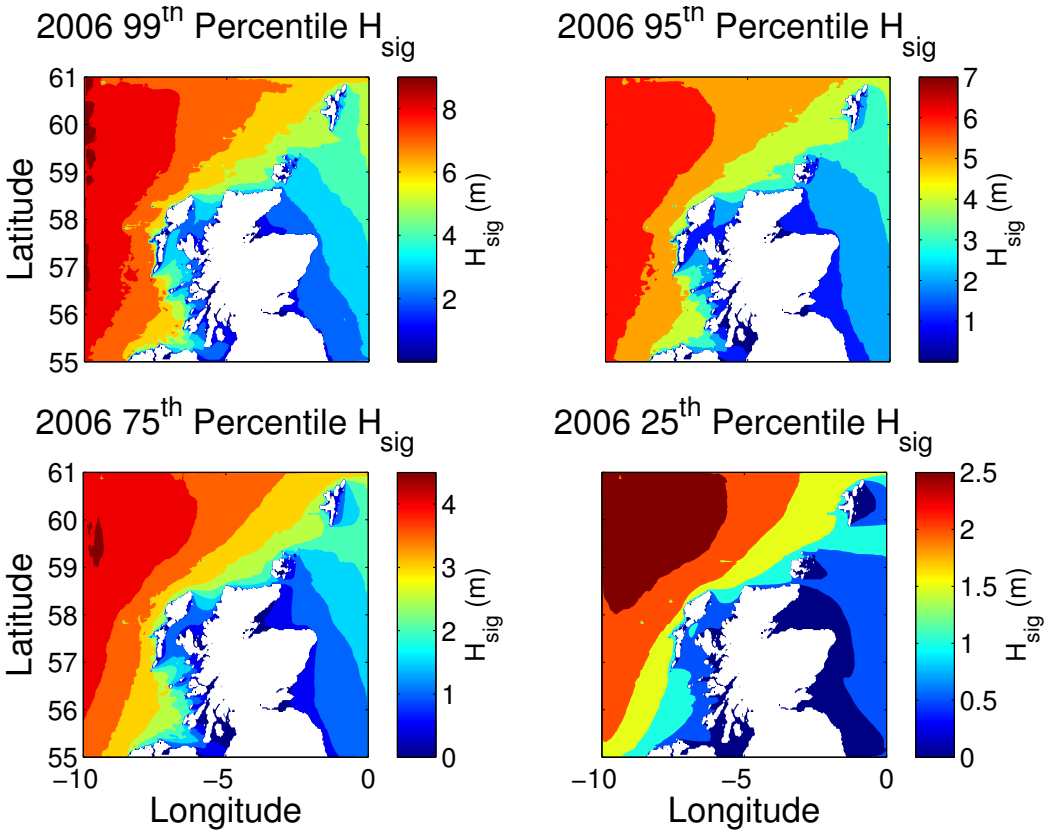

Figure D.25: Annual percentiles 2006

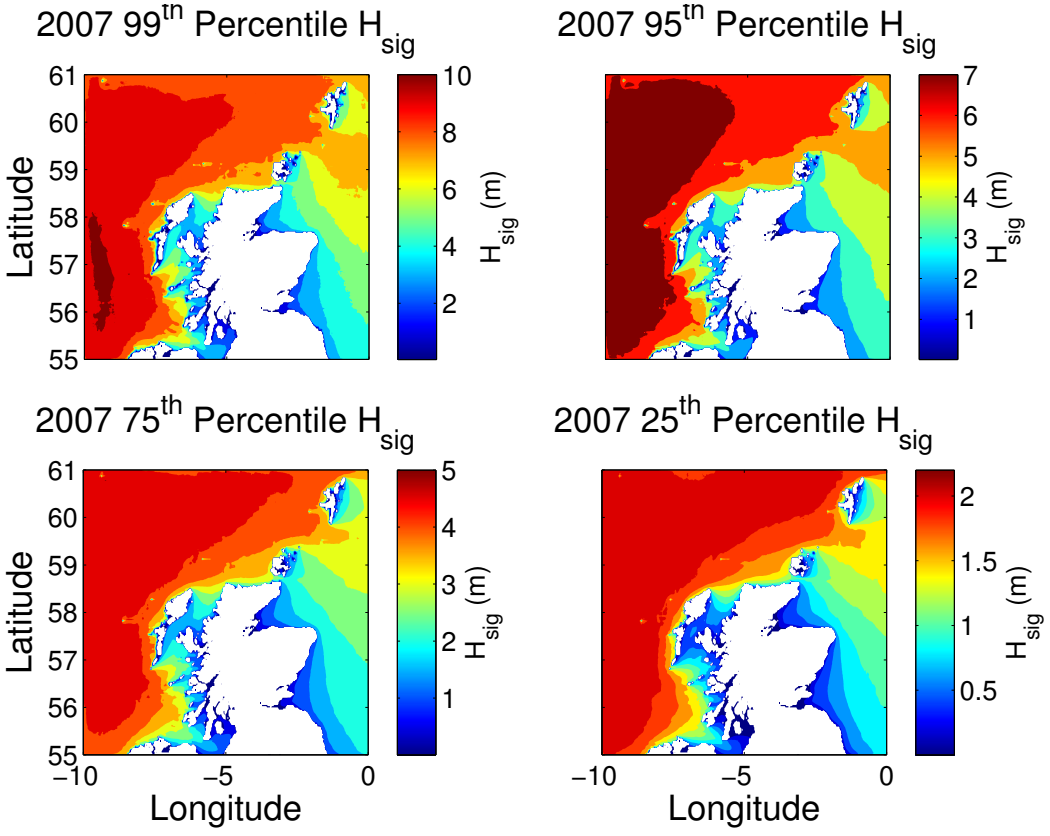

Figure D.26: Annual percentiles 2007

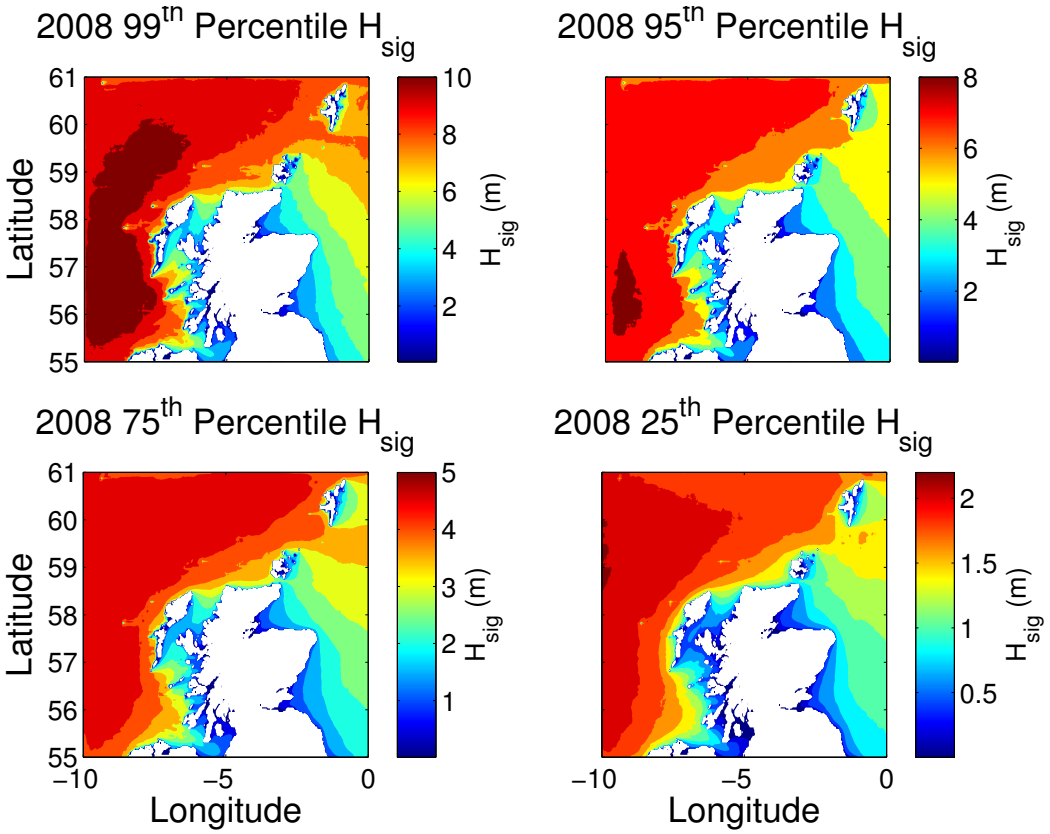

Figure D.27: Annual percentiles 2008

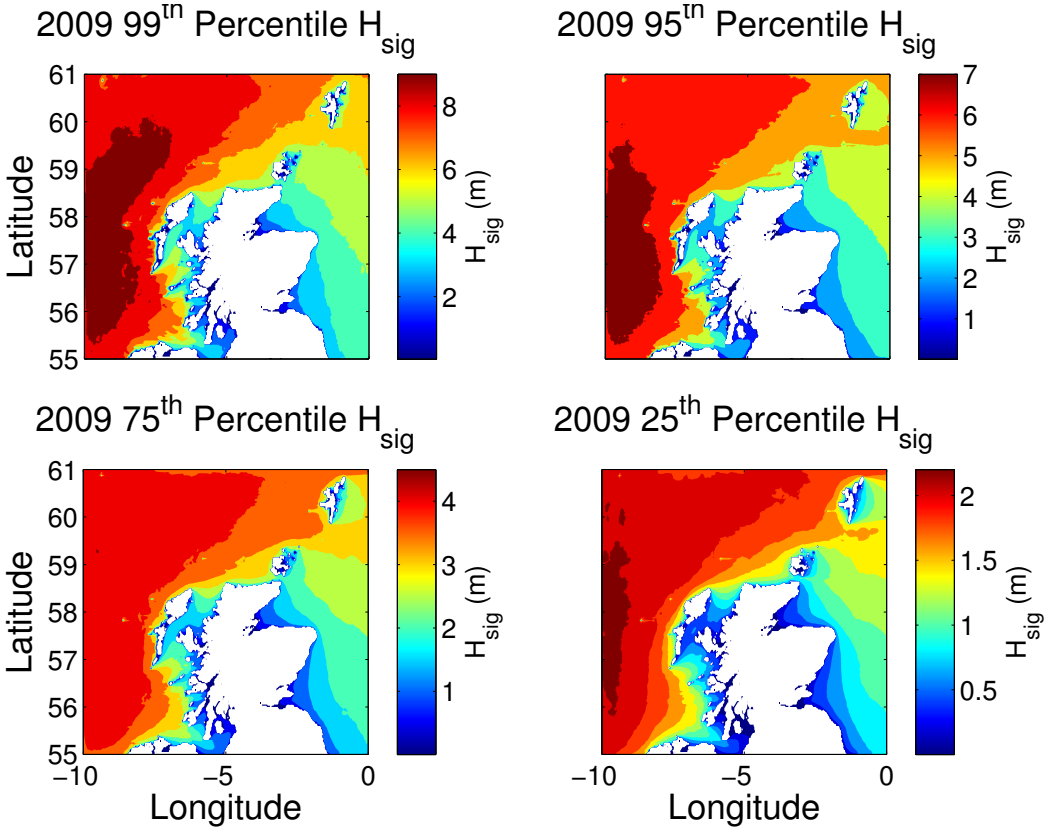

Figure D.28: Annual percentiles 2009

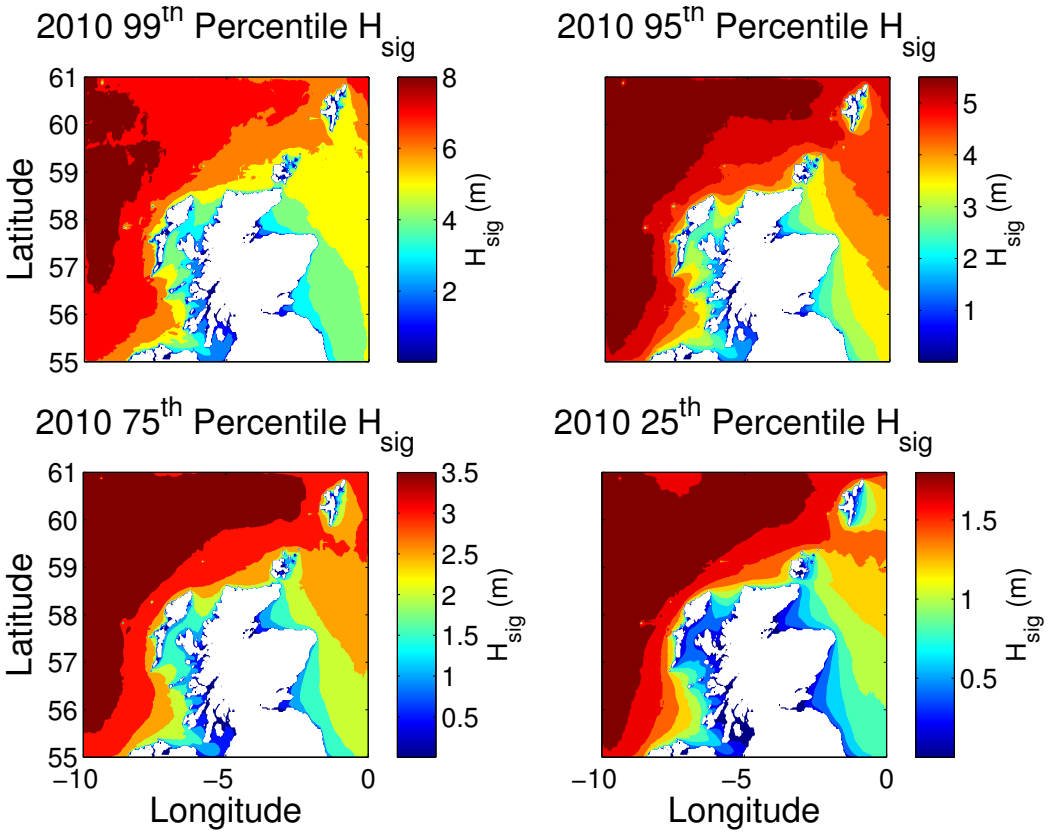

Figure D.29: Annual percentiles 2010

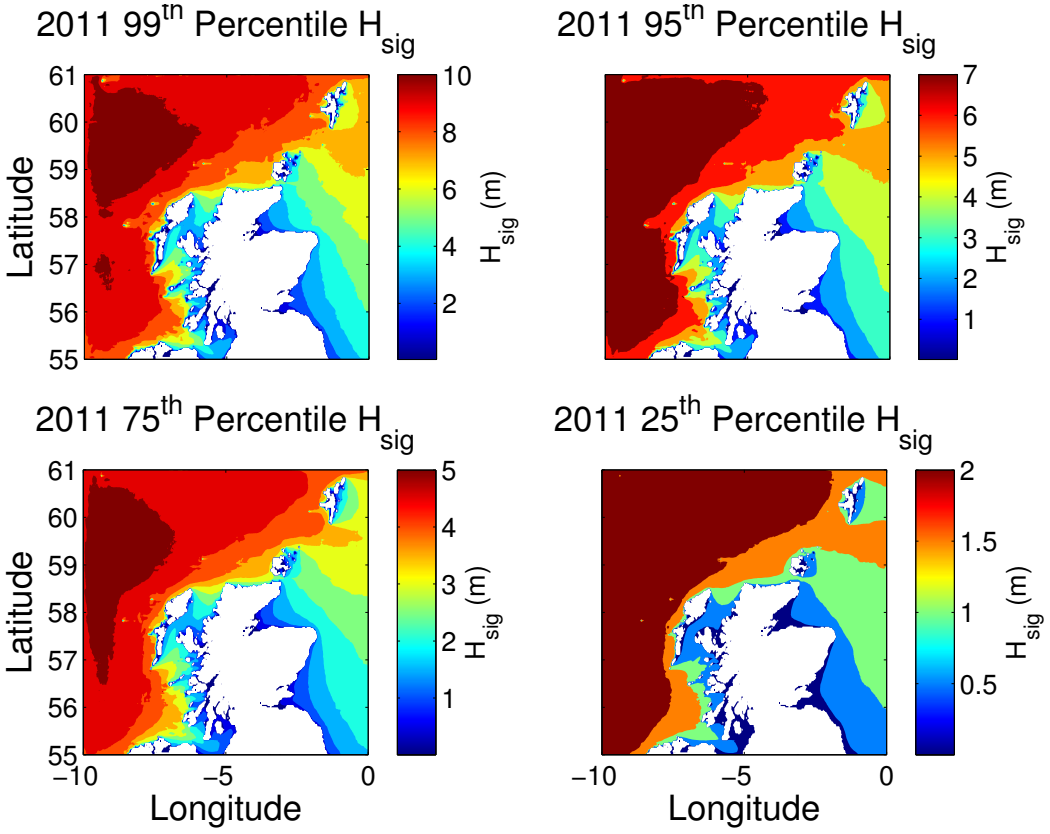

Figure D.30: Annual percentiles 2011

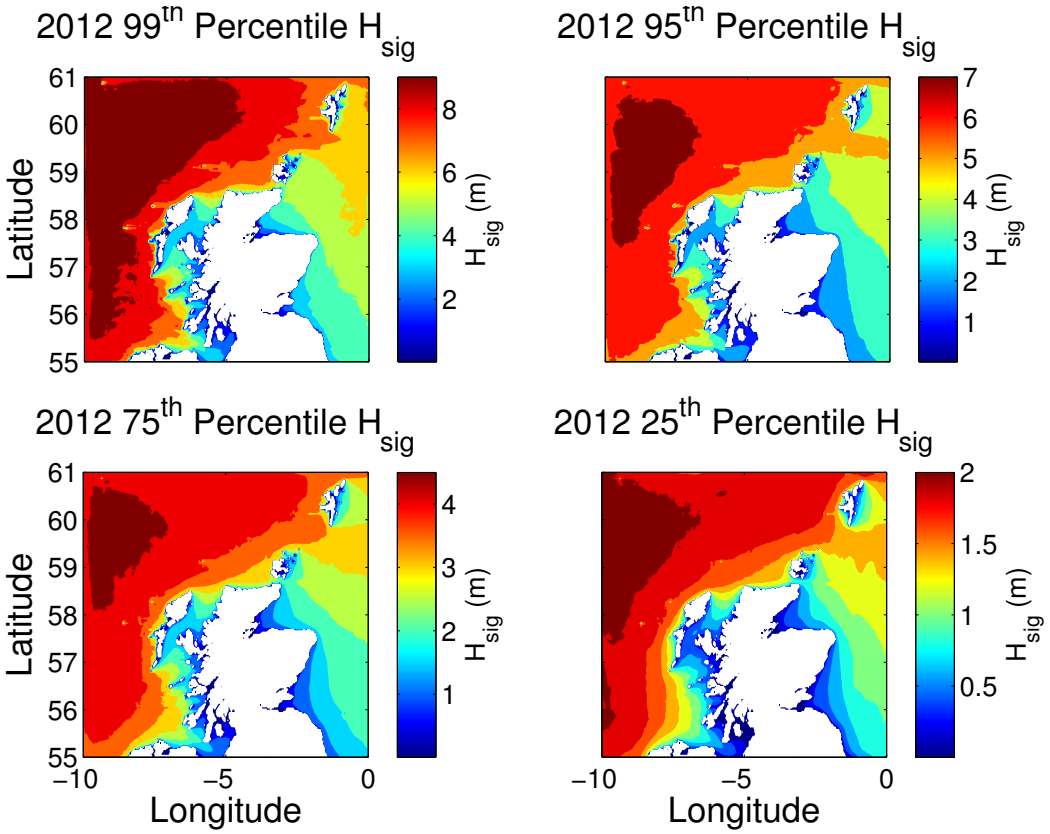

Figure D.31: Annual percentiles 2012

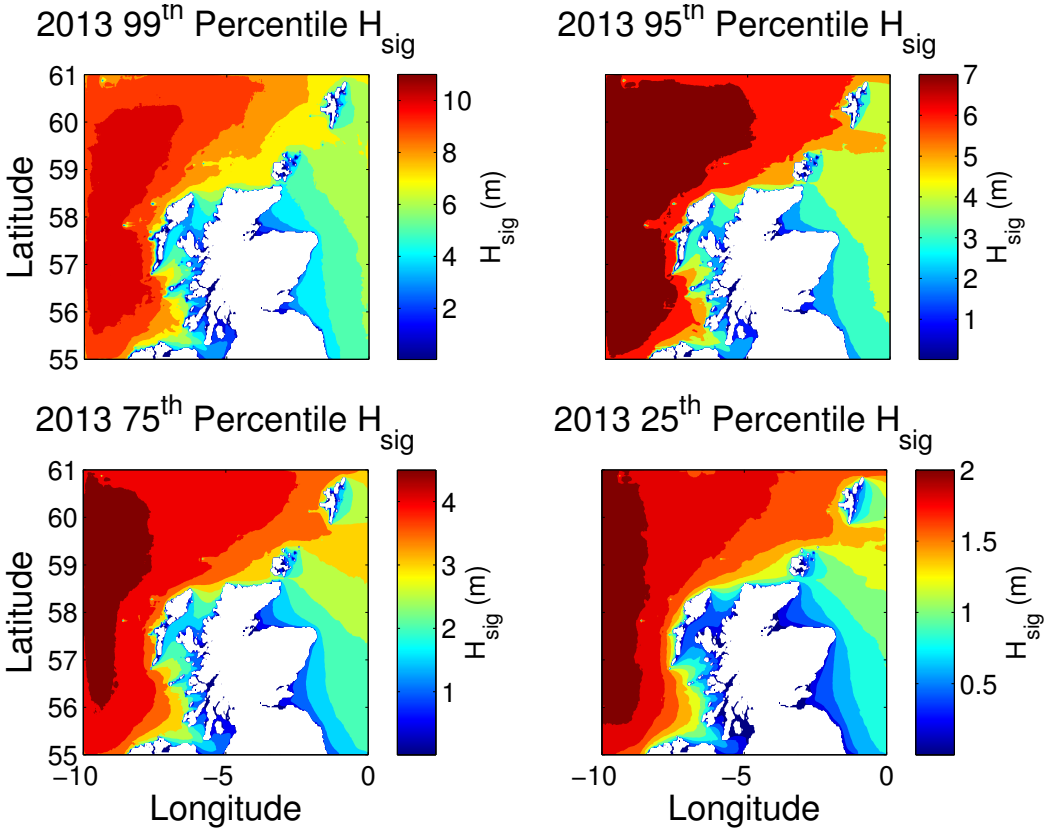

Figure D.32: Annual percentiles 2013

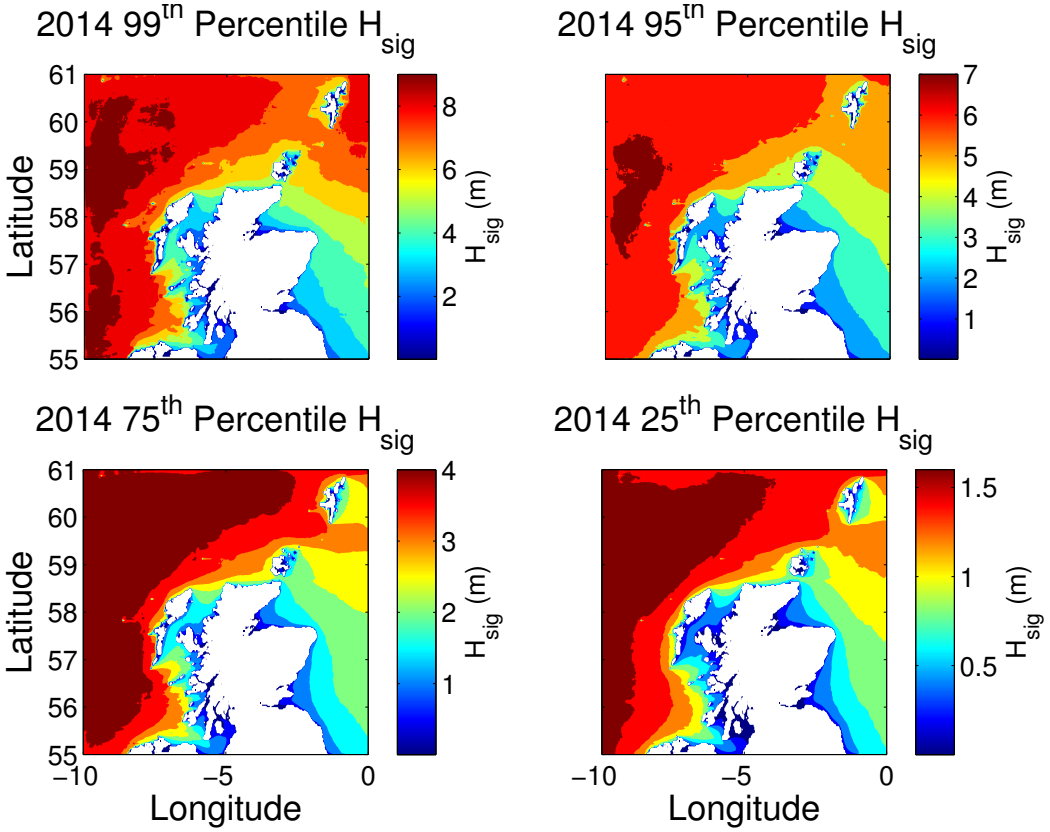

Figure D.33: Annual percentiles 2014

Bibliography

Report of the Tropical Pacific Observing System 2020 Workshop VOLUME II White Papers (TPOS 2020). Technical Report January, Scripps Institution of Oceanography, San Diego, United States, 27-30th January 2014, 2014.

Aarnes, O. J., Breivik, Ø., and Reistad, M. Wave Extremes in the Northeast Atlantic. *J. Clim.*, 25(5):1529–1543, 2012. ISSN 0894-8755. doi: 10.1175/JCLI-D-11-00132.1. URL http://journals.ametsoc.org/doi/abs/10.1175/JCLI-D-11-00132.1.

Agarwal, A. *A long-term analysis of the wave climate in the North East Atlantic and North Sea.* Ph.d thesis, University of Edinburgh, Edinburgh, 2015.

Agarwal, A., Venugopal, V., and Harrison, G. P. The assessment of extreme wave analysis methods applied to potential marine energy sites using numerical model data. *Renew. Sustain. Energy Rev.*, 27:244–257, nov 2013. ISSN 13640321. doi: 10.1016/j.rser.2013.06.049. URL http://linkinghub.elsevier.com/retrieve/pii/S1364032113004401.

Akpinar, A. and Kömürcü, M. Ä. Wave energy potential along the south-east coasts of the Black Sea. *Energy*, 42(1):289–302, jun 2012. ISSN 03605442. doi: 10.1016/j.energy.2012.03.057. URL http://linkinghub.elsevier.com/retrieve/pii/S0360544212002605.

Akpinar, A. and Kömürcü, M. Ä. Assessment of wave energy resource of the Black Sea based on 15-year numerical hindcast data. *Appl. Energy*, 101:502–512, jan 2013. ISSN 03062619. doi: 10.1016/j.apenergy.2012.06.005. URL http://linkinghub.elsevier.com/retrieve/pii/S0306261912004461.

Allan, G., Gilmartin, M., McGregor, P., and Swales, K. Levelised costs of Wave and Tidal energy in the UK: Cost competitiveness and the importance of "banded" renewables obligation certificates. *Energy Policy*, 39(1):23–39, 2011. ISSN 03014215. doi: 10.1016/j.enpol.2010.08.029. URL http://dx.doi.org/10.1016/j.enpol.2010.08.029.

Alves, J.-H. G., Banner, L. M., and Young, I. A Revisiting the Pierson-Moskowitz Asymptotic Limits for Fully Developed Wind Waves. pages 1301–1323, 2003.

Amante, C. and Eakins, B. ETOPO1 1 Arc-Minute Global Relief Model: Procedures, Data Sources and Analysis. NOAA Technical Memorandum NESDIS NGDC-24, 2014. URL http://maps.ngdc.noaa.gov/viewers/wcs-client/.

Andrés, A. D., Macgillivray, A., Guanche, R., and Jeffrey, H. Factors affecting LCOE of Ocean energy technologies : a study of technology and deployment attractiveness. In *5th Int. Conf. Ocean Energy, Halifax Factors*, pages 1–11, 2014.

Antonini, A., Bologna, U., Archetti, R., Bozzi, S., Milano, P., and Passoni, G. OMAE2014-23445 Assessment of the surge effects in a heaving point absorber in the Mediterranean Sea. In *ASME 2014 33rd Int. Conf. Ocean. Offshore Arct. Eng. OMAE2014, June 8-13, San Fr. California, USA*, pages 1–8, 2014.

Aquamarine. Aquamarine Power, 2015. URL http://www.aquamarinepower.com/.

Ardhuin, F., Herbers, T. H. C., Watts, K. P., van Vledder, G. P., Jensen, R., and Graber, H. C. Swell and Slanting-Fetch Effects on Wind Wave Growth. *J. Phys. Oceanogr.*, 37(4):908–931, apr 2007. ISSN 0022-3670. doi: 10.1175/JPO3039.1. URL http://journals.ametsoc.org/doi/abs/10.1175/JPO3039.1.

Athens, U. Wave Forecast by University of Athens, 2014. URL http://forecast.uoa.gr/wamindx.php.

Ayat, B. Wave power atlas of Eastern Mediterranean and Aegean Seas. *Energy*, 54:251–262, jun 2013. ISSN 03605442. doi: 10.1016/j.energy.2013.02.060. URL http://linkinghub.elsevier.com/retrieve/pii/S036054421300193X.

Babarit, A., Ben Ahmed, H., Clément, A., Debusschere, V., Duclos, G., Multon, B., and Robin, G. Simulation of electricity supply of an Atlantic island by offshore wind turbines and wave energy converters associated with a medium scale local energy storage. *Renew. Energy*, 31 (2):153–160, feb 2006. ISSN 09601481. doi: 10.1016/j.renene.2005.08.014. URL http://linkinghub.elsevier.com/retrieve/pii/S0960148105002223.

Babarit, a., Hals, J., Muliawan, M., Kurniawan, A., Moan, T., and Krokstad, J. Numerical benchmarking study of a selection of wave energy converters. *Renew. Energy*, 41:44–63, may 2012. ISSN 09601481. doi: 10.1016/j.renene.2011.10.002. URL http://linkinghub.elsevier.com/retrieve/pii/S0960148111005672.

Balmaseda, M., Kumar, A., Andersson, E., Takaya, Y., Anderson, D., Janssen, P., Martin, M., and Fujii, Y. White Paper 4-Operational Forecasting Systems. Technical Report November, Report of the Tropical Pacific Observing System 2020 Workshop VOLUME II âĂŞ White Papers (TPOS 2020), 2013.

Battjes, J. a. Long-term wave height distributions at seven stations around the British Isles. *Dtsch. Hydrogr. Zeitschrift*, 25:179–189, 1972. ISSN 00120308. doi: 10.1007/BF02312702.

Battjes, J. a. and Groenendijk, H. W. Wave height distributions on shallow foreshores. *Coast. Eng.*, 40(3):161–182, 2000. ISSN 03783839. doi: 10.1016/S0378-3839(00)00007-7.

Berr. Atlas of UK marine renewable energy. *Dep. Bus. Enterp. Regul. Reform*, (March):1–26, 2008.

Bertotti, L. and Cavaleri, L. Wind and wave predictions in the Adriatic Sea. *J. Mar. Syst.*, 78: S227–S234, nov 2009. ISSN 09247963. doi: 10.1016/j.jmarsys.2009.01.018. URL http://linkinghub.elsevier.com/retrieve/pii/S0924796309001511.

Bertotti, L. and Cavaleri, L. Modelling waves at Orkney coastal locations. *J. Mar. Syst.*, 96-97:116–121, aug 2012. ISSN 09247963. doi: 10.1016/j.jmarsys.2012.02.012. URL http://linkinghub.elsevier.com/retrieve/pii/S092479631200067X.

Bidlot, J.-R., Janssen, P., and Abdalla, S. Extreme waves in the ECMWF operational wave forecasting system. In *9th Int. Work. wave hindcasting Forecast.*, 2006.

Bilgili, A., Smith, K. W., and Lynch, D. R. BatTri: A two-dimensional bathymetry-based unstructured triangular grid generator for finite element circulation modeling. *Comput. Geosci.*, 32(5):632–642, jun 2006. ISSN 00983004. doi: 10.1016/j.cageo.2005.09.007. URL http://linkinghub.elsevier.com/retrieve/pii/S0098300405001950.

Blanco, G., Waniek, D., Olsina, F., Garcés, F., and Rehtanz, C. Flexible investment decisions in the European interconnected transmission system. *Electr. Power Syst. Res.*, 81(4):984–994, apr 2011. ISSN 03787796. doi: 10.1016/j.epsr.2010.12.001. URL http://linkinghub.elsevier.com/retrieve/pii/S0378779610003056.

Bolaños-Sanchez, R., Sanchez-Arcilla, a., and Cateura, J. Evaluation of two atmospheric models for windâĂŞwave modelling in the NW Mediterranean. *J. Mar. Syst.*, 65(1-4): 336–353, mar 2007. ISSN 09247963. doi: 10.1016/j.jmarsys.2005.09.014. URL http://linkinghub.elsevier.com/retrieve/pii/S0924796306003009.

Booij, N., Ris, R. C., and Holthuijsen, L. H. A third-generation wave model for coastal regions: 1. Model description and validation. *J. Geophys. Res.*, 104(C4):7649, 1999. ISSN 0148-0227. doi: 10.1029/98JC02622. URL http://doi.wiley.com/10.1029/98JC02622.

Bottema, M. and van Vledder, G. Effective fetch and non-linear four-wave interactions during wave growth in slanting fetch conditions. *Coast. Eng.*, 55(3):261–275, mar 2008. ISSN 03783839. doi: 10.1016/j.coastaleng.2007.11.001. URL http://linkinghub.elsevier.com/retrieve/pii/S0378383907001263.

Bozzi, S., Milano, P., and Passoni, G. MEDITERRANEAN SEA : COMPARISON AMONG DIFFERENT TECHNOLOGIES. In *ASME 2011 30th Int. Conf. Ocean. Offshore Arct. Eng. Vol. 5 Ocean Sp. Util. Ocean Renew. Energy Rotterdam, Netherlands, June 19âĂŞ24, 2011*, pages 1–6, 2011a. doi: 978-0-7918-4437-3.

Bozzi, S., Milano, P., and Passoni, G. Omae2011-49372 Feasibility Study of Wave Energy Farm in the Western Mediterranean Sea : Comparison Among Different Technologies. In *Proc. ASME 2011 30th Int. Conf. Ocean. Arct. Eng. OMAE2011*, pages 1–6, 2011b. doi: 978-0-7918-4437-3.

British Oceanographic Data Centre. BODC British Oceanographic Data Centre. URL http://www.bodc.ac.uk/.

Brodtkorb, P., Johannesson, P., Lindgren, G., Rychlik, I., Ryden, J., and Sja, E. WAFO - a Matlab toolbox for analysis of random waves and loads. In *10th Int.Offshore Polar Eng. Conf.*, pages 343–350, Seattle,USA, 2010.

Caires, S. and Gent, M. V. Wave height distribution in constant and finite depths. *Coast. Eng. Proc.*, 2012.

Caires, S., Sterl, A., Bidlot, J.-R., Graham, N., and Swail, V. Intercomparison of Different Wind-Wave Reanalyses. *J. Clim.*, 17(10):1893–1913, 2004.

Caires, S., Groeneweg, J., and Sterl, A. Past and Futures Changes in the North Sea Extreme Waves. *ICCE*, 19(2006):7666, 2008.

Caires, S. and Sterl, A. A new nonparametric method to correct model data: Application to significant wave height from the ERA-40 re-analysis. *J. Atmos. Ocean. Technol.*, 22(4): 443–459, 2005. ISSN 07390572. doi: 10.1175/JTECH1707.1.

Cañellas, B., Orfila, A., Méndez, F., Menéndez, M., and Tintoré, J. Application of a POT model to estimate the extreme significant wave height levels around the Balearic Sea (Western Mediterranean). *J. Coast. Res. Spec. Issue*, 50(50):329–333, 2007. ISSN 07490208. URL http://costabalearsostenible.com/PDFs/ICS2007{_}final3{_}.pdf.

Carballo, R. and Iglesias, G. A methodology to determine the power performance of wave energy converters at a particular coastal location. *Energy Convers. Manag.*, 61:8–18, 2012. ISSN 01968904. doi: 10.1016/j.enconman.2012.03.008. URL http://dx.doi.org/10.1016/j.enconman.2012.03.008.

Carbon Trust and AMEC. Carbon Trust Foreword to UK Wave Resource Study . Technical Report October, 2012.

Carter, D. J. T. *Estimating extreme wave heights in the NE Atlantic from Geosat data.* HSE-Health & Safety Executive, 1993. ISBN 0 11 882139 3.

Cavaleri, L. and Holthuijsen, L. H. Wave modelling in the WISE group. In *5th Int. Work. Wave hindcast Forecast*, number i, pages 498–508, 1998.

Cavaleri, L., Alves, J.-H., Ardhuin, F., Babanin, A., Banner, M., Belibassakis, K., Benoit, M., Donelan, M., Groeneweg, J., Herbers, T., Hwang, P., Janssen, P., Janssen, T., Lavrenov, I., Magne, R., Monbaliu, J., Onorato, M., Polnikov, V., Resio, D., Rogers, W., Sheremet, A., McKee Smith, J., Tolman, H., van Vledder, G., Wolf, J., and Young, I. Wave modelling âĂŞ The state of the art. *Prog. Oceanogr.*, 75(4):603–674, dec 2007. ISSN 00796611. doi: 10.1016/j.pocean.2007.05.005. URL http://linkinghub.elsevier.com/retrieve/pii/S0079661107001206.

Cavaleri, L. Wave Modeling-Missing the Peaks. *J. Phys. Oceanogr.*, 39(11):2757–2778, nov 2009. ISSN 0022-3670. doi: 10.1175/2009JPO4067.1. URL http://journals.ametsoc.org/doi/abs/10.1175/2009JPO4067.1.

Cavaleri, L. and Bertotti, L. The improvement of modelled wind and wave fields with increasing resolution. *Ocean Eng.*, 33(5-6):553–565, apr 2006. ISSN 00298018. doi: 10.1016/j.oceaneng.2005.07.004. URL http://linkinghub.elsevier.com/retrieve/pii/S0029801805001782.

Cavaleri, L. and Sclavo, M. A wind and wave atlas for the Mediterranean Sea. *Eur. Sp. Agency, (Special Publ. ESA SP*, (614):0–5, 2006a. ISSN 03796566.

Cavaleri, L. and Sclavo, M. The calibration of wind and wave model data in the Mediterranean Sea. *Coast. Eng.*, 53(7):613–627, 2006b. ISSN 03783839. doi: 10.1016/j.coastaleng.2005.12.006.

CEFAS, Center for Environment, F. &. A. S. CEFAS, 2014. URL http://www.cefas.defra.gov.uk/home.aspx.

Cherneva, Z., Andreeva, N., Pilar, P., Valchev, N., Petrova, P., and Guedes Soares, C. Validation of the WAMC4 wave model for the Black Sea. *Coast. Eng.*, 55(11):881–893, nov 2008. ISSN 03783839. doi: 10.1016/j.coastaleng.2008.02.028. URL http://linkinghub.elsevier.com/retrieve/pii/S0378383908000471.

Coles, S. *An Introduction to Statistical modelling of extreme values*. Springer Series in Statistics, 2001. ISBN 1852334592.

Connolly, D., Lund, H., Mathiesen, B., Pican, E., and Leahy, M. The technical and economic implications of integrating fluctuating renewable energy using energy storage. *Renew. Energy*, 43:47–60, jul 2012. ISSN 09601481. doi: 10.1016/j.renene.2011.11.003. URL http://linkinghub.elsevier.com/retrieve/pii/S0960148111006057.

Cornett, A. M. A Global Wave Energy Resource Assessment. *Proc. Eighteenth Int. Offshore Polar Eng. Conf. Vancouver,BC,Canada July 6-11*, 8:318–326, 2008.

Cradden, L. and Sarantis, S. Site Assessment. *Deliv. D2.1, Mar. Platf.*, pages 1–28, 2010.

Cradden, L., Mouslim, H., Duperray, O., and Ingram, D. Joint Exploitation of Wave and Offshore Wind Power. *Energy*, 2012.

CrownEstates. The Crown Estates-Energy and Infrastructure, 2014. URL http://www.thecrownestate.co.uk/energy-infrastructure/.

Cruz, J. *Ocean Wave Energy: Current Status and Future Perspectives*. 2008. ISBN 978-3-540-74894-6.

Dalton, G. J., Alcorn, R., and Lewis, T. Case study feasibility analysis of the Pelamis wave energy convertor in Ireland, Portugal and North America. *Renew. Energy*, 35(2):443–455, 2010. ISSN 09601481. doi: 10.1016/j.renene.2009.07.003. URL http://dx.doi.org/10.1016/j.renene.2009.07.003.

de Andres, A., Guanche, R., Vidal, C., and Losada, I. Adaptability of a generic wave energy converter to different climate conditions. *Renew. Energy*, 78:322–333, 2015. ISSN 09601481. doi: 10.1016/j.renene.2015.01.020. URL http://linkinghub.elsevier.com/retrieve/pii/S0960148115000270.

De Decker, J. and Woyte, A. Review of the various proposals for the European offshore grid. *Renew. Energy*, 49:58–62, jan 2013. ISSN 09601481. doi: 10.1016/j.renene.2012.01.066. URL http://linkinghub.elsevier.com/retrieve/pii/S0960148112000778.

Dean, R. G. and Dalrymple, R. A. *Water Wave Mechanics of engineers and scientists*. Prentice-Hall Inc, advanced s edition, 1984. ISBN 9810204205.

Delft, T. SWAN User Manual Cycle III version 41.01, 2014a.

Delft, T. *SWAN scientific documentation Cycle III version 41.01*. Delft University of Technology Faculty of Civil Engineering and Geosciences Environmental Fluid Mechanics Section, 2014b.

Delft University of Technology, H. E. SWAN, 2014. URL http://www.swan.tudelft.nl/.

Delucchi, M. a. and Jacobson, M. Z. Providing all global energy with wind, water, and solar power, Part II: Reliability, system and transmission costs, and policies. *Energy Policy*, 39 (3):1170–1190, mar 2011. ISSN 03014215. doi: 10.1016/j.enpol.2010.11.045. URL http://linkinghub.elsevier.com/retrieve/pii/S0301421510008694.

DHI. MIKE21, 2014. URL http://www.mikebydhi.com/products/mike-21.

Dietrich, J., Zijlema, M., Westerink, J., Holthuijsen, L., Dawson, C., Luettich, R., Jensen, R., Smith, J., Stelling, G., and Stone, G. Modeling hurricane waves and storm surge using integrally-coupled, scalable computations. *Coast. Eng.*, 58(1):45–65, jan 2011. ISSN 03783839. doi: 10.1016/j.coastaleng.2010.08.001. URL http://linkinghub.elsevier.com/retrieve/pii/S0378383910001250.

Dietrich, J., Zijlema, M., Allier, P.-E., Holthuijsen, L., Booij, N., Meixner, J., Proft, J., Dawson, C., Bender, C., Naimaster, A., Smith, J., and Westerink, J. Limiters for spectral propagation velocities in SWAN. *Ocean Model.*, nov 2012. ISSN 14635003. doi: 10.1016/j.ocemod.2012.11.005. URL http://linkinghub.elsevier.com/retrieve/pii/S1463500312001655.

Dodet, G., Bertin, X., and Taborda, R. Wave climate variability in the North-East Atlantic Ocean over the last six decades. *Ocean Model.*, 31(3-4):120–131, 2010. ISSN 14635003. doi: 10.1016/j.ocemod.2009.10.010. URL http://dx.doi.org/10.1016/j.ocemod.2009.10.010.

DTI. Quantifying the system cost of additional renewables in 2020. Technical report, 2002.

Dunnett, D. and Wallace, J. S. Electricity generation from wave power in Canada. *Renew. Energy*, 34:179–195, 2009. ISSN 09601481. doi: 10.1016/j.renene.2008.04.034.

Durrant, T. H., Greenslade, D. J., and Simmonds, I. The effect of statistical wind corrections on global wave forecasts. *Ocean Model.*, (November), nov 2013. ISSN 14635003. doi: 10.1016/j.ocemod.2012.10.006. URL http://linkinghub.elsevier.com/retrieve/pii/S1463500312001515.

ECMWF. ERA Interim, 2014. URL http://www.ecmwf.int/.

EMEC. Assessment of Wave Energy Resource. *Renew. Energy*, pages 1–36, 2009. URL www.emec.org.uk/standards/assessment-of-wave-energy-resource/.

EMEC. European Marine Energy Centre, 2013. URL http://www.emec.org.uk/.

Energy Information Administation Agency U.S. Annual Energy Outlook 2014, 2014. URL http://www.eia.gov/forecasts/aeo/electricity{_}generation.cfm.

European Climate Foundation. Roadmap 2050. Technical Report April, 2010. URL http://www.roadmap2050.eu/.

Falcão, A. F. D. O. Wave energy utilization: A review of the technologies. *Renew. Sustain. Energy Rev.*, 14(3):899–918, apr 2010. ISSN 13640321. doi: 10.1016/j.rser.2009.11.003. URL http://linkinghub.elsevier.com/retrieve/pii/S1364032109002652.

Ferreira, J. A. and Soares, C. G. Modelling bivariate distributions of significant wave height and mean wave period. *Appl. Ocean Res.*, 24(24):6–8, 2002.

Fusco, F., Nolan, G., and Ringwood, J. V. Variability reduction through optimal combination of wind/wave resources-An Irish case study. *Energy*, 35(1):314–325, jan 2010. ISSN 03605442. doi: 10.1016/j.energy.2009.09.023. URL http://linkinghub.elsevier.com/retrieve/pii/S0360544209004095.

Galanis, G., Chu, P. C., Kallos, G., Kuo, Y.-H., and Dodson, C. T. J. Wave height characteristics in the north Atlantic ocean: a new approach based on statistical and geometrical techniques. *Stoch. Environ. Res. Risk Assess.*, 26:83–103, 2012. ISSN 1436-3240. doi: 10.1007/s00477-011-0540-2.

Garrad, A. The lessons learned from the development of the wind energy industry that might be applied to marine industry renewables. *Philos. Trans. A. Math. Phys. Eng. Sci.*, 370 (1959):451–71, jan 2012. ISSN 1364-503X. doi: 10.1098/rsta.2011.0167. URL http://www.ncbi.nlm.nih.gov/pubmed/22184671.

Giannoulis, E. and Haralambopoulos, D. Distributed Generation in an isolated grid: Methodology of case study for Lesvos -Greece. *Appl. Energy*, 88(7):2530–2540, jul 2011. ISSN 03062619. doi: 10.1016/j.apenergy.2011.01.046. URL http://linkinghub.elsevier.com/retrieve/pii/S030626191100064X.

Gleizon, P. Modelling wave energy in archipelagos-case of northern scotland. In *EIMR2014-968*, number May, pages 1–4, 2014.

Goda, Y. *Random seas and desing of maritime structures*. World Scientific Co.Pte.Ltd., 2nd editio edition, 2000. ISBN 981-02-3256-X.

Greenwood, C. E., Venugopal, V., Christie, D., Morrison, J., and Vogler, A. OMAE2013-11356 Wave modelling for potential wave energy sites around the outer Hebrides. In *ASME 2013 32nd Int. Conf. Ocean. Offshore Arct. Eng. OMAE2013, June 9-14, Nantes,France*, pages 1–9, 2013.

Gulev, S. K. and Hasse, L. Changes of wind waves in the North Atlantic over the last 30 years. *Int. J. Climatol.*, 19:1091–1117, 1999. ISSN 08998418. doi: 10.1002/(SICI)1097-0088(199908)19:10<1091::AID-JOC403>3.0.CO;2-U.

Gunn, K. and Stock-Williams, C. Quantifying the global wave power resource. *Renew. Energy*, 44:296–304, 2012. ISSN 09601481. doi: 10.1016/j.renene.2012.01.101. URL http://dx.doi.org/10.1016/j.renene.2012.01.101.

Hagerman, G. Southern New England Wave Energy Resource Potential. In *Build. Energy*, number March, 2001.

Hansen, R. H. and Kramer, M. M. Modelling and Control of the Wavestar Prototype. *Proc. 9th Eur. Wave Tidal Energy Conf.*, pages 1–10, 2011.

Harrison, G. P. and Wallace, a. R. Climate sensitivity of marine energy. *Renew. Energy*, 30(12):1801–1817, oct 2005. ISSN 09601481. doi: 10.1016/j.renene.2004.12.006. URL http://linkinghub.elsevier.com/retrieve/pii/S0960148105000170.

Hasselmann, K. On the non-linear energy transfer in a gravity-wave spectrum Part 1.General theory. *J. Fluid Mech.*, 12(1960), 1961.

Hasselmann, K. On the non-linear energy transfer i n a gravity wave spectrum Part 2.Conservation;wave particle analogy;irreversibility. *J. Fluid Mech.*, 15:273–281, 1962a.

Hasselmann, K. On the non-linear energy transfer in a gravity- wave spectrum Part 3. Evaluation of the energy flux and swell-sea interactin for a Neumann spectrum. *J. Fluid Mech.*, 15:385–398, 1962b.

Hasselmann, K. On the spectral dissipation of ocean waves due to whitecapping. pages 107–127, 1974.

Hasselmann, K., Barnett, T. P., Bouws, E., Carlson, H., Cartwright, D. E., Enke, K., Ewing, J. A., Gienapp, H., Hasselmann, D. E., Kruseman, P., Meerburg, A., Muller, P., Olbers, D. J., Richter, K., Sell, W., and Walden, H. *Measurements of Wind-Wave Growth and Swell Decay during the Joint North Sea Wave Project (JONSWAP)*, volume A(8). Hamburg, 1973. doi: citeulike-article-id:2710264.

Hasselmann, S., Hasselmann, K., Allender, J., and Barnett, T. Computations and Parameterizations of the Nonlinear Energy Transfer in a Gravity-Wave Specturm. Part II: Parameterizations of the Nonlinear Energy Transfer for Application in Wave Model. *Phys. Oceanogr.*, 15:1378–1391, 1985.

Hawkins, S. *A High Resolution Reanalysis of Wind Speeds over the British Isles for Wind Energy Integration.* Ph.d thesis, University of Edinburgh, 2012.

Hedegaard, K. and Meibom, P. Wind power impacts and electricity storage-A time scale perspective. *Renew. Energy*, 37(1):318–324, jan 2012. ISSN 09601481. doi: 10.1016/j.renene.2011.06.034. URL http://linkinghub.elsevier.com/retrieve/pii/S0960148111003594.

Hellenic Centre for Marine for Research, H. Monitoring, Forecasting System Oceanographic information for the Greek Seas (POSEIDON), 2014. URL http://www.poseidon.hcmr.gr/.

Hervás Soriano, F. and Mulatero, F. EU Research and Innovation (R&I) in renewable energies: The role of the Strategic Energy Technology Plan (SET-Plan). *Energy Policy*, 39(6):3582–3590, jun 2011. ISSN 03014215. doi: 10.1016/j.enpol.2011.03.059. URL http://linkinghub.elsevier.com/retrieve/pii/S0301421511002485.

Holick, M. *Introduction to Probability and Statistics for Engineers.* Springer-Verlag Berlin Heidelberg, 2013. ISBN 9783642382994. doi: 10.1007/978-3-642-38300-7.

Holthuijsen, L. *Waves in oceanic and coastal waters*. Cambridge University Press, 2007. ISBN 9780521129954. URL http://www.cambridge.org/gb/academic/subjects/earth-and-environmental-science/oceanography-and-marine-science/waves-oceanic-and-coastal-waters?format=PB.

IEA. International Energy Agency, 2015. URL http://www.iea.org/.

Ingram, D., Smith, G., Bittencourt-Ferreira, C., and Smith, H. *EquiMar: Protocols for the Equitable Assessment of Marine Energy Converters*. Number 213380. 2011a. ISBN 9780950892016. doi: 978-0-9508920-3-0.

Ingram, D., Smith, G. H., Ferriera, C., and Smith, H. Protocols for the Equitable Assessment of Marine Energy Converters. Technical report, Institute of Energy Systems, University of Edinburgh, School of Engineering, 2011b.

Janssen, P. *The Interaction of Ocean Waves and Wind*. Cambridge University Press, Cambridge, 2009. ISBN 9780511525018. doi: 10.1017/CBO9780511525018. URL http://ebooks.cambridge.org/ref/id/CBO9780511525018.

Janssen, P. A. Wave - induced Stress and drag of air flow over sea waves.pdf. *J. Phys. Oceanogr.*, 19(6):745–754, 1988.

Janssen, P. A. Quasi-Linear theory of Wind-Wave Generation applied to wave forecasting. *J. Phys. Oceanogr.*, 6:1631–1642, 1991.

Janssen, P. A. Progress in ocean wave forecasting. *J. Comput. Phys.*, 227(7):3572–3594, mar 2008. ISSN 00219991. doi: 10.1016/j.jcp.2007.04.029. URL http://linkinghub.elsevier.com/retrieve/pii/S0021999107001659.

Jin, K.-R. and Ji, Z.-G. Calibration and verification of a spectral windâĂŞwave model for Lake Okeechobee. *Ocean Eng.*, 28(5):571–584, may 2001. ISSN 00298018. doi: 10.1016/S0029-8018(00)00009-3. URL http://linkinghub.elsevier.com/retrieve/pii/S0029801800000093.

Kaldellis, J. *Stand-alone and hybrid wind energy systems: technology, energy storage and applications*. Woodhead Ltd., woodhead p edition, 2010.

Kaldellis, J. *Stand-alone and hybrid wind energy systems.Technology, energy storage and applications*. Woodhead Publishing Limited, Great Abington, Cambridge CB21 6AH, UK, 2011. ISBN 9781845695804.

Karathanasi, F., Soukissian, T., and Sifnioti, D. Offshore wave potential of the Mediterranean Sea. In *Int. Conf. Renew. Energies Power Qual. (ICREPQ 2015),La Coruna*, number 13, Spain, 25-27 March, 2015.

Kinsman, B. *Wind Waves their generation and propagation on the Ocean Surface*. Prentice-Hall, Englewood Cliffs, N.J, dover edit edition, 1965. ISBN 0-486-64652-1.

Komen, G., Hasselmann, S., and Hasselmann, K. On the Existence of a Fully Developed Wind-Sea Spectrum.pdf. *Phys. Oceanogr.*, 14:1271–1285, 1984.

Komen, G., Cavaleri, L., Donelan, M., Hasselmann, S., and Janssen, P. *Dynamics and Modelling of Ocean waves*. Cambridge University Press, 1994. ISBN 0-521-47047-1. URL www.cambridge.org/9780521470476.

Korres, G., Papadopoulos, A., Katsafados, P., Ballas, D., Perivoliotis, L., and Nittis, K. A 2-year intercomparison of the WAM-Cycle4 and the WAVEWATCH-III wave models implemented within the Mediterranean Sea. *Sci. Mediterr. Mar.*, 2011.

Krozer, Y. Cost and benefit of renewable energy in the European Union. *Renew. Energy*, 50:68–73, feb 2013. ISSN 09601481. doi: 10.1016/j.renene.2012.06.014. URL http://linkinghub.elsevier.com/retrieve/pii/S0960148112003643.

Larsén, X. G., Kalogeri, C., Galanis, G., and Kallos, G. A statistical methodology for the estimation of extreme wave conditions for offshore renewable applications. *Renew. Energy*, 80, 2014. ISSN 09601481. doi: 10.1016/j.renene.2015.01.069.

Lavidas, G., Venugopal, V., and Friedrich, D. On Investigating Wind -Wave Resource To Enhance Predictability In Offshore Wave Energy Deployments. In *Int. Conf. Offshore Renew. Energy 2014 ASRANET 15th-17th Sept. Glas. 2014*, Glasgow, 2014a.

Lavidas, G., Venugopal, V., and Friedrich, D. Investigating the opportunities for wave energy in the Aegean Sea. In *7th Int. Sci. Conf. Energy Clim. Chang. 8-10 Oct. 2014 Athens*, Athens, 2014b. PROMITHEAS The Energy and Climate Change Policy Network.

Lavidas, G., Venugopal, V., Friedrich, D., and Agarwal, A. Wave energy assessment and wind correlation for the North region of Scotland, hindcast resource and calibration, investigating for improvements of physical model for adaptation to temporal correlation. In *ASME 2014 33rd Int. Conf. Ocean. Offshore Arct. Eng. Vol. 9B Ocean Renew. Energy*, volume Conference, pages 1–11, San Francisco, California, USA, June 8âĂŞ13, 2014, 2014c. ASME. doi: 978-0-7918-4554-7. URL http://proceedings.asmedigitalcollection.asme.org/proceeding.aspx?articleid=1912194{&}resultClick=3.

Liang, B., Fan, F., Liu, F., Gao, S., and Zuo, H. 22-Year wave energy hindcast for the China East Adjacent Seas. *Renew. Energy*, 71:200–207, nov 2014. ISSN 09601481. doi: 10.1016/j.renene.2014.05.027. URL http://linkinghub.elsevier.com/retrieve/pii/S096014811400278X.

Liberti, L., Carillo, A., and Sannino, G. Wave energy resource assessment in the Mediterranean, the Italian perspective. *Renew. Energy*, 50:938–949, feb 2013. ISSN 09601481. doi: 10.1016/j.renene.2012.08.023. URL http://linkinghub.elsevier.com/retrieve/pii/S0960148112004934.

Lin, W., Sanford, L. P., and Suttles, S. E. Wave measurement and modeling in Chesapeake Bay. *Cont. Shelf Res.*, 22(February 2001):2673–2686, 2002.

Longuet-Higgins, M. S. On the distribution of the heights of sea waves: Some effects of nonlinearity and finite band width. *J. Geophys. Res.*, 85(2):1519, 1980. ISSN 0148-0227. doi: 10.1029/JC085iC03p01519.

Lund, H. Large-scale integration of optimal combinations of PV, wind and wave power into the electricity supply. *Renew. Energy*, 31(4):503–515, apr 2006. ISSN 09601481. doi: 10.1016/j.renene.2005.04.008. URL http://linkinghub.elsevier.com/retrieve/pii/S0960148105000893.

Mackay, E. B., Bahaj, A. S., and Challenor, P. G. Uncertainty in wave energy resource assessment. Part 1: Historic data. *Renew. Energy*, 35(8):1792–1808, 2010a. ISSN 09601481. doi: 10.1016/j.renene.2009.10.026. URL http://dx.doi.org/10.1016/j.renene.2009.10.026.

Mackay, E. B., Bahaj, A. S., and Challenor, P. G. Uncertainty in wave energy resource assessment. Part 2: Variability and predictability. *Renew. Energy*, 35(8):1809–1819, 2010b. ISSN 09601481. doi: 10.1016/j.renene.2009.10.027. URL http://dx.doi.org/10.1016/j.renene.2009.10.027.

Manwell, J., McGowan, J., and Rogers, A. *Wind Energy Explained: Theory, Design and Application*. John Wiley & Sons Ltd., 2nd edition, 2009.

Mathiesen, B. V., Lund, H., and Karlsson, K. 100% Renewable energy systems, climate mitigation and economic growth. *Appl. Energy*, 88(2):488–501, feb 2011. ISSN 03062619. doi: 10.1016/j.apenergy.2010.03.001. URL http://linkinghub.elsevier.com/retrieve/pii/S0306261910000644.

Mathiesen, M., Goda, Y., Hawkes, P. J., Mansard, E., Martín, M. J., Peltier, E., Thompson, E. F., and Van Vledder, G. Recommended practice for extreme wave analysis. *J. Hydraul. Res.*, 32(6):803–814, 1994. ISSN 0022-1686. doi: 10.1080/00221689409498691.

Mazarakis, N., Kotroni, V., Lagouvardos, K., and Bertotti, L. High-resolution wave model validation over the Greek maritime areas. *Nat. Hazards Earth Syst. Sci.*, 12(11):3433–3440, nov 2012. ISSN 1684-9981. doi: 10.5194/nhess-12-3433-2012. URL http://www.nat-hazards-earth-syst-sci.net/12/3433/2012/.

Medatlas Group. Wind and Wave Atlas of the Mediterranean Sea. Technical Report April, Western European Union, 2004.

Melo, A. and J.Huckerby. Annual Report 2012, Implementing Agreement on Ocean Energy Systems (OES-IA). *Ocean Energy Syst.*, 2012.

Mentaschi, L., Besio, G., Cassola, F., and Mazzino, A. Performance evaluation of Wavewatch III in the Mediterranean Sea. *Ocean Model.*, 2015. ISSN 14635003. doi: 10.1016/j.ocemod.2015.04.003. URL http://linkinghub.elsevier.com/retrieve/pii/S1463500315000578.

Michalena, E. and Hills, J. M. Renewable energy issues and implementation of European energy policy: The missing generation? *Energy Policy*, 45:201–216, jun 2012. ISSN 03014215. doi: 10.1016/j.enpol.2012.02.021. URL http://linkinghub.elsevier.com/retrieve/pii/S0301421512001383.

Miles, J. W. On the generation of surface waves by shear flows. *J. Fluid Mech.*, pages 185–204, mar 1957. ISSN 0022-1120. doi: 10.1017/S0022112057000567. URL http://www.journals.cambridge.org/abstract{_}S0022112057000567.

NCAR. NCAR/CISL Research data archive, 2014. URL https://rda.ucar.edu/index.html?hash=data{_}user{&}action=showsignedin.

Neill, S. P. and Hashemi, M. R. Wave power variability over the northwest European shelf seas. *Appl. Energy*, 106:31–46, jun 2013. ISSN 03062619. doi: 10.1016/j.apenergy.2013.01.026. URL http://linkinghub.elsevier.com/retrieve/pii/S0306261913000354.

Nobre, A., Pacheco, M., Jorge, R., Lopes, M., and Gato, L. Geo-spatial multi-criteria analysis for wave energy conversion system deployment. *Renew. Energy*, 34(1):97–111, jan 2009. ISSN 09601481. doi: 10.1016/j.renene.2008.03.002. URL http://linkinghub.elsevier.com/retrieve/pii/S0960148108000852.

O'Connor, M., Lewis, T., and Dalton, G. Techno-economic performance of the Pelamis P1 and Wavestar at different ratings and various locations in Europe. *Renew. Energy*, 50:889–900, 2013. ISSN 09601481. doi: 10.1016/j.renene.2012.08.009. URL http://dx.doi.org/10.1016/j.renene.2012.08.009.

OEE. Ocean Energy Europe, 2015. URL http://www.oceanenergy-europe.eu/index.php.

Pallares, E., Sánchez-Arcilla, A., and Espino, M. Wave energy balance in wave models (SWAN) for semi-enclosed domains-Application to the Catalan coast. *Cont. Shelf Res.*, 87:41–53, sep 2014. ISSN 02784343. doi: 10.1016/j.csr.2014.03.008. URL http://linkinghub.elsevier.com/retrieve/pii/S0278434314001022.

Park, S. Part VII : ECMWF Wave Model IFS DOCUMENTATION-Cy33r1 Operational implementation 3 June 2008 PART VII : ECMWF WAVE MODEL. Technical Report June, The European Centre for Medium-Range Weather Forecast (ECMWF), 2008.

Parliament, E. The European Parliament. Directive of the European Parliament and of the Council on the promotion of the use of energy from renewable sources amending and subsequently repealing directives 2001/77/ec and 2003/30/ec. Technical report, 2009.

Pepermans, G., Driesen, J., Haeseldonckx, D., Belmans, R., and D'Haeseleer, W. Distributed generation: definition, benefits and issues. *Energy Policy*, 33(6):787–798, apr 2005. ISSN 03014215. doi: 10.1016/j.enpol.2003.10.004. URL http://linkinghub.elsevier.com/retrieve/pii/S0301421503003069.

Pereira, Belo, M., Muacho, S., and Varvalho, A. Implementaion and evaluation of an operational ocean wave forecasting system along the coast of West Iberia. *J. Oper. Oceanogr.*, (March 2015):37–41, 2014. doi: 10.1080/1755876X.2014.11020157.

Pierson, W. J. and Moskowitz, L. A proposed spectral form for fully developed wind seas based on the similarity theory of S. A. Kitaigorodskii. *J. Geophys. Res.*, 69(24):5181–5190, dec 1964. ISSN 01480227. doi: 10.1029/JZ069i024p05181. URL http://doi.wiley.com/10.1029/JZ069i024p05181.

Pierson, W. J. and Stacy, R. A. The elevation, slope and curvature spectra of a wind roughened sea surface. Technical Report December, NASA, Washington D.C, 1973.

Pilar, P., Soares, C. G., and Carretero, J. C. 44-year wave hindcast for the North East Atlantic European coast. *Coast. Eng.*, 55(11):861–871, 2008. ISSN 03783839. doi: 10.1016/j.coastaleng.2008.02.027. URL http://dx.doi.org/10.1016/j.coastaleng.2008.02.027.

Ratsimandresy, a. W., Sotillo, M. G., Carretero Albiach, J. C., Álvarez Fanjul, E., and Hajji, H. A 44-year high-resolution ocean and atmospheric hindcast for the Mediterranean Basin developed within the HIPOCAS Project. *Coast. Eng.*, 55(11):827–842, 2008. ISSN 03783839. doi: 10.1016/j.coastaleng.2008.02.025. URL http://dx.doi.org/10.1016/j.coastaleng.2008.02.025.

Reguero, B. G., Menéndez, M., Méndez, F. J., Mínguez, R., and Losada, I. J. A Global Ocean Wave (GOW) calibrated reanalysis from 1948 onwards. *Coast. Eng.*, 65:38–55, 2012. ISSN 03783839. doi: 10.1016/j.coastaleng.2012.03.003. URL http://dx.doi.org/10.1016/j.coastaleng.2012.03.003.

Reguero, B., Losada, I., and Méndez, F. A global wave power resource and its seasonal, inter-annual and long-term variability. *Appl. Energy*, 148:366–380, 2015. ISSN 03062619. doi: 10.1016/j.apenergy.2015.03.114. URL http://linkinghub.elsevier.com/retrieve/pii/S030626191500416X.

Resio, D. T., Pihl, J. H., Tracy, B. A., and Vincent, C. L. Nonlinear energy fluxes and the finite depth equilibrium range in wave spectra. *J. Geophys. Res.*, 106(2000):6985–7000, 2001.

Richardson, D. S., Bidlot, J., Ferranti, L., Haiden, T., Hewson, T., Janousek, M., Prates, F., and Vitart, F. Evaluation of ECMWF forecasts, including 2012 âĂŞ 2013 upgrades. Technical Report November, European Centre for Medium-Range Forecasts (ECMWF), 2013.

Rienecker, M. M., Suarez, M. J., Gelaro, R., Todling, R., Bacmeister, J., Liu, E., Bosilovich, M. G., Schubert, S. D., Takacs, L., Kim, G.-K., Bloom, S., Chen, J., Collins, D., Conaty, A., da Silva, A., Gu, W., Joiner, J., Koster, R. D., Lucchesi, R., Molod, A., Owens, T., Pawson, S., Pegion, P., Redder, C. R., Reichle, R., Robertson, F. R., Ruddick, A. G., Sienkiewicz, M., and Woollen, J. MERRA: NASA's Modern-Era Retrospective Analysis for Research and Applications. *J. Clim.*, 24(14):3624–3648, jul 2011. ISSN 0894-8755. doi: 10.1175/JCLI-D-11-00015.1. URL http://journals.ametsoc.org/doi/abs/10.1175/JCLI-D-11-00015.1.

Ris, R. C., Holthuijsen, L. H., and Booij, N. A third-generation wave model for coastal regions: 2.Verification. 104:7667–7681, 1999.

Rogers, W. E. and Van Vledder, G. P. Frequency width in predictions of windsea spectra and the role of the nonlinear solver. *Ocean Model.*, 70:52–61, oct 2013. ISSN 14635003. doi: 10.1016/j.ocemod.2012.11.010. URL http://linkinghub.elsevier.com/retrieve/pii/S1463500312001710.

Rogers, W. E., Kaihatu, J. M., Hsu, L., Jensen, R. E., Dykes, J. D., and Holland, K. T. Forecasting and hindcasting waves with the SWAN model in the Southern California Bight. *Coast. Eng.*, 54(1):1–15, jan 2007. ISSN 03783839. doi: 10.1016/j.coastaleng.2006.06.011. URL http://linkinghub.elsevier.com/retrieve/pii/S0378383906000937.

Rogers, W., Hwang, P., and Wang, W. Investigation of Wave Growth and Decay in the SWAN Model : Three Regional-Scale Applications. *Phys. Oceanogr.*, pages 366–389, 2002a.

Rogers, W., Kaihatu, J., Petit, H., Booij, N., and Holthuijsen, L. Diffusion reduction in an arbitrary scale third generation wind wave model. *Ocean Eng.*, 29(11):1357–1390, sep 2002b. ISSN 00298018. doi: 10.1016/S0029-8018(01)00080-4. URL http://linkinghub.elsevier.com/retrieve/pii/S0029801801000804.

Rusu, E. and Guedes Soares, C. Numerical modelling to estimate the spatial distribution of the wave energy in the Portuguese nearshore. *Renew. Energy*, 34(6):1501–1516, jun 2009. ISSN 09601481. doi: 10.1016/j.renene.2008.10.027. URL http://linkinghub.elsevier.com/retrieve/pii/S0960148108003935.

Rusu, L. and Ivan, A. Modelling wind waves in the romanian coastal environment. *Environ. Eng. Manag. J.*, 9(4):547–553, 2010.

Salmon, J., Holthuijsen, L., Smit, P., van Vledder, G., and Zijlema, M. Alternative source terms for SWAN in the coastal region. *Coast. Eng.*, pages 1–13, 2014.

Sathyajith, M. *Wind Energy Fundamentals,Resource Analysis and Economics*. Springer-Verlag Berlin Heidelberg, 2006. ISBN 978-3-540-30905-5.

Schaber, K., Steinke, F., and Hamacher, T. Transmission grid extensions for the integration of variable renewable energies in Europe: Who benefits where? *Energy Policy*, 43:123–135, apr 2012a. ISSN 03014215. doi: 10.1016/j.enpol.2011.12.040. URL http://linkinghub.elsevier.com/retrieve/pii/S0301421511010469.

Schaber, K., Steinke, F., Mühlich, P., and Hamacher, T. Parametric study of variable renewable energy integration in Europe: Advantages and costs of transmission grid extensions. *Energy Policy*, 42:498–508, mar 2012b. ISSN 03014215. doi: 10.1016/j.enpol.2011.12.016. URL http://linkinghub.elsevier.com/retrieve/pii/S0301421511010081.

Sharkey, F., Bannon, E., Conlon, M., and Gaughan, K. Dynamic Electrical Ratings and the Economics of Capacity Factor for Wave Energy Converter Arrays. *Proc. 9th Eur. Wave Tidal Energy Conf.*, pages 1–8, 2011.

Siadatmousavi, S. M., Jose, F., and Stone, G. Evaluation of two WAM white capping parameterizations using parallel unstructured SWAN with application to the Northern Gulf of Mexico, USA. *Appl. Ocean Res.*, 33(1):23–30, feb 2011. ISSN 01411187. doi: 10.1016/j.apor.2010.12.002. URL http://linkinghub.elsevier.com/retrieve/pii/S0141118710000969.

Silva, D., Rusu, E., and Soares, C. G. Evaluation of various technologies for wave energy conversion in the portuguese nearshore. *Energies*, 6:1344–1364, 2013. ISSN 19961073. doi: 10.3390/en6031344.

Smith, H. and Maisondieu, C. Resource Assessment for Cornwall , Isles of Scilly and PNMI. Technical Report April, 2014.

Smith, H. C. M., Haverson, D., and Smith, G. H. A wave energy resource assessment case study: Review, analysis and lessons learnt. *Renew. Energy*, 60:510–521, 2013. ISSN 09601481. doi: 10.1016/j.renene.2013.05.017. URL http://dx.doi.org/10.1016/j.renene.2013.05.017.

Soukissian, T., Gizari, N., Fytilis, D., Papadopoulos, A., Korres, G., and Prospathopoulos, A. Wind and Wave Potential in Offshore Locations of the Greek Seas. In *Proc. Twenty-second Int. Offshore Polar Eng. Conf. June 17-22*, volume 4, pages 525–532, 2012.

Soukissian, T. H., Prospathopoulos, A. M., and Diamanti, C. Wind and Wave Data Analysis for the Aegean Sea - Preliminary Results. *J. Atmos. Ocean Sci.*, 8(2-3):163–189, 2002. ISSN 1741-7538. doi: 10.1080/1023673029000003525.

Soukissian, T. H., Prospathopoulos, A., Korres, G., Papadopoulos, A., Maria, H., and Maria, K. A new wind and wave atlas of the Hellenic Seas. In *Proc. ASME 2008 27th Int. Conf. Ocean. Arct. Eng. OMAE2008*, pages 1–9, Estoril,Portugal, 2008. ASME.

Soukissian, T. and Pospathopoulos, A. The Errors-in-Variables approach for the validation of the WAM wave model in the Aegean Sea. *Sci. Mediterr. Mar.*, 7(1):47–62, 2006.

Standards, B. British Standards - Maritime structures. 3(1):1–254, 2000.

Sterl, A., Komen, G. J., and Cotton, P. D. Fifteen years of global wave hindcasts using winds from the European Centre for Medium-Range Weather Forecasts reanalysis: Validating the reanalyzed winds and assessing the wave climate. *J. Geophys. Res.*, 103:5477–5492, 1998.

Sterl, A. and Caires, S. Climatology, variability and extrema of ocean waves: The web-based KNMI/ERA-40 wave atlas. *Int. J. Climatol.*, 25(7):963–977, 2005. ISSN 08998418. doi: 10.1002/joc.1175.

Stopa, J. E. and Cheung, K. F. Intercomparison of wind and wave data from the ECMWF Reanalysis Interim and the NCEP Climate Forecast System Reanalysis. *Ocean Model.*, 75:65–83, mar 2014. ISSN 14635003. doi: 10.1016/j.ocemod.2013.12.006. URL http://linkinghub.elsevier.com/retrieve/pii/S1463500313002205.

Stopa, J. E., Cheung, K. F., Tolman, H. L., and Chawla, A. Patterns and cycles in the Climate Forecast System Reanalysis wind and wave data. *Ocean Model.*, 70:207–220, oct 2013. ISSN 14635003. doi: 10.1016/j.ocemod.2012.10.005. URL http://linkinghub.elsevier.com/retrieve/pii/S1463500312001503.

Stoutenburg, E. D., Jenkins, N., and Jacobson, M. Z. Power output variations of co-located offshore wind turbines and wave energy converters in California. *Renew. Energy*, 35(12): 2781–2791, dec 2010. ISSN 09601481. doi: 10.1016/j.renene.2010.04.033. URL http://linkinghub.elsevier.com/retrieve/pii/S0960148110002004.

Swail, V. R., Ceccacci, E. a., Cox, a. T., and Cob, C. The AES40 North Atlantic Wave Reanalysis: Valdation and Climate Assessment. (1994), 2000.

Taylor, J., Wallace, R., and Bialek, J. Matching Renewable Electricity Generation with Demand. *Scottish Exec.*, (February), 2006.

Tolman, H. L. A Generalized Multiple Discrete Interaction Approximation for resonant four-wave interactions in wind wave models. *Ocean Model.*, 70:11–24, oct 2013. ISSN 14635003. doi: 10.1016/j.ocemod.2013.02.005. URL http://linkinghub.elsevier.com/retrieve/pii/S1463500313000310.

Tolman, H. L. and development Group, W. I. *User manual and system documentation of WAVEWATCH III version 4.18*. Number 316. Environmental Modeling Center Marine Modeling and Analysis Branch, 2014.

Tomawac. TOMAWAC wave model, 2014. URL http://www.opentelemac.org/index.php/modules-list/20-tomawac.

Tucker, M, J. *Waves in Ocean Engineering Measurements, Analysis, Interpretation*. Ellis Horwood Ltd., 1991. ISBN 0-13-932955-2.

van der Westhuysen, A. J., Zijlema, M., and Battjes, J. a. Nonlinear saturation-based whitecapping dissipation in SWAN for deep and shallow water. *Coast. Eng.*, 54(2):151–170, feb 2007. ISSN 03783839. doi: 10.1016/j.coastaleng.2006.08.006. URL http://linkinghub.elsevier.com/retrieve/pii/S037838390600127X.

van Os, J., Caires, S., and Gent, M. How to Carry Out Metocean Studies. *Proc. Twenty-first Int. Offshore Polar Eng. Conf. 19-14*, 8:290–297, 2011. doi: 10.1115/OMAE2011-49066.

van Vledder, G., Zijlema, M., and Holthuijsen, L. Revisiting the JONSWAP bottom friction formulation. In *Proc. 32nd Conf. Coast. Eng. Shanghai, China, 2010*, pages 1–8. Proceedings of the International Conference on Coastal Engineering; No 32, 2010.

van Vledder, G. P. Improved method for obtaining the integration space for the computation of nonlinear quadruplet wave-wave interactions. In *Wave Work. ECMWF*, number 1, 2000.

van Vledder, G. P. The WRT method for the computation of non-linear four-wave interactions in discrete spectral wave models. *Coast. Eng.*, 53(2-3):223–242, feb 2006. ISSN 03783839. doi: 10.1016/j.coastaleng.2005.10.011. URL http://linkinghub.elsevier.com/retrieve/pii/S0378383905001377.

van Vledder, G. P. Personal Communication on DIA problems, 2015.

Vannuchi, V. and Cappietti, L. OMAE2013-10183 Wave Energy estimation in four Italian nearshore areas. In *ASME 2013 32nd Int. Conf. Ocean. Offshore Arct. Eng. OMAE2013, June 9-14, Nantes,France*, pages 1–7, 2013.

Veigas, M., Ramos, V., and Iglesias, G. A wave farm for an island: Detailed effects on the nearshore wave climate. *Energy*, 69:801–812, may 2014. ISSN 03605442. doi: 10.1016/j.energy.2014.03.076. URL http://linkinghub.elsevier.com/retrieve/pii/S0360544214003405.

Venugopal, V., Wolfram, J., and Linfoot, B. The properties of extreme waves. Technical report, Health and Safety Executive, 2005.

Venugopal, V. and Nemalidinne, R. Wave resource assessment for Scottish waters using a large scale North Atlantic spectral wave model. *Renew. Energy*, 76:503–525, 2015. ISSN 0960-1481. doi: 10.1016/j.renene.2014.11.056. URL http://dx.doi.org/10.1016/j.renene.2014.11.056.

Venugopal, V., Davey, T., Smith, H., Smith, G., Cavaleri, L., Bertotti, L., and John, L. Equitable testing and evaluation of Marine Energy Extraction Devices of Performance, Cost and Environmental Impact. Deliverable 2.3 Application of Numerical Models. Technical report, 2010.

Verbruggen, A., Fischedick, M., Moomaw, W., Weir, T., Nadaï, A., Nilsson, L. J., Nyboer, J., and Sathaye, J. Renewable energy costs, potentials, barriers: Conceptual issues. *Energy Policy*, 38(2):850–861, feb 2010. ISSN 03014215. doi: 10.1016/j.enpol.2009.10.036. URL http://linkinghub.elsevier.com/retrieve/pii/S0301421509007836.

Verma, Y. P. and Kumar, A. Potential impacts of emission concerned policies on power system operation with renewable energy sources. *Int. J. Electr. Power Energy Syst.*, 44(1):520–529, jan 2013. ISSN 01420615. doi: 10.1016/j.ijepes.2012.03.053. URL http://linkinghub.elsevier.com/retrieve/pii/S0142061512004334.

Vinoth, J. and Young, I. R. Global Estimates of Extreme Wind Speed and Wave Height. *J. Clim.*, 24(6):1647–1665, mar 2011. ISSN 0894-8755. doi: 10.1175/2010JCLI3680.1. URL http://journals.ametsoc.org/doi/abs/10.1175/2010JCLI3680.1.

Vledder, G. P. V. Efficient algorithms for non-linear four-wave interactions. In *ECMWF Work. Ocean Waves,25-27 June 2012*, number June, pages 25–27, 2012.

Vögler, A. and Venugopal, V. OMAE2012-83658 Hebridean Marine Energy Resources: Wave-Power Characterisation Using a Buoy Network. In ASME, editor, *Proc. ASME 2012 31st Int. Conf. Ocean. Offshore Arct. Eng. June10-15,Rio Janeiro, Brazil*, pages 1–11, Rio de Janeiro, Brazil, 2012.

WAFO-group. WAFO - A Matlab Toolbox for Analysis of Random Waves and Loads - A Tutorial. *Math. Stat., Cent. Math. Sci., Lund Univ., Lund, Sweden*, 2000. URL http://www.maths.lth.se/matstat/wafo.

WAMDI, G. The WAM Model-a Third Generation Ocean Wave Prediction Model. *Phys. Oceanogr.*, 18:1775–1810, 1988.

WaveDragon. WaveDragon, 2015. URL http://www.wavedragon.net/index.php?option=com{_}frontpage{&}Itemid=1.

Waveplam. Methodology for Site Selection (D3.1). *Intell. Energy Eur.*, (November):1–35, 2009.

WaveStar. WaveStar, 2015. URL http://wavestarenergy.com/.

Wu, J. Wind-Stress Over Sea Surface From Breeze to Hurricane. *J. Geophys. Res.*, 87(12): 9704–9706, 1982.

Young, I. R. Seasonal variability of the global ocean wind and wave climate. *Int. J. Climatol.*, 950(19):931–950, 1999a.

Young, I. R., Vinoth, J., Zieger, S., and Babanin, a. V. Investigation of trends in extreme value wave height and wind speed. *J. Geophys. Res.*, 117, mar 2012. ISSN 0148-0227. doi: 10.1029/2011JC007753. URL http://doi.wiley.com/10.1029/2011JC007753.

Young, I. *Wind Generated Ocean Waves-volume 2*. Elsevier Ocean Engineering Book Series, 1st edition, 1999b. ISBN 0-08-043317-0.

Young, I. and van Vledder, G. The central role of non linear wave interactions in wind wave evolution. *Philos. Trans. R. Soc. London*, 342:505–524, 1993.

Zafirakis, D., Chalvatzis, K., and Kaldellis, J. "Socially just" support mechanisms for the promotion of renewable energy sources in Greece. *Renew. Sustain. Energy Rev.*, 21: 478–493, may 2013. ISSN 13640321. doi: 10.1016/j.rser.2012.12.030. URL http://linkinghub.elsevier.com/retrieve/pii/S1364032112007332.

Zijlema, M. Computation of wind-wave spectra in coastal waters with SWAN on unstructured grids. *Coast. Eng.*, 57(3):267–277, mar 2010. ISSN 03783839. doi: 10.1016/j.coastaleng.2009.10.011. URL http://linkinghub.elsevier.com/retrieve/pii/S0378383909001616.

Zijlema, M., van Vledder, G., and Holthuijsen, L. Bottom friction and wind drag for wave models. *Coast. Eng.*, 65:19–26, jul 2012. ISSN 03783839. doi: 10.1016/j.coastaleng.2012.03.002. URL http://linkinghub.elsevier.com/retrieve/pii/S0378383912000440.

Zijlema, M. Personal Communication on Unstructured meshes, 2014.

Zijlema, M. and van der Westhuysen, A. J. On convergence behaviour and numerical accuracy in stationary SWAN simulations of nearshore wind wave spectra. *Coast. Eng.*, 52(3):237–256, mar 2005. ISSN 03783839. doi: 10.1016/j.coastaleng.2004.12.006. URL http://linkinghub.elsevier.com/retrieve/pii/S0378383904001681.

Zodiatis, G., Galanis, G., Nikolaidis, A., Kalogeri, C., Hayes, D., Georgiou, G. C., Chu, P. C., and Kallos, G. Wave energy potential in the Eastern Mediterranean Levantine Basin. An integrated 10-year study. *Renew. Energy*, 69:311–323, sep 2014. ISSN 09601481. doi: 10.1016/j.renene.2014.03.051. URL http://linkinghub.elsevier.com/retrieve/pii/S0960148114002158.